RECEIVED
CENTRAL FAX CENTER

DEC 0 6 2011

IN THE UNITED STATES PATENT AND TRADEMARK OFFICE

APPLICANT(S)	: BOWEN, Philip J. et al
SERIAL NO.	: 10/502,080
FILED	: October 8, 2004
FOR	: SOLENOPSIN A, B AND ANALOGS AS NOVEL ANGIOGENESIS INHIBITORS
GROUP ART UNIT	: 1628
Examiner	: Paul E. Zarek

Mail Stop Amendment
Commissioner for Patents
P.O. Box 1450
Alexandria, VA 22313-1450

FURTHER DECLARATION OF DR. JACK L. ARBISER

I, Jack L. Arbiser declare as follows:

1. I am a co-inventor of the subject matter of the above-referenced patent application.

2. In 1983, I received a B.S. degree in Chemistry from Emory University, Atlanta, Georgia.

3. In 1991, I received a Ph.D. degree in Genetics and a MD degree in Medicine from Harvard Medical School, Boston, Massachusetts.

5. From 1994-1998, I participated in the Howard Hughes Postdoctoral Fellowship, Laboratory of Judah Folkman, M.D., Harvard Medical School, Boston Massachusetts.

6. Since 1991, I have studied the mechanisms of how oncogenes and tumor suppressor genes regulate angiogenesis and tumorigenesis. This work has resulted in the

discovery of small molecule inhibitors of tumor growth, and a novel method of predicting tumor signaling based upon loss of tumor suppressor genes p53 and p19ink4a. I have substantial scientific and medical expertise in cancer and clinical oncology.

7. I am presently a Professor of Dermatology, Emory University School of Medicine, Atlanta, Georgia. I have held this position since September, 2009.

8. I am also presently an Attending Physician, Atlanta Veterans Administration Medical Center, Atlanta Georgia. I have held this position since 2001.

9. In 2008, I was the Chief of Service of Dermatology and the Chief of Dermatology, Atlanta Veterans Administration Medical Center, Atlanta Georgia.

10. In 2007, I was the Director of Research, Department of Dermatology, Emory University School of Medicine, Atlanta, Georgia.

11. From 2004 to 2009, I was an Associate Professor in the Department of Dermatology, Emory University School of Medicine, Atlanta, Georgia.

12. From 1998 to 2004, I was an Assistant Professor in the Department of Dermatology, Emory University School of Medicine, Atlanta, Georgia.

13. In 1998, I was an Attending Physician, Emory University School of Medicine, Atlanta, Georgia

14. From 1995 to 1998, I was an Instructor in the Department of Dermatology, Harvard Medical School, Boston, Massachusetts.

15. From 1992 to 1994, I was a Resident in Dermatology, Massachusetts General

Hospital, Boston, Massachusetts.

16. From 1991 to 1992, I was an Intern in Internal Medicine, Beth Israel Hospital, Boston, Massachusetts.

17. From 1985 to 1991, I was in the Medical Scientist Training Program, Department of Genetics, Harvard Medical School, Boston, Massachusetts.

18. In 1984, I was a Research Assistant, Department of Rheumatology, Massachusetts General Hospital, Boston, Massachusetts.

19. In 1983, I was a Research Assistant, Department of Pediatrics, Emory University, Atlanta, Georgia.

20. In 1979, I was an Undergraduate Research Assistant, Department of Chemistry, Emory University, Atlanta, Georgia.

21. I have received numerous awards and honors for my scientific work including receiving the Albert E. Levy Scientific Research Award for Senior Investigator in 2007, and receiving the Emory School of Medicine Dean's Clinical Scholar award from 2000-2003 and 2004-2006 among other awards and honors.

22. I am a member of the Emory Medical Student Research Committee (2001-present) and the VA Research and Development Committee (2007-present). I am also a member of the Dermatology Foundation Medical and Scientific Committee External Advisory Board, University of Arizona Cancer Center, the Sturge-Weber Foundation Scientific Advisory Board (2001-present) and the American Academy of Dermatology-NAID Liaison (1998-present). I was an Organizer for the 48th Montagna Annual Symposium on the Biology of Skin, Snowmass Colorado (1999). I have been a Membership Chair of the Society for Investigative Dermatology

(2001-2002) and a Resident/Fellow Representative for the Society of Investigative Dermatology (1995-1997).

23. I have been a member of the following societies: the American Association for Cancer Research, The Society for Investigative Dermatology, the American Academy of Dermatology, the Tuberous Sclerosis Alliance, the Dermatology Foundation and the Sturge-Weber Foundation.

24. I am on the Editorial Boards for Pigment Cell Research (2007-present) and Journal of Investigative Dermatology (2001-present). I have been on the Editorial Boards for Journal of the Cutaneous Medicine and Surgery (2002-2005) and Journal of the American Academy of Dermatology (2001-2004). I was also a Guest Editor for Seminars in Cancer Biology, Karolinska Institute.

25. I have published over 200 scientific papers and I have published extensively in the scientific area of cancer research, including the mechanism by which cancer occurs, including the role of angiogenesis in cancer pathogenesis, including tumorigenesis.

26. The above paragraphs clearly establish a foundation for my medical and scientific expertise in cancer, including experimental cancer and clinical oncology, in providing the instant declaration.

27. I am familiar with United States patent application serial number 10/502,080, of which I am a co-inventor. I understand that the presently pending claims are directed to a method of treating cancer or a tumor in a patient comprising administering to a patient in need an effective amount of a composition which comprises a compound as otherwise set forth in the presently pending claims, namely claims 40, 50-56 and 66. Essentially, the presently pending claims are directed to the discovery that compositions which contain effective amounts of a compound as claimed are effective to treat a number of cancers and tumors. This is based upon

the fact that the compounds which are set forth in presently pending claims 40, 50-56 and 66 inhibit cancer and/or tumor growth by a mechanism which inhibits angiogenesis in the cancer/tumor tissue. By inhibiting angiogenesis, the presently claimed methods provide a generic approach to the treatment of any number of cancers and tumors as set forth in presently pending claims 40, 50-56 and 66.

28. It is my opinion that the presently claimed methods of treating tumors and/or cancer are useful and are expected to work as described and claimed, given that angiogenesis is an important generic mechanism by the way tumors and/or cancer grow and elaborate, and the presently claimed methods set forth in pending claims 40, 50-56 and 66 are directed to methods which utilize the inhibition of angiogenesis as a general mechanism to treat tumor and/or cancer. The compound which is claimed for use in the present method, solenopsin A, is an excellent anti-angiogenesis compound which exhibits broad activity against a large number of cancers, reflective of that mechanism as an angiogenesis inhibitor.

29. Angiogenesis comprises the development of a new vasculature for a tissue with increased metabolic demand. In adult life, the new tissue is likely to be a tumor or cancer, either benign or malignant, or an inflammatory process, such as psoriasis, inflammatory bowel disease, arthritis, asthma, multiple sclerosis, type II diabetes, lupus, and other diseases. The major sources of the blood vessel cells (endothelial cells) that are required for this process are recruitment of blood vessel cells from local pre-existing capillaries, or recruitment of cells from bone marrow that can turn into endothelial cells. Both processes contribute to the vascularization of a tumor or an inflammatory process. One of the commonalities of both inflammatory and tumor derived (neoplastic processes) is that they elaborate factors that recruit endothelial cells. The major factors for these processes include vascular endothelial growth factor (VEGF), basic fibroblast growth factor (bFGF), inflammatory cytokines (such as interleukin-8, and other factors), which stimulate the migration and proliferation of endothelial cells. The laboratory of Judah Folkman, MD, proved the absolute requirement of angiogenesis for the growth of malignant tumors. Based upon Dr. Folkman's pioneering work, angiogenesis

inhibitors have been developed for the treatment of human diseases, in particular the treatment of tumors and cancer.

26. Two strategies have been developed for the assessment of angiogenesis inhibitors. The first is direct inhibition, in which the activity of growth factors on the receptors is directly antagonized. The second is indirect inhibition, in which the ability of tumors to produce growth factors is inhibited. The phosphoinositol-3 kinase pathway, which is activated in virtually all tumors, is implicated in both direct and indirect angiogenesis inhibition.

27. Direct antiangiogenesis inhibition is now in clinical use for the treatment of cancer. The most prominent example is that of avastin (bevacizumab) that directly blocks the activity of VEGF on endothelial cells. Avastin is commonly used for the treatment of kidney and colon cancer, and more recently in brain cancer (glioblastoma). While avastin has been shown to be of clinical benefit, it is not curative and has well known side effects, such as hypertension and bleeding. In addition, the tumor hypoxia that is induced by avastin is thought to cause adaptation in the tumor, such as increased local invasion and elaboration of more growth factors in order to relieve the avastin-induced tumor hypoxia. Other strategies are being developed, but it is likely that any strategy that increased tumor hypoxia by itself will ultimately not cure a tumor.

28. Indirect inhibition of angiogenesis is an attractive strategy that has not been sufficiently explored. My studies in the Folkman lab, published in the Proceedings of the National Academy, were the first to demonstrate that blockade of phosphoinositol-3 kinase was able to inhibit the growth of a tumor *in vivo*. Blockade of phosphoinositol-3 kinase is an attractive strategy for several reasons. First, it blocks the production of growth factors by the tumor. Second, it causes increased apoptosis (programmed cell death) in tumors themselves. Finally, it is believed to prevent the metabolic adaptations in tumors caused by antiangiogenic therapies. Since phosphoinositol-3 kinase is such an important target, we regard it as a major focus to inhibit this pathway and to treat tumors and cancer. We discovered that solenopsin, a

naturally occurring alkaloid in the venom of the fire ant (Solenopsis invicta), is a potent inhibitor of this enzyme. In addition, we have shown that this compound claimed in the present invention is a potent inhibitor of angiogenesis in the zebrafish model and that solenopsin is stable and may be used as a pharmaceutical agent. See the previously submitted references, Arbiser, et al, *Blood*, 15 January 2007, Volume 109, Number 2, pages 560-565, which teaches the inhibition of angiogenesis by solenopsin consistent with its use as an anticancer agent, and Park, et al., *Journal of Infectious Diseases*, 15 October 2008, 198, 1198-201, which teaches that solenopsin is stable and may be used as a small molecule pharmaceutical agent as set forth in the present invention. The inhibitory activity, small molecular size and stability of solenopsin, which make it amenable to topical, systemic and oral administration, make it an attractive molecule for the treatment of tumors and cancer. It thus represents close to an ideal compound for providing generic therapy against a variety of cancerous tissue.

29. By way of cellular experimental evidence, recently the following experiments on a benign tumor cell line (FP52-SV) and malignant sarcoma cell (tsc2ang1) were conducted. In these experiments, the anti-proliferative/anticancer activity of solenopsin A (a compound claimed in the present application) were tested in the two cell lines. More specifically, 10,000 cells from benign tumors (FP52-SV40) or malignant sarcoma cells (tsc2ang1) were plated in 24 well plates. 24 hours after plating, the cells were treated with solenopsin in concentrations ranging from 0-20 micromolar or vehicle control. A number of other compounds were also tested. 24 hours after solenopsin treatment, the cells were trypsinized and counted with a cell culture.

30. The results of the experiments which are described in paragraph 29, above are shown in the attached Exhibits 1 and 2. In the first assay, the proliferation assay performed on the benign tumor cell line FP52 SV40, the anti-proliferative effect of solenopsin on the cells is clearly evidenced (see attached Exhibit 1). Noted is the fact that a concentration of solenopsin at 10 micromolar provided significant inhibition of cell proliferation (approximately 80%). The graph also evidences that anti-proliferative activity of solenopsin was synergistic with

imipramine blue where both compounds were used at a concentration of 1 micromolar. In the second experiment, the effect of solenopsin at varying concentrations was tested against malignant sarcoma TSC2ang1 cells (Exhibit 2). In this experiment, solenopsin exhibited excellent antiproliferative/anticancer activity against the sarcoma cell line with a concentration of 10 micromolar solenopsin being particularly effective, with concentration of solenopsin of 15 and 20 micromolar being slightly less effective than the lower concentration of 10 micromolar. In a third experiment, solenopsin was tested against a malignant melanoma cell line A375 (Exhibit 3). In this experiment, solenopsin exhibited excellent antiproliferative/anticancer activity against the melanoma cell line at a concentration of 10 micromolar with significant anticancer activity at a concentration of 10 micromolar. In all three experiments, the results of which are presented in attached Exhibits 1, 2 and 3, solenopsin showed substantial antiproliferative/anticancer activity in cell-based assays consistent with its use as a generic anticancer agent as claimed in the present invention.

31. Recently, solenopsin A was tested by the National Cancer Institute (NCI) against a number of cancer cell lines. This *in vitro* testing was conducted in 60 human tumor cell lines in the following cancers: breast, central nervous system, colon, leukemia, melanoma, non-small cell lung, ovarian, prostate and renal. Pursuant to NSC guidelines, each drug (in this case, NSC 166588 (Solenopsin A) is exposed to 60 humor tumor cell lines of the various cancer cited above at five different doses for 48 hours. The results of the *in vitro* testing in the 60 cell lines is presented in attached Exhibit 4. The NCI results evidenced that in all of the tumor cell lines tested, solenopsin exhibited substantial anti-cancer activity at 1 to 100 micromolar concentrations, depending on the cell line, consistent with its use as an anti-cancer agent. All cell lines were impacted by the Solenopsin treatment, evidencing that Solenopsin exhibited anti-cancer activity against every cell line in the 60 cell-line panel.

32. In addition to the experimental data which is presented in attached Exhibits 1-4, which clearly evidences that solenopsin exhibits generic anticancer activity against a number of different cancers and a large number of cell lines, the mechanism of action of

solenopsin and its anticancer activity is completely consistent with its use in a number of additional cancers. In particular, a review of the literature evidences that the inhibition of phosphatidyl inositol 3-kinase as part of an anti-angiogenesis mechanism is relevant to cancer treatment in a broad range of cancers, including skin cancer, colorectal cancer, head and neck cancer, breast cancer, including metaplastic breast cancer, lung cancer, pancreatic cancer and skin cancers, including basal cell carcinoma, squamous cell carcinoma and melanoma. In support of the generic utility of the present invention as a treatment for numerous cancers, enclosed herewith are a number of peer reviewed publications in the scientific literature which evidences that inhibition of phosphatidyl inositol 3-kinase (the inhibition of the pathway through which solenopsin exhibits its generic anti-cancer effect) is consistent with cancer growth inhibition and apoptosis of cancer cells. This mechanism is shown to be important for the treatment of a number of cancers including skin cancers (see Anto, et al., *The Journal of Biological Chemistry*, 278, 28, pp. 25490-25498. August, 2003, copy enclosed), colorectal cancer (see Baba, et al., *Cancer*, April 1, 2011, pp. 1399-1408, copy enclosed), head and neck cancer (see Bian, et al., *Cancer Res.*, 2009, July 15; 69(14), pp. 5918-5926, copy enclosed), breast cancer (see Capodanno, et al., *Human Pathology*, 2009, 40, 1408-1417 and Hennessy, et al., *Cancer Res.*, 2009, May 15, 69(10) pp. 4116-4124, copies enclosed), lung cancer (see Capuzzo, et al., *Journal of the National Cancer Institute*, 96, 15, August 4, 2004, pp. 1133-1141, copy enclosed), pancreatic cancer (Chen, et al., *Pathol. Oncol. Res.*, 2011, 17:257 pp. 257-261, copy enclosed), skin cancers, including melanoma, squamous cell carcinoma and basal cell carcinoma (see Jee, et al, *The Journal of Investigative Dermatology*, 119, 5, pp. 1121- 1127, 2002 and Ming, et al., *The Journal of Investigative Dermatology*, 129, pp. 2109-2112, 2009, copies enclosed), brain cancer (see Rong,et al., *PNAS*, 101, 52, pp. 18200-18205, December 28, 2004, copy enclosed) and ovarian cancer (see Wang,et al., *Oncogene*,24, 3574-3582, 2005, copy enclosed). These references evidence the dramatic generic role that phosphatidyl inositol 3-kinase plays in a variety of cancers and also evidences that inhibition of this enzyme is material to the treatment of these cancers.

33. Given the exceptional inhibitory activity solenopsin displays against

phosphoinositol-3 kinase and the direct and indirect role that phosphoinositol-3 kinase plays in promoting angiogenesis, a critically important process in tumor/cancer growth and elaboration, as evidenced by the literature cited and enclosed, as well as the experimental test results which are described in paragraphs 29-31, above, it is my expectation that solenopsin will prove to be an effective agent against tumors and cancer by inhibiting angiogenesis in cancer tissue through inhibition of phosphoinositol-3 kinase. This expectation is corroborated by the favorable antiproliferative/anticancer activity exhibited by solenopsin in the cell-based assays which are described above and in attached Exhibits 1-4, as well as the literature cited which further evidences the broad generic role that phosphoinositol 3-kinase plays in cancer treatment. By virtue of the inhibitory activity of the compounds which are presently claimed in the pending method claims, it is my expectation that these compounds will prove to be effective anti-cancer agents against a broad range of tumors and cancer.

34. As a separate point, I understand that Examiner Zarek has objected to Figure 5 in the original application for the reasons which are cited in the July, 2011 office action on pages 6-7. Applicants submit that the entry for Solenopsin in figure 5, in particular for the entry at a concentration of 6 micrograms/mL, which presents data for an SVR inhibition assay conducted prior to the filing of the present application, is an artifact of the experimental conditions run at the time the figure was generated. The SVR assay, the results of which are presented in the original specification, may be viewed as a screen for preliminary results. The 6 microgram test result from the SVR assay of Figure 5 is an experimental artifact that may be attributed to a number of factors, including but not limited to aggregation effects, solubility, sample purity, etc. Occasionally, in the SVR assay, concentration effects have been observed. In such cases either the assay is repeated or other experiments are carried out. In this case, we have repeated this experiment several times and a more accurate experiment is presented in figure 2 of the previously submitted *Blood* 2007 paper, referenced above in paragraph 29. We have repeated the experiment several times with the same results which are presented in figure 2 of the *Blood 2007* paper. The combination of experiments described above unambiguously demonstrates that solenopsin A is inhibiting angiogenesis and by the akt

pathway.

35. I further declare that all statements made herein of my own personal knowledge are true and that all statements made on information and belief are believed to be true; and further that these statements were made with the knowledge that willful false statements and the like so made are punishable by fine or imprisonment, or both, under Section 1001 of Title 18 of the United States Code, and that such willful false statements may jeopardize the validity of the application or any patent issued thereon.

Date: _____ _____

Jack L. Abiser, MD, PhD

pathway.

35. I further declare that all statements made herein of my own personal knowledge are true and that all statements made on information and belief are believed to be true; and further that these statements were made with the knowledge that willful false statements and the like so made are punishable by fine or imprisonment, or both, under Section 1001 of Title 18 of the United States Code, and that such willful false statements may jeopardize the validity of the application or any patent issued thereon.

Date: 11/5/11

Jack L. Abiser, MD, PhD

EXHIBIT 1

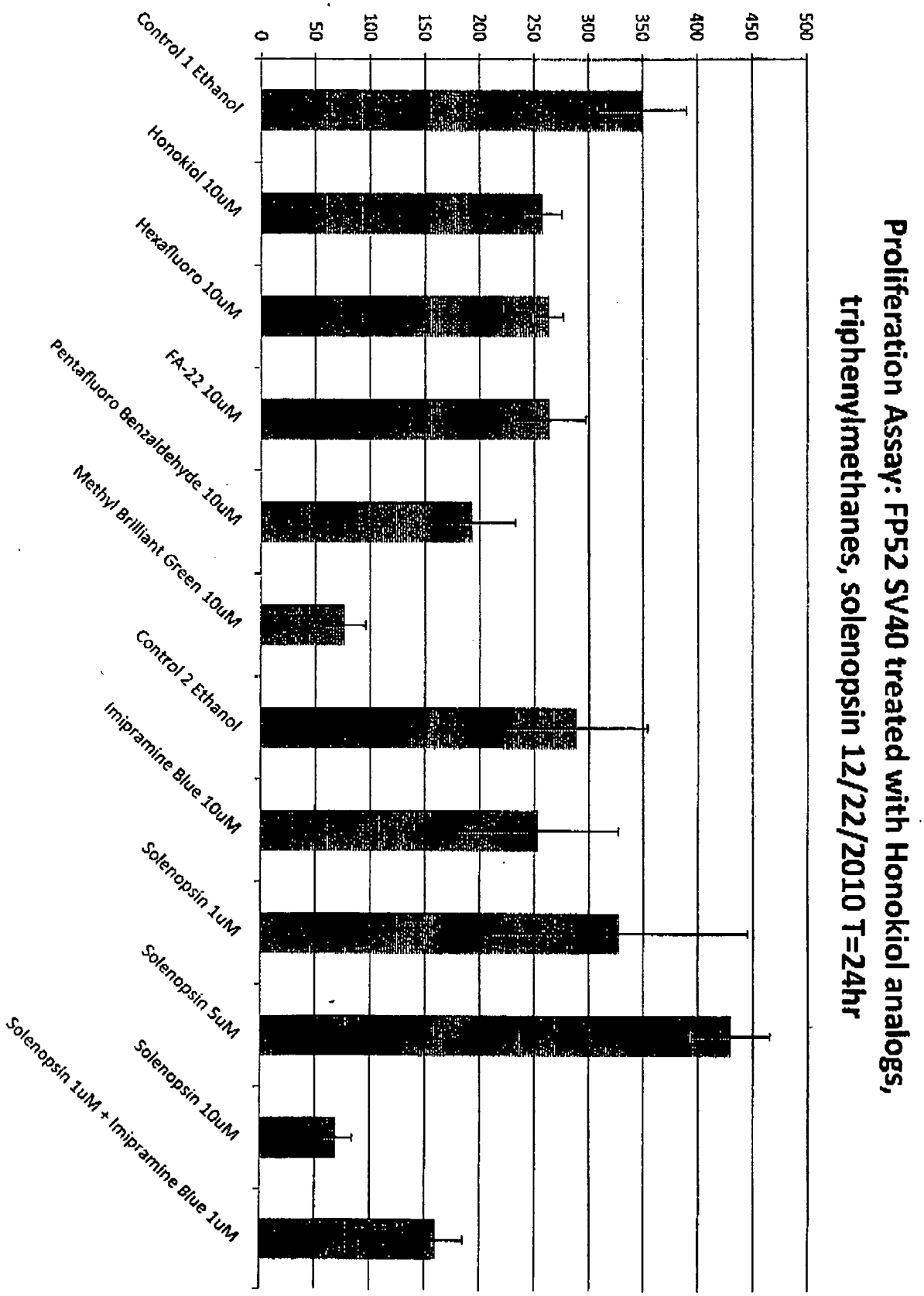
Proliferation Assay: FP52 SV40 treated with Honokiol analogs, triphenylmethanes, solenopsin 12/22/2010 T=24hr
0
50
100
150
200
250
300
350
400
450
500
Control 1 Ethanol
Honokiol 10uM
Hexafluoro 10uM
FA-22 10uM
Pentafluoro Benzaldehyde 10uM
Methyl Brilliant Green 10uM
Control 2 Ethanol
Imipramine Blue 10uM
Solenopsin 1uM
Solenopsin 5uM
Solenopsin 10uM
Solenopsin 1uM + Imipramine Blue 1uM

EXHIBIT 2

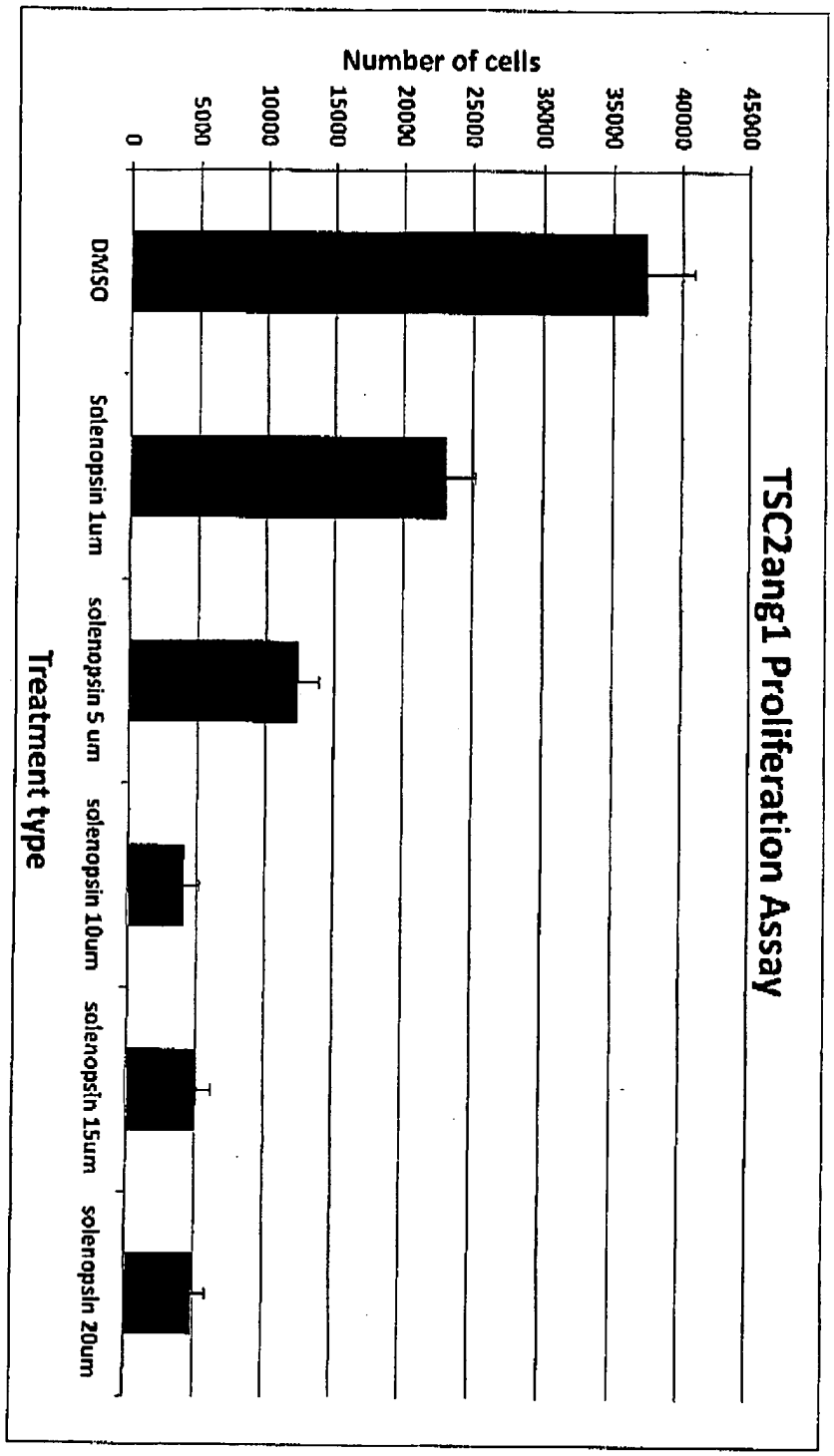
TSC2ang1 Proliferation Assay
Number of cells
0
5000
10000
15000
20000
25000
30000
35000
40000
45000
DMSO
Solenopsin 1um
solenopsin 5 um
solenopsin 10um
solenopsin 15um
solenopsin 20um
Treatment type

EXHIBIT 3

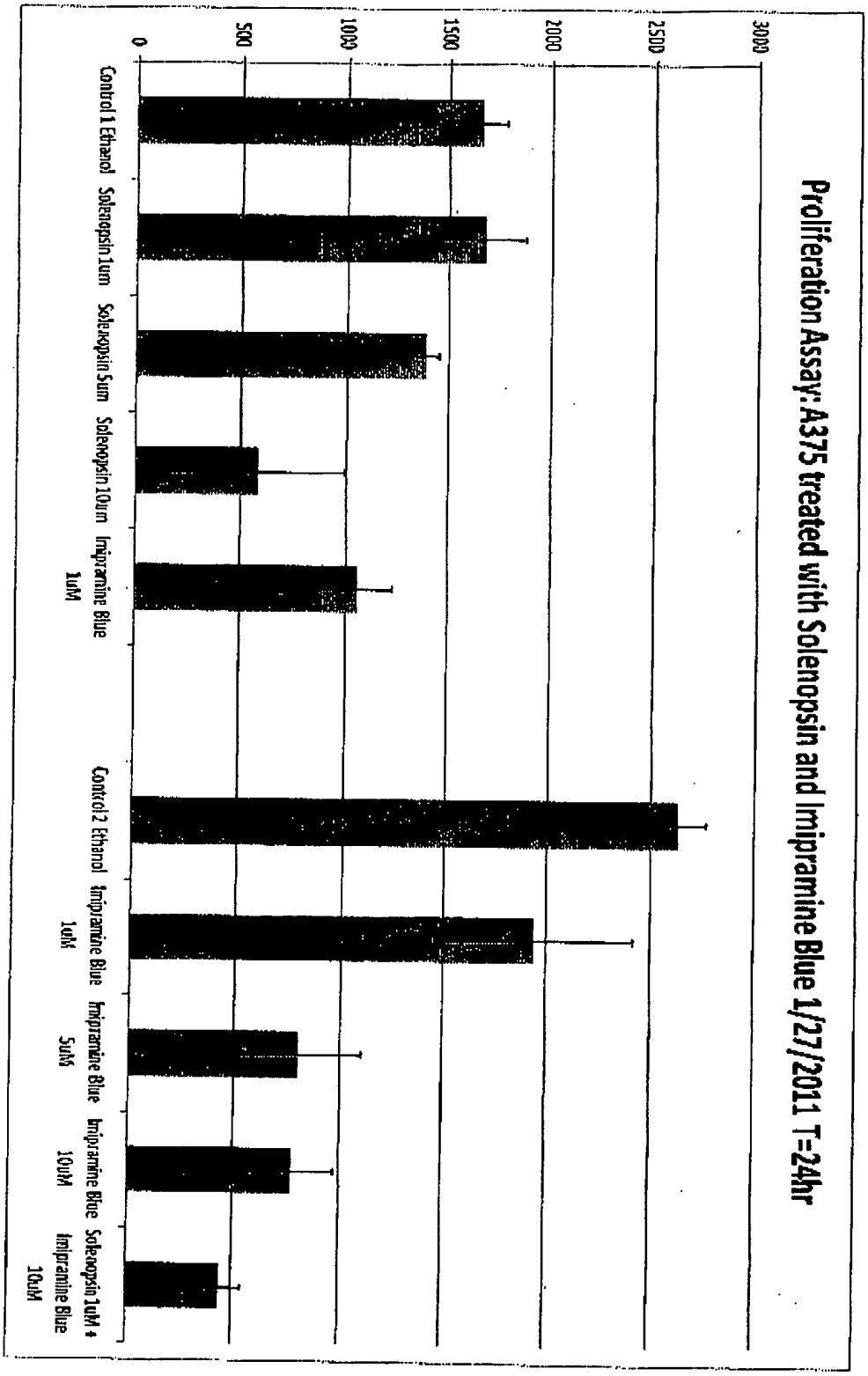
Proliferation Assay: A375 treated with Solenopsin and Imipramine Blue 1/27/2011 T=24hr
0
500
1000
1500
2000
2500
3000
Control 1 Ethanol
Solenopsin 1um
Solenopsin 5um
Solenopsin 10um
Imipramine Blue 1uM
Control 2 Ethanol
Imipramine Blue 1uM
Imipramine Blue 5uM
Imipramine Blue 10uM
Solenopsin 1uM + Imipramine Blue 10uM

EXHIBIT 4

NATIONAL CANCER INSTITUTE DEVELOPMENTAL THERAPEUTICS PROGRAM
DOSE RESPONSE CURVES FOR NSC 166588
(SOLENOPSIN A)

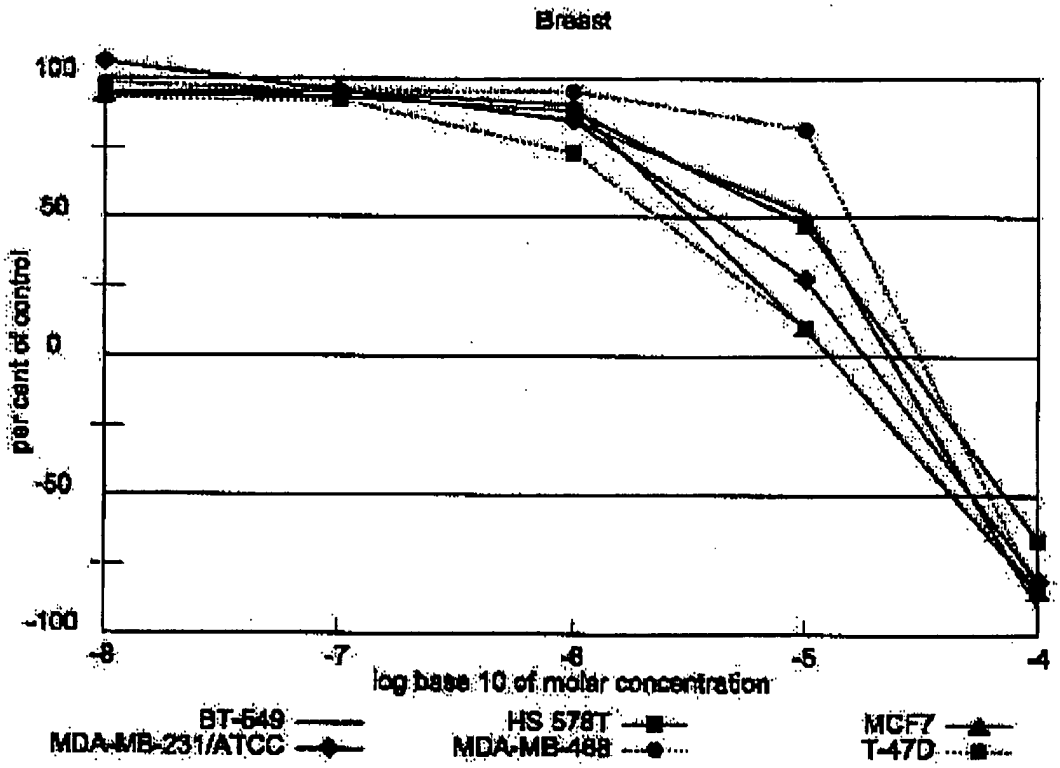

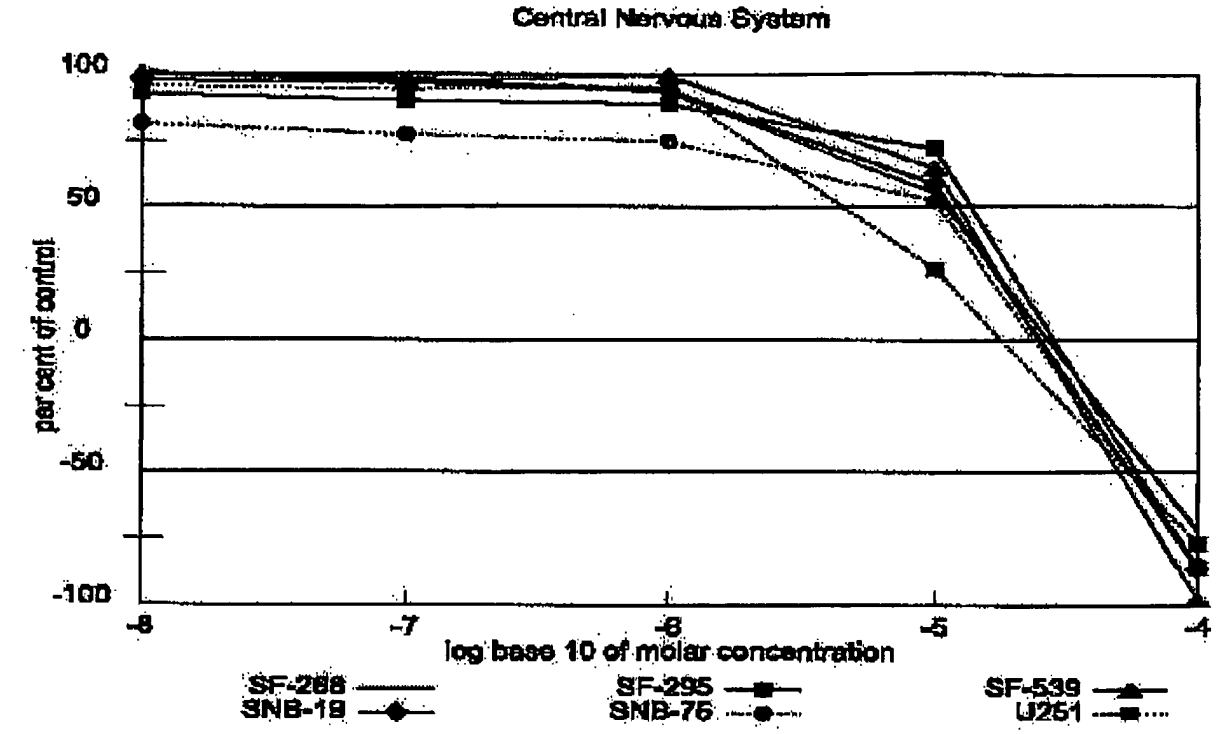
Central Nervous System
100
50
0
-50
-100
per cent of control
-8
-7
-6
-5
-4
log base 10 of molar concentration
SF-268
SF-295
SF-539
SNB-19
SNB-75
U251

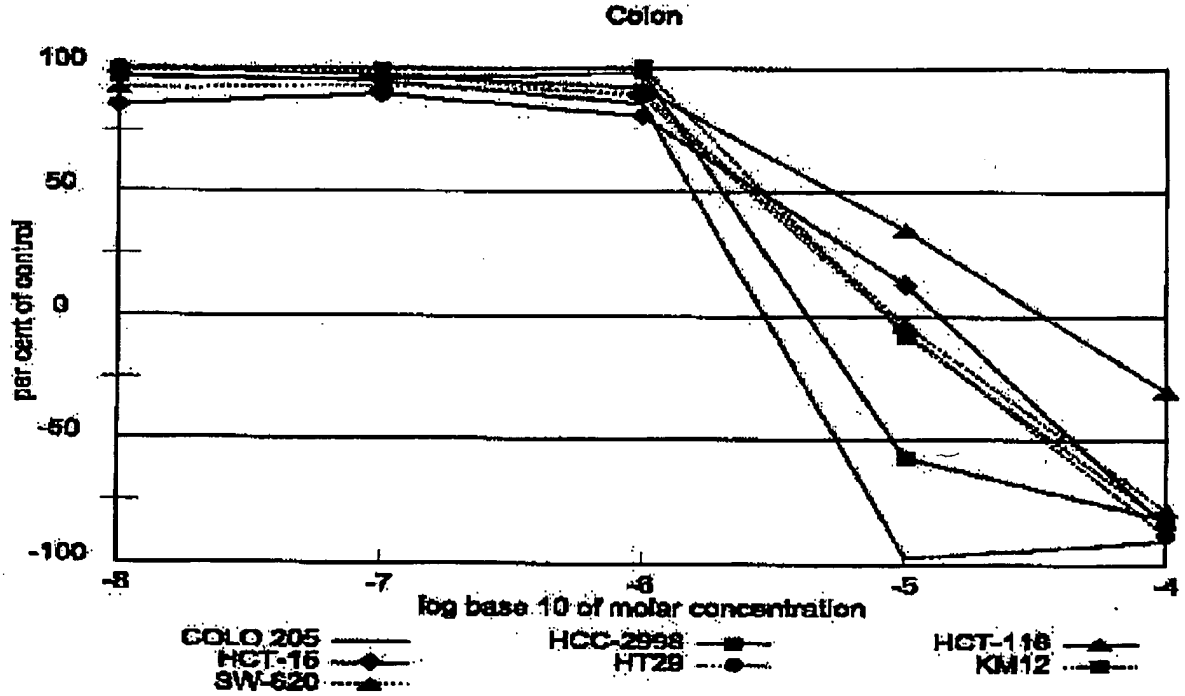
Colon
100
50
0
-50
-100
per cent of control
-8
-7
-6
-5
-4
log base 10 of molar concentration
COLO 205
HCC-2998
HCT-116
HCT-15
HT29
KM12
SW-620

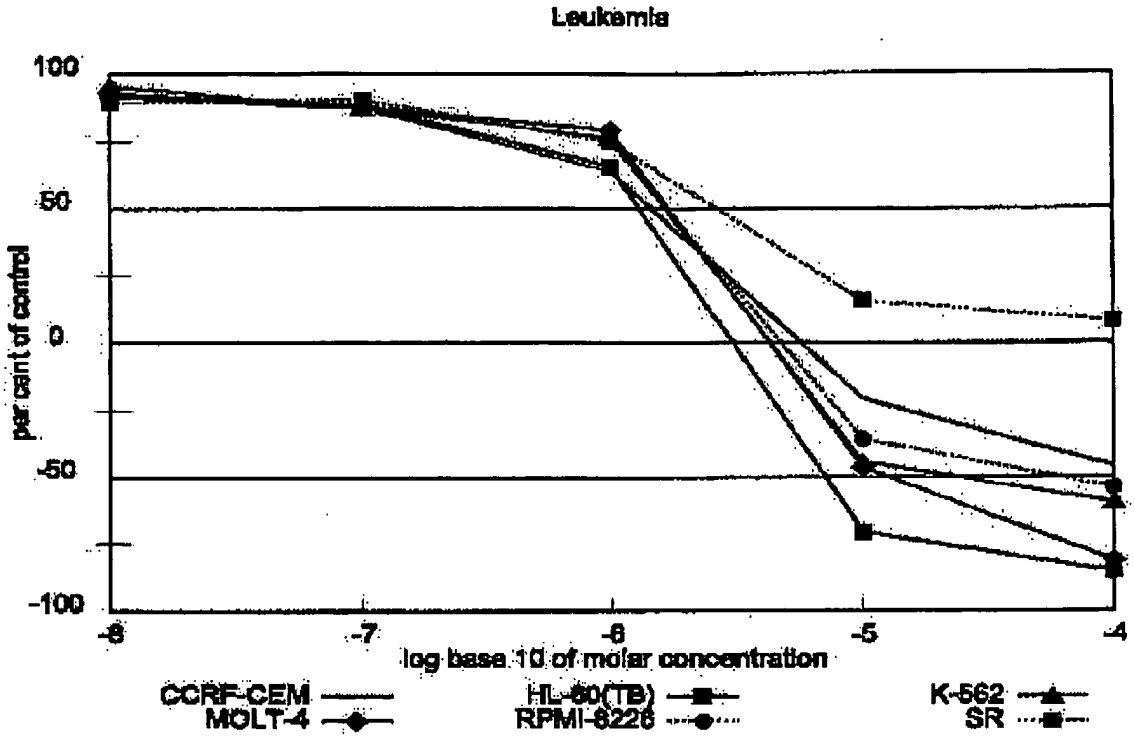
Leukemia
100
50
0
-50
-100
per cent of control
-8
-7
-6
-5
-4
log base 10 of molar concentration
CCRF-CEM
MOLT-4
HL-60(TB)
RPMI-8226
K-562
SR

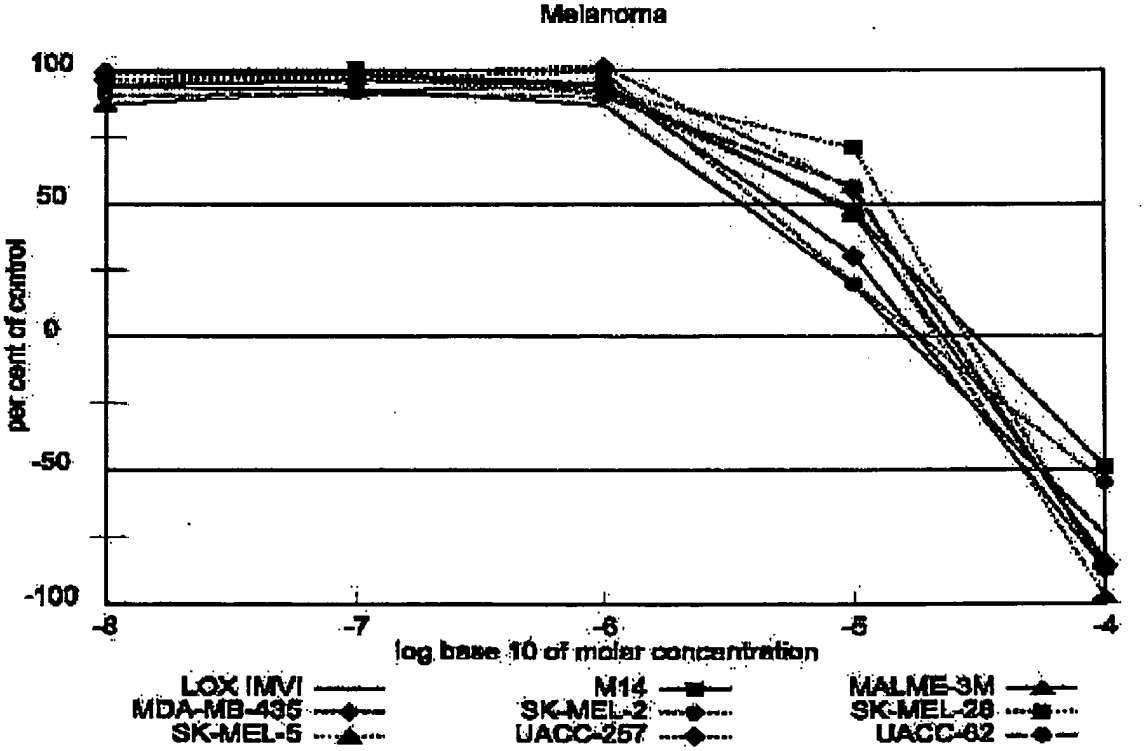
Melanoma
100
50
0
-50
-100
per cent of control
-8
-7
-6
-5
-4
log base 10 of molar concentration
LOX IMVI
MDA-MB-435
SK-MEL-5
M14
SK-MEL-2
UACC-257
MALME-3M
SK-MEL-28
UACC-62

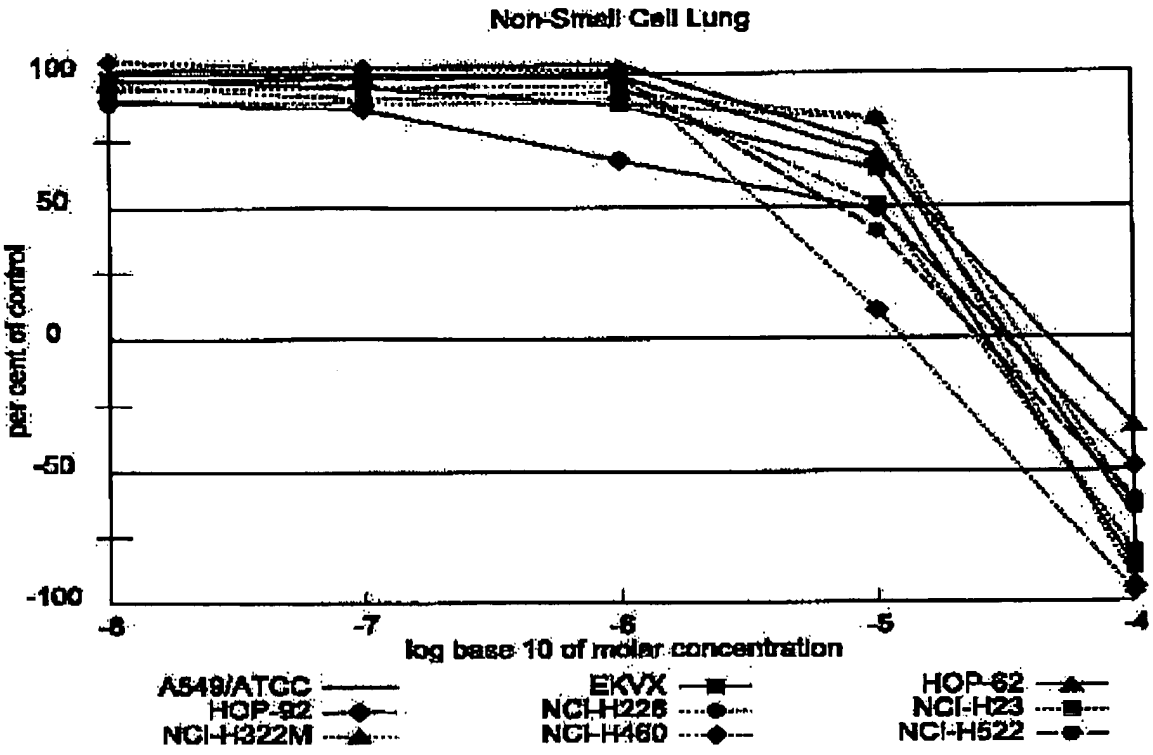
Non-Small Cell Lung
100
50
0
-50
-100
per cent of control
-8
-7
-6
-5
-4
log base 10 of molar concentration
A549/ATCC
HOP-92
NCI-H322M
EKVX
NCI-H226
NCI-H460
HOP-62
NCI-H23
NCI-H522

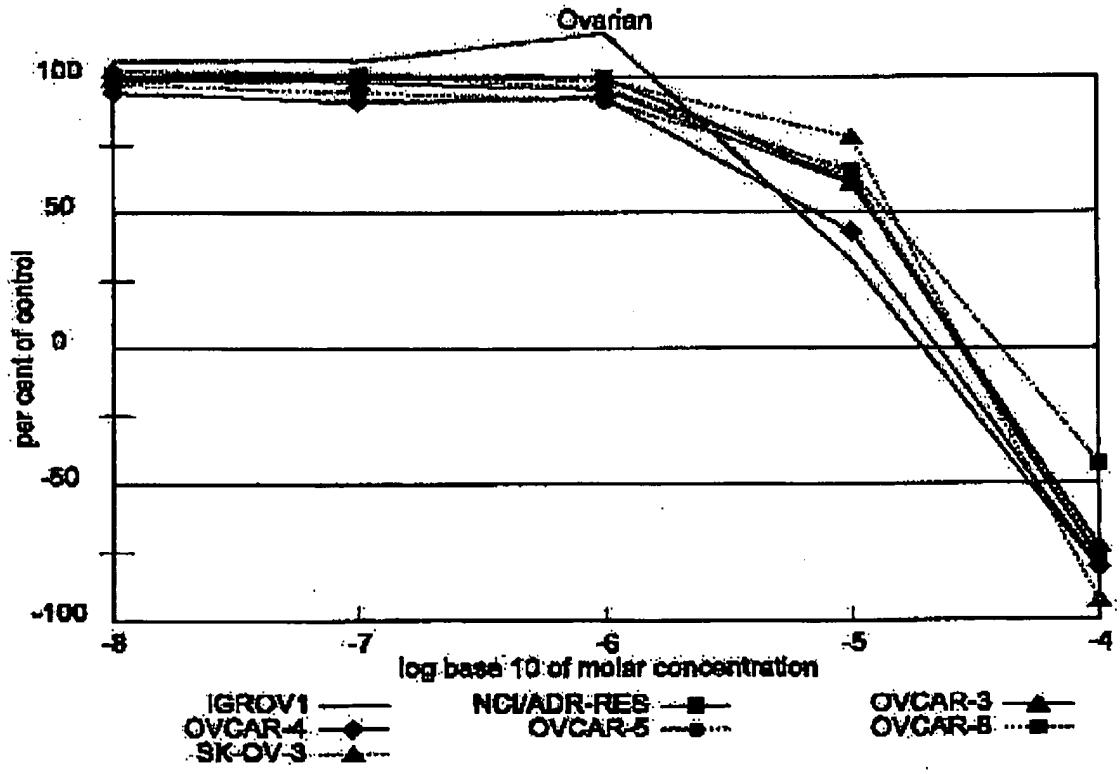
Ovarian
100
50
0
-50
-100
per cent of control
-8
-7
-6
-5
-4
log base 10 of molar concentration
IGROV1
OVCAR-4
SK-OV-3
NCI/ADR-RES
OVCAR-5
OVCAR-3
OVCAR-8

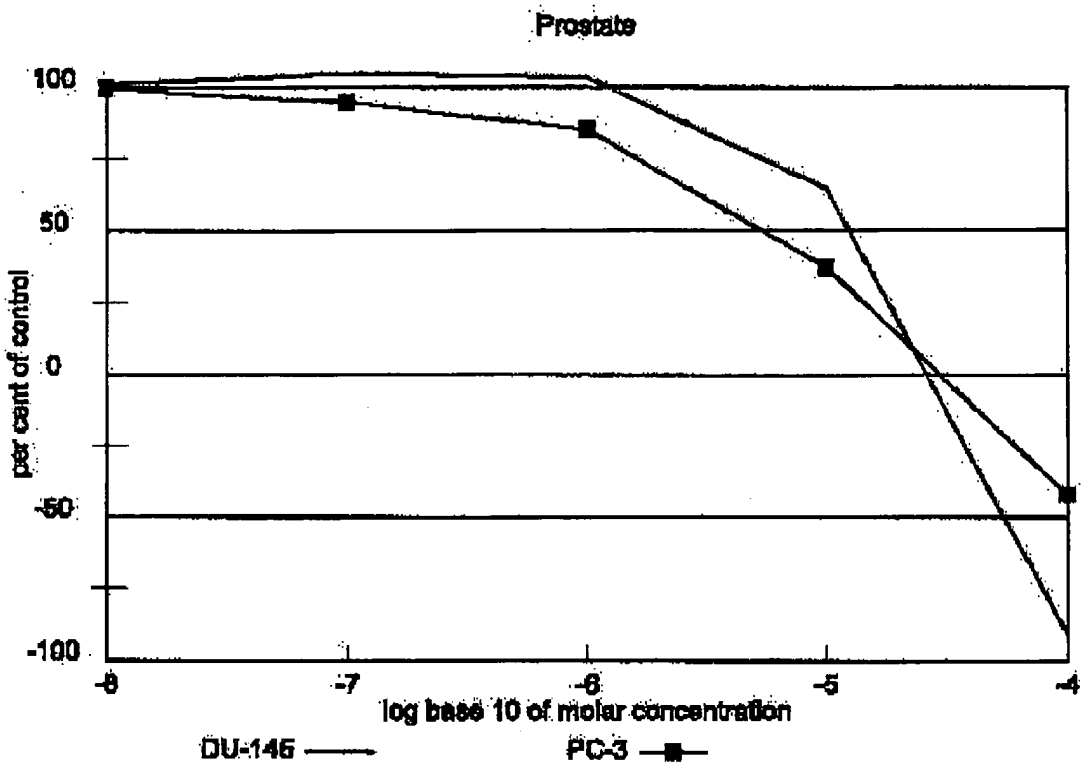
Prostate
100
50
0
-50
-100
per cent of control
-8
-7
-6
-5
-4
log base 10 of molar concentration
DU-145
PC-3

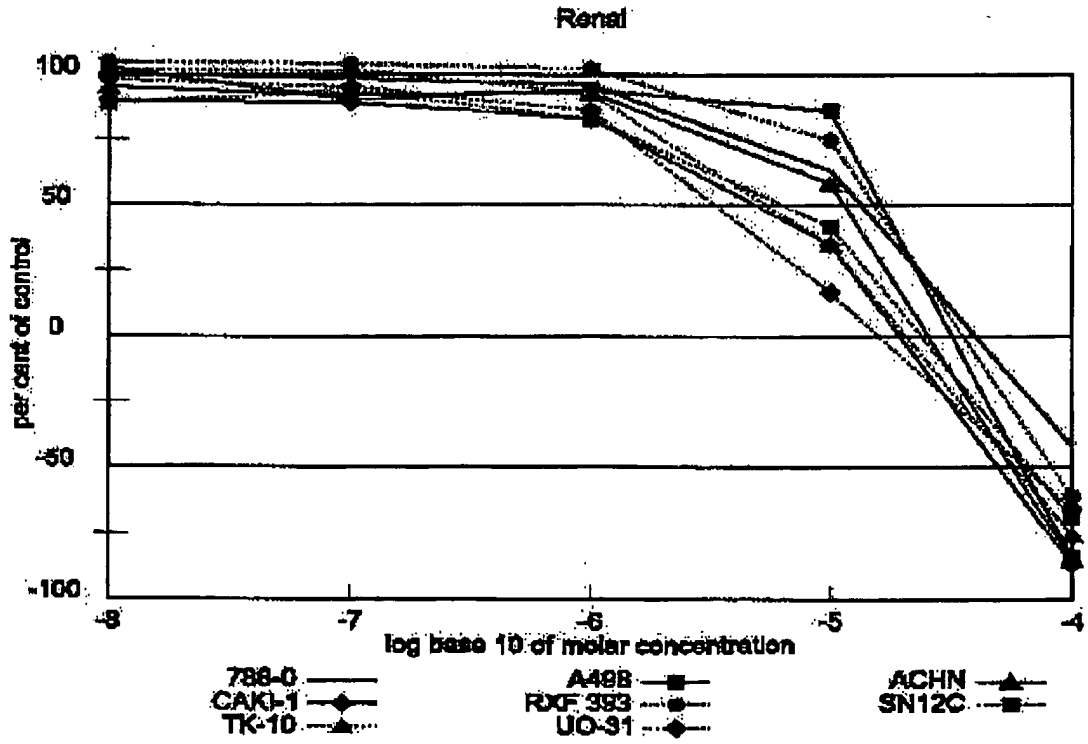
Renal
100
50
0
-50
-100
per cent of control
-8
-7
-6
-5
-4
log base 10 of molar concentration
786-0
CAKI-1
TK-10
A498
RXF 393
UO-31
ACHN
SN12C

THE JOURNAL OF BIOLOGICAL CHEMISTRY
Vol. 278, No. 28, Issue of July 11, pp. 25490–25498, 2003
Printed in U.S.A.

Inhibition of NF-κB Sensitizes A431 Cells to Epidermal Growth Factor-induced Apoptosis, whereas Its Activation by Ectopic Expression of RelA Confers Resistance*

Received for publication, February 19, 2003, and in revised form, April 16, 2003
Published, JBC Papers in Press, April 24, 2003, DOI 10.1074/jbc.M301790200

Ruby John Anto, Manickam Venkatraman‡, and Devarajan Karunagaran§
From the Division of Cancer Biology, Rajiv Gandhi Center for Biotechnology, Thiruvananthapuram, Kerala-695014, India

Epidermal growth factor (EGF) is a well known mitogen, but it paradoxically induces apoptosis in cells that overexpress its receptor. We demonstrate for the first time that the EGF-induced apoptosis is accelerated if NF-κB is inactivated. To inactivate NF-κB, human epidermoid carcinoma cells (A431) that overexpress EGF receptor were stably transfected with an IκB-α double mutant construct. Under the NF-κB-inactivated condition, A431 cells were more sensitive to EGF with decreased cell viability and increased externalization of phosphatidylserine on the cell surface, DNA fragmentation, and activation of caspases (3 and 8 but not 9), typical features of apoptosis. These results were further supported by the potentiation of the growth inhibitory effects of EGF by chemical inhibitors of NF-κB (curcumin and sodium salicylate) and the protective role of RelA evidenced by the resistance of A431-RelA cells (stably transfected with RelA) to EGF-induced apoptosis. EGF treatment or ectopic expression of RelA in A431 cells induced DNA binding activity of NF-κB (p50 and RelA) and the expression of c-IAP1, a downstream target of NF-κB. A431-RelA cells exhibited spontaneous phosphorylation of Akt (a downstream target of phosphatidylinositol 3-kinase and regulator of NF-κB) and EGF treatment stimulated it further. Blocking this basal Akt phosphorylation with LY294002, an inhibitor of phosphatidylinositol 3-kinase, did not affect their viability but blocking of EGF-induced phosphorylation of Akt sensitized the otherwise resistant A431-RelA cells to EGF-mediated growth inhibition. Our results favor an anti-apoptotic role for NF-κB in the regulation of EGF-induced apoptosis.

Epidermal growth factor (EGF)[1] is a polypeptide (6-kDa) that belongs to the EGF family of ligands (heparin binding EGF, transforming growth factor-α, amphiregulin, β-cellulin, epiregulin, and neuregulins) binding to specific cell surface receptors (1, 2). Upon ligand binding, the epidermal growth factor receptor (EGFR) dimerizes, autophosphorylates itself, and recruits a cascade of signaling molecules before transmitting potent mitogenic signals in many cellular systems (1, 3). EGFR is overexpressed in a number of human malignancies including cancers of the lung, head and neck, brain, bladder, and breast (4). Furthermore, increased EGFR expression correlates with a poorer clinical outcome for patients with breast and ovarian cancers (5, 6). Whereas EGF is a potent mitogen, it paradoxically induces apoptosis in cells that overexpress EGFR such as A431 (7). Experimentally increasing the level of EGFR expression in epithelial, mesenchymal, or glial cells also leads to ligand-dependent apoptosis (8). Another ligand of the EGF family, heregulin (also known as neuregulin), is known to induce apoptosis in cells that overexpress ErbB2, the second member of the EGFR family (9). In addition, epiregulin also inhibited cell growth in EGFR-overexpressing cells (10). Induction of amphiregulin mRNA was observed in EGF-induced apoptosis (11) and interaction of EGF with pro-heparin-binding EGF leads to growth inhibition and apoptosis (12). Growth factors other than EGF such as platelet-derived growth factor and hepatocyte growth factor can also trigger cell cycle arrest and death in a variety of cells (13, 14) and in addition, EGF enhanced the apoptotic effect of platelet-derived growth factor (14). An EGF-related protein, Cripto-1, promotes apoptosis in HC-11 mouse mammary epithelial cells (15). Anoikis, activation of EGFR tyrosine kinase, Ras-MAP kinase signaling, and the elevation of Stat1 and p21 levels have been advocated as mechanisms driving EGF-induced apoptosis (11, 16–18) but, the actual mechanism appears to be more elusive and complicated.

Apoptosis or programmed cell death is a physiological process characterized by distinct morphological and biochemical features that include membrane blebbing, chromatin condensation, cytoplasmic shrinking, DNA fragmentation, and activation of different caspases (19). Typically two different pathways, extrinsic receptor-mediated and intrinsic mitochondria-mediated, leading to apoptosis have been identified (20, 21). Mostly cytokines of the tumor necrosis factor (TNF) superfamily induce apoptosis by interaction of the ligand with its death receptor, which sequentially recruits TNF receptor-associated death domain, Fas-associated death domain, caspase 8, and caspase 3, the last then cleaves various substrates leading to apoptosis. In contrast, the mitochondria-mediated pathway involves the release of cytochrome c from the mitochondria, and cytochrome c together with Apaf1 activates caspase 9, and the latter then activates caspase 3, resulting in apoptosis (20, 21). Tumor cells often evade apoptosis by expressing several anti-apoptotic proteins such as Bcl-2, down-regulation and mutation of pro-apoptotic genes and alterations of p53, PI-3K/Akt, or NF-κB

* This work was supported in part by grants from the Department of Science and Technology, Government of India and the Science, Technology and Environment committee, Government of Kerala, India (to D. K.). The costs of publication of this article were defrayed in part by the payment of page charges. This article must therefore be hereby marked "*advertisement*" in accordance with 18 U.S.C. Section 1734 solely to indicate this fact.

‡ Supported by a Senior Research Fellowship from the Council of Scientific and Industrial Research, India.

§ To whom correspondence should be addressed. Tel.: 91-471-2347975; Fax: 91-471-2348096; E-mail: dkarunagaran@hotmail.com.

[1] The abbreviations used are: EGF, epidermal growth factor; ECL, enhanced chemiluminescence; EGFR, epidermal growth factor receptor; EMSA, electrophoretic mobility shift assay; HA, hemagglutinin; IκB, inhibitor κB; IKK, IκB kinase; MTT, 3-(4,5-dimethylthiazol-2-yl)-2,5-diphenyltetrazolium bromide; NF-κB, nuclear factor κB; PARP, poly(ADP-ribose) polymerase; PBS, phosphate-buffered saline; PI, propidium iodide; PS, phosphatidylserine; TNF, tumor necrosis factor; IAP, inhibitor of apoptosis protein; PI-3K, phosphatidylinositol 3-kinase; AFC, 7-amino-4-trifluoromethyl coumarin; DTT, dithiothreitol; CHAPS, 3-[(3-cholamidopropyl)dimethylammonio]-1-propanesulfonic acid.

pathways that give them survival advantage and thereby resist therapy-induced apoptosis (20).

NF-κB is a family of transcription factors activated by a diverse number of stimuli including EGF, cytokines, such as TNF-α and interleukin-1, UV irradiation, and lipopolysaccharides (22). EGF has been reported to activate NF-κB in smooth muscle cells, fibroblasts, and in several EGFR-overexpressing cell lines (23–25). Binding of IκB to NF-κB masks nuclear localization signals and prevents its translocation to the nucleus (26). Stimulation of cells with a diverse array of stimuli results in phosphorylation of IκB-α on serines 32 and 36 at its NH_2-terminal. This leads to the ubiquitination and degradation of IκB-α, allowing NF-κB to translocate to the nucleus and activate transcription (22, 26). Inhibition of NF-κB activity potentiates cell killing of human breast cancer and fibrosarcoma cell lines by TNF-α, ionizing radiation, and daunorubicin (27–29). NF-κB inhibition sensitized tumors in mice to chemotherapeutic compound CPT-11-mediated cell killing (30). NF-κB directly causes increased expression of proteins that contribute to the survival of tumor cells such as inhibitors of apoptotic proteins (IAPs) (31, 32). Results from our laboratory have shown earlier that ectopic expression of the RelA subunit of NF-κB into murine fibrosarcoma cells protects them from curcumin-induced apoptosis (33).

To understand whether NF-κB plays any role in EGF-induced apoptosis, we used A431 cells that overexpress EGFR and stably transfected them with a mutant IκB (known to inactivate NF-κB) or RelA (known to activate NF-κB). Using several parameters to assess apoptosis such as viability, externalization of phosphatidylserine (PS) on the cell surface, DNA fragmentation, and activation of caspases we report that A431 cells are more sensitive to EGF-induced apoptosis under NF-κB-inactivated conditions whereas its activation confers resistance.

EXPERIMENTAL PROCEDURES

Reagents, Chemicals, and Antibodies—EGF (isolated from male mouse submaxillary glands), Dulbecco's minimum essential medium, and fetal bovine serum were procured from Invitrogen. Curcumin, sodium salicylate, MTT (3-(4,5-dimethylthiazol-2-yl)-2,5-diphenyltetrazolium bromide), nitro blue tetrazolium/5-bromo-4-chloro-3-indolyl phosphate substrate mixture, and a mouse monoclonal antibody to β-actin (A-5441) were purchased from Sigma. Fluorimetric substrates for caspase 3 (Ac-DEVD-AFC number 264157) and caspase 9 (Ac-LEHD-AFC number 218765) were obtained from Calbiochem. Rabbit polyclonal antibodies to p50 (sc-7178), RelA (sc-109), hemagglutinin (HA) (sc-7392), IκB-α (sc-271), and c-IAP1 (sc-7943) were procured from Santa Cruz Biotechnology (Santa Cruz, CA). Mouse monoclonal antibody to caspase 8 (1C12), rabbit polyclonal PARP antibody (number 9542), and phospho-Akt pathway sampler kit (number 9916 containing antibodies to Akt and phospho-Akt, and LY294002) were purchased from Cell Signaling Technology (Beverly, MA), and the mouse monoclonal EGFR antibody (clone 111) raised against the extracellular domain of EGFR was a gift from Dr. Yosef Yarden, Weizmann Institute of Science, Israel.

Cell Lines and Culture—Human epidermoid carcinoma cell line A431 was obtained from the National Center for Cell Science, Pune, India. The cells were grown as monolayer cultures in Dulbecco's modified Eagle's medium supplemented with 10% fetal bovine serum and antibiotics (Invitrogen). Cells were incubated at 37 °C in a humidified atmosphere of 5% CO_2 and 95% air.

Transient and Stable Transfections—A431-IκB-α cells were transiently transfected with *relA* in pMT2T vector (33, 34) using the calcium-phosphate transfection kit (Invitrogen) according to the manufacturer's protocol. Stable transfections in A431 cells with *relA* in pMT2T vector (co-transfected with pcDNA3) or the empty vector pcDNA3 or pcDNA3-IκB-α were carried out by the LipofectAMINE method (35). For the preparation of liposome solution, 20 μmol/ml of stock (prepared by mixing 6.6 μmol of dimethyl dioctadecyl ammonium bromide and 13.4 μmol of dioleyl-L-phosphatidylethanolamine in 1 ml of ethanol) was diluted into 1 nmol/μl in water. For transfection, the cells were seeded to attain 70% confluence in 35-mm Petri dishes. For each dish, 2 μg of DNA and 24 μl of liposome solution were mixed in 500 μl of Dulbecco's minimum essential medium free from serum and antibiotics, vortexed, and incubated at room temperature for 30 min. The liposome solution (1 ml) was layered over the cells previously rinsed with serum-free medium and left for 4 h in a CO_2 incubator and then the medium was replenished with 20% fetal bovine serum and reverted back to 10% fetal bovine serum after 24 h. After 72 h, cells were grown in selection medium (400 μg/ml G418) and clones formed were picked up and maintained separately with 100 μg/ml G418.

Western Blotting—Cells were lysed in whole cell lysis buffer (20 mM Tris, pH 7.4, 250 mM NaCl, 2 mM EDTA, 0.1% Triton X 100, 1 mM DTT, 5 μg/ml aprotinin, 5 μg/ml leupeptin, 0.5 mM phenylmethylsulfonyl fluoride, and 4 mM sodium orthovanadate). Equal amounts of total protein for each sample were separated by SDS-PAGE and electrotransferred onto nitrocellulose filters, probed with the primary antibodies and appropriate peroxidase-conjugated secondary antibodies, and visualized with the enhanced chemiluminescence (ECL) method as per the manufacturer's protocol (Amersham Biosciences). For some experiments, alkaline phosphatase-conjugated secondary antibodies from Sigma were used and the bands were detected using nitro blue tetrazolium/5-bromo-4-chloro-3-indolyl phosphate as substrate.

Electrophoretic Mobility Shift Assay (EMSA)—Cells were washed with cold PBS and suspended in 160 μl of lysis buffer (10 mM HEPES (pH 7.9), 10 mM KCl, 0.1 mM EDTA, 0.1 mM EGTA, 1 mM DTT, 0.5 mM phenylmethylsulfonyl fluoride, 2 μg/ml leupeptin, 2 μg/ml aprotinin, and 0.5 mg/ml benzamidine). The cells were allowed to swell for 30 min, after which 4.5 μl of 10% Nonidet P-40 was added, vortexed, and centrifuged, and the pellet was suspended in 25 μl of nuclear extraction buffer (20 mM HEPES, pH 7.9, 0.4 M NaCl, 1 mM EDTA, 1 mM EGTA, 1 mM DTT, 1 mM phenylmethylsulfonyl fluoride, 2 μg/ml leupeptin, 2 μg/ml aprotinin, and 0.5 mg/ml benzamidine). The nuclear extract (8 μg of protein) collected after 30 min by centrifugation was used to perform EMSA by incubating it with 16 fmol of ^{32}P-end labeled 45-mer double stranded NF-κB oligonucleotide from the human immunodeficiency virus-1 long terminal repeat (5′-TTGTTACAAGGGACTTTCCGCTGGGGACTTTCCAGGGAGGCGTGG-3′) in the presence of 1 μg/ml poly(dI-dC) in a binding buffer (25 mM HEPES (pH 7.9), 50 mM NaCl, 0.5 mM EDTA, 0.5 mM DTT, 1% Nonidet P-40, and 5% glycerol) for 30 min at 37 °C and the DNA-protein complex was resolved using a 6.6% native polyacrylamide gel. The gels were dried and the radioactive bands were visualized by phosphorimaging (Bio-Rad Personal FX).

MTT Assay—For MTT assay, 25 μl of MTT solution (5 mg/ml in PBS) was added to cells (untreated and treated) cultured in 96-well plates. Cells were incubated for 2 h and 0.1 ml of the extraction buffer (20% sodium dodecyl sulfate in 50% dimethyl formamide) was added after removal of MTT with a PBS wash. After an overnight incubation at 37 °C, the optical densities at 570 nm were measured using a plate reader (Bio-Rad), with the extraction buffer as a blank. The relative cell viability in percentage was calculated as (A_{570} of treated samples/A_{570} of untreated samples) × 100.

[^{3}H]Thymidine Incorporation—Cells grown in 96-well plates were treated with or without the indicated concentrations of EGF and at the end of 18 h, [^{3}H]thymidine was added to each well (0.5 μCi/well) and the incubation was continued for a total period of 24 h. The culture medium was then removed, washed twice with PBS, and the proteins were precipitated with 5% trichloroacetic acid. The supernatant was removed and after washing with ethanol, the cells were solubilized with 0.2 N NaOH, and the radioactivity was counted using a liquid scintillation counter.

Annexin-PI Staining—The cells (10^6 cells/well) were seeded in 48-well plates and treated with or without EGF for 16 h. Then the cells were washed with PBS and treated with 1× assay buffer, annexin-fluorescein isothiocyanate and propidium iodide (PI) as per the protocol described in the annexin V apoptosis detection kit (sc-4252 AK) from Santa Cruz Biotechnology. After 10–20 min, the wells were washed with PBS and greenish apoptotic cells were viewed using a Nikon fluorescent microscope and photographed.

Comet Assay—Comet assay was carried out essentially as described (36). Briefly, the cells (treated with or without EGF) were pelleted and resuspended in 0.5% low melting point agarose at 37 °C and layered on a frosted microscope slide previously coated with a thin layer of 0.5% normal melting agarose and kept for 5 min at 4 °C. After solidification, the slides were immersed in lysing solution (2.5 M NaCl, 100 mM EDTA, 10 mM Tris, pH 10.5, 1% Triton X-100, and 10% Me_2SO) for 1 h at 4 °C. The slides were then electrophoresed for 20 to 30 min at 25 V. The slides after electrophoresis were washed with 0.4 M Tris (pH 7.5) and stained with ethidium bromide (1 μg/ml) and observed under a Nikon fluorescent microscope.

Assays of Caspase 3 and Caspase 9—The enzymatic activities of caspase 3 or caspase 9 were assayed spectrofluorimetrically (37). Briefly, the whole cell lysate was incubated with 50 μM fluorimetric substrates of caspase 3 (Ac-DEVD-AFC) or caspase 9 (Ac-LEHD-AFC) in a total volume of 500 μl of reaction buffer (50 mM HEPES-KOH, pH 7.0, 10% glycerol, 0.1% CHAPS, 2 mM EDTA, 2 mM DTT) at 37 °C for 1 h. The released AFC was quantitated using a spectrofluorimeter (PerkinElmer LS-50 B) with the excitation and emission wavelengths of 380 and 460 nm, respectively. Values of relative fluorescence units released per mg of protein were calculated.

RESULTS

EGF Induces NF-κB DNA Binding Activity in A431-Neo but Not A431-IκB-α Cells—The human epidermoid carcinoma cell line, A431, overexpresses EGFRs (about 2×10^6 EGFRs/cell) and has been extensively used as a model system to study the effects of EGF on cell proliferation (7, 38–40). To study the role of NF-κB in EGF-induced apoptosis, we used A431 cells and stably transfected them with either the empty vector (pcDNA3) or pcDNA3-IκB-α, a double mutant construct in which both the serines (32 and 36) at the amino-terminal of IκB-α are mutated to alanine. Because the double mutant form of IκB-α lacks the crucial serine residues that need to be phosphorylated by NF-κB activators, it is popularly employed to strongly inhibit NF-κB (28). As the construct, pcDNA3-IκB-α, contains the hemagglutinin tag (HA tag), Western blotting of HA protein was used to ascertain the presence of the mutant IκB protein. As expected, all six clones of A431-IκB-α cells (selected by G418) showed the presence of HA protein whereas the A431-Neo cells transfected with control vector (pcDNA3) did not show its expression (Fig. 1*A*). Further experiments with IκB-transfected cells were done using only clone 6 of A431-IκB-α cells (showing very high HA expression) unless stated otherwise. Western blotting with a polyclonal IκB-α antibody confirmed that clone 6 had indeed a higher level of IκB-α expression compared with that in the parental as well as A431-Neo cells (Fig. 1*B*). For the Western blots, β-actin was used as a control and the results confirm equal loading of the samples (Fig. 1, *A* and *B*). To see whether transfection procedures affected the level of EGFR, Western blotting was carried out in parental, A431-Neo, and A431-IκB-α cells and the results confirmed that EGFR levels remained unaffected in these cells (Fig. 1*C*). Because the very purpose of stable transfection was to inactivate NF-κB, it was logical to check whether EGF could stimulate the NF-κB DNA binding activity in A431-Neo and A431-IκB-α cells (clone 6) by EMSA. Whereas 50 ng/ml EGF enhanced the NF-κB DNA binding activity in A431-Neo cells, even 100 ng/ml EGF could not induce it in A431-IκB-α cells and in the absence of EGF there were no active DNA-binding complexes of NF-κB in both the cells (Fig. 1*D*). To confirm whether the active complex contains the classical NF-κB partners, p50 and RelA, the nuclear extracts prepared from A431-Neo cells stimulated with 50 ng/ml EGF were incubated with antibodies to RelA or p50 and then EMSA was carried out. As shown in Fig. 1*E*, both antibodies shifted the active NF-κB complex (supershift) whereas incubation with excess of an unlabeled oligonucleotide containing the NF-κB binding site removed the active complex. Fig. 1*E* also shows that transient transfection of A431-IκB-α cells with *relA* restored the NF-κB active complex, and *relA* transfection was used by us earlier to constitutively activate NF-κB in L-929 cells (33). These results confirm that the A431-IκB-α cells express the mutant form of IκB-α that inactivated NF-κB and hence, EGF could not stimulate NF-κB DNA binding activity in these cells. The results also indicate that EGF can induce the NF-κB DNA binding activity in A431-Neo cells and the active NF-κB complex contains the heterodimers, p50 and RelA. In addition, the results show that RelA, being one of the heterodimeric partners of active NF-κB, favors the formation of active NF-κB DNA binding complexes and has the potential to reverse the NF-κB-inactivating effect of IκB.

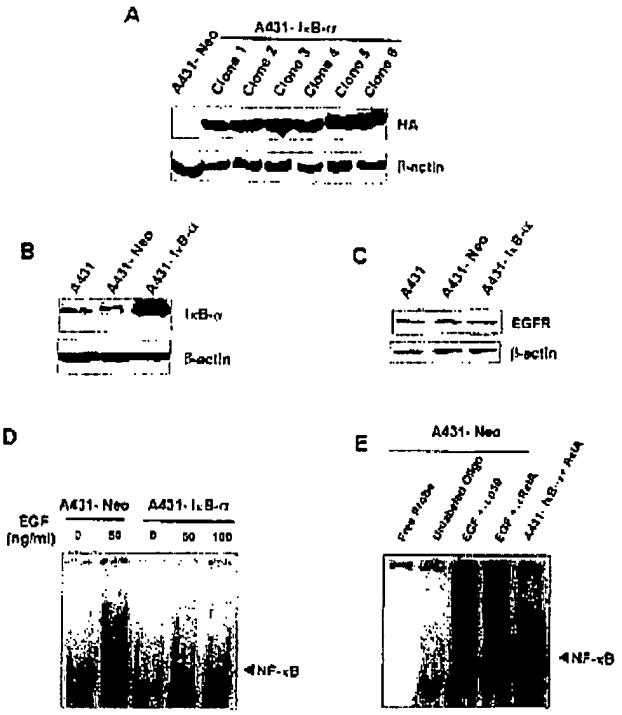

FIG. 1. **Western blotting for HA and IκB-α, and assessment of NF-κB DNA binding activity in transfected and untransfected A431 cells.** *A*, A431 cells were transfected with pcDNA3 vector or the pcDNA3-IκB-α construct using LipofectAMINE and the G418-resistant clones were selected as described under "Experimental Procedures." Cell lysates (40 μg of protein) from the vector-transfected A431-Neo cells and the different clones of A431-IκB-α cells were subjected to SDS-PAGE and immunoblotted with HA antibody or β-actin (control) by ECL as described under "Experimental Procedures." *B*, cell lysates from A431, A431-Neo, and the clone-6 of A431-IκB-α cells were subjected to Western blotting with an antibody to IκB-α or β-actin (control) as described above. *C*, similarly, the cell lysate from A431, A431-Neo, or A431-IκB-α cells was subjected to Western blotting with an antibody to EGFR or β-actin (control). *D*, A431-Neo cells or A431-IκB-α cells grown in 35-mm Petri dishes (1×10^6 cells/dish) were treated with EGF at the indicated concentrations at 37 °C for 1 h. Nuclear extracts were prepared and EMSA was done as described under "Experimental Procedures." *E*, A431-Neo cells were treated with 50 ng/ml EGF as described above and EMSA was done as before. The nuclear extracts from EGF-stimulated cells were also incubated with either RelA or p50 antibody or with 10 times excess of unlabeled oligo. One of the lanes had the nuclear extract prepared from A431-IκB-α cells transiently transfected with *relA* as described under "Experimental Procedures" and another lane contained the labeled oligo (free probe) without the addition of nuclear extract. All the experiments above were done at least two times with similar results. The *arrowheads* shown in *panels D* and *E* indicate the positions of the active DNA-binding complexes of NF-κB.

A431-IκB-α Cells Are More Sensitive to EGF-induced Cytotoxicity and DNA Fragmentation Than A431-Neo Cells—To study the effects of EGF on cell growth under conditions of NF-κB inactivation, A431-Neo and A431-IκB-α cells were exposed to various concentrations of EGF and the cell viability in percentage over untreated control was determined after 72 h by MTT assay. The MTT assay is a convenient screening assay for the measurement of cell death while it does not discriminate between apoptosis and necrosis. EGF treatment at 0.01 and 0.1 ng/ml had a stimulatory effect on A431-Neo cells with cell viabilities of 130 and 110%, respectively, if the viability of untreated control was taken as 100% at the end of 72 h (Fig. 2*A*). In contrast, EGF inhibited the A431-IκB-α cells with only 81 and 67% of cells being alive for the concentrations of 0.01

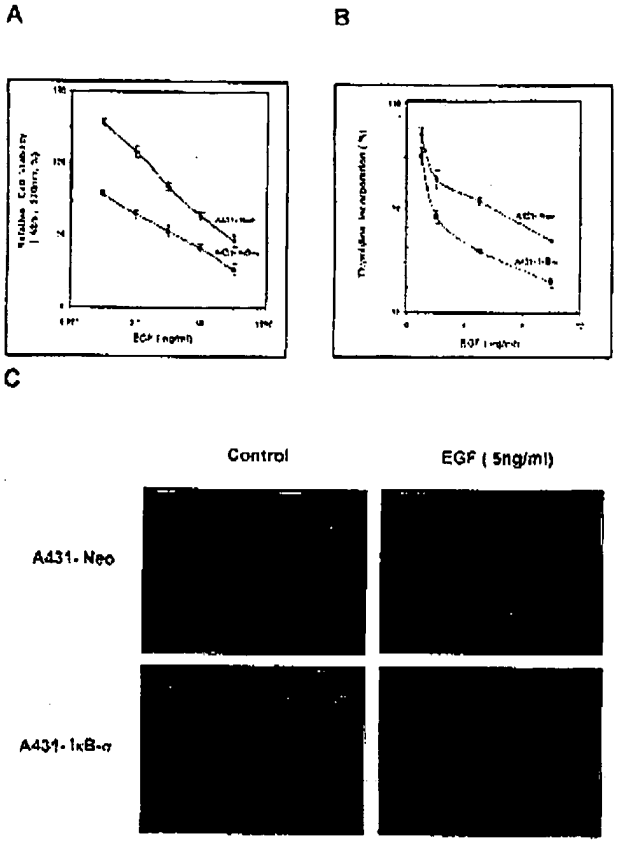

FIG. 2. **Inhibition of growth and DNA synthesis and induction of DNA fragmentation in A431-Neo and A431-IκB-α cells by EGF.** *A*, cells grown in 96-well plates (5×10^3 cells/well) were incubated for 72 h either with medium or different concentrations of EGF as indicated and cell viability was assessed by the MTT assay as described under "Experimental Procedures." *B*, cells grown in 96-well plates (5×10^3 cells/well) were incubated with different concentrations of EGF for 24 h, and then the thymidine incorporation as a measure of DNA synthesis was determined as described under "Experimental Procedures" and the results are expressed as percentage over the control (untreated cells). The above experiments were repeated two times with similar results and all determinations were made in triplicate and the *error bars* show the standard deviations. *C*, cells (1×10^6) were seeded in 35-mm Petri dishes and incubated with 5 ng/ml EGF for 24 h. After incubation, cells were trypsinized, pelleted, and the comet assay was done as described under "Experimental Procedures." The experiment was repeated once more with similar results.

and 0.1 ng/ml, respectively, compared with the control (Fig. 2*A*). As can be seen in Fig. 2*A*, EGF at a concentration of 1 ng/ml and above was inhibitory to both A431-Neo and A431-IκB-α cells. Thus, even at concentrations that were stimulatory to A431-Neo cells, EGF inhibited the growth of A431-IκB-α cells (Fig. 2*A*) suggesting that A431-IκB-α cells are much more sensitive to EGF-induced cytotoxicity and these results were also confirmed in 2 other clones of A431-IκB-α (data not shown). We also examined the effect of EGF on DNA synthesis by the method of thymidine incorporation after exposing the cells to different concentrations of EGF (1–10 ng/ml) found to be inhibitory to both A431-Neo and A431-IκB-α cells by the MTT assay. EGF inhibited DNA synthesis in both A431-Neo and A431-IκB-α cells in a dose-dependent manner and again the A431-IκB-α cells were more sensitive to EGF-induced inhibition of DNA synthesis (Fig. 2*B*). DNA fragmentation is another hallmark of apoptosis and to detect this, we have used the single cell gel electrophoresis (Comet assay), a sensitive technique that allows detection of DNA strand breaks. DNA strand breaks create fragments that when embedded in agarose gels migrate in an electric field. Cells with damaged DNA when stained with ethidium bromide appear like a comet and the length of the comet tail represents the extent of DNA damage. Fig. 2*C* clearly indicates that well formed comets are more in number in A431-IκB-α than A431-Neo cells when induced with 5 ng/ml EGF while the untreated cells did not exhibit the comet morphology in both the cells. These results suggest that A431-IκB-α cells with inactivated NF-κB are more susceptible to cell death induced by EGF compared with A431-Neo cells.

Relatively More A431-IκB-α Cells Undergo EGF-induced Externalization of Phosphatidylserine—To assess whether the cell death induced by EGF involves typical changes encountered during apoptosis, we first looked for changes in PS on the cell membrane. Under defined salt and calcium concentrations, annexin V is predisposed to bind PS that is externalized to the cell surface in the very early stages of apoptosis (41, 42). Hence, apoptotic cells were detected using annexin V labeled with fluorescein isothiocyanate and photographed with a camera-attached fluorescent microscope. Addition of PI helps to distinguish the early apoptotic cells from late apoptotic or necrotic cells because PI cannot enter the cells in the early stages of apoptosis when the membrane integrity is intact (41, 42). In A431-IκB-α cells 37 and 65% were annexin positive after treatment with 5 and 10 ng/ml EGF, respectively, whereas only 9 and 23% of the A431-Neo cells showed annexin positivity (greenish yellow) for the same corresponding EGF concentrations (Fig. 3). Untreated A431-Neo and A431-IκB-α cells either did not show annexin positivity or had a very minimum number of positively stained cells (Fig. 3). However, a small percentage of A431-Neo and A431-IκB-α cells also showed typical PI staining (yellowish red) suggesting the appearance of late apoptotic or necrotic cells with 10 ng/ml EGF treatment (Fig. 3). These results indicate that in comparison with A431-Neo cells, a relatively large number of A481-IκB-α cells exhibit externalization of PS, a typical feature of apoptosis upon treatment with EGF.

A431-IκB-α Cells Are More Sensitive to EGF-induced Apoptosis That Involves Cleavage of PARP, Activation of Caspases 3 and 8, but Not Caspase 9—In many systems caspase 8 and caspase 9 act as initiator caspases and caspase 3, the effector, signals for the final execution of the cells. Pro-caspase 8 was cleaved into its active fragments (p43/41 and p18) by 10 ng/ml EGF in A431-Neo cells while even 5 ng/ml EGF could easily do it in A431-IκB-α cells as visualized by Western blotting and the untreated cells did not show any of the cleavage products (Fig. 4*A*). Caspase 3 activity was determined spectrofluorimetrically using a substrate, Ac-DEVD-AFC, an acetylated synthetic tetrapeptide corresponding to the upstream amino acid sequence of the caspase 3 cleavage site in PARP, and the fluorphor AFC (7-amino-4-trifluromethyl coumarin). Whereas EGF-induced caspase 3 activity was 2.1-fold more than the untreated control in A431-IκB-α cells, it was only 1.2-fold more than the control in A431-Neo cells (Fig. 4*B*). Caspase 9 activity was also determined fluorimetrically and EGF treatment could not induce caspase 9 activity in A431-IκB-α and A431-Neo cells, whereas curcumin used as a positive control activated caspase 9 in both cells (Fig. 4*C*). We also examined the cleavage of a well characterized caspase 3 substrate, PARP, from its 116-kDa intact form into the 89-kDa fragment by Western blotting. When A431-IκB-α cells were treated with 5 or 10 ng/ml EGF, the 116-kDa form of PARP decreased and the 89-kDa form increased indicating that the full-length PARP was converted to an apoptotic fragment while the untreated cells showed only the uncleaved fragment (Fig. 4*D*). In A431-Neo cells, both control and 5 ng/ml EGF-treated cells did not exhibit the cleaved

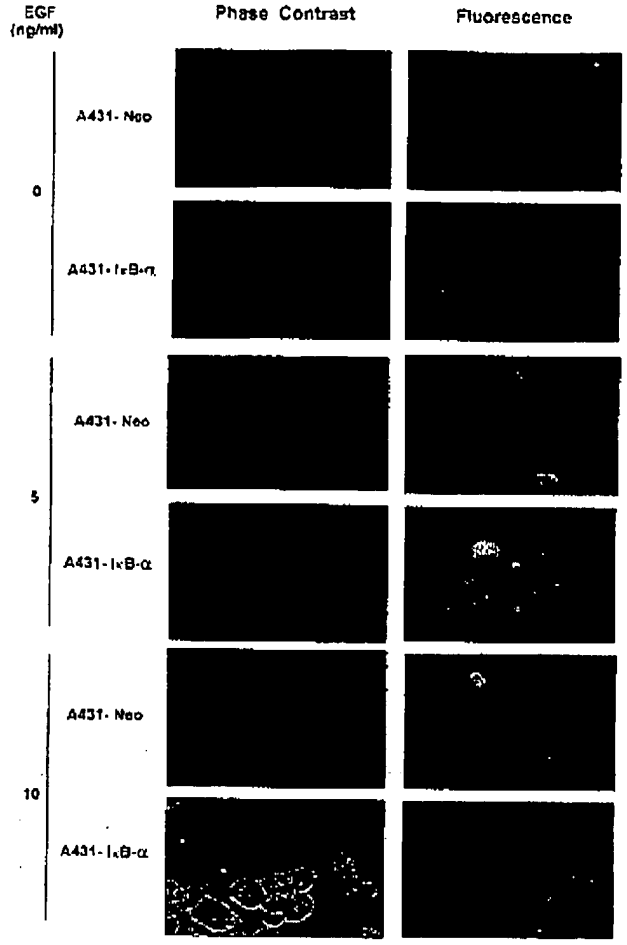

FIG. 3. **EGF-induced changes in annexin-PI staining.** Cells were incubated with or without the indicated concentrations of EGF for 16 h, and stained for annexin-PI positivity (not shown in color) as described under "Experimental Procedures." The same results were confirmed in another independent experiment.

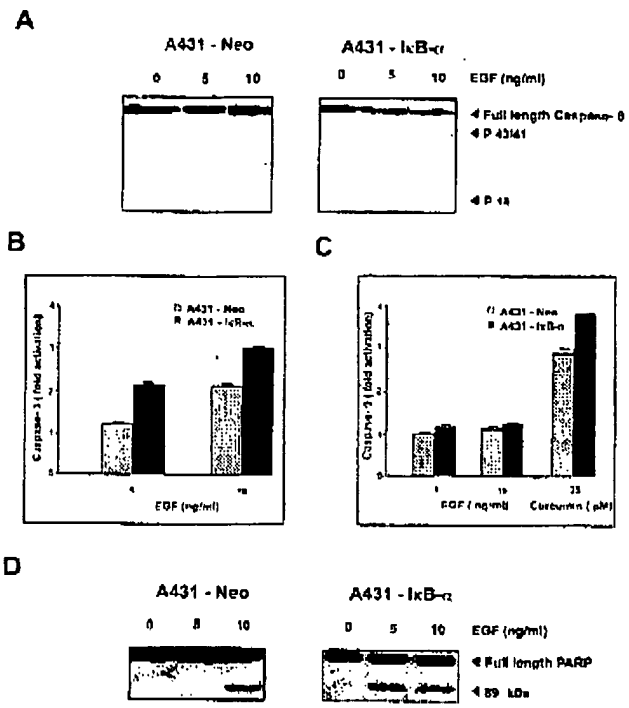

FIG. 4. **Effects of EGF on the activities of caspases 8, 3, and 9, and PARP cleavage.** *A*, cells (1×10^6) were seeded in 35-mm Petri dishes and treated with or without EGF for 24 h. To detect the active caspase 8 fragments, the cell lysates were resolved on 12% SDS-PAGE, electrotransferred onto a nitrocellulose membrane, probed with caspase 8 antibody (1:3000), and detected by the alkaline phosphatase method using nitro blue tetrazolium/5-bromo-4-chloro-3-indolyl phosphate as substrate. *B*, cells (1×10^6) were seeded in 35-mm Petri dishes and treated with or without EGF for 24 h. Fifty micrograms of total protein was incubated with 50 μM caspase 3 fluorimetric substrate in a total volume of 500 μl of the reaction buffer and the fluophor released was quantitated spectrofluorimetrically as described under "Experimental Procedures." *C*, cells (1×10^6) were seeded in 35-mm Petri dishes and treated with EGF or curcumin along with untreated control for 24 h. Fifty micrograms of total protein was incubated with 50 μM caspase 9 fluorimetric substrate and the activity was quantitated spectrofluorimetrically as above. The reproducibility of these experiments was ascertained by repeating them at least two times. *D*, cells (1×10^6) were seeded in 35-mm Petri dishes and treated with or without EGF for 24 h. To detect the cleavage of PARP, whole cell lysate (40 μg) was resolved on a 7.5% polyacrylamide gel, electrotransferred, probed with PARP antibody (1:3000), and detected by ECL reagent as described earlier. Similar results were obtained when the experiment was repeated.

product and even 10 ng/ml EGF could induce only a slight PARP cleavage (Fig. 4*D*). The above results confirm that the A431-IκB-α cells are more sensitive to EGF-induced apoptosis than A431-Neo cells by showing increased PARP cleavage and higher activation of caspases 3 and 8 but not 9 suggesting the operation of a caspase 8-mediated extrinsic pathway.

Chemical Inhibitors of NF-κB Enhance the Susceptibility of A431-Neo Cells whereas Activation of NFκB by RelA Reverses the Susceptibility of A431-IκB-α Cells to EGF-induced Cytotoxicity—To know whether chemical inhibitors of NF-κB would also enhance EGF-induced apoptosis, the A431-Neo cells were treated with known inhibitors of NF-κB such as sodium salicylate (50 μM) or curcumin (10 μM) for 2 h prior to EGF treatment. When compared with untreated cells, 77% A431-Neo cells were alive in wells treated with 5 ng/ml EGF for 24 h (Fig. 5*A*). If the viability of A431-Neo cells treated with 10 μM curcumin alone for 24 h was taken as 100, treatment with EGF after pretreatment with curcumin reduced it to 71% (Fig. 5*A*). Similarly, if 50 μM sodium salicylate pretreatment is compared with or without EGF the viability of A431-Neo cells was only 61% (Fig. 5*A*). If IκB-mediated inhibition of NF-κB can positively regulate EGF-induced apoptosis, then this effect is expected to be reversed by NF-κB. As expected, the transient transfection of *relA* into A431-IκB-α cells partly reversed the cytotoxic effect of EGF as measured by an MTT assay (Fig. 5*B*). The higher expression of RelA in the transfected cells was confirmed by Western blotting and to ensure that proteins were loaded equally, β-actin controls were used (Fig. 5*B*, *inset*). These results suggest that similar to IκB, NF-κB inhibitors also have the potential to enhance EGF-induced cell death and NF-κB has a protective role suggested by the higher level of resistance of A431-IκB-α cells transiently transfected with *relA* to EGF-induced cytotoxicity.

RelA Protects A431 Cells from EGF-induced Apoptosis—Because RelA reversed the effect of IκB-α it became relevant to know whether, on its own, it can protect the parental A431 cells from EGF-induced apoptosis. To this end, we transfected the A431 cells stably with *relA* and confirmed the higher expression of RelA in A431-RelA cells (clone 1 and clone 2) compared with A431 and A431-Neo cells by Western blotting (Fig. 6*A*). When A431-Neo and A431-RelA cells (clone 1) were compared for their relative viability in the presence of varying concentrations of EGF by the MTT assay, A431-RelA cells were notably more resistant to EGF (Fig. 6*B*) and these results were also confirmed using clone 2 (data not shown)

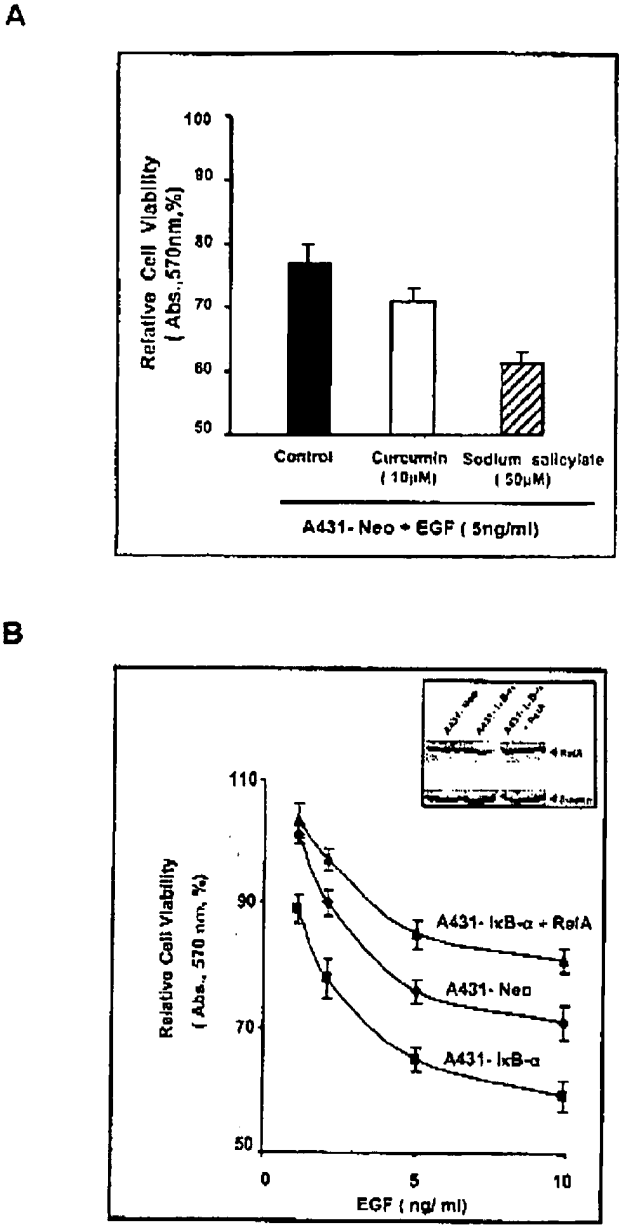

FIG. 5. **Influence of chemical inhibitors of NF-κB and *relA* transfection on EGF-mediated growth inhibition of A431-Neo and A431-IκB-α cells, respectively.** *A*, A431-Neo cells (5×10^3/well) were seeded into 96-well plates and pretreated with 10 μM curcumin, 50 μM sodium salicylate, or medium alone for 2 h. The cells were then treated with or without 5 ng/ml EGF for 24 h and the MTT assay was done as described earlier. Triplicate samples were used and the *error bars* indicate the standard deviations and the results were confirmed in another independent experiment. *B*, A431-IκB-α cells were transiently transfected with *relA* as described under Fig. 1*E*. A431-Neo and A431-IκB-α and the transfected cells (A431-IκB-α+RelA) were seeded into 96-well plates (5×10^3/well) and treated with the indicated concentrations of EGF for 24 h and the MTT assay was done as described earlier. Triplicate samples were used and the *error bars* indicate the standard deviations. The results were confirmed in another independent experiment. The *inset* shows Western blots of RelA and β-actin control in A431-Neo, A431-IκBα, and the transfected cells (*A431-IκB-α+RelA*).

but further experiments were done using clone 1 of A431-RelA cells. Similarly EGF-mediated inhibition of thymidine incorporation was relatively more in A431-Neo than A431-RelA cells confirming the protective role of RelA against

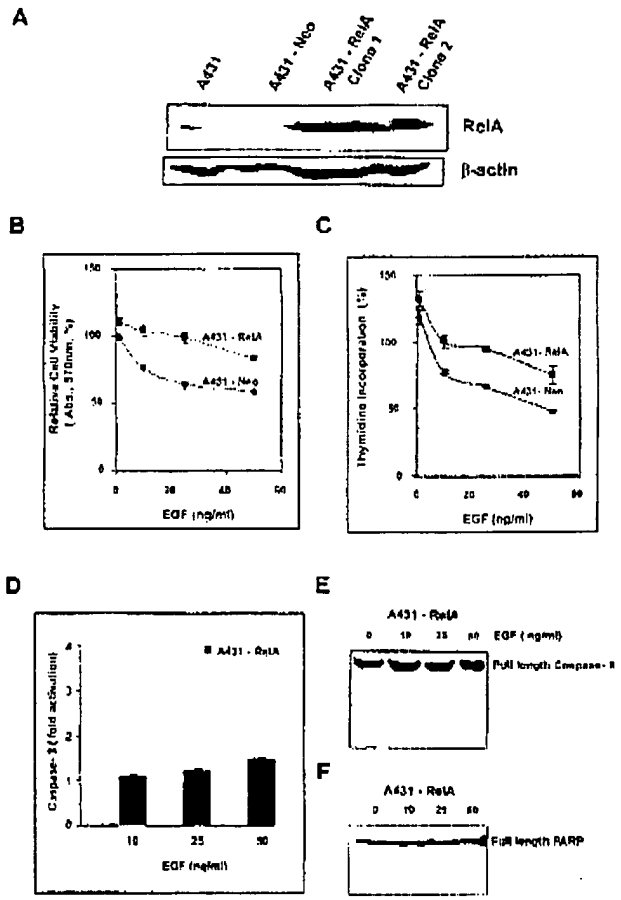

FIG. 6. **Western blotting for RelA and EGF-mediated changes in growth, DNA synthesis, caspase activation, and PARP cleavage.** *A*, A431 cells were cotransfected with pcDNA3 vector and *relA* PMT2T construct using LipofectAMINE and the G418-resistant clones were selected as described under "Experimental Procedures." Cell lysates (60 μg of protein) from the vector-transfected A431-Neo cells and different clones of A431-RelA cells were subjected to SDS-PAGE and immunoblotted with RelA or β-actin (control) antibody by the alkaline phosphatase method as described under "Experimental Procedures." *B*, cells were treated with or without the indicated concentrations of EGF for 24 h and the MTT assay was done under the conditions described for Fig. 2. Triplicate samples were used and the *error bars* indicate the standard deviations. The results were confirmed in another independent experiment. *C*, cells were treated with or without the indicated concentrations of EGF for 24 h and thymidine incorporation assays were done under the conditions described for Fig. 2. Triplicate samples were used and the *error bars* indicate the standard deviations. The results were confirmed in another independent experiment. *D*, A431-RelA cells were treated with or without the indicated concentrations of EGF for 24 h and caspase 8 activity was determined as described for Fig. 4. *E*, cells were treated with or without the indicated concentrations of EGF for 24 h and caspase 3 activity was determined as described for Fig. 4. *F*, cells were treated with or without the indicated concentrations of EGF for 24 h and PARP cleavage was determined as described for Fig. 4.

EGF-mediated cell death (Fig. 6*C*). In addition, varying EGF concentrations even up to 50 ng/ml could not induce caspase 8 (Fig. 6*D*) or caspase 3 (Fig. 6*E*) activities or PARP cleavage (Fig. 6*F*) in A431-RelA cells.

EGF Up-regulates the Expression of c-IAP1 in A431-Neo Cells and Its Basal Expression Is Higher in A431-RelA Cells—As IAP is considered to be one of the survival proteins induced by NF-κB, it was of interest to study the effect of EGF and RelA on IAP expression. Expression of c-IAP1 was observed by Western blotting in A431-Neo cells stimulated with 10 ng/ml EGF for

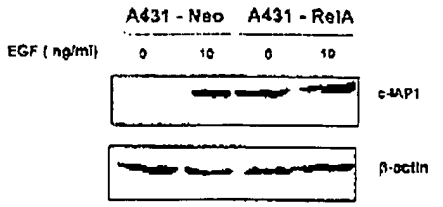

FIG. 7. **Effects of EGF on IAP expression in A431-Neo and A431-RelA cells.** Cells (1×10^6) were seeded in 35-mm Petri dishes and treated with or without EGF (10 ng/ml) for 24 h. To detect IAP expression, the cell lysates were resolved on 10% SDS-PAGE, electrotransferred onto a nitrocellulose membrane, probed with c-IAP1 or β-actin (control) antibody, and detected by ECL as described under "Experimental Procedures." The results were confirmed in another independent experiment.

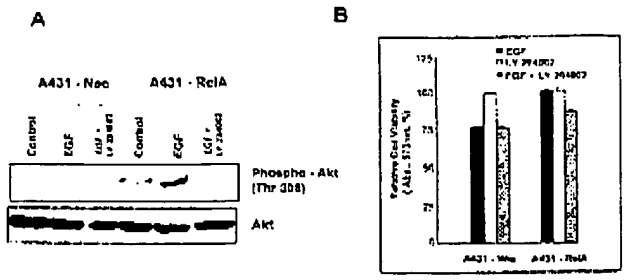

FIG. 8. **Effect of LY294002 on Akt phosphorylation and survival of A431-Neo and A431-RelA cells.** *A*, cells (1×10^6) grown in 35-mm Petri dishes were pretreated with LY294002 (20 μM) for 2 h and then treated with EGF (10 ng/ml) for 1 h and the cells that received no treatment served as control. Cell lysates were probed with phospho-Akt (Thr^{308}) antibody (1:1000) by Western blotting by ECL as described above and the same blot was reprobed with an antibody (1:1000) to Akt. *B*, cells were pretreated with LY294002 (20 μM) for 2 h and then with EGF (10 ng/ml) and incubated for 24 h and the MTT assay was done as described under "Experimental Procedures." The above experiments were repeated with similar results.

24 h and A431-RelA cells had a higher basal level of c-IAP1 that was not further increased by EGF (Fig. 7). These results suggest that RelA up-regulates the expression of c-IAP1 and EGF up-regulates it presumably through the activation of NF-κB.

LY294002, an Inhibitor of PI-3K, Sensitizes A431-RelA Cells but Not A431-Neo Cells to EGF-induced Cytotoxicity—We also examined for the involvement of the PI-3K pathway known to activate Akt that enables survival of cells by the activation of NF-κB. In Western blot analysis using a phosphorylation-specific antibody to Akt, there was no detectable phosphorylation of Akt in A431-Neo cells in the presence or absence of EGF, whereas even the unstimulated A431-RelA cells exhibited phosphorylation of Akt that was further enhanced by EGF (Fig. 8*A*). An inhibitor of PI-3K, LY294002, inhibited EGF-induced phosphorylation of Akt in A431-RelA cells whereas the expression of total Akt protein remained unaffected by EGF treatment in A431-Neo and A431-RelA cells (Fig. 8*A*). EGF decreased the growth of A431-Neo cells whereas LY294002 alone did not affect their viability and addition of LY294002 together with EGF had no further effect on the growth of A431-Neo cells (Fig. 8*B*). In contrast, EGF did not inhibit the growth of A431-RelA cells but addition of LY294002 together with EGF decreased their viability (Fig. 8*B*). These results suggest that RelA could activate Akt and EGF could activate it further in A431-RelA cells and even though inhibition of PI-3K by LY294002 could not enhance EGF-induced cell death of A431-Neo cells, it did sensitize A431-RelA cells to EGF.

Taken together, the results of the present study suggest that EGF induces typical features of apoptosis in A431 cells such as the externalization of PS, DNA fragmentation, and activation of caspases (3 and 8 but not 9). These hallmarks of apoptosis induced by EGF were potentiated by NF-κB inhibition by IκB-α and RelA relieved the effects of IκB-α on EGF-mediated cytotoxicity. The chemical inhibitors of NF-κB also enhanced the growth inhibitory effects of EGF and these results together support an anti-apoptotic role for NF-κB. This is further supported by the protective role of RelA observed in A431-RelA cells against EGF-mediated apoptosis. A model for the regulation of EGF-induced apoptosis incorporating the known mechanisms and contributions from the present study is shown in Fig. 9.

DISCUSSION

Several studies have reported that high (nanomolar) concentrations of EGF caused growth inhibition and apoptosis of A431 cells while low (picomolar) concentrations of EGF promoted cell proliferation (7, 38, 40, 43, 44). Many hypotheses have been proposed to explain the mechanisms by which EGF inhibits cell proliferation, arrests cell cycle, and induces apoptosis. Increase in EGFR tyrosine kinase activity because of excessive ligand binding is said to result in growth inhibition and programmed cell death and the level of EGFR tyrosine kinase activity regulates the expression of p21 (17, 38). It has also been suggested that EGF arrests cell cycle progression through Stat1 activation and elevation of p21 that eventually inhibits cdk2 activity (43–45). However, Stat1 activation by EGF was not detected in a number of cancer cell lines with abnormal EGFR expression (18, 45). The dual effect of EGF on the proliferation of A431 cells is also attributed to differential activation of p42 MAP kinase at low and high concentrations of EGF (11, 46). Another hypothesis proposes that EGF-induced apoptosis is the result of a decline in cell adhesion (47), and detachment of cells because of anoikis is said to be responsible for the paradoxical anti-proliferative effects of EGF (16, 48). Our results do not support the view that EGF-induced apoptosis results from the loss of cell-substratum attachment and many other workers also have not observed EGF-induced anoikis of A431 or other EGFR-overexpressing cells (8, 11, 49, 50). The results of the present study suggest that EGF-induced apoptosis operates through the extrinsic pathway mediated through caspase 8 and not the mitochondrial pathway involving caspase 9. In contrast, EGF-induced apoptosis of MDA-MB-468 breast cancer cells that also overexpress EGFR has been reported to involve the mitochondrial pathway of caspase activation (16). Similar to our results with EGF, heregulin also enhanced the degradation of PARP but unlike EGF, heregulin activated caspase 9 without any significant activation of caspase 3 (51). Cripto-1 mediates the induction of caspase 3-like protease and down-regulates the expression of Bcl-XL (15). UCVA-1 cells, derived from human pancreas adenocarcinoma, have a high number of EGFRs but their growth is not inhibited by EGF, highlighting the complexity of the mechanisms involved in EGF-induced apoptosis (52). Thus, the regulation of EGF-induced apoptosis appears to be a complex process involving the interplay of several regulatory molecules.

In addition to the mechanisms by which the growth factors exhibit both stimulatory and inhibitory activity in a single cell, the final outcome is presumably influenced by a host of regulatory molecules other than the growth factors and their receptors (53, 54). It is thus clearly important to recognize that a potent mitogen like EGF also sends out apoptotic signals and identify conditions in which these signals are regulated. In the present study, we have hypothesized such a condition and demonstrated for the first time that NF-κB inhibition makes A431 cells more susceptible to EGF-induced apoptosis whereas RelA protects them against it. EGF stimulation in A431 cells

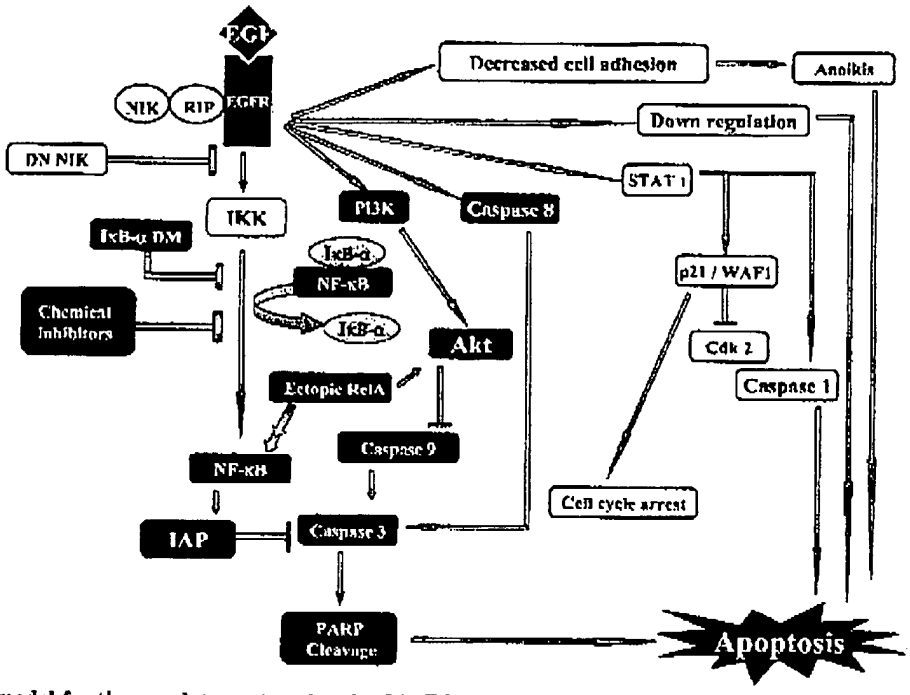

FIG. 9. **Proposed model for the regulatory steps involved in EGF-induced apoptosis.** EGF-induced activation of its receptor is said to decrease cell adhesion leading to anoikis and apoptosis. Down-regulation of EGFR is also postulated to induce apoptosis, and activation of Stat-1 has been reported to induce p21/WAF-1 or caspase 1 that may result in cell cycle arrest or apoptosis, respectively. In addition to these mechanisms that induce apoptosis, anti-apoptotic regulation also exists that includes activation of Akt or NF-κB. EGF-induced activation of EGFR is known to recruit NIK and RIP to activate IKK resulting in the activation of NF-κB that blocks apoptosis through IAPs. Ectopic expression of RelA activates Akt and also induces c-IAP1 and blocks apoptosis while the use of chemical inhibitors or IκB-α DM accelerates EGF-induced apoptosis.

enhances the degradation of IκB-α, but not IκB-β and proteasome inhibitors such as ALLN or MG132, block EGF-mediated NF-κB activation, indicating that EGF-induced NF-κB activation requires proteasome-dependent IκB degradation (25). Similar to the findings of the present study, EGF-induced DNA binding complex of NF-κB in A431 was found to be composed of p50/RelA heterodimers, but not c-Rel (25). In agreement with our results, a recent report has shown that both the protein kinase C inhibitor Go6976 (also inhibits NF-κB) and expression of dominant-negative NF-κB inhibitor kinase mutants caused apoptosis of EGF-stimulated mammary tumor cells whereas EGF alone did not induce apoptosis in these cells (55). In contrast to our results, it has been reported that infection of adenoviral vectors expressing IκB reversed the EGF-induced cell growth inhibition of A431 cells (56). Use of high concentrations of EGF (100 ng/ml), transient expression of IκB, and drawing conclusions only based upon cell counting (proportion of live and dead cells not shown) may account for this discrepancy. Furthermore, caspase activities or other apoptotic parameters were not measured in that study. Consistent with our results, blocking Ras (known to activate NF-κB) with dominant negative Ras mutants in EGFR overexpressing cells also potentiated EGF-induced apoptosis (8). EGF did not affect the levels of several proteins that regulate apoptotic pathways, including Bcl-2, Bcl-XL, Bax, and p53 in human ovarian cancer cells (57). Many workers have shown that Akt, a serine/threonine protein kinase and a downstream target of PI-3K, suppresses apoptosis by activating NF-κB (58–60) and accordingly blocking the EGF-induced phosphorylation of Akt sensitizes the otherwise resistant A431-RelA cells to EGF-mediated growth inhibition. However, the spontaneous phosphorylation of Akt in A431-RelA cells places Akt as a downstream target of NF-κB and it is interesting to note that blocking this basal phosphorylation with LY294002 does not affect their viability. Consistent with our results, overexpression of RelA stimulated the phosphorylation of Akt in NIH 3T3 cells and in addition increased the expression of Akt mRNA and protein (61). Akt does not seem to be involved in EGF-induced NF-κB activation of MDA-MB-468 cells that also overexpress EGFR (62). The mechanism by which ectopic expression of RelA results in the phosphorylation of Akt is not known and further work is in progress to understand the contribution of Akt in EGF-induced apoptosis. Similar to the EGF-induced expression of c-IAP1 in the present study, TNF also stimulated its expression (63). Cbl-b inhibits EGF-induced apoptosis by enhancing ubiquitination and degradation of activated EGFR (64).

Our results support an anti-apoptotic role for NF-κB and suggest the possibility that EGF-induced apoptosis *in vivo* may be regulated by NF-κB. However, whether EGF-induced apoptosis occurs *in vivo* in tumor cells is not known. If EGF-induced apoptosis does not occur *in vivo*, it is still logical to think that anti-apoptotic factors such as NF-κB guard the tumor cells against responding to such apoptotic stimuli. Consistent with this speculation, NF-κB is constitutively activated in a number of tumors (22, 26). In addition, tumor cells are also known to express many anti-apoptotic proteins such as Bcl-2 and their role in EGF-induced apoptosis remains to be determined. Our identification of a role for NF-κB in EGF-induced apoptosis opens up new lines of investigation pertaining to EGF receptor-mediated signaling. Further studies on the role of NF-κB and its regulators in EGF-induced apoptosis are likely to be relevant for a better understanding of the biology of human tumors as well as EGF-induced normal growth.

Acknowledgments—We thank Drs. Yosef Yarden for providing EGFR antibody, Sudhir Krishna for HA-tagged pcDNA3-IκB-α construct, Paul Chiao for *relA* in pMT2T vector, and Bova Smitha and Goodwin Jinesh for technical help.

REFERENCES

1. Grant, S., Qiao, L., and Dent, P. (2002) *Front. Biosci.* **7**, 376–389
2. Yarden, Y. (2001) *Eur. J. Cancer* **37**, Suppl. 4, S3–S8
3. Schlessinger, J. (2000) *Cell* **103**, 211–225
4. Gullick, W. J. (1991) *Br. Med. Bull.* **47**, 87–98
5. Harris, A. L. (1994) *Breast Cancer Res. Treat.* **29**, 1–2
6. Bartlett, J. M., Langdon, S. P., Simpson, B. J., Stewart, M., Katsaros, D., Sismondi, P., Love, S., Scott, W. N., Williams, A. R., Lessells, A. M., Macleod, K. G., Smyth, J. F., and Miller, W. R. (1996) *Br. J. Cancer* **73**, 301–306
7. Barnes, D. W. (1982) *J. Cell Biol.* **93**, 1–4
8. Hoganson, T., Chatterjee, S., Vartanian, T., Ratan, R. R., Ernewein, K. M., and Habib, A. A. (2001) *FEBS Lett.* **491**, 9–15
9. Daly, J. M., Olayioye, M. A., Wong, A. M., Neve, R., Lane, H. A., Maurer, F. G., and Hynes, N. E. (1999) *Oncogene* **18**, 3440–3451
10. Xi, Q. S., Pan, W., Zhang, Q., Qian, X. G., Li, Z. P., and Gao, R. B. (2000) *Sheng Wu Hua Xue Yu Sheng Wu Wu Li Xue Bao (Shanghai)* **32**, 601–604
11. Silva, M., Martin, P. M., Chajry, N., and Berthois, Y. (1998) *Endocrinology* **139**, 2382–2391
12. Iwamoto, R., Handa, K., and Mekada, E. (1999) *J. Biol. Chem.* **274**, 25906–25912
13. Conner, E. A., Teramoto, T., Wirth, P. J., Kiss, A., Garfield, S., and Thorgeirsson, S. S. (1999) *Carcinogenesis* **20**, 583–590
14. Kim, H. R., Upadhyay, S., Li, G., Palmer, K. C., and Deuel, T. F. (1995) *Proc. Natl. Acad. Sci. U. S. A.* **92**, 9500–9504
15. De Santis, M. L., Martinez-Lacaci, I., Bianco, C., Seno, M., Wallace-Jones, B., Kim, N., Ebert, A., Wechselberger, C., and Salomon, D. S. (2000) *Cell Death Differ.* **7**, 189–198
16. Kottke, T. J., Blajeski, A. L., Martins, L. M., Mesner, P. W., Jr., Davidson, N. E., Earnshaw, W. C., Armstrong, D. K., and Kaufmann, S. H. (1999) *J. Biol. Chem.* **274**, 15927–15936
17. Roddy, K. B., Keshamouni, V. G., and Chen, Y. Q. (1999) *Int. J. Oncol.* **15**, 801–806
18. Chin, Y. E., Kitagawa, M., Kuida, K., Flavell, R. A., and Fu, X. Y. (1997) *Mol. Cell. Biol.* **17**, 5328–5337
19. Strasser, A., O'Connor, L., and Dixit, V. M. (2000) *Annu. Rev. Biochem.* **69**, 217–245
20. Igney, F. H., and Krammer, P. H. (2002) *Nat. Rev. Cancer* **2**, 277–288
21. Sun, X. M., MacFarlane, M., Zhuang, J., Wolf, B. B., Green, D. R., and Cohen, G. M. (1999) *J. Biol. Chem.* **274**, 5053–5060
22. Karin, M., Cao, Y., Greten, F. R., and Li, Z. W. (2002) *Nat. Rev. Cancer* **2**, 301–310
23. Ohata, H., Biro, S., Arima, N., Kaieda, H., Kihara, T., Eto, H., Miyata, M., and Tanaka, H. (1996) *Biochem. Biophys. Res. Commun.* **224**, 27–33
24. Biswas, D. K., Cruz, A. P., Gansberger, E., and Pardee, A. B. (2000) *Proc. Natl. Acad. Sci. U. S. A.* **97**, 8542–8547
25. Sun, L., and Carpenter, G. (1998) *Oncogene* **16**, 2095–2102
26. Rayet, B., and Gelinas, C. (1999) *Oncogene* **18**, 6938–6947
27. Beg, A. A., and Baltimore, D. (1996) *Science* **274**, 782–784
28. Van Antwerp, D. J., Martin, S. J., Kafri, T., Green, D. R., and Verma, I. M. (1996) *Science* **274**, 787–789
29. Wang, C. Y., Mayo, M. W., and Baldwin, A. S., Jr. (1996) *Science* **274**, 784–787
30. Cusack, J. C., Jr., Liu, R., Houston, M., Abendroth, K., Elliott, P. J., Adams, J., and Baldwin, A. S., Jr. (2001) *Cancer Res.* **61**, 3535–3540
31. Chu, Z. L., McKinsey, T. A., Liu, L., Gentry, J. J., Malim, M. H., and Ballard, D. W. (1997) *Proc. Natl. Acad. Sci. U. S. A.* **94**, 10057–10062
32. You, M., Ku, P. T., Hrdlickova, R., and Bose, H. R., Jr. (1997) *Mol. Cell. Biol.* **17**, 7328–7341
33. Anto, R. J., Mukhopadhyay, T. T., and Karunagaran, D. (2000) *J. Biol. Chem.* **275**, 15601–15604
34. Bours, V., Bonif, P. R., Brown, K., Villalobos, J., Park, S., Ryseck, R. P., Bravo, R., Kelly, K., and Siebenlist, U. (1992) *Mol. Cell. Biol.* **12**, 685–695
35. Taylor, N. A., and Docherty, K. (1996) in *Gene Transcription: RNA Analysis* (Docherty, K., ed) pp. 96–97, John Wiley & Sons Ltd., London
36. Singh, N. P., McCoy, M. T., Tice, R. R., and Schneider, E. L. (1988) *Exp. Cell Res.* **175**, 184–191
37. Ito, A., Uehara, T., Tokumitsu, A., Okuma, Y., and Nomura, Y. (1999) *Biochim. Biophys. Acta* **1452**, 263–274
38. Gulli, L. F., Palmer, K. C., Chen, Y. Q., and Reddy, K. B. (1996) *Cell Growth Differ.* **7**, 173–178
39. Filmus, J., Pollak, M. N., Cailleau, R., and Buick, R. N. (1985) *Biochem. Biophys. Res. Commun.* **128**, 898–905
40. Gill, G. N., and Lazar, C. S. (1981) *Nature* **293**, 305–307
41. Homburg, C. H., de Haas, M., von dem Borne, A. E., Verhoeven, A. J., Reutelingsperger, C. P., and Roos, D. (1995) *Blood* **85**, 532–540
42. Vermes, I., Haanen, C., Steffens-Nakken, H., and Reutelingsperger, C. (1995) *J. Immunol. Methods* **184**, 39–51
43. Fan, Z., Lu, Y., Wu, X., DeBlasio, A., Koff, A., and Mendelsohn, J. (1995) *J. Cell Biol.* **131**, 235–242
44. Jakus, J., and Yeudall, W. A. (1996) *Oncogene* **12**, 2369–2376
45. Chin, Y. E., Kitagawa, M., Su, W. C., You, Z. H., Iwamoto, Y., and Fu, X. Y. (1996) *Science* **272**, 719–722
46. Chajry, N., Martin, P. M., Pages, G., Cochet, C., Affet, K., and Berthois, Y. (1994) *Biochem. Biophys. Res. Commun.* **203**, 984–990
47. Cao, L., Yao, Y., Lee, V., Kiani, C., Spaner, D., Lin, Z., Zhang, Y., Adams, M. E., and Yang, B. B. (2000) *J. Cell. Biochem.* **77**, 569–583
48. Generash, E., Schneider, D. W., Sauer, G., Khazaie, K., Schuppan, D., and Lichtner, R. B. (1998) *Int. J. Cancer* **75**, 205–209
49. Lee, K., Tanaka, M., Hatanaka, M., and Kuze, F. (1987) *Exp. Cell Res.* **173**, 156–162
50. Dong, X. F., Berthois, Y., and Martin, P. M. (1991) *Anticancer Res.* **11**, 737–743
51. Le, X. F., Marcelli, M., McWatters, A., Nan, B., Mills, G. B., O'Brian, C. A., and Bast, R. C., Jr. (2001) *Oncogene* **20**, 8258–8269
52. Hiral, M., Kobayashi, M., and Shimizu, N. (1990) *Cell. Signalling* **2**, 245–252
53. Sporn, M. B., and Roberts, A. B. (1988) *Nature* **332**, 217–219
54. Lohto, V. P. (2001) *FEBS Lett.* **491**, 1–3
55. Biswas, D. K., Martin, K. J., McAlister, C., Cruz, A. P., Graner, E., Dai, S. C., and Pardee, A. B. (2003) *Cancer Res.* **63**, 290–295
56. Ohtsubo, M., Takayanagi, A., Gomou, S., and Shimizu, N. (2000) *J. Cell. Physiol.* **184**, 131–137
57. Ceuni, B., Achi, S., Nehme, A., and Christen, R. D. (2001) *Cancer Chemother. Pharmacol.* **47**, 397–403
58. Romashkova, J. A., and Makarov, S. S. (1999) *Nature* **401**, 86–90
59. Pianetti, S., Arsura, M., Romieu-Mourez, R., Coffey, R. J., and Sonenshein, G. E. (2001) *Oncogene* **20**, 1287–1299
60. Ozes, O. N., Mayo, L. D., Gustin, J. A., Pfeffer, S. R., Pfeffer, L. M., and Donner, D. B. (1999) *Nature* **401**, 82–85
61. Meng, F., Liu, L., Chin, P. C., and D'Mello, S. R. (2002) *J. Biol. Chem.* **277**, 29674–29680
62. Habib, A. A., Chatterjee, S., Park, S. K., Ratan, R. R., Lefebvre, S., and Vartanian, T. (2001) *J. Biol. Chem.* **276**, 8865–8874
63. Wang, C. Y., Mayo, M. W., Korneluk, R. G., Goeddel, D. V., and Baldwin, A. S., Jr. (1998) *Science* **281**, 1680–1683
64. Ettenberg, S. A., Rubinstein, Y. R., Banerjee, P., Nau, M. M., Keane, M. M., and Lipkowitz, S. (1999) *Mol. Cell. Biol. Res. Commun.* **2**, 111–118

Original Article

Phosphorylated AKT Expression Is Associated With *PIK3CA* Mutation, Low Stage, and Favorable Outcome in 717 Colorectal Cancers

Yoshifumi Baba, MD[1]; Katsuhiko Nosho, MD[1]; Kaori Shima, PhD[1]; Marika Hayashi, BS[1]; Jeffrey A. Meyerhardt, MD[1]; Andrew T. Chan, MD[2]; Edward Giovannucci, MD[3,4]; Charles S. Fuchs, MD[1,4]; and Shuji Ogino, MD[1,5]

BACKGROUND: AKT (AKT1, AKT2, and AKT3) was a downstream effector of phosphatidylinositide-3-kinase (PI3K) and played crucial roles in protein synthesis, cellular metabolism, survival, and proliferation. The PI3K/AKT pathway was commonly activated in human cancers and was recognized as a potential target for anticancer therapy. Nonetheless, clinical, molecular, or prognostic features of AKT-activated colon cancer remained uncertain. **METHODS:** Using a database of 717 colon and rectal cancers in the Nurses' Health Study and the Health Professionals Follow-up Study, Ser473 phosphorylated AKT (p-AKT) expression was detected in 448 (62%) tumors by immunohistochemistry. Cox proportional hazards model was used to compute mortality hazards ratio (HR), adjusting for clinical and tumoral features, including *PIK3CA*, *KRAS*, *BRAF*, microsatellite instability (MSI), CpG island methylator phenotype (CIMP), LINE-1 methylation, TP53 (p53), and FASN (fatty acid synthase). **RESULTS:** Tumor p-AKT expression was associated with *PIK3CA* mutation (odds ratio [OR], 1.77; 95% confidence interval [CI], 1.12-2.80; $P = .015$). p-AKT expression was significantly associated with longer colorectal cancer-specific survival in Kaplan-Meier analysis (log-rank $P = .0005$), univariate Cox regression (HR, 0.62; 95% CI, 0.47-0.82; $P = .0006$) and multivariate analysis (adjusted HR, 0.75; 95% CI, 0.56-0.99; $P = .048$) adjusting for clinical and molecular variables including *PIK3CA*, MSI, CIMP and LINE-1 hypomethylation. p-AKT expression was inversely associated with high stage (III-IV) (adjusted OR, 0.63; 95% CI, 0.45-0.88, $P = .0071$). **CONCLUSIONS:** p-AKT expression in colorectal cancer is associated with low stage and good prognosis. p-AKT may serve as a tissue biomarker to identify patients with superior prognosis and a possible therapeutic target (analogous to estrogen receptor ESR1 in breast cancer). *Cancer* 2011;117:1399-408. © *2010 American Cancer Society.*

KEYWORDS: pAKT, PI3K, clinical outcome, personalized medicine, colorectal carcinoma.

AKT, a serine/threonine protein kinase, is a major downstream effector of phosphatidylinositide-3-kinase (PI3K).[1-3] AKT has 3 isoforms, including AKT1, AKT2 and AKT3, and plays crucial roles in regulating a wide range of cellular processes, including protein synthesis, cell survival, proliferation, and metabolism.[1-3] In human cancer, the PI3K/AKT pathway is aberrantly activated by growth factor stimulation and subsequent activation of receptor tyrosine kinases, as well as by a mutation, deletion, or amplification of a key pathway component (eg, *PIK3CA*, *PTEN*, or *AKT1*).[1-3] Therefore, this pathway has been recognized as an attractive target for anticancer therapy.[4-6] Thus, better understanding of the role of AKT activation in human cancer is increasingly important. However, prognostic significance of AKT activation in human cancers remains inconclusive; phosphorylated AKT (p-AKT) expression (ie, AKT activation) has been associated with poor prognosis in some types of cancers,[7-9] but with favorable prognosis in other types of cancers.[10-14] Studies have shown that p-AKT expression in colorectal cancer is not associated with patient survival[15-18]; however, they are all limited by lack of *PIK3CA* mutation data and/or low statistical power ($N < 160$ in all[16-18] but 1 study[15]). Given accumulating evidence on vital roles of AKT in cellular metabolism, we hypothesized that AKT-activated cancers and AKT-inactive cancers might behave differently.

Corresponding author: Shuji Ogino, MD, PhD, MS(Epidemiology), Center for Molecular Oncologic Pathology, Dana-Farber Cancer Institute, 44 Binney St., Room JF-215C, Boston, MA 02115; Fax: (617) 277 9015; shuji_ogino@dfci.harvard.edu

[1]Department of Medical Oncology, Dana-Farber Cancer Institute and Harvard Medical School, Boston, Massachusetts; [2]Gastrointestinal Unit, Massachusetts General Hospital, Boston, Massachusetts; [3]Department of Epidemiology and Nutrition, Harvard School of Public Health, Boston, Massachusetts; [4]Channing Laboratory, Department of Medicine, Brigham and Women's Hospital and Harvard Medical School, Boston, Massachusetts; [5]Department of Pathology, Brigham and Women's Hospital and Harvard Medical School, Boston, Massachusetts

Y.B., K.N., and K.S. contributed equally.

DOI: 10.1002/cncr.25630, **Received:** July 1, 2010; **Revised:** July 28, 2010; **Accepted:** August 3, 2010, **Published online** November 8, 2010 in Wiley Online Library (wileyonlinelibrary.com)

To test this hypothesis, we used a database of 717 stage I-IV colorectal cancers in two prospective cohort studies and examined the prognostic role of p-AKT expression. Microsatellite instability (MSI), the CpG island methylator phenotype (CIMP) status, and LINE-1 hypomethylation (ie, global DNA hypomethylation) reflect global genomic and epigenomic aberrations in tumor cells and determine clinical, pathologic, molecular, and prognostic characteristics of colorectal cancer.[19] It is widely accepted that activating mutations in *PIK3CA*, *KRAS*, and *BRAF* play vital roles in colorectal carcinogenesis. *TP53* is a crucial tumor suppressor gene in the pathogenesis of colorectal cancer. FASN (fatty acid synthase) is physiologically regulated by energy balance and may interact with the PI3K/AKT pathway.[20] Prognostic effect of FASN expression in colon cancer differs according to body mass index.[21] Since we concurrently assessed these important molecular variables, we could evaluate the independent effect of p-AKT on patient survival after controlling for these molecular events. Our findings of the relationship between p-AKT expression and good outcome suggest that p-AKT may serve as a tissue biomarker to identify patients with better prognosis and a possible therapeutic target (analogous to estrogen receptor ESR1 in breast cancer).

MATERIALS AND METHODS

Study Group

We used the database of two prospective cohort studies: the Nurses' Health Study (N = 121,701 women followed since 1976),[22] and the Health Professionals Follow-up Study (N = 51,529 men followed since 1986).[22] We collected paraffin-embedded tissue blocks from hospitals where patients underwent colorectal cancer resections. Tissue sections from all colorectal cancers were reviewed by a pathologist (S.O.). Based on availability of adequate tissue specimens and follow-up data, a total of 717 colorectal cancers (diagnosed up to 2004) were included. Patients were observed until death or June 30, 2009, whichever came first. Tissue collection and analyses were approved by the Harvard School of Public Health and Brigham and Women-s Hospital Institutional Review Boards.

Sequencing of KRAS, BRAF and PIK3CA and MSI Analysis

DNA was extracted from tumor. Polymerase chain reaction (PCR) and pyrosequencing targeted for *KRAS*,[23] *BRAF*,[24] and *PIK3CA* were performed.[25] MSI-high was defined as ≥30% unstable microsatellite markers, and MSI-low/microsatellite stable (MSS) as 0-29% unstable markers.[26]

Methylation Analyses for CpG Islands and LINE-1

Bisulfite DNA treatment and real-time PCR (MethyLight) were validated.[27] We quantified DNA methylation in 8 CIMP-specific promoters (*CACNA1G*, *CDKN2A* (p16), *CRABP1*, *IGF2*, *MLH1*, *NEUROG1*, *RUNX3*, and *SOCS1*).[28-30] CIMP-high was defined as the presence of ≥6/8 methylated promoters, CIMP-low as 1/8-5/8 methylated promoters, and CIMP-0 as the absence (0/8) of methylated promoters.[30,31] To accurately quantify LINE-1 methylation, we used pyrosequencing.[32,33]

Immunohistochemistry

Tissue microarrays (TMAs) were constructed.[22] Two 0.6-mm tissue cores each from tumor and normal colonic mucosa were placed in each TMA block. Methods of immunohistochemistry were previously described for TP53 (p53) and FASN.[21,26] AKT1 is partially activated through phosphorylation of Thr308 and reaches its maximum activity after phosphorylation of Ser473 in tandem with that of Thr308. Similar phosphorylation sites are present in AKT2 and AKT3. To date, the most successful biomarker for evaluating the status of AKT activation is Ser473 phosphorylated form of AKT.[34] In our current study, we used the pan-AKT antibody (rabbit monoclonal anti-phospho-Akt [Ser473] [736E11], Cell Signaling Technology, Boston, Mass), which detects AKT1 only when phosphorylated at Ser 473, and AKT2 and AKT3 only when phosphorylated at equivalent sites, according to previous studies.[8-10,15,17]

For phosphorylated-AKT (p-AKT) staining, deparaffinized tissue sections in Antigen Retrieval Citra Solution (Biogenex Laboratories, San Ramon, CA) were treated with microwave in a pressure cooker (25 min). Tissue sections were incubated with 5% normal goat serum (Vector Laboratories, Burlingame, CA) in phosphate-buffered saline (30 min). Primary antibody against p-AKT (1:100 dilution) was applied, and the slides were maintained at 4°C for overnight, followed by rabbit secondary antibody (Vector Laboratories) (60 min), an avidin-biotin complex conjugate (Vector Laboratories) (60 min), diaminobenzidine (5 min), and methyl-green counterstain. Appropriate positive and negative controls were included in each run of immunohistochemistry. In each

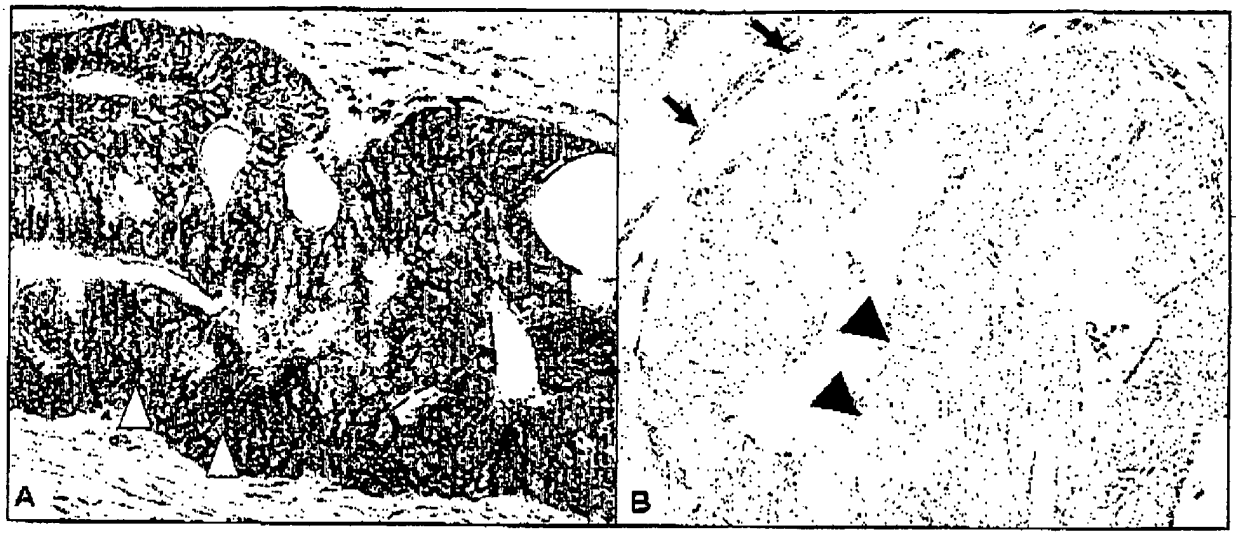

Figure 1. Immunohistochemistry for p-AKT expression in colorectal cancer (A) Positive for p-AKT cytoplasmic expression in colon cancer cells (white arrowheads). (B) Negative for p-AKT expression in colon cancer cells (black arrowheads). Stromal cells serve as an internal positive control for p-AKT expression (arrows).

case, we recorded cytoplasmic p-AKT expression as no expression, weak expression, moderate expression, or strong expression compared to normal colonic epithelial cells (Fig. 1). Considering that AKT is downstream of the PI3K pathway,[1-3] we used *PIK3CA* mutation frequency data to determine a cutoff for p-AKT positivity.

We randomly selected 364 tumors as a training set, leaving the remaining 353 as a validation set. Using the training set, the frequency of *PIK3CA* mutation was as follows: 13% (16/119) in tumors with no expression, 20% (19/94) in tumors with weak expression, and 19% (21/110) in tumors with moderate/strong expression. Thus, p-AKT positivity was defined as the presence of weak to strong expression. In the remaining validation set, p-AKT positivity was associated with *PIK3CA* mutation (odds ratio [OR], 2.00; 95% confidence interval [CI], 1.02-3.94; $P = .040$), confirming the validity of the cutoff for p-AKT positivity, although it might not be the best cutoff. There was no perfect correlation between *PIK3CA* mutation and p-AKT, in part because there were other mechanisms of AKT activation (ie, *PTEN* loss and/or methylation, *PIK3CA* amplification, and *PIK3R1* mutation). p-AKT expression might serve as a surrogate of AKT activation by any of these causes.

Each immunohistochemical maker was visually interpreted by one of the investigators (p-AKT by Y.B.; TP53 and FASN by S.O.) unaware of other data. For agreement studies, a random selection of 108-246 cases was examined for each marker by a second pathologist (p-AKT by K.S., TP53 and FASN by K.N.) unaware of other data. The concordance between the two pathologists (all $P < .0001$) was 0.81 ($\kappa = 0.59$, N = 132) for p-AKT, 0.87 ($\kappa = 0.75$, N = 108) for TP53, and 0.93 ($\kappa = 0.57$, N = 246) for FASN, indicating good agreement.

Statistical Analysis

We used the SAS program (Version 9.1, SAS Institute, Cary, NC). All P values were two-sided. When we performed multiple hypothesis testing, a P value for significance was adjusted by Bonferroni correction to $p = 0.0031$. For categorical data, the chi-square test was performed. To assess independent relationship between p-AKT and disease stage (an outcome variable), a multivariate logistic regression analysis was performed, initially including sex, age at diagnosis (continuous), body mass index (BMI, <30 vs. ≥30 kg/m^2), family history of colorectal cancer in any first-degree relative (present vs. absent), tumor location (rectum vs. colon), tumor grade (high vs. low), CIMP (high vs. low/0), MSI (high vs. low/MSS), LINE-1 methylation (continuous), *BRAF*, *KRAS*, *PIK3CA*, TP53, FASN, and p-AKT expression. A backward stepwise elimination with a threshold of $P = .20$ was used to select variables in the final model. For cases with missing information in any of categorical variables (BMI,

0.1%; tumor grade, 0.4%; TP53, 0.6%; FASN, 0.8%; CIMP, 1.7%; MSI, 2.0%; *BRAF*, 1.5%; *KRAS*, 1.1%; and *PIK3CA*, 10%), we included those cases in a majority category of that missing variable in the initial model. After the selection was done, we assigned separate missing indicator variables to those cases with missing information in any of the categorical covariates in the final model.

For survival analysis, Kaplan-Meier method and log-rank test were used. For analyses of colorectal cancer-specific mortality, deaths as a result of causes other than colorectal cancer were censored. To assess independent effect of p-AKT on mortality, tumor stage (I, IIA, IIB, IIIA, IIIB, IIIC, IV, unknown) was used as a stratifying variable in Cox models using the strata option in the SAS proc phreg command to avoid residual confounding and overfitting. We constructed a multivariate proportional hazards model to compute a hazards ratio (HR) according to p-AKT status, initially containing sex, age, BMI, family history of colorectal cancer, year of diagnosis, tumor location, tumor grade, TP53, FASN, CIMP, MSI, *BRAF*, *KRAS*, *PIK3CA*, and LINE-1 methylation. A backward stepwise elimination with a threshold of $P = .20$ was used to select variables in the final model. The proportionality of hazard assumption was satisfied by evaluating time-dependent variables, which were the cross-product of the p-AKT variable and survival time ($P > .31$). An interaction was assessed by including the cross-product of p-AKT variable and another variable of interest (without data-missing cases) in a multivariate Cox model, and the Wald test was performed.

RESULTS

p-AKT Expression in Colorectal Cancer

Among 717 colorectal cancers, we observed phosphorylated AKT (p-AKT) expression in 448 tumors (62%) by immunohistochemistry (Fig. 1). Although variability of p-AKT staining between tissue cores in a given case was not substantial, we obtained 4 tissue cores from each case to overcome within-tumor heterogeneity. Table 1 shows p-AKT status in relation to clinical, pathologic and molecular features. Notably, there was no difference in frequencies of p-AKT positivity between cases prior to 1995 and those in 1995 or after ($P = .85$), suggesting that the age of tissue block might not substantially influence our results. Consistent with a possible causal link between *PIK3CA* mutation and p-AKT expression, p-AKT expression was significantly associated with *PIK3CA* mutation (OR, 1.77; 95% CI, 1.12-2.80; $p = 0.015$). In addition, p-AKT expression was associated positively with FASN expression ($p = 0.0025$), and inversely with stage III-IV disease ($p = 0.0022$) and high tumor grade ($P < .0001$).

In multivariate logistic regression analysis assessing the independent relationship between p-AKT expression and disease stage, p-AKT expression was inversely associated with high disease stage (stage III-IV) (adjusted OR, 0.63; 95% CI, 0.45-0.88; $P = .0071$) (Table 2).

p-AKT Expression and Patient Survival

During follow-up of 717 patients with survival data (median follow-up time 11.6 years for censored cases), there were 341 deaths, including 210 deaths due to colorectal cancer. In Kaplan-Meier analysis, p-AKT expression was associated with longer colorectal cancer-specific survival (log-rank $P = .0005$) and overall survival (log-rank $P = .014$) (Fig. 2).

Compared to p-AKT-negative cases, p-AKT-positive cases experienced a significantly lower colorectal cancer-specific mortality in univariate analysis (HR, 0.62; 95% CI, 0.47-0.82; $P = .0006$) and multivariate analysis (adjusted HR, 0.75; 95% CI, 0.56-0.99; $P = .048$) (Table 3). The attenuation in the effect of p-AKT expression in the multivariate analysis was principally the result of adjusting for disease stage; when we simply adjusted for disease stage, p-AKT overexpression was associated with HR of 0.72 (95% CI, 0.54-0.94). Similar results, although somewhat attenuated, were observed in analysis for overall mortality (Table 3). Our data suggest that, despite the role of AKT activation in carcinogenesis, p-AKT expression marks a subtype of colorectal cancers with indolent behavior, which is analogous to estrogen receptor (ESR1) expression in breast cancer.

Interaction Between p-AKT Expression and Another Variable in Survival Analyses

We examined the influence of p-AKT positivity on cancer-specific mortality across strata of other potential predictors of survival, including age, sex, year of diagnosis, BMI, family history of colorectal cancer, tumor location, stage, MSI, CIMP, *KRAS*, *BRAF*, *PIK3CA*, LINE-1 methylation, TP53, and FASN. There was no evidence for significant effect modification by any of the variables examined (all P interaction $\geq .10$). Notably, the effect of p-AKT did not significantly differ between the two independent cohort studies (P interaction = .53), or between tumors prior to 1995 and those in 1995 or after (P interaction = .15).

Table 1. p-AKT Expression in Colorectal Cancer[a]

Clinical or Molecular Feature	Total N	p-AKT Expression		P
		(-)	(+)	
All cases	717	269	448	
Sex				.0035
Male	259 (36%)	79 (29%)	180 (40%)	
Female	458 (64%)	190 (71%)	268 (60%)	
Age (years)				.17
<65	265 (37%)	108 (40%)	157 (35%)	
≥65	452 (63%)	161 (60%)	291 (65%)	
Body mass index (BMI, kg/m^2)				.30
<25	313 (44%)	126 (47%)	187 (42%)	
25-29	281 (39%)	96 (36%)	185 (41%)	
≥30	122 (17%)	47 (17%)	75 (17%)	
Family history of colorectal cancer in any first-degree relative				.60
(-)	546 (76%)	202 (75%)	344 (77%)	
(+)	171 (24%)	67 (25%)	104 (23%)	
Year of diagnosis				.65
Prior to 1995	275 (38%)	102 (38%)	173 (39%)	
1995 to 2004	442 (62%)	167 (62%)	275 (61%)	
Tumor location				.29
Rectum	141 (20%)	61 (23%)	81 (18%)	
Distal colon (splenic flexure to sigmoid)	221 (31%)	80 (30%)	141 (31%)	
Proximal colon (cecum to transverse)	355 (50%)	128 (48%)	227 (51%)	
Stage				.0022
I	161 (22%)	41 (15%)	120 (27%)	
II	221 (31%)	80 (30%)	141 (31%)	
III	200 (28%)	89 (33%)	111 (25%)	
IV	98 (14%)	44 (16%)	54 (12%)	
Unknown	37 (5.2%)	15 (5.6%)	22 (4.9%)	
Tumor grade				<.0001
Low	648 (91%)	227 (85%)	421 (94%)	
High	66 (9.2%)	40 (15%)	26 (5.8%)	
MSI status				.25
MSI-low/MSS	583 (83%)	213 (81%)	370 (84%)	
MSI-high	121 (17%)	51 (19%)	70 (16%)	
CIMP status				.17
CIMP-0	296 (42%)	105 (40%)	191 (43%)	
CIMP-low	291 (41%)	105 (40%)	186 (42%)	
CIMP-high	118 (17%)	53 (20%)	65 (15%)	
***BRAF* mutation**				.53
(-)	597 (85%)	222 (83%)	375 (85%)	
(+)	109 (15%)	44 (17%)	65 (15%)	
***KRAS* mutation**				.61
(-)	441 (62%)	168 (63%)	273 (61%)	
(+)	268 (38%)	97 (37%)	171 (39%)	
***PIK3CA* mutation**				.015
(-)	534 (83%)	210 (88%)	324 (80%)	
(+)	108 (17%)	29 (12%)	79 (20%)	
LINE-1 methylation level (Mean±SD)	61.3±9.4	61.3±9.1	61.3±9.7	.94
TP53 expression				.46
(-)	432 (61%)	167 (62%)	265 (60%)	
(+)	281 (39%)	101 (38%)	180 (40%)	
FASN expression				.0025
(-)	598 (84%)	238 (89%)	360 (81%)	
(+)	113 (16%)	28 (11%)	85 (19%)	

[a](%) indicates the proportion of cases with a specific clinical, pathologic, or molecular feature among p-AKT (+) cases [or p-AKT (-) cases]; CIMP, CpG island methylator phenotype; FASN, fatty acid synthase; MSI, microsatellite instability; MSS, microsatellite stable; p-AKT, phosphorylated AKT; SD, standard deviation.

Table 2. Multivariate Logistic Regression Analysis of the Relationship Between p-AKT Expression and Colorectal Cancer Stage (as an Outcome Variable)*

Variables in the Final Model for Disease Stage III-IV (vs. I-II) as an Outcome Variable	Multivariate OR (95% CI)	P
p-AKT expression	0.63 (0.45-0.88)	.0071
Other variables		
MSI-high (vs. MSI-low/MSS)	0.28 (0.16-0.51)	<.0001
High tumor grade (vs. low tumor grade)	3.51 (1.82-6.77)	.0002
Age at diagnosis (for a 10-year increase)	0.96 (0.95-0.99)	.0006
KRAS mutation	1.60 (1.12-2.29)	.0096
Family history of colorectal cancer	0.62 (0.42-0.92)	.017
BRAF mutation	1.76 (1.03-3.00)	.038
TP53 expression	1.66 (1.01-2.76)	.048

*The multivariate logistic regression analysis assessing the relations with cancer stage (as an outcome variable) initially included p-AKT, age, sex, family history of colorectal cancer, body mass index, tumor location, tumor grade, *KRAS*, *BRAF*, *PIK3CA*, LINE-1 methylation, microsatellite instability (MSI), CpG island methylator phenotype, TP53, and FASN. A backward stepwise elimination with threshold of $P = .20$ was used to select variables in the final model. Variables with $P < .05$ are listed.

CI indicates confidence interval; MSI, microsatellite instability; MSS, microsatellite stable; OR, odds ratio; p-AKT, phosphorylated AKT.

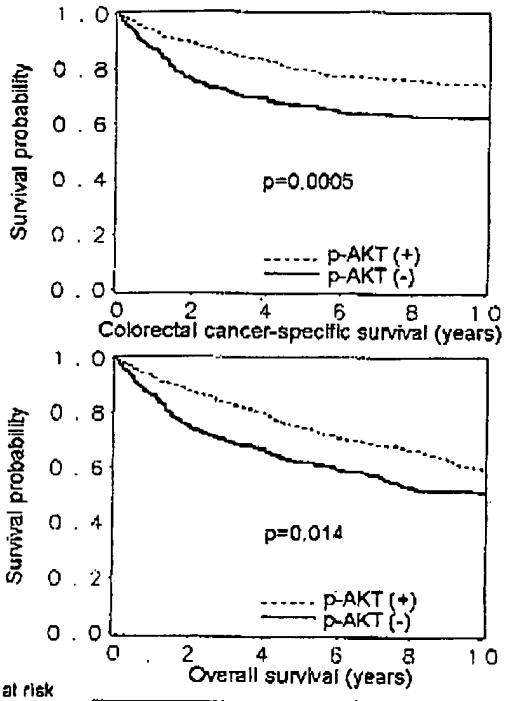

Number at risk

Year	0	2	4	6	8	10
p-AKT (+) - - -	448	395	359	297	239	168
p-AKT (-) ——	269	202	179	148	114	93

Figure 2. Kaplan-Meier curves for colorectal cancer-specific survival (*Top*) and for overall survival (*Bottom*) according to p-AKT status in colorectal cancer. The bottom table indicates the number of patients who were alive and at risk of death at each time point after the diagnosis of colorectal cancer.

DISCUSSION

We conducted this study to examine the relationship between phosphorylated AKT (p-AKT) expression and patient survival in a large cohort of stage I-IV colorectal cancers. AKT has emerged as a central node in cell signaling pathways, downstream of growth factors, cytokines, and other cellular stimuli.[1-3] AKT is aberrantly activated in a wide variety of human cancers and is increasingly important as a promising target for cancer therapy.[4-6] We have found that p-AKT expression in colorectal cancer is associated with early stage and favorable prognosis (Fig. 3), suggesting that p-AKT may be a biomarker to identify patients with superior outcome and a possible therapeutic target (analogous to ESR1 in breast cancer).

Examining tumor factors and clinical outcome is important in cancer research.[35-39] Studies examining the relation between p-AKT expression and prognosis in human cancers have yielded variable results.[7-12] Previous studies on colorectal cancer have suggested no prognostic role of p-AKT expression.[15-18] Notably, in the study with over 1000 colorectal cancers,[15] tumoral p-AKT expression was associated with early lymph node stage, but not independently with patient survival. However, that study[15] lacked *PIK3CA* mutation data. A difference in the prognostic data by that study[15] and our current study might be due to a difference in the patient cohorts or the methods to assess p-AKT expression, or simply due to a chance variation between independent studies. In addition, all but one[15] of the studies[16-18] were limited by small sample sizes ($N < 160$). Our current study ($N = 717$) has shown that p-AKT expression is associated with *PIK3CA* mutation as expected from their causal link, and that our method and cutoff for p-AKT positivity are reasonable for evaluating AKT activation levels in paraffin-embedded tissues. Furthermore, in contrast to the prior studies,[15-18] we assessed the prognostic effect of p-AKT expression independent of *PIK3CA* mutation and other molecular events that have been documented to be critical in colorectal carcinogenesis.

Considering experimental data suggesting that AKT plays critical roles in tumor proliferation, survival, invasion, and angiogenesis,[1-3,40] one would expect that p-

Table 3. p-AKT Expression in Colorectal Cancer and Patient mortality[a]

	Total N	Colorectal Cancer-Specific Mortality				Overall Mortality			
		Deaths/ Person-Years	Univariate HR (95% CI)	Stage-Matched HR (95% CI)	Multivariate Stage-Matched HR (95% CI)	Deaths/ Person-Years	Univariate HR (95% CI)	Stage-Matched HR (95% CI)	Multivariate Stage-Matched HR (95% CI)
p-AKT (-)	269 (38%)	97/2056	1 (referent)	1 (referent)	1 (referent)	139/2056	1 (referent)	1 (referent)	1 (referent)
p-AKT (+)	448 (62%)	113/3962	0.62 (0.47-0.82)	0.72 (0.54-0.94)	0.75 (0.56-0.99)	202/3962	0.76 (0.61-0.95)	0.82 (0.66-1.03)	0.78 (0.62-0.98)
P			.0006	.018	.048		.014	.083	.029

[a]The multivariate, stage-matched conditional Cox regression model included age, year of diagnosis, sex, family history of colorectal cancer, body mass index, tumor location, grade, *KRAS*, *BRAF*, *PIK3CA*, FASN, TP53, LINE-1 methylation, microsatellite instability, CpG island methylator phenotype and p-AKT. A backward stepwise elimination with threshold of $P = .20$ was used to select variables in the final model.CI indicates confidence interval; HR, hazards ratio; p-AKT, phosphorylated AKT.

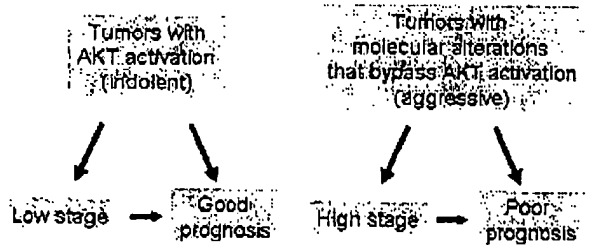

Figure 3. Schematic representation of possible relations between AKT activation, disease stage, and patient prognosis.

AKT' expression would imply poor prognosis. It is very common to conceive that the presence of oncogene activation (or tumor suppressor inactivation) should imply aggressive tumor behavior. However, this preconception does not always hold true. Colon cancers develop through accumulation of multiple genetic and epigenetic events, and each tumor has its own unique combination of molecular aberrations. Some tumors activate AKT, while others do not. In order to acquire malignant characteristics, those AKT-inactive tumors need to have aberrations which can be an alternative to AKT activation: those aberrations may lead to more aggressive behavior than AKT activation actually does (Fig. 3). This is well exemplified by the association between estrogen receptor (ESR1, or ER-alpha) expression in breast cancer and good prognosis. ESR1 is known to contribute to breast cancer development; yet ESR1 expression marks tumors with favorable outcome.[41] This is probably because breast cancer without ESR1 expression might have developed through more detrimental events than ESR1 expression. Another example is MSI in colorectal cancer. MSI is known to cause inactivation of a number of tumor suppressors; yet MSI marks tumors with good prognosis.[42] The aforementioned preconception that oncogene activation (or tumor suppressor inactivation) should be associated with poor outcome can cause serious publication bias, because reports consistent with this preconception have been regarded favorably during journal's decision process, whereas reports inconsistent with the preconception have been treated unfavorably.[43]

Another possible explanation for the relationship between AKT activation and good prognosis may be due to "tumor suppressive" roles of AKT.[44] AKT has blocked cancer cell mortality and invasion through the transcription factor NFAT[45] or down-regulation of RHO activity.[46] Another study has reported that AKT1 activation

can promote tumorigenesis but suppresses tumor invasion.[47] The inhibitory effect of AKT activation on cancer cell cycle has been reported.[48] In addition, it is possible that each AKT isoform may have different functions.[49,50] Future studies are necessary to confirm our observations as well as to elucidate biological mechanisms by which AKT activation affects colorectal tumor behavior.

Interestingly, we found that p-AKT expression was independently associated with FASN expression and low tumor grade; the latter association is consistent with a previous study.[15] Inhibition of FASN has resulted in the down-regulation of AKT pathway.[20] The PI3K/AKT pathway activation has modulated the expression and/or nuclear maturation of the transcription factor SREBF1, stimulating FASN expression.[20] Our finding of the relationship between p-AKT and FASN expression may be consistent with these experimental data.

There are limitations in this study. For example, data on cancer treatment were unavailable. Nonetheless, it is unlikely that chemotherapy use substantially differed according to AKT status in tumor, since such data were unavailable for treatment decision making. In addition, our multivariate survival analysis adjusted for disease stage as finely as possible (I, IIA, IIB, IIIA, IIIB, IIIC, IV, unknown) on which treatment decision making was mostly based. As another limitation, beyond cause of mortality, data on cancer recurrences were unavailable in these cohort studies. Nonetheless, colorectal cancer-specific survival might be a reasonable surrogate of colorectal cancer-specific outcome.

Immunohistochemical evaluation of p-AKT expression in cancer tissue has been a challenge, and there is no standardized method. Preanalytical variables such as tissue processing may have considerable impact on antigenicity of p-AKT, which may be substantially influenced by a slight difference in conditions of immunohistochemical procedure. We tried to minimize such an external source of noise in a number of ways. We constructed TMAs and performed the immunohistochemical procedure in a very similar condition for all specimens. The quality of tissue sections, which depends on age of tissue and time after cutting the TMA blocks, should be considered. In our current study, p-AKT expression was not associated with age of tissue (ie, year of diagnosis), supporting that p-AKT antigen might not substantially be deteriorated over time. With regard to time after block cutting, because we cut all TMA blocks into sections around the same time, time after block cutting was uniform from case to case. In addition, we obtained 4 tissue cores from each case to overcome within-tumor heterogeneity. Interpretation of protein expression took into account background noise if any, and we calibrated against such background noise in each case. Furthermore, any preanalytical variability was largely nondifferential (ie, random) in nature, and thus, might have conservatively biased our results toward the null hypothesis. Because of a large sample size, we were still able to detect the biologically reasonable relationship between *PIK3CA* mutation and p-AKT expression as well as the relations of p-AKT expression with disease stage and prognosis. The cutoff for p-AKT used in this current study needs to be validated in an independent data set.

There are advantages in using the database of the two prospective cohort studies, the Nurses' Health Study and the Health Professionals Follow-up Study, to examine prognostic significance of tumor biomarkers. Anthropometric measurements, family history, cancer staging, and other clinical, pathologic, and tumoral molecular data were prospectively collected, blinded to patient outcome. Cohort participants who developed cancer were treated at hospitals throughout the United States (in 48 states except for North Dakota and Alaska), and thus more representative colorectal cancers in the general US population than patients in one to a few academic hospitals. There were no demographic differences between cases with tumor tissue analyzed and those without tumor tissue analyzed.[22] Finally, our rich tumor database enabled us to simultaneously assess pathologic and tumoral molecular correlates and control for confounding by a number of tumoral molecular alterations.

In summary, our large cohort study has shown that p-AKT expression in colorectal cancer is associated with *PIK3CA* mutation, early disease stage and favorable prognosis. The high percentage of p-AKT positive patients in this study certainly supports a vital role of AKT activation in the pathogenesis of colorectal cancer. Our findings suggest a possibility that AKT activation may have a predictive role in a manner analogous to ESR1 in breast cancer, identifying a subgroup of patients with better prognosis and serving as a therapeutic target at the same time.

CONFLICT OF INTEREST DISCLOSURES

Funding: U.S. National Institute of Health (NIH) grants P01 CA87969 (to S. Hankinson), P01 CA55075 (to W. Willett), P50 CA127003 (to C.S.F.), K07 CA122826 (to S.O.), and R01 CA151993 (to S.O.); the Bennett Family Fund; and the Entertainment Industry Foundation through National Colorectal Cancer Research Alliance. Y.B. was supported by a fellowship grant from the Uehara Memorial Foundation. The content is solely

the responsibility of the authors and does not necessarily represent the official views of NCI or NIH. The funders had no role in study design, data collection and analysis, decision to publish, or preparation of the manuscript.

REFERENCES

1. Engelman JA. Targeting PI3K signalling in cancer: opportunities, challenges and limitations. *Nat Rev Cancer.* 2009;9:550-562.
2. Manning BD, Cantley LC. AKT/PKB signaling: navigating downstream. *Cell.* 2007;129:1261-1274.
3. Franke TF. PI3K/Akt: getting it right matters. *Oncogene.* 2008;27:6473-6488.
4. Courtney KD, Corcoran RB, Engelman JA. The PI3K pathway as drug target in human cancer. *J Clin Oncol.* 2010;28:1075-1083.
5. Ma WW, Adjei AA. Novel agents on the horizon for cancer therapy. *CA Cancer J Clin.* 2009;59:111-137.
6. Grant S. Cotargeting survival signaling pathways in cancer. *J Clin Invest.* 2008;118:3003-3006.
7. Li R, Dai H, Wheeler TM, et al. Prognostic value of Akt-1 in human prostate cancer: a computerized quantitative assessment with quantum dor technology. *Clin Cancer Res.* 2009;15:3568-3573.
8. Tomita Y, Morooka T, Hoshida Y, et al. Prognostic significance of activated AKT expression in soft-tissue sarcoma. *Clin Cancer Res.* 2006;12:3070-3077.
9. Dai DL, Martinka M, Li G. Prognostic significance of activated Akt expression in melanoma: a clinicopathologic study of 292 cases. *J Clin Oncol.* 2005;23:1473-1482.
10. Cappuzzo F, Magrini E, Ceresoli GL, et al. Akt phosphorylation and gefitinib efficacy in patients with advanced non-small-cell lung cancer. *J Natl Cancer Inst.* 2004;96:1133-1141.
11. Nam SY, Lee HS, Jung GA, et al. Akt/PKB activation in gastric carcinomas correlates with clinicopathologic variables and prognosis. *Apmis.* 2003;111:1105-1113.
12. Shah A, Swain WA, Richardson D, et al. Phospho-akt expression is associated with a favorable outcome in non-small cell lung cancer. *Clin Cancer. Res* 2005;11:2930-2936.
13. Javle MM, Yu J, Khoury T, et al. Akt expression may predict favorable prognosis in cholangiocarcinoma. *J Gastroenterol Hepatol.* 2006;21:1744-1751.
14. Chadha KS, Khoury T, Yu J, et al. Activated Akt and Erk expression and survival after surgery in pancreatic carcinoma. *Ann Surg Oncol.* 2006;13:933-939.
15. Lugli A, Zlobec I, Minoo P, et al. Role of the mitogen-activated protein kinase and phosphoinositide 3-kinase/AKT pathways downstream molecules, phosphorylated extracellular signal-regulated kinase, and phosphorylated AKT in colorectal cancer-a tissue microarray-based approach. *Hum Pathol.* 2006;37:1022-1031.
16. Kato S, Iida S, Higuchi T, et al. PIK3CA mutation is predictive of poor survival in patients with colorectal cancer. *Int J Cancer.* 2007;121:1771-1778.
17. Schmitz KJ, Wohlschlaeger J, Alakus H, et al. Activation of extracellular regulated kinases (ERK1/2) but not AKT predicts poor prognosis in colorectal carcinoma and is associated with k-ras mutations. *Virchows Arch.* 2007;450:151-159.
18. Colakoglu T, Yildirim S, Kayaselcuk F, et al. Clinicopathological significance of PTEN loss and the phosphoinositide 3-kinase/Akt pathway in sporadic colorectal neoplasms: is PTEN loss predictor of local recurrence? *Am J Surg.* 2008;195:719-725.
19. Ogino S, Goel A. Molecular classification and correlates in colorectal cancer. *J Mol Diagn.* 2008;10:13-27.
20. Menendez JA, Lupu R. Fatty acid synthase and the lipogenic phenotype in cancer pathogenesis. *Nat Rev Cancer.* 2007;7:763-777.
21. Ogino S, Nosho K, Meyerhardt JA, et al. Cohort study of fatty acid synthase expression and patient survival in colon cancer. *J Clin Oncol.* 2008;26:5713-5720.
22. Chan AT, Ogino S, Fuchs CS. Aspirin and the risk of colorectal cancer in relation to the expression of COX-2. *N Engl J Med.* 2007;356:2131-2142.
23. Ogino S, Kawasaki T, Brahmandam M, et al. Sensitive sequencing method for KRAS mutation detection by Pyrosequencing. *J Mol Diagn.* 2005;7:413-421.
24. Ogino S, Kawasaki T, Kirkner GJ, Loda M, Fuchs CS. CpG island methylator phenotype-low (CIMP-low) in colorectal cancer: possible associations with male sex and KRAS mutations. *J Mol Diagn.* 2006;8:582-588.
25. Nosho K, Kawasaki T, Ohnishi M, et al. PIK3CA mutation in colorectal cancer: relationship with genetic and epigenetic alterations. *Neoplasia.* 2008;10:534-541.
26. Ogino S, Brahmandam M, Cantor M, et al. Distinct molecular features of colorectal carcinoma with signet ring cell component and colorectal carcinoma with mucinous component. *Mod Pathol.* 2006;19:59-68.
27. Ogino S, Kawasaki T, Brahmandam M, et al. Precision and performance characteristics of bisulfite conversion and real-time PCR (MethyLight) for quantitative DNA methylation analysis. *J Mol Diagn.* 2006;8:209-217.
28. Ogino S, Cantor M, Kawasaki T, et al. CpG island methylator phenotype (CIMP) of colorectal cancer is best characterised by quantitative DNA methylation analysis and prospective cohort studies. *Gut.* 2006;55:1000-1006.
29. Weisenberger DJ, Siegmund KD, Campan M, et al. CpG island methylator phenotype underlies sporadic microsatellite instability and is tightly associated with BRAF mutation in colorectal cancer. *Nat Genet.* 2006;38:787-793.
30. Nosho K, Irahara N, Shima K, et al. Comprehensive biostatistical analysis of CpG island methylator phenotype in colorectal cancer using a large population-based sample. *PLoS One.* 2008;3:e3698.
31. Ogino S, Kawasaki T, Kirkner GJ, Kraft P, Loda M, Fuchs CS. Evaluation of markers for CpG island methylator phenotype (CIMP) in colorectal cancer by a large population-based sample. *J Mol Diagn.* 2007;9:305-314.
32. Ogino S, Kawasaki T, Nosho K, et al. LINE-1 hypomethylation is inversely associated with microsatellite instability and CpG island methylator phenotype in colorectal cancer. *Int J Cancer.* 2008;122:2767-2773.
33. Irahara N, Nosho K, Baba Y, et al. Precision of pyrosequencing assay to measure LINE-1 methylation in colon cancer, normal colonic mucosa, and peripheral blood cells. *J Mol Diagn.* 2010;12:177-183.
34. Cicenas J. The potential role of Akt phosphorylation in human cancers. *Int J Biol Markers.* 2008;23:1-9.
35. Horst D, Reu S, Kriegl L, Engel J, Kirchner T, Jung A. The intratumoral distribution of nuclear beta-catenin is a prognostic marker in colon cancer. *Cancer.* 2009;115:2063-2070.

36. Zlobec I, Minoo P, Baumhoer D, et al. Multimarker phenotype predicts adverse survival in patients with lymph node-negative colorectal cancer. *Cancer.* 2008;112:495-502.
37. Buergy D, Fuchs T, Kambakamba P, et al. Prognostic impact of extracellular matrix metalloprotease inducer: immunohistochemical analyses of colorectal tumors and immunocytochemical screening of disseminated tumor cells in bone marrow from patients with gastrointestinal cancer. *Cancer.* 2009;115:4667-4678.
38. Watanabe T, Kobunai T, Sakamoto E, et al. Gene expression signature for recurrence in stage III colorectal cancers. *Cancer.* 2009;115:283-292.
39. Vilkin A, Niv Y, Nagasaka T, et al. Microsatellite instability, MLH1 promoter methylation, and BRAF mutation analysis in sporadic colorectal cancers of different ethnic groups in Israel. *Cancer.* 2009;115:760-769.
40. Itoh N, Semba S, Ito M, Takeda H, Kawata S, Yamakawa M. Phosphorylation of Akt/PKB is required for suppression of cancer cell apoptosis and tumor progression in human colorectal carcinoma. *Cancer.* 2002;94:3127-3134.
41. Payne SJ, Bowen RL, Jones JL, Wells CA. Predictive markers in breast cancer--the present. *Histopathology.* 2008;52:82-90.
42. Popat S, Hubner R, Houlston RS. Systematic review of microsatellite instability and colorectal cancer prognosis. *J Clin Oncol.* 2005;23:609-618.
43. Fanelli D. Do pressures to publish increase scientists' bias? An empirical support from US States Data. *PLoS One.* 2010;5:e10271.
44. Wyszomierski SL, Yu D. A knotty turnabout?: Akt1 as a metastasis suppressor. *Cancer Cell.* 2005;8:437-439.
45. Yoeli-Lerner M, Yiu GK, Rabinovitz I, Erhardt P, Jauliac S, Toker A. Akt blocks breast cancer cell motility and invasion through the transcription factor NFAT. *Mol Cell.* 2005;20:539-550.
46. Liu H, Radisky DC, Nelson CM, et al. Mechanism of Akt1 inhibition of breast cancer cell invasion reveals a protumorigenic role for TSC2. *Proc Natl Acad Sci U S A.* 2006;103:4134-4139.
47. Hutchinson JN, Jin J, Cardiff RD, Woodgett JR, Muller WJ. Activation of Akt-1 (PKB-alpha) can accelerate ErbB-2-mediated mammary tumorigenesis but suppresses tumor invasion. *Cancer Res.* 2004;64:3171-3178.
48. Kodama Y, Baxter RC, Martin JL. Insulin-like growth factor-I inhibits cell growth in the a549 non-small lung cancer cell line. *Am J Respir Cell Mol Biol.* 2002;27:336-344.
49. Irie HY, Pearline RV, Grueneberg D, et al. Distinct roles of Akt1 and Akt2 in regulating cell migration and epithelial-mesenchymal transition. *J Cell Biol.* 2005;171:1023-1034.
50. Samuels Y, Diaz LA, Jr., Schmidt-Kittler O, et al. Mutant PIK3CA promotes cell growth and invasion of human cancer cells. *Cancer Cell.* 2005;7:561-573.

Published in final edited form as:
Cancer Res. 2009 July 15; 69(14): 5918–5926. doi:10.1158/0008-5472.CAN-08-4623.

Progressive Tumor Formation in Mice with Conditional Deletion of TGF-β Signaling in Head and Neck Epithelia Is Associated with Activation of the PI3k/Akt Pathway

Yansong Bian[1], **Anita Terse**[1], **Juan Du**[1], **Bradford Hall**[1], **Alfredo Molinolo**[2], **Pin Zhang**[3], **Wanjun Chen**[3], **Kathleen C. Flanders**[4], **J. Silvio Gutkind**[2], **Lalage M. Wakefield**[4], and **Ashok B. Kulkarni**[1]

[1] Functional Genomics Section, Laboratory of Cell and Developmental Biology, National Cancer Institute, NIH, Bethesda, MD 20892

[2] Oral and Pharyngeal Cancer Branch, National Cancer Institute, NIH, Bethesda, MD 20892

[3] Mucosal Immunity Section, Oral Immunity and Infection Branch, National Institute of Dental and Craniofacial Research, National Cancer Institute, NIH, Bethesda, MD 20892

[4] Cancer Biology of TGF-β Section, Laboratory of Cancer Biology and Genetics, National Cancer Institute, NIH, Bethesda, MD 20892

Abstract

The precise role of TGF-β signaling in head and neck squamous cell carcinoma (HNSCC) is not yet fully understood. Here we report generation of an inducible head- and neck-specific knockout mouse model by crossing TGF-β receptor I (*Tgfbr1*) floxed mice with *K14-CreER*^{tam} mice. By applying tamoxifen (TM) to oral cavity of the mouse to induce Cre expression, we were able to conditionally delete *Tgfbr1* in the mouse head and neck epithelia. Upon tumor induction with 7, 12-dimethylbenzanthracene (DMBA), 45% of *Tgfbr1* conditional knockout (cKO) mice (n=42) developed squamous cell carcinomas (SCCs) in the head and neck area starting from 16 weeks after treatment. However, no tumors were observed in the control littermates. A molecular analysis revealed an enhanced proliferation and loss of apoptosis in the basal layer of the head and neck epithelia of *Tgfbr1* cKO mice 4 weeks after TM and DMBA treatment. The most notable finding of our study is that the phosphoinositide 3-kinase (PI3K)/Akt pathway was activated in SCCs that developed in the *Tgfbr1* cKO mice upon inactivation of TGF-β signaling through Smad2/3 and DMBA treatment. These observations suggest that activation of Smad-independent pathways may contribute cooperatively with inactivation of Smad-dependent pathways to promote head and neck carcinogenesis in these mice. Our results revealed the critical role of the TGF-β signaling pathway and its crosstalk with the PI3K/Akt pathway in suppressing head and neck carcinogenesis.

Keywords

TGF-β; PI3K/Akt; Head and Neck Squamous Cell Carcinoma (HNSCC); Conditional Knockout; Cancer Mouse Model

Requests for reprints: Ashok B. Kulkarni, Functional Genomics Section, Laboratory of Cell and Developmental Biology, National Institute of Dental and Craniofacial Research, NIH, 30 Convent Drive, Building 30, Room 130, Bethesda, MD 20892-4330. Phone: 301-435-2887 ; Fax : 301-435-2888 ; ak40m@nih.gov.

Potential conflicts of Intrest: None

Introduction

Head and neck squamous cell carcinoma (HNSCC) is one of the most common types of human cancer (1). Tobacco, alcohol consumption and viral agents are the major risk factors for development of HNSCC. These risk factors together with genetic susceptibility result in the accumulation of multiple genetic and epigenetic alterations in a multistep process of cancer development (2). However, the underlying cellular and molecular mechanisms that contribute to the initiation and progression from normal epithelia to invasive squamous cell carcinoma have not been clearly delineated (3).

There is accumulating evidence which suggests that the TGF-β signal transduction pathway is involved in head and neck carcinogenesis (4,5). TGF-β is a multifunctional cytokine with diverse biological effects on cellular processes, including cell proliferation, migration, differentiation, and apoptosis. The 3 mammalian TGF-β isoforms, TGF-β_1, -β_2 and -β_3, exert their functions through a cell surface receptor complex composed of type I (TGFBR1) and type II (TGFBR2) serine/threonine kinase receptors. Intracellular signaling is initiated once TGFBR1 has been phosphorylated by TGFBR2, which in turn phosphorylates Smad2 or Smad3. Phosphorylated Smad2 or Smad3 binds to Smad4, and then the complexes translocate from the cytoplasm into the nucleus. This results in the transcriptional activation of TGF-β-responsive genes that mediate the effects of TGF-β at the cellular level. Independent of SMAD proteins, receptor activation also induces other downstream targets, including Ras, RhoA, TAK1, MEKK1, PI3K, and PP2A, to produce the full spectrum of TGF-β responses (6–8).

The effects of TGF-β signaling in carcinogenesis largely depend on the tissue of origin and the tumor type. In most types of human cancer, TGF-β plays a paradoxical role in cancer development by acting as a tumor suppressor in early stages (9), and a tumor promoter in later stages (10,11). In HNSCC, it is known that TGF-β functions as a potent tumor suppressor (12). However, it is not clear whether TGF-β acts in a pro-oncogenic manner in advanced late-stage HNSCC. The human oral carcinoma cell line, which contained a normal Ras but was growth-inhibited by TGF-β1, led to an increase in cell migration and invasion, and metastasis when transfected with dominant negative *TGFBR2* (*dn RII*) cDNA (13). When TGF-β receptor II (*Tgfbr2*) was conditionally deleted in mouse head and neck epithelia, 35% of the DMBA-initiated $Tgfbr2^{-/-}$ mice developed jugular lymph node metastasis, suggesting TGF-β may actually in fact suppress metastasis rather than promote it (14).

The correlation between TGF-β receptor-mediated signaling and cancer development has been studied extensively. However, much less attention has been paid to the role of TGFBR1 in carcinogenesis when compared to that of TGFBR2. Although several reports have noted that mutations and polymorphisms of *TGFBR1* are associated with HNSCC (15–17), the precise molecular nature of TGFBR1-mediated pro-oncogenic effects is still unknown. In the current study, we conditionally deleted *Tgfbr1* in mouse head and neck epithelia using the *Cre-LoxP* approach to show that deletion of *Tgfbr1* alone is not sufficient for spontaneous tumor formation, though it can increase the susceptibility to tumor development initiated by DMBA. The most notable finding of our study is that, in SCCs that developed in the *Tgfbr1* cKO mice, the PI3K/Akt pathway, one of the most important Smad-independent receptor-I signaling pathways, was clearly activated in addition to inactivation of the Smad-dependent TGF-β signaling pathway. Our studies identified the critical role of the TGFBR1-mediated signaling pathway and its crosstalk with the PI3K/Akt pathway in suppressing head and neck carcinogenesis. The *Tgfbr1* cKO mouse will be a valuable animal model for studying genetic alterations and signaling pathways that play important roles in HNSCC.

Materials and Methods

Generation of *Tgfbr1* cKO mice

The *Tgfbr1* cKO mice (*K14-CreER^{tam};Tgfbr1$^{f/f}$*) were generated from crosses between *Tgfbr1$^{f/f}$* mice (mixed genetic strains of C57BL/6, 129SV/J and FVB/N) (18,19) and *K14-CreER^{tam}* mice (genetic strain CD-1) (20). The *Tgfbr1* cKO mice and their controls (*Tgfbr1$^{f/f}$*, *Tgfbr1$^{f/+}$*, and *K14-CreER^{tam};Tgfbr1$^{f/+}$* mice) were from the same litter and therefore had exactly the same mixed genetic background. The treatment procedures of Tamoxifen and DMBA have been described (20,14). Additional details are provided in the Supplementary Data.

Histology, immunostaining, and BrdU labeling

Immunohistochemical staining (IHC) and quantifications of IHC slides were performed using a previously published method (21). Intratumoral microvessel density (iMVD) was determined as previously described (22). BrdU labeling and primary antibodies are described in the Supplementary Data.

Western blot analysis

Normal buccal mucosa and tongue from 6 pairs of *Tgfbr1$^{f/f}$* and *Tgfbr1* cKO mice, together with tumors that developed in DMBA-initiated *Tgfbr1* cKO mice, were carefully dissected. A total amount of 40 μg protein from each sample was denatured and then loaded in each lane of NuPAGE 4–12% Bis-Tris precast gel. Additional details are provided in Supplementary Data.

Additional Methods

Information on TUNEL assay, Cre-mediated recombination assessment, quantitative real-time PCR and flow cytometry analysis is detailed in the Supplementary Data.

Statistical analysis

Statistical differences in the levels of mRNA expression between controls and experimental samples were determined using the Student's *t*-test.

Results

Inducible deletion of *Tgfbr1* in head and neck epithelia is not sufficient for SCC formation in mice

We generated an inducible head- and neck-specific knockout mouse model by crossing *Tgfbr1* floxed mice with *K14-CreER^{tam}* mice. K14 is expressed in proliferating keratinocytes of the basal layer of the epidermis. It is also active in stem cells that regenerate the epidermis, sebaceous glands, hair follicles, and the oral mucosa. Therefore TM treatment causes permanent excision of *Tgfbr1* in both epithelia and epidermis of the head and neck region including buccal mucosa, tongue and ears. The *Tgfbr1* cKO mice and controls (*Tgfbr1$^{f/f}$*) were dissected 10 days after TM treatment. Genomic DNA was extracted from all major organs and tissues. *Cre*-mediated recombination of the *Tgfbr1$^{f/f}$* allele was assessed using a PCR-based assay. Deletions of *Tgfbr1* were detected in the buccal mucosa (BM), tongue (Tg), and ear (Er), but not in the esophagus (Es), forestomach (FS), back skin (SK), or any other nonstratified epithelial organs of *Tgfbr1* cKO mice (Supplementary Fig. 1). No recombination was detected prior to TM administration. *Tgfbr1* mRNA expression was examined by quantitative RT-PCR (qRT-PCR). The expression levels of *Tgfbr1* mRNA in *Tgfbr1$^{f/f}$* mice were normalized as 1.00 ± 0.23 in the buccal mucosa and 1.00 ± 0.08 in the tongue. The mRNA expression levels were significantly reduced to a mean of 0.65 ± 0.17 in the buccal mucosa ($p<0.01$) and 0.07 ± 0.05

in SCC of *Tgfbr1* cKO mice as well as 0.46 ± 0.05 in the tongue ($p<0.001$) (Fig. 1*A*). Using immunostaining, the Tgfbr1 protein level was found to be significantly decreased in the tongue of *Tgfbr1* cKO mice, as compared to that of *Tgfbr1*$^{f/f}$ mice. A similar decrease was also observed in phosphorylated Smad2, an activated mediator of TGF-β signaling (Fig. 1*B*). However, the expression of both Tgfbr1 and p-Smad2 in the back skin of the same mice remained normal (data not shown). This suggests that, upon oral administration of TM, the deletion of *Tgfbr1* and the inactivation of its downstream signaling was localized only in the head and neck epithelia. These results were further confirmed by Western blot (Fig. 1*C*).

Out of 31 *Tgfbr1* cKO mice, only 3 (9.7%, 3/31) developed spontaneous tumors including 2 SCCs in the periobital region and one in the upper lateral neck. No significant pathological changes in the head and neck region were observed in the remaining *Tgfbr1* cKO mice during 1 year of observation. Thus, our results indicate that inactivation of TGF-β signaling alone is not sufficient to promote tumor formation in head and neck epithelia of these mice.

Deletion of *Tgfbr1* in the head and neck epithelia together with DMBA initiation induced SCCs in mice

Because spontaneous tumor formation in *Tgfbr1* cKO mice was rare, we induced tumors in *Tgfbr1* cKO mice by applying a single dose (50 μg per mouse) of DMBA to the mouse oral cavity 10 days after the last TM treatment. DMBA is a commonly used chemical carcinogen, which can induce *H-ras* mutations in sporadic cells (24). After tumor initiation with DMBA, *Tgfbr1* cKO mice started to develop SCCs in the head and neck area as early as 16 weeks, and by 1 year after treatment, 19 out of 42 (45%) *Tgfbr1* cKO mice had developed SCCs (Fig. 2*B*–2*E*). The sites of tumors that developed in DMBA-treated *Tgfbr1* cKO mice included the oral cavity, periorbital region, muzzle area, and skin around the head and neck area (Fig. 2*A*). 16% (3/19) of mice with tumors had developed metastases in the jugular lymph nodes and/or lungs by the time the mice were dissected (10–12 months after TM and DMBA treatment) (Fig. 2*F*, 2*G*). No tumors developed in the heterozygous mice (*K14-CreER*^{tam};*Tgfbr1*$^{f/+}$, $n = 27$) or the *Tgfbr1* floxed homozygous (*Tgfbr1*$^{f/f}$, $n = 34$) control littermates (also treated with TM and DMBA) during the same time period (Fig. 2*H*). However, only partial excision of *Tgfbr1* in mouse head and neck epithelia were noted by IHC and Western blot, due to relatively low efficiency of the tamoxifen-induced *K14-CreER*^{tam} mouse line being used in this study (20) (Fig. 1*B*, 1*C*).

Enhanced cell proliferation, inhibition of apoptosis, and down-regulation of cell cycle inhibitors in the head and neck epithelia of *Tgfbr1* cKO mice

TGF-β has effects on both cell growth and apoptosis. Four weeks after DMBA treatment, an increased expression of a proliferative marker Ki67 was detected in the basal layer of the tongue of *Tgfbr1* cKO mice but not in *Tgfbr1*$^{f/f}$ mice. A decreased apoptosis was also observed, indicating that the imbalance between cell proliferation and apoptosis occurs early in the head and neck epithelia of *Tgfbr1* cKO mice (Fig. 3*A*). Using BrdU assays, we found a significantly increased number of proliferative cells in *Tgfbr1* cKO mice head and neck epithelia and SCCs when compared to those of *Tgfbr1*$^{f/f}$ mice (Fig. 3*B, 3D*). However, we did not observe any apoptotic cells in SCCs by TUNEL assays (data not shown). Immunostaining revealed that CDKN1A expression was reduced in tongue and SCCs of *Tgfbr1* cKO mice compared to that in *Tgfbr1*$^{f/f}$ mice. In contrast, c-Myc was overexpressed in tongue of *Tgfbr1* cKO mice and its expression was even more remarkable in SCCs (Fig. 3*B, 3D*). These results were further confirmed by Western blot analysis (Fig 3*C*). Our results indicate the existence of an imbalance between cell proliferation, differentiation, and apoptosis in SCCs that developed in *Tgfbr1* cKO mice, as well as in normal *Tgfbr1* cKO mice head and neck epithelia.

Enhanced paracrine effect of TGF-β on tumor stroma of *Tgfbr1* cKO mice

Increased inflammation and angiogenesis have been found in human HNSCCs (25). Deletion of *Tgfbr2* in mouse head and neck epithelia resulted in enhanced paracrine effect of TGF-β on tumor stroma (14). To investigate the paracrine effect of TGF-β in tumor progression in the DMBA-treated *Tgfbr1* cKO mice, we analyzed the expression level of Cyclooxygenase-2 (Cox-2) (26), Endoglin (CD105) (27), and α-Smooth Muscle Actin (SMA) in tumor stroma (28,29). We found that Cox-2 expression was absent in normal buccal mucosa and tongue of $Tgfbr1^{f/f}$ mice, as well as in *Tgfbr1* cKO mice, but its expression was significantly increased in SCCs, suggesting increased inflammation in tumors (Fig. 4*A*, 4*B*). Increased angiogenesis indicated by Endoglin (CD105)-stained microvessels in the stroma surrounding SCCs were also observed (Fig. 4*A*, 4*B*). Using immunofluorescent staining, we found that α-SMA, a hallmark of the myofibroblastic phenotype, strongly expressed in the stroma surrounding SCCs, but was not detected in the tongues of $Tgfbr1^{f/f}$ mice (Fig. 4*A*). To determine whether these enhanced paracrine effects correlate with endogenous TGF-β1 levels in the area surrounding the SCCs, we examined *Tgfb1* mRNA expression by qRT-PCR. In comparison to tissues from $Tgfbr1^{f/f}$ mice, the levels of *Tgfb1* mRNA expression were increased 2.42 ± 0.31 fold and 27.08 ± 4.42 fold ($p<0.01$) in DMBA-treated *Tgfbr1* cKO mice tongues and SCCs, respectively (Fig. 4*D*). Immunofluorescent staining indicated significantly increased expression of Tgfb1 located only in the tumor stroma (Fig. 4*C*).

Evasion of the immune response is one of the most important features of TGF-β-mediated tumor progression (30,31). We analyzed the immune status of the *Tgfbr1* cKO mice using flow cytometry analysis. Compared with their control littermates, *Tgfbr1* cKO mice showed significantly reduced numbers of both $CD4^+$ and $CD8^+$ effector T cells in jugular lymph nodes. In contrast, the regulatory T cells ($CD4^+CD25^+Foxp3^+$) were increased, indicating active immune suppression in *Tgfbr1* cKO mice. Gross changes in inflammation within tumors were noted by H&E staining (Supplementary Fig. 2*A*, 2*B*).

Activation of PI3K/Akt signaling in SCCs of *Tgfbr1* cKO mice

The PI3K/Akt pathway is important in suppressing apoptosis and in promoting cell growth and proliferation. Hyperactivation of PI3K/Akt in HNSCC is induced either by mutations or by enhanced activity of its upstream activators, including the *Ras* oncogene or inactivation of *PTEN* (phosphatase and tensin homolog deleted on chromosome 10) (32). *PTEN* is a potent tumor suppressor gene and a negative regulator of the PI3K/Akt pathway. Mutations of *PTEN* have been found in a wide range of human cancers (33). In our study, a significantly increased level of unphosphorylated PTEN, an active form of the protein, was detected in all of the tumors that developed in the DMBA-treated *Tgfbr1* cKO mice (Fig. 5*B*). However, despite the elevated PTEN levels, we observed consistently increased levels of the phosphorylated form of Akt (p-Akt) and its downstream target, the mammalian target of rapamycin (mTOR), in all of the tumors analyzed both by immunostaining and Western blot (Fig. 5*A*, 5*B*). These results indicate that in spite of the increased expression of PTEN, the PI3K/Akt pathway was activated in the SCCs that developed in the DMBA-treated *Tgfbr1* cKO mice. Our results suggest that Akt activation in the SCCs is independent of effects on PTEN in this mouse model, and that other mechanisms are involved in the activation of this pathway. One of these might be the *H-ras* mutations caused by DMBA initiation. Indeed, *H-ras* mutations were detected in 9 out of 17 tumors (53%) at codon 61 in exon 2 of the gene. No *K-ras* mutations were found in any of these tumors (data not shown). However, the mechanisms underlying the activation of the PI3K/Akt pathway upon *TβRI* deletion warrant further investigation. A proposed TGF-β signaling alteration that promotes HNSCC in mice through activation of PI3K/Akt pathway is shown in Fig. 6.

Discussion

TGF-β is a potent growth inhibitor for epithelial cells (34). Inactivating mutations or experimental deletion of components of the TGF-β pathway have been shown to promote tumorigenesis in a variety of organ systems (35,36). However, the precise role of TGF-β signaling in head and neck carcinogenesis has not been fully understood. As with other organ systems, existing research has been mainly focused on TGFBR2. Inactivation of *Tgfbr2* by overexpression of dominant negative receptor constructs or by targeted deletion promotes tumorigenesis in the mammary gland, prostate, pancreas, anogenital region, as well as in the head and neck area (37–40,14). With one exception (40), inactivation of *Tgfbr2* does not result in tumor formation unless cooperating oncogenic lesions are present, suggesting that loss of TGF-β response plays a tumor promoting rather than initiating role (14,41). Interestingly, mice that harbored an inactivated *Tgfbr2* in stromal cells developed intraepithelial neoplasia of the prostate and invasive SCCs in the forestomach. This suggests that alterations in the TGF-β signaling pathway within cells of the tumor microenvironment can also contribute to cancer development and progression (38). Even in cases where the TGF-β pathway is compromised specifically in the epithelium, the effects of this perturbation appear to extend to the stroma. Thus mice with inactivated *Tgfbr2* in the mammary epithelium show increased recruitment of $F4/80^+$ cells, increased expression of pro-inflammatory genes, and altered composition of the fibrovascular stroma- all effects that may promote further tumor progression (42). It is clear that perturbations in TGF-β signaling can have far reaching effects throughout the ecosystem of the tumor.

It is important to note that TGFBR2 not only interacts with TGFBR1, but also forms functional complexes with other type I receptors such as ActRI/ALK2, ALK3 or ALK1 (43,44). Signaling through TGFBR2/Alk1 complexes activates Smad1, Smad5, and Smad8, whereas signaling through the TGFBR2/TGFBR1 complex results in phosphorylation of Smad2 and Smad3. In fact, TGF-β signaling through TGFBR1 and ALK1, in a complex with TGFBR2, showed opposing activities in endothelial cell migration and proliferation (45). Importantly, in epithelial cells TGFBR2 can also directly phosphorylate Par6 without involvement of TGFBR1, and release Par6 from the Par6-TGFBR1 complex. This allows Par6 to trigger the dissolution of tight junctions in the context of epithelial-mesenchymal transitions (46). Therefore, knocking out *Tgfbr2* affects not only Smad-mediated TGF-β signaling, but also direct receptor-II–mediated alternative signaling via Par6. Thus knocking out TGFBR1 or TGFBR2 individually could affect downstream signaling differently, leading to distinct biological outcomes.

TGFBR1 forms heterotetrameric complexes with TGFBR2 on the cell surface and is critical for the downstream phosphorylation and activation of the Smads. Mutations and polymorphisms of *TGFBR1* have been described; *TGFBR1(6A)*, a 9 bp deletion coding for 3 alanine residues within the 9 alanine repeat region of exon 1, has been particularly associated with HNSCC (15–17). In an earlier study, we showed that 35% of mice with a targeted deletion of *Tgfbr1* developed spontaneous SCCs in periorbital and/or perianal regions (19). To specifically study the role of Tgfbr1-mediated signaling in the progression of HNSCCs, we developed a novel inducible knockout mouse model by deleting *Tgfbr1* in head and neck epithelia.

Most of our findings on the *Tgfbr1* cKO mouse model are consistent with the findings from DMBA-initiated *Tgfbr2* cKO mice (14), suggesting that *Tgfbr1* functions similarly to *Tgfbr2* in the progression of HNSCCs. The lack of spontaneous tumor formation in *Tgfbr1* cKO mice, together with the fact that DMBA treatment facilitates tumor development in these mice, suggests that rather than initiation, loss of *Tgfbr1* may play a more crucial role in tumor progression in mouse HNSCC. This is also the case for other epithelia, with the sole exception

of the anogenital region (40). However, several differences have also been noted in our DMBA-initiated *Tgfbr1* cKO mice compared with DMBA-initiated *Tgfbr2* cKO mice. For example, none of our DMBA-initiated *Tgfbr1* heterozygous mice (*K14-CreER^{tam};Tgfbr1$^{f/+}$*) developed HNSCCs, while about 33% of mice with a heterozygous *Tgfbr2* deletion (*K5-CrePR1;Tgfbr2$^{f/+}$*) in the head and neck epithelia developed HNSCCs after DMBA initiation. Therefore tumor suppressor activities of TGF-β require a higher threshold level of Tgfbr2 than of Tgfbr1. Furthermore, only 16% of our DMBA-initiated *Tgfbr1* cKO mice with tumors developed metastases in jugular lymph nodes and/or lungs by the time the mice were dissected. However, up to 35% of the DMBA-initiated *Tgfbr2* cKO mice developed jugular lymph node metastases by 20–39 wks of age. While this difference between the two mouse models may be attributable to differences in mouse genetic background and/or the *Cre* mouse line being used in the studies, it may also indicate that Tgfbr1 and Tgfbr2 function differently. For example, Tgfbr2 may have more suppressive effects in later stages of cancer development, possibly due to TGFBR1-independent effects.

It is widely believed that TGF-β can affect cancer progression through both autocrine and paracrine effects. Paracrine effects of TGF-β, which are generally tumor promoting, include stimulation of inflammation and angiogenesis, escape from immunosurveillance, and recruitment of myofibroblasts. Autocrine effects of TGF-β in premalignant epithelial cells are tumor suppressive, while more advanced cancer cells with a functional TGF-β receptor complex may exhibit tumor-promoting autocrine effects, due to a convergence of TGF-β signaling with other signaling pathways (47). In the current study, we saw evidence for both types of effect. We found that upon deletion of *Tgfbr1* in mouse head and neck epithelia, there is an enhanced cell proliferation and down-regulation of cell cycle inhibitors, due to inactivation of Smad2/3 mediated signaling. An inhibition of apoptosis through activation of the PI3K/Akt pathway in SCCs that developed in *Tgfbr1* cKO mice was also observed. These results suggest that in the head and neck epithelia, TGF-β is an early tumor suppressor. In the SCCs that developed in *Tgfbr1* cKO mice, we found increased inflammation, angiogenesis, and myofibroblast formation. Similar results have been observed in other mouse models when TGF-β signaling was disrupted (14,48). Furthermore, elevated levels of endogenous TGF-β1 were detected in tumor stroma of *Tgfbr1* cKO mice, as they have been in other studies (14). Therefore, on one hand, the deletion of *Tgfbr1* in mouse head and neck epithelia prevents the surrounding increased TGF-β1 from exerting its tumor suppressive effects. On the other hand, the expression of Tgfbr1 in tumor stroma would certainly enhance its tumor promoting function through paracrine effects. Consequently, we believe that the elevated level of TGF-β1 in tumor stroma has direct involvement in the creation of microenvironment for tumor progression (4).

Alternative modes of TGF-β signaling have been categorized (8). Recent work showed that TGF-β induces apoptosis through repression of PI3K/Akt signaling, indicating that there may be negative crosstalk between the TGF-β tumor suppressor and PI3K/Akt pathways (49). The most notable finding of our current study is that in addition to inactivation of the Smad-dependent TGF-β signaling pathway and in spite of increased PTEN levels after deletion of *Tgfbr1* in mouse head and neck epithelia and DMBA treatment, the PI3K/Akt pathway is activated in all SCCs that developed in the *Tgfbr1* cKO mice. The results from our study indicate that decreased Tgfbr1 expression in *Tgfbr1* cKO mice leads to increased cell proliferation and cell survival through PTEN independent activation of PI3K/Akt pathway. This is possibly due to DMBA induced *H-ras* mutation as well as other unknown mechanisms. These changes accompanied by increased TGF-β1 in tumor stroma, which leads to increased invasion, angiogenesis, inflammation and immune suppression through paracrine effect of TGF-β, switch TGF-β signaling from tumor suppression in normal cells to tumor promotion in head and neck carcinogenesis of *Tgfbr1* cKO mice.

In summary, we generated an inducible conditional gene targeting mouse model for head and neck cancer research. We have demonstrated that targeted deletion of *Tgfbr1* in the head and neck epithelia is apparently not sufficient for spontaneous tumor formation, but could increase susceptibility to tumor development initiated by DMBA. TGF-β is a major tumor suppressor, and inactivation of TGF-β signaling, in the context of *ras* mutations and aberrant activation of the PI3K/Akt pathway, may contribute cooperatively to the promotion of head and neck carcinogenesis in these mice. Our results underscore a critical role of the TGF-β signaling pathway and its crosstalk with the PI3K/Akt pathway in suppressing head and neck carcinogenesis. These findings have significant implications for the development of effective therapeutic strategies targeting both the TGF-β and the PI3K/Akt pathways for the treatment of HNSCCs.

Acknowledgments

Grant support: Intramural Research Program, National Institute of Dental and Craniofacial Research, NIH.

We would like to thank Dr Stefan Karlsson for providing us with the *Tgfbr1* flox mice, Dr Hynda Kleinman for critical reading of this manuscript, Dr Raj Puri and Dr Andrew Doyle for helpful discussion, and Shelagh Powers for editorial assistance.

References

1. Jemal A, Siegel R, Ward E, et al. Cancer statistics, 2008. CA Cancer J Clin 2008;58:71–96. [PubMed: 18287387]
2. Kim MM, Califano JA. Molecular pathology of head-and-neck cancer. Int J Cancer 2004;112:545–53. [PubMed: 15382034]
3. Mao L, Hong WK, Papadimitrakopoulou VA. Focus on head and neck cancer. Cancer Cell 2004;5:311–6. [PubMed: 15093538]
4. Lu SL, Reh D, Li AG, et al. Overexpression of transforming growth factor beta1 in head and neck epithelia results in inflammation, angiogenesis, and epithelial hyperproliferation. Cancer Res 2004;64:4405–10. [PubMed: 15231647]
5. Qiu W, Schönleben F, Li X, Su GH. Disruption of transforming growth factor beta-Smad signaling pathway in head and neck squamous cell carcinoma as evidenced by mutations of SMAD2 and SMAD4. Cancer Lett 2007;245:163–70. [PubMed: 16478646]
6. Roberts AB, Wakefield LM. The two faces of transforming growth factor β in carcinogenesis. Proc Natl Acad Sci USA 2003;100:8621–3. [PubMed: 12861075]
7. Derynck R, Zhang YE. Smad-dependent and Smad-independent pathways in TGF-beta family signaling. Nature 2003;425:577–84. [PubMed: 14534577]
8. Massagué J. TGF-β in Cancer. Cell 2008;134:215–30. [PubMed: 18662538]
9. Engle SJ, Hoying JB, Boivin GP, Ormsby I, Gartside PS, Doetschman T. Transforming growth factor β1 suppresses nonmetastatic colon cancer at an early stage of tumorigenesis. Cancer Res 1999;59:3379–86. [PubMed: 10416598]
10. Pick E, Roberts AB. Suppressor and oncogenic roles of transforming growth factor-beta and its signaling pathways in tumorigenesis. Adv Cancer Res 2001;83:1–54. [PubMed: 11665716]
11. Tang B, Vu M, Booker T, et al. TGF-beta switches from tumor suppressor to prometastatic factor in a model of breast cancer progression. J Clin Invest 2003;112:1116–24. [PubMed: 14523048]
12. Xie W, Bharathy S, Kim D, Haffty BG, Rimm DL, Reiss M. Frequent alterations of Smad signaling in human head and neck squamous cell carcinomas: a tissue microarray analysis. Oncol Res 2003;14:61–73. [PubMed: 14649540]
13. Huntley SP, Davies M, Matthews JB, et al. Attenuated type II TGF-beta receptor signaling in human malignant oral keratinocytes induces a less differentiated and more aggressive phenotype that is associated with metastatic dissemination. Int J Cancer 2004;110:170–6. [PubMed: 15069677]

14. Lu SL, Herrington H, Reh D, et al. Loss of transforming growth factor-beta type II receptor promotes metastatic head-and-neck squamous cell carcinoma. Genes Dev 2006;20:1331–42. [PubMed: 16702406]
15. Chen T, Yan W, Wells RG, et al. Novel inactivating mutations of transforming growth factor-beta type I receptor gene in head-and-neck cancer metastases. Int J Cancer 2001;93:653–61. [PubMed: 11477574]
16. Knobloch TJ, Lynch MA, Song H, et al. Analysis of TGF-beta type I receptor for mutations and polymorphisms in head and neck cancers. Mutat Res 2001;479:131–9. [PubMed: 11470488]
17. Pasche B, Knobloch TJ, Bian Y, et al. Somatic acquisition and signaling of TGFBR1*6A in cancer. JAMA 2005;294:1634–46. [PubMed: 16204663]
18. Larsson J, Goumans MJ, Sjöstrand LJ, et al. Abnormal angiogenesis but intact hematopoietic potential in TGF-beta type I receptor-deficient mice. EMBO J 2001;20:1663–73. [PubMed: 11285230]
19. Honjo Y, Bian Y, Kawakami K, et al. TGF-beta receptor I conditional knockout mice develop spontaneous squamous cell carcinoma. Cell Cycle 2007;6:1360–6. [PubMed: 17534148]
20. Vasioukhin V, Degenstein L, Wise B, Fuchs E. The magical touch: genome targeting in epidermal stem cells induced by tamoxifen application to mouse skin. Proc Natl Acad Sci U S A 1999;96:8551–6. [PubMed: 10411913]
21. Czerninski R, Amornphimoltham P, Patel V, Molinolo AA, Gutkind JS. Targeting mammalian target of rapamycin by rapamycin prevents tumor progression in an oral-specific chemical carcinogenesis model. Cancer Prev Res 2009;2:27–36.
22. Weidner N, Semple JP, Welch WR, Folkman J. Tumor angiogenesis and metastasis--correlation in invasive breast carcinoma. N Engl J Med 1991;324:1–8. [PubMed: 1701519]
23. Liu Y, Zhang P, Li J, Kulkarni AB, Perruche S, Chen W. A critical function for TGF-beta signaling in the development of natural CD4+CD25+Foxp3+ regulatory T cells. Nat Immunol 2008;9:632–40. [PubMed: 18438410]
24. Kim TW, Chen Q, Shen X, et al. Oral mucosal carcinogenesis in SENCAR mice. Anticancer Res 2002;22:2733–40. [PubMed: 12529989]
25. Chen Z, Malhotra PS, Thomas GR, et al. Expression of proinflammatory and proangiogenic cytokines in patients with head and neck cancer. Clin Cancer Res 1999;5:1369–79. [PubMed: 10389921]
26. Goulart Filho JA, Nonaka CF, da Costa Miguel MC, de Almeida Freitas R, Galvão HC. Immunoexpression of cyclooxygenase-2 and p53 in oral squamous cell carcinoma. Am J Otolaryngol 2009;30:89–94. [PubMed: 19239949]
27. Wikström P, Lissbrant IF, Stattin P, Egevad L, Bergh A. Endoglin (CD105) is expressed on immature blood vessels and is a marker for survival in prostate cancer. Prostate 2002;51:268–75. [PubMed: 11987155]
28. Orimo A, Gupta PB, Sgroi DC, et al. Stromal fibroblasts present in invasive human breast carcinomas promote tumor growth and angiogenesis through elevated SDF-1/CXCL12 secretion. Cell 2005;121:335–48. [PubMed: 15882617]
29. Lewis MP, Lygoe KA, Nystrom ML, et al. Tumour-derived TGF-beta1 modulates myofibroblast differentiation and promotes HGF/SF-dependent invasion of squamous carcinoma cells. Br J Cancer 2004;90:822–32. [PubMed: 14970860]
30. Smyth MJ, Dunn GP, Schreiber RD. Cancer immunosurveillance and immunoediting: the roles of immunity in suppressing tumor development and shaping tumor immunogenicity. Adv Immunol 2006;90:1–50. [PubMed: 16730260]
31. Kim BG, Li C, Qiao W, et al. Smad4 signalling in T cells is required for suppression of gastrointestinal cancer. Nature 2006;441:1015–9. [PubMed: 16791201]
32. Molinolo AA, Amornphimoltham P, Squarize CH, Castilho RM, Patel V, Gutkind JS. Dysregulated molecular networks in head and neck carcinogenesis. Oral Oncol. 2008
33. Eng C. PTEN: one gene, many syndromes. Hum Mutat 2003;22:183–98. [PubMed: 12938083]
34. Massagué J, Gomis RR. The logic of TGF-β signaling. FEBS Lett 2006;580:2811–20. [PubMed: 16678165]
35. Levy L, Hill CS. Alterations in components of the TGF-beta superfamily signaling pathways in human cancer. Cytokine Growth Factor Rev 2006;17:41–58. [PubMed: 16310402]

36. Bierie B, Moses HL. Tumour microenvironment: TGFbeta: the molecular Jekyll and Hyde of cancer. Nat Rev Cancer 2006;6:506–20. [PubMed: 16794634]
37. Siegel PM, Shu W, Cardiff RD, Muller WJ, Massagué J. Transforming growth factor beta signaling impairs Neu-induced mammary tumorigenesis while promoting pulmonary metastasis. Proc Natl Acad Sci U S A 2003;100:8430–5. [PubMed: 12808151]
38. Bhowmick NA, Chytil A, Plieth D, et al. TGF-beta signaling in fibroblasts modulates the oncogenic potential of adjacent epithelia. Science 2004;303:848–51. [PubMed: 14764882]
39. Ijichi H, Chytil A, Gorska AE, et al. Aggressive pancreatic ductal adenocarcinoma in mice caused by pancreas-specific blockade of transforming growth factor-beta signaling in cooperation with active Kras expression. Genes Dev 2006;20:3147–60. [PubMed: 17114585]
40. Guasch G, Schober M, Pasolli HA, Conn EB, Polak L, Fuchs E. Loss of TGFbeta signaling destabilizes homeostasis and promotes squamous cell carcinomas in stratified epithelia. Cancer Cell 2007;12:313–27. [PubMed: 17936557]
41. Biswas S, Chytil A, Washington K, et al. Transforming growth factor beta receptor type II inactivation promotes the establishment and progression of colon cancer. Cancer Res 2004;64:4687–92. [PubMed: 15256431]
42. Bierie B, Stover DG, Abel TW, et al. Transforming growth factor-beta regulates mammary carcinoma cell survival and interaction with the adjacent microenvironment. Cancer Res 2008;68:1809–19. [PubMed: 18339861]
43. Feng XH, Derynck R. Specificity and versatility in tgf-beta signaling through Smads. Annu Rev Cell Dev Biol 2005;21:659–93. [PubMed: 16212511]
44. Daly AC, Randall RA, Hill CS. Transforming growth factor beta-induced Smad1/5 phosphorylation in epithelial cells is mediated by novel receptor complexes and is essential for anchorage-independent growth. Mol Cell Biol 2008;28:6889–902. [PubMed: 18794361]
45. Goumans MJ, Valdimarsdottir G, Itoh S, Rosendahl A, Sideras P, ten Dijke P. Balancing the activation state of the endothelium via two distinct TGF-beta type I receptors. EMBO J 2002;21:1743–53. [PubMed: 11927558]
46. Ozdamar B, Bose R, Barrios-Rodiles M, Wang HR, Zhang Y, Wrana JL. Regulation of the polarity protein Par6 by TGFbeta receptors controls epithelial cell plasticity. Science 2005;307:1603–9. [PubMed: 15761148]
47. De Wever O, Mareel M. Role of tissue stroma in cancer cell invasion. J Pathol 2003;200:429–47. [PubMed: 12845611]
48. Go C, Li P, Wang XJ. Blocking transforming growth factor beta signaling in transgenic epidermis accelerates chemical carcinogenesis: a mechanism associated with increased angiogenesis. Cancer Res 1999;59:2861–8. [PubMed: 10383147]
49. Wang J, Yang L, Yang J, et al. Transforming growth factor beta induces apoptosis through repressing the phosphoinositide 3-kinase/AKT/survivin pathway in colon cancer cells. Cancer Res 2008;68:3152–60. [PubMed: 18451140]

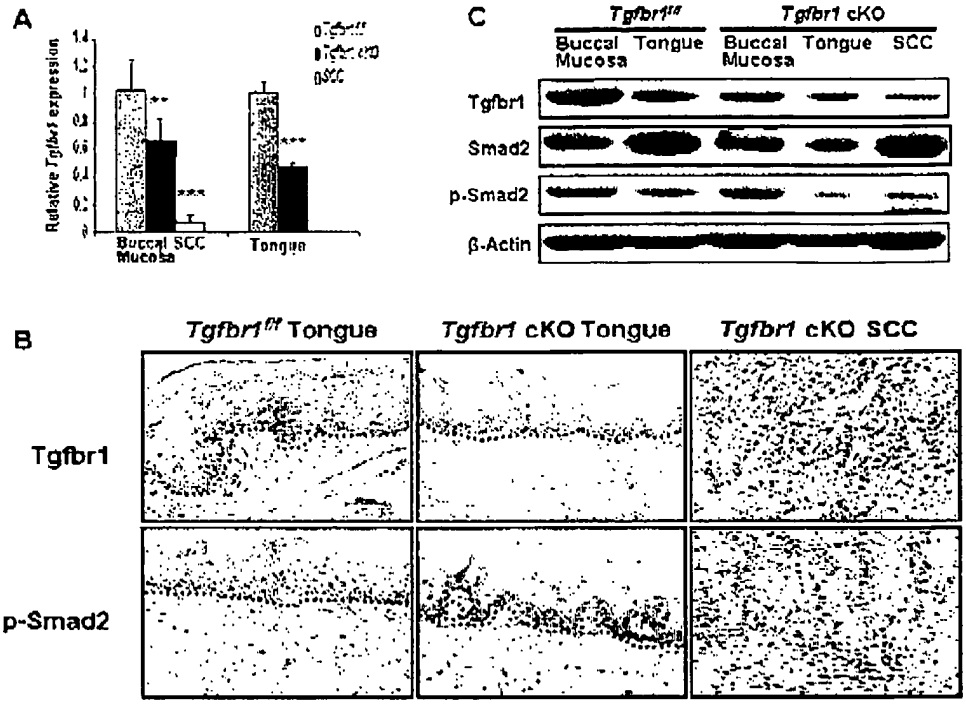

Figure 1.

Decreased TGF-β signaling in *Tgfbr1* cKO mice. *A. Tgfbr1* mRNA significantly reduced in the head and neck epithelia and SCCs of *Tgfbr1* cKO mice by qRT-PCR (n=3). **, P<0.01; ***, P<0.001. *B.* Tgfbr1 and p-Smad2 expression were reduced in the tongue and SCC of *Tgfbr1* cKO mice by IHC. The dotted lines delineate the adjacent epithelial compartment. The changes in staining patterns are seen in the epithelium (above the dotted line) in which *Tgfbr1* was knocked out. *Bar*, 50μm. *C.* Western blot analysis demonstrates that Tgfbr1 and p-Smad2 were reduced in buccal mucosa, tongue and SCCs of *Tgfbr1* cKO mice compared to that of *Tgfbr1*$^{f/f}$ mice.

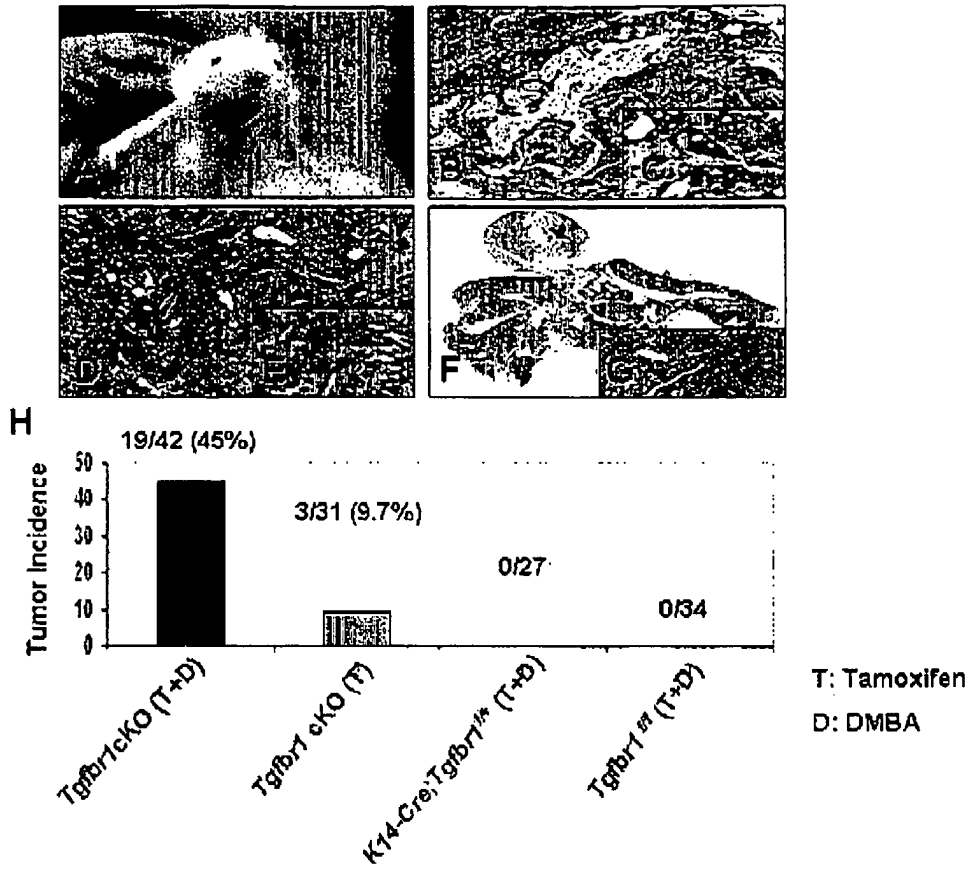

Figure 2.

DMBA-initiated *Tgfbr1* cKO mice develop HNSCCs. *A*, Tumor developed in the oral cavity of *Tgfbr1* cKO mice. Pathological sections of oral squamous cell carcinoma (*B*) and infiltrating squamous cell carcinoma (*D*); (*F*) Low magnification of the heart (thick black arrow) and lung block. Examples of intrapulmonary metastases are indicated by black arrows; extrapulmonary (lymph nodes) with a white arrow, and non-compromised lung parenchyma by a block white arrow. Inset: the metastasis (black block arrow) is surrounded by compressed lung parenchyma (white block arrow). The arrow indicates a bronchus. The insets in (*C*), (*E*) and (*G*) depict fine details of the malignant cells (magnifications, 20× and 200× for main figure and inset, respectively). *H*, DMBA-treated *Tgfbr1* cKO mice develop SCCs more frequently than *Tgfbr1* cKO mice. No tumors were observed in *K14-CreER*^{tam};*Tgfbr1*$^{f/+}$ or *Tgfbr1*$^{f/f}$ control littermates during 1 year of observation after TM and DMBA treatment.

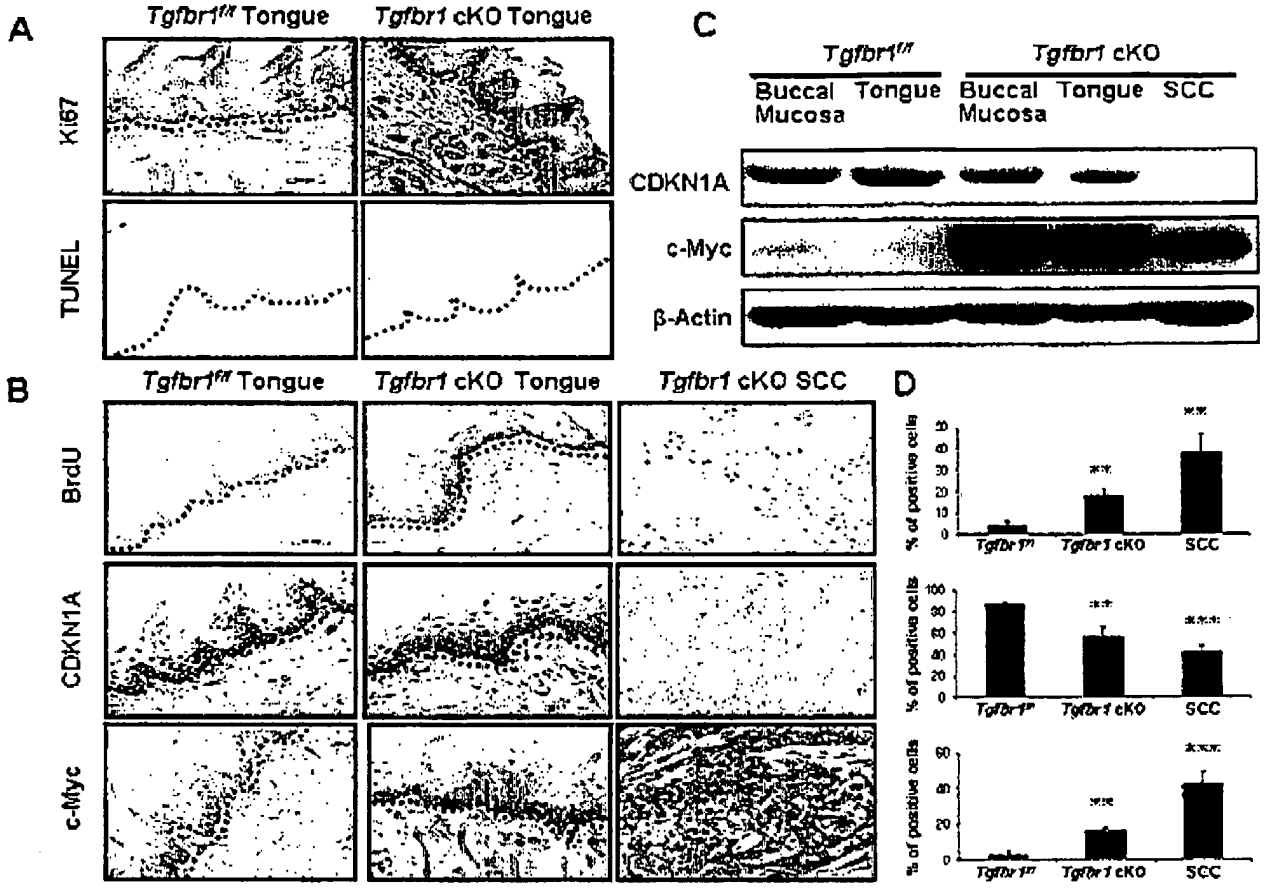

Figure 3.

Enhanced growth-promotion and down-regulation of cell cycle inhibitors in *Tgfbr1* cKO mice. *A*, Increased expression of Ki67 and loss of apoptosis in the basal layer of tongue of the *Tgfbr1* cKO mice 4 weeks after TM and DMBA treatment. ***B***, A significantly increased number of proliferative cells in tongue and SCCs of *Tgfbr1* cKO mice by BrdU assays. CDKN1A expression was reduced in tongue and SCCs of *Tgfbr1* cKO mice compared to that in *Tgfbr1*$^{f/f}$ mice. In contrast, c-Myc was overexpressed in tongue of *Tgfbr1* cKO mice and its expression was even more remarkable in SCCs. The results were further confirmed by Western blot (***C***). ***D***, Percentage of positive cells in tongue or SCCs of *Tgfbr1* cKO mice compared with that of *Tgfbr1*$^{f/f}$ mice. *Columns*, average of three to five immunostained sections; the dotted lines delineate the adjacent epithelial compartment. *Bar*, 50 μm. **, $P<0.01$; ***, $P<0.001$.

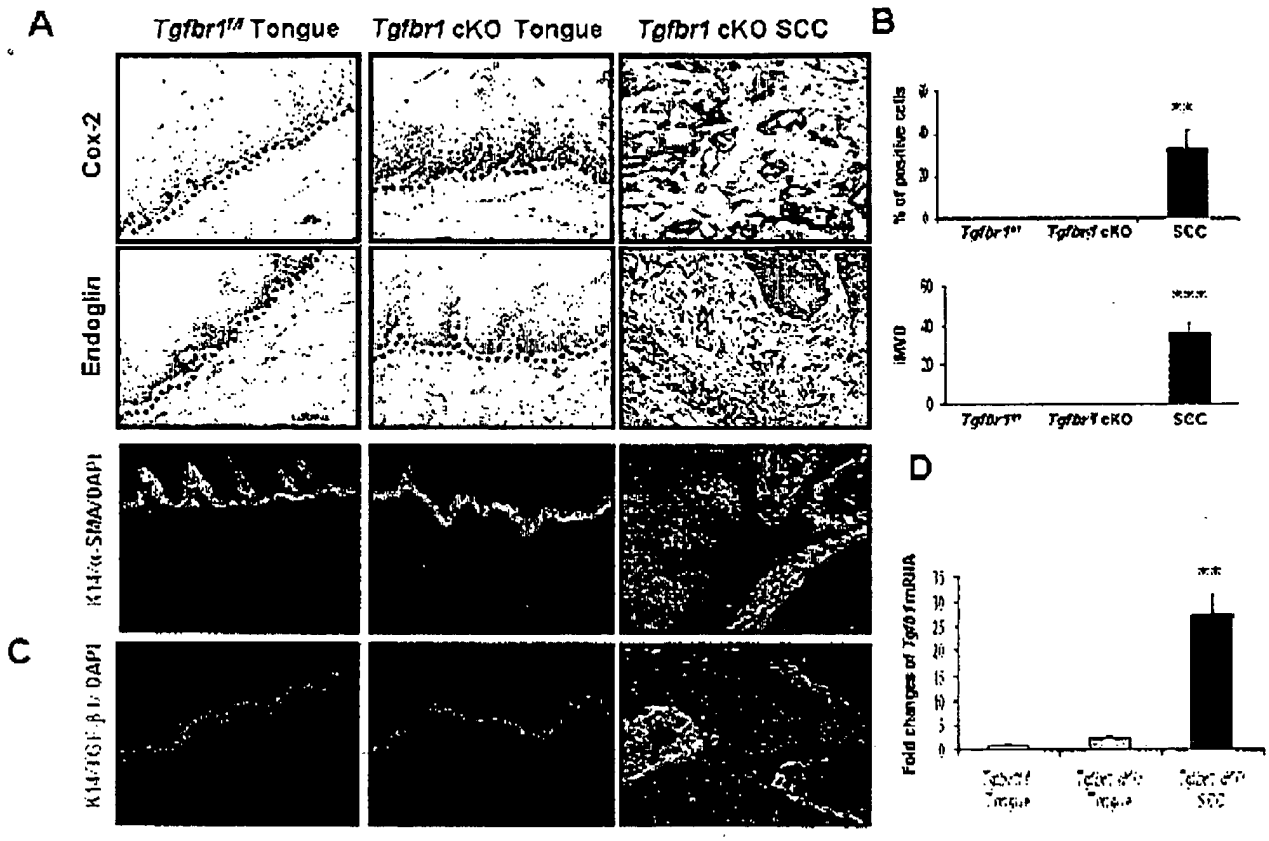

Figure 4.

A, Enhanced paracrine effects of TGF-β in *Tgfbr1* cKO mice. *A*, Significantly increased expression of Cox-2 in SCCs as well as overexpression of Endoglin (CD105), α-SMA in the stroma surrounding SCCs of *Tgfbr1* cKO mice (magnifications, 200×). No expression was detected in normal tongue of $Tgfbr1^{f/f}$ or *Tgfbr1* cKO mice. The dotted lines delineate the adjacent epithelial compartment. *Bar*, 50 μm. *B*, Percentage of Cox-2 positive cells and intratumoral microvessel density (iMVD) indicated by Endoglin (CD105)-stained microvessels per 200 × field in tumor stroma of *Tgfbr1* cKO mice. *Columns*, five immunostained sections. **, $P<0.01$; ***, $P<0.001$. *C*, Tgfb1 expression in the tumor stroma by immunofluorescent staining (magnifications, 200×). *D*, *Tgfb1* mRNA expression by qRT-PCR.

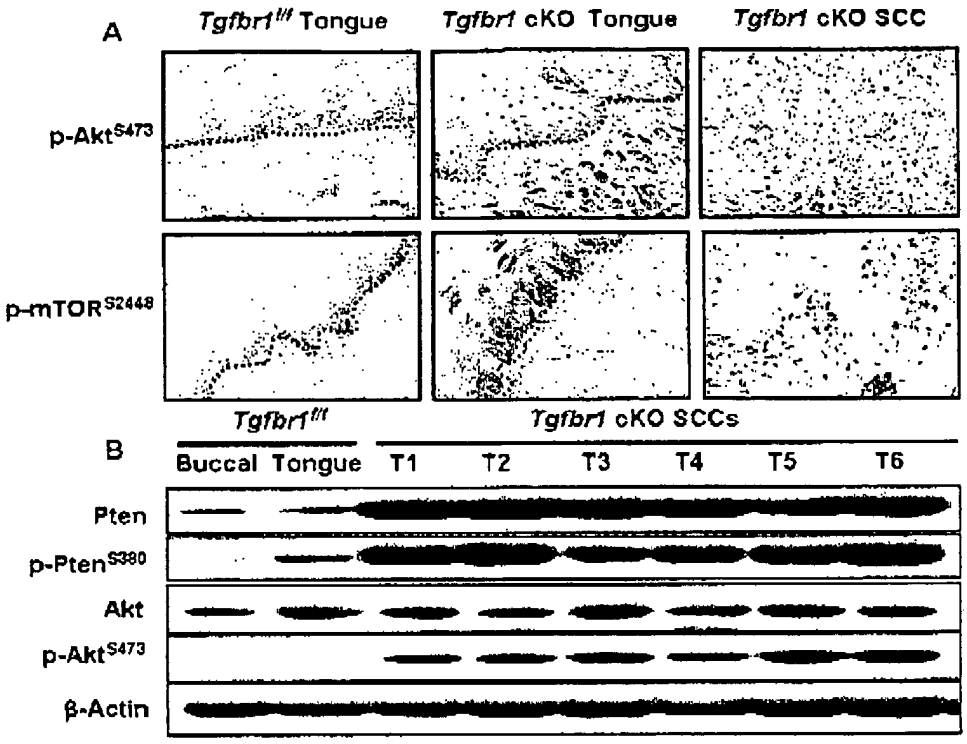

Figure 5.

Activation of the PI3K/Akt pathway in *Tgfbr1* cKO mice. *A*, Immunostaining revealed a significantly increased number of positive cells of p-Akt, p-mTOR in the SCCs that developed in *Tgfbr1* cKO mice. The dotted lines delineate the adjacent epithelial compartment. *Bar*, 50 μm. *B*, A significantly increased level of unphosphorylated PTEN, an active form of the protein, was detected in all SCCs that developed in the DMBA-treated *Tgfbr1* cKO mice. However, comparable elevated levels of the phosphorylated form of Akt (p-Akt) were also observed in SCCs by Western blot analysis.

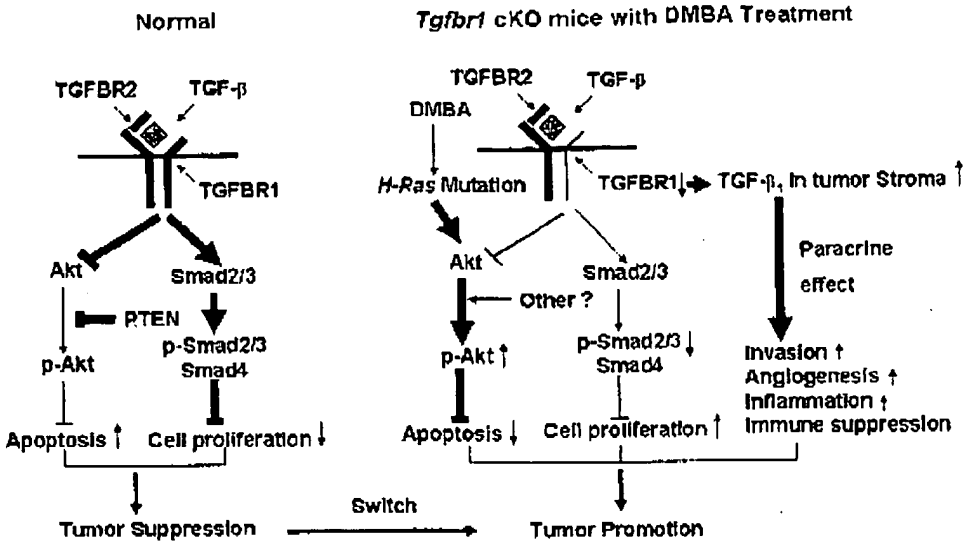

Figure 6.

A schematic presentation of the proposed TGF-β signaling alteration that promotes HNSCC in mice. In normal cells, TGF-β inhibits cell proliferation through the Smad-dependent pathway. It also induces apoptosis by repressing the PI3K/Akt pathway results in tumor suppression. Decreased Tgfbr1 expression in *Tgfbr1* cKO mice leads to increased cell proliferation and cell survival through PTEN independent activation of the PI3K/Akt pathway. DMBA treatment, which causes *H-ras* mutation as well as other mechanisms, may also play an important role in Akt activation. Decreased TGFBR1 can also increase TGF-β1 in tumor stroma by as yet unidentified mechanisms, which leads to increased invasion, angiogenesis, and inflammation, as well as immune suppression through the paracrine effect of TGF-β. In summary, inactivation of TGF-β signaling, in the context of *ras* mutations and aberrant activation of the PI3K/Akt pathway and accompanied by increased paracrine effect of TGF-β, switches TGF-β signaling from tumor suppression in normal cells to tumor promotion in head and neck carcinogenesis of *Tgfbr1* cKO mice.

Human Pathology (2009) 40, 1408–1417

ELSEVIER

Human PATHOLOGY

www.elsevier.com/locate/humpath

Original contribution

Dysregulated PI3K/Akt/PTEN pathway is a marker of a short disease-free survival in node-negative breast carcinoma

Alessandra Capodanno PhD[a], Andrea Camerini MD[b,c], Cinzia Orlandini MD[b], Editta Baldini MD[b], Maria Letizia Resta MD[d], Generoso Bevilacqua MD[a], Paola Collecchi PhD[a,*]

[a]*Division of Surgical, Molecular and Ultrastructural Pathology, University of Pisa and Pisa University Hospital, 56126 Pisa, Italy*
[b]*Division of Medical Oncology, University of Pisa and Pisa University Hospital, 56126 Pisa, Italy*
[c]*Division of Medical Oncology, Versilia Hospital, 55041 Lido di Camaiore-Lucca, Italy*
[d]*Clinical Pathology, University of Messina, 98100 Messina, Italy*

Received 1 November 2008; revised 12 February 2009; accepted 13 February 2009

Keywords:
PI3K/Akt/PTEN pathway;
Tumor progression;
Node-negative breast carcinoma;
Prognosis

Summary The phosphoinositide 3-kinase/Akt pathway is involved in the pathogenesis of several human cancers. In this study, the biological and prognostic value of phosphoinositide 3-kinase/Akt pathway dysregulation was assessed by immunohistochemistry in a well-characterized series of 72 patients with node-negative breast cancer with a long-term follow-up. Phosphorylated Akt and PTEN expression was reduced in 32% and 12.5% of the tumors, respectively. Phosphorylated Akt or PTEN status was not associated with the main clinicopathologic and biological parameters, whereas their expression was tightly related to their downstream targets cyclin D1 and $p27^{Kip1}$ which are involved in cell proliferation. Survival analysis showed a strong association between a shorter disease-free survival and the dysregulated expression of phosphorylated Akt ($P = .036$), PTEN ($P = .003$), $p27^{Kip1}$ ($P = .008$), and Ki67 ($P = .0007$), or the distinct subtypes of breast tumors (luminal, HER2 overexpressing, and basal-like; $P = .03$). Moreover, multivariate analysis using the Cox proportional-hazards regression model showed that PTEN and Ki67 were independent predictive factors of disease recurrence and that their simultaneous dysregulation strongly increased the hazards ratio of the patients with node-negative breast cancer (hazards ratio, 38.30; $P = .0014$). In conclusion, our results show that the dysregulation of the phosphoinositide 3-kinase/Akt/PTEN pathway is relevant to the prognosis in node-negative breast carcinoma and that the evaluation of key components of this pathway might be a useful tool to identify the patients with node-negative breast cancer at high-risk of disease recurrence.

1. Introduction

Patients with node-negative breast cancer have an excellent prognosis despite a 10-year recurrence rate of 30%. Several prognostic and/or predictive factors have been proposed to identify the patients at high risk of disease

Abbreviations: CI, confidence interval; CK, cytokeratin; DFS, disease-free survival; ER, estrogen receptor; HR, hazards ratio; pAkt, phosphorylated Akt; PI3K, phosphoinositide 3-kinase; PIP_2, phosphatidylinositol-3,4-bisphosphate; PIP_3, phosphatidylinositol-3,4,5-trisphosphate; PTEN, phosphatase tensin homologue deleted on chromosome 10.

* Corresponding author.
E-mail address: p.collecchi@med.unipi.it (P. Collecchi).

0046-8177/$ – see front matter © 2009 Elsevier Inc. All rights reserved.
doi:10.1016/j.humpath.2009.02.005

recurrence. However, they do not accurately predict the clinical outcome of patients with node-negative breast cancer and the research of reliable prognostic markers remains the main purpose in many studies.

The dysregulation of the phosphoinositide 3-kinase (PI3K)/Akt pathway has been recently found to be involved in the pathogenesis of several human cancers, such as breast, colon, ovarian, pancreas, and prostate cancer [1-3]. The PI3K/Akt pathway regulates essential cell functions, such as cell proliferation, cell growth, apoptosis, metabolism, transcription, protein synthesis, angiogenesis, and tissue invasion [4,5].

The activation of PI3K by receptors with protein tyrosine kinase activity or coupled with G proteins leads to the phosphorylation of cell membrane phosphatidylinositol at the D3 position of the inositol ring, thereby generating phosphatidylinositol-3,4-bisphosphate (PIP_2) and phosphatidylinositol-3,4,5-trisphosphate (PIP_3). PIP_2 and PIP_3 act as a docking site and bind to the pleckstrin homology domain of the serine/threonine kinase Akt, leading to its recruitment to the inner plasma membrane. PIP_2 and PIP_3 binding causes a conformational change in Akt that results in the exposure of 2 conserved threonine and serine residues lying within the kinase and regulatory domain, respectively, and in subsequent kinase activation [4,5]. Akt plays a key role in a variety of cell processes that are relevant to cancer cells, affecting cell survival, proliferation, cell growth, and invasion, through the phosphorylation of several downstream substrates [1-5].

The major antagonist of the Akt kinase is the dual-specificity protein and lipid phosphatase PTEN (phosphatase tensin homologue deleted on chromosome 10) that counteracts the PI3K-dependent Akt activation by dephosphorylating the D3 position of PIP_2 and PIP_3 [6]. Several studies have shown that PTEN plays an important role in the regulation of apoptosis and cell cycle through its lipid and protein phosphatase activity, respectively [7-9]. PTEN affects apoptosis through the inhibition of Akt phosphorylation and the upregulation of the cyclin-dependent kinase inhibitor $p27^{Kip1}$ via its lipid phosphatase activity [7-10], and cell cycle through the downregulation of the mitogen-activated protein kinase pathway and cyclin D1 protein level and nuclear localization via its protein phosphatase activity [7-11].

PTEN expression is lost by mutation, deletion, or promoter methylation at high frequency in many primary and metastatic human cancers [12-14]. The observation that *PTEN* gene alterations occur in the advanced stages of a large number of tumors and the involvement of PTEN in cell migration and focal adhesion formation in tumor cells suggest that loss of PTEN activity might have an important role in tumor invasion and metastatic progression [12-15].

Based on the key role of the PI3K/Akt/PTEN pathway in cancer pathogenesis and progression, we investigated the potential prognostic value of this pathway in patients with node-negative breast cancer to identify the patients at high risk of disease recurrence. To this purpose, we analyzed the expression of phosphorylated Akt (pAkt) and PTEN in relation to the tumor features, some proteins of the PI3K/Akt/PTEN pathway involved in cell proliferation, and patients' survival.

2. Materials and methods

2.1. Patient characteristics and tissue samples

Seventy-two consecutive node-negative breast carcinomas from patients with primary diagnosis of breast cancer were collected at the Santa Chiara University Hospital of Pisa (Italy) between 1988 and 1998. The node-negative status was defined according to the TNM system after axillary node dissection or sentinel lymphadenectomy for 10 of the 72 patients.

Patients who had undergone quadrantectomy received complementary radiotherapy. According to individual risk factors, the patients received chemotherapy and/or hormonal therapy. The chemotherapy treatment was an association of cyclophosphamide, methotrexate, and 5-fluorouracil or an anthracycline-containing regimen, whereas the hormonal treatment mainly consisted of tamoxifen. The relapsed and not-relapsed groups included a similar percentage of patients who received chemotherapy, hormonal therapy, or no therapy.

Histologic type, tumor size, and tumor grade according to the Bloom and Richardson method were evaluated (Table 1). The median age of the patients at diagnosis was 55 years (range, 34-82 years). The median follow-up was 10 years and 23 (32%) of the 72 patients relapsed within 5 years from diagnosis.

The selection of the patients did not require approval by the institutional ethics committee because samples were coded and the names of the patients were not revealed. Survival data were obtained from the medical records or from the local registry office.

2.2. Immunohistochemistry

PTEN, pAkt, estrogen receptor (ER), Ki67, HER2, cytokeratin 5/6 (CK 5/6), cyclin D1, and $p27^{Kip1}$ expression was evaluated by immunohistochemistry. Tumor sections (3 μm) from formalin-fixed and paraffin-embedded tissues were immunostained using monoclonal antibodies against human PTEN (clone A2B1; Santa Cruz Biotech, Santa Cruz, CA), phospho-Akt (Ser473) (clone 587F11; Cell Signalling, Danvers, MA), ER (clone 6F11; Ventana Medical Systems, Tucson, AZ), Ki67 (clone MIB1; Immunotech, Marseille, France), HER2 (clone 4B5, Ventana Medical Systems), CK 5/6 (clone D5/16B4, Ventana Medical Systems), cyclin D1 (clone DCS-6; Novocastra, Florence, Italy), and $p27^{Kip1}$ (clone 57; BD Transduction Lab, San Diego, CA). Anti-PTEN, pAkt, $p27^{Kip1}$, cyclin D1, and Ki67 antibodies were diluted 1:100, whereas ER, HER2, and CK 5/6 antibodies were applied without dilution.

Table 1 PTEN and pAkt expression in relation to the clinicopathologic features and biological markers in 72 consecutive patients with node-negative breast cancer

Parameter	PTEN$^-$	PTEN$^+$	*P* value[a]	pAkt$^-$	pAkt$^+$	*P* value[a]
pAkt status[b]						
pAkt$^+$	23 (36)	40 (64)	.07			
pAkt$^-$	0 (0)	9 (100)				
Age						
≤50 y	8 (31)	18 (69)	.80	2 (8)	24 (92)	.57
>50 y	15 (33)	31 (67)		7 (15)	39 (85)	
Tumor size						
pT1 ≤ 2 cm	14 (30)	33 (70)	.56	5 (11)	42 (89)	.73
pT2 > 2 cm	9 (36)	16 (64)		4 (16)	21 (84)	
Histology						
Ductal	21 (30)	48 (70)	.49	9 (13)	60 (87)	.82
Lobular	2 (67)	1 (33)		0 (0)	3 (100)	
Tumor grade						
I	3 (37)	5 (63)	.98	1 (12)	7 (88)	.14
II	11 (28)	28 (72)		3 (8)	36 (92)	
III	7 (32)	15 (68)		5 (23)	17 (77)	
ER status[b]						
ER$^+$	15 (33)	30 (67)	.87	6 (13)	39 (87)	.90
ER$^-$	8 (30)	19 (70)		3 (11)	24 (89)	
Ki67 status[b]						
Ki67$^+$	12 (32)	25 (68)	.81	4 (11)	33 (89)	.60
Ki67$^-$	11 (31)	24 (69)		5 (14)	30 (86)	
Molecular classification						
Luminal	15 (33)	30 (67)	.37	6 (13)	39 (87)	.97
HER2 overexpressing	1 (10)	9 (90)		1 (10)	9 (90)	
Basal-like	7 (41)	10 (59)		2 (12)	15 (88)	
Disease recurrence						
No evidence of disease	10 (20)	39 (80)	*.005*	9 (18)	40 (82)	.07
Relapse	13 (56)	10 (44)		0 (0)	23 (100)	

NOTE. Values are shown as *n* (%).

[a] *P* value assessed using χ^2 test. Significant *P* values are in italics.

[b] Cut-off ≥10% positive cells or nuclei.

Briefly, deparaffinized sections were rehydrated through a graded series of alcohols and endogenous peroxidase activity was blocked with 1% H_2O_2 in methanol. Antigen retrieval was performed by microwave irradiation at 750 W for 15 minutes in 10 mmol/L sodium citrate buffer (pH 6.0). The immunoperoxidase (avidin-biotin-peroxidase complex) technique was applied using an automatic immunostaining device (Ventana Medical Systems). Negative controls were obtained omitting the primary antibodies. Normal glandular epithelium and vascular endothelial cells were used as internal positive controls for PTEN and pAkt [16], whereas for the other analyzed markers specimens with known positive immunostaining were used as positive controls according to the manufacturers' instructions.

All slides were evaluated independently by 2 investigators and discrepant results were reviewed jointly.

PTEN and pAkt status was determined according to the widely reported immuno-scoring criteria based on a proportional and an intensity score. Tumors were regarded as PTEN positive (PTEN$^+$) and pAkt positive (pAkt$^+$) when an equal or increased staining intensity compared to the corresponding normal tissue was observed in more than 10% of the tumor cells at cytoplasmic and/or nuclear level [16-19].

On the basis of the median values observed for ER, cyclin D1, $p27^{Kip1}$, and Ki67 in our series of tumors, the value of 10% positively stained tumor nuclei was used as the cut-off to identify ER-positive (ER$^+$), cyclin D1–positive (cyclin D1$^+$), $p27^{Kip1}$-positive ($p27^{Kip1+}$), and Ki67-positive (Ki67$^+$) tumors.

As to the HER2 and CK 5/6 expression, tumors were classified as HER2 positive (HER2$^+$) when an intense and complete cell membrane staining was observed in 30% or more of the tumor cells, whereas they were scored as CK 5/6 positive (CK 5/6$^+$) if any cytoplasmic tumor cell staining was observed as has been previously reported by Nielsen et al [20].

The different subtypes of breast carcinoma were identified on the basis of the immunohistochemical expression profiles of the ER, HER2, and CK 5/6 markers. Tumors were classified as luminal, HER2 overexpressing, and basal-like if they were ER$^+$, ER$^-$/HER2$^+$, and ER$^-$/HER2$^-$/CK 5/6$^+$, respectively [20-23].

2.3. Statistical analysis

The association between the biological parameters was performed using the analysis of variance test. The contingency tables and χ^2 test were used for categorical data analysis, whereas the Student t test was used to compare mean values.

Disease-free survival (DFS) was defined as the interval between surgery and the first documented evidence of disease in locoregional area, distant sites, contralateral breast, or their combination. Disease relapse was accurately assessed by clinical, radiological, and, whenever feasible, histopathological examination.

DFS analysis was performed by the Kaplan-Meier method and the log-rank test was used to compare the survival curves. A multivariate Cox proportional-hazards regression model was designed for factors that are relevant to prognosis to assess the independent contribution of each variable to the DFS. The results of the multivariate analysis were expressed in terms of hazards ratio (HR) along with their 95% confidence intervals (CI).

Statistical analyses were performed using the StatView 5.0 software (Abacus Concepts, Berkeley, CA). All tests were 2 tailed and a P value of less than .05 was considered significant.

3. Results

3.1. PTEN and pAkt expression in node-negative breast carcinoma

PTEN and pAkt expression was evaluated by immunohistochemistry in 72 consecutive patients with node-negative breast cancer. PTEN and pAkt proteins showed both a cytoplasmic and a nuclear localization (Fig. 1A and B), but no significant difference was observed between their subcellular distribution and the analyzed tumor clinicopathologic and biological features (data not shown).

A reduced or absent expression of PTEN and pAkt was observed in 23 (32%) and 9 (12.5%) of the 72 tumors, respectively. All the pAkt$^-$ tumors were PTEN$^+$ tumors, although no statistical association between PTEN and pAkt expression was observed (Table 1).

3.2. PTEN and pAkt status and clinicopathologic and biological parameters

PTEN and pAkt expression was not associated with the main clinicopathologic and biological parameters, such as

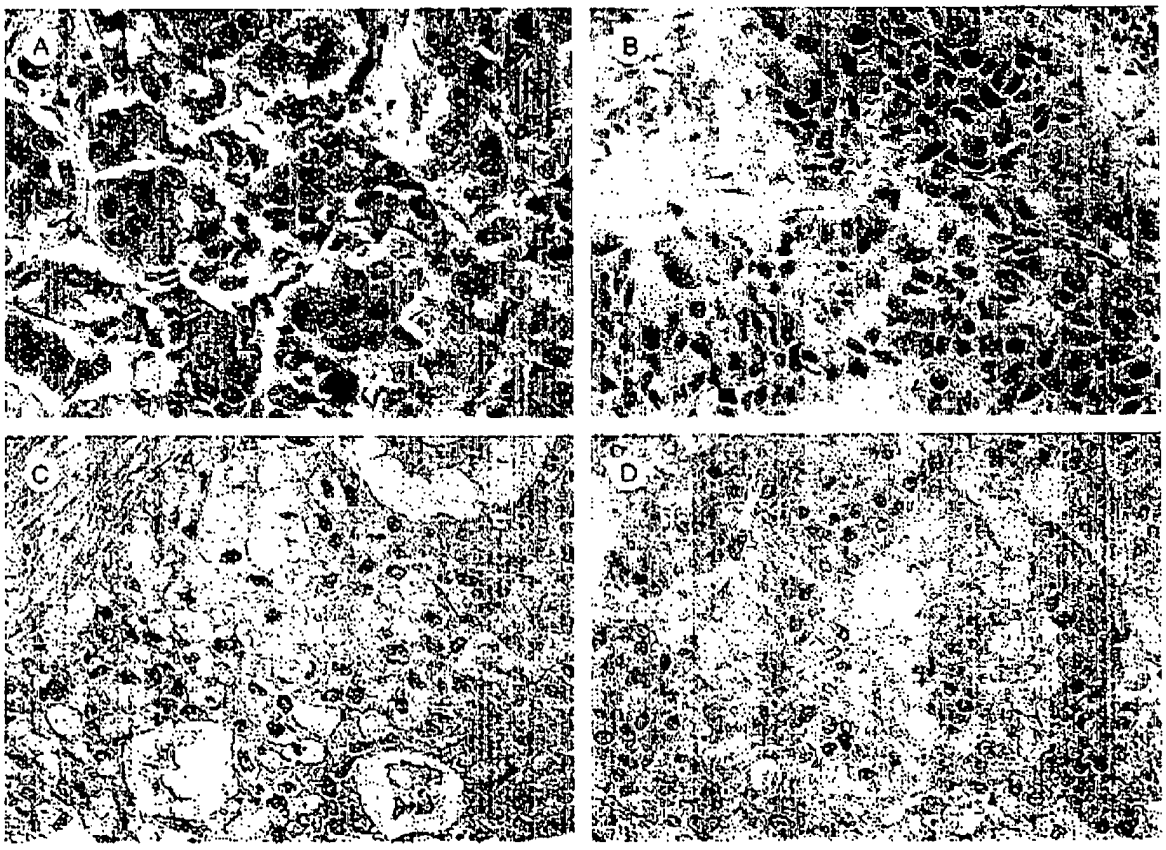

Fig. 1 Representative immunohistochemistry of (A) PTEN, (B) pAkt, (C) $p27^{Kip1}$, and (D) cyclin D1 expression in node-negative breast cancers. Original magnification ×40.

the age, tumor size, histology, tumor grade, ER status, and the proliferation of the tumor evaluated by the Ki67 expression (Table 1).

According to the new molecular classification of breast cancer derived from DNA microarray profiling [20-23], 45 (62.5%), 10 (13.9%), and 17 (23.6%) of the 72 tumors were classified as luminal (ER^+), HER2 overexpressing (ER^-/HER2$^+$), and basal-like (ER^-/$HER2^-$/CK 5/6$^+$), respectively. However, neither PTEN nor pAkt status was significantly associated with the 3 distinct breast cancer subtypes, as shown in Table 1.

Statistical analysis revealed a highly significant association between PTEN expression and the absence of disease recurrence (P = .005). In fact, 39 (80%) of the

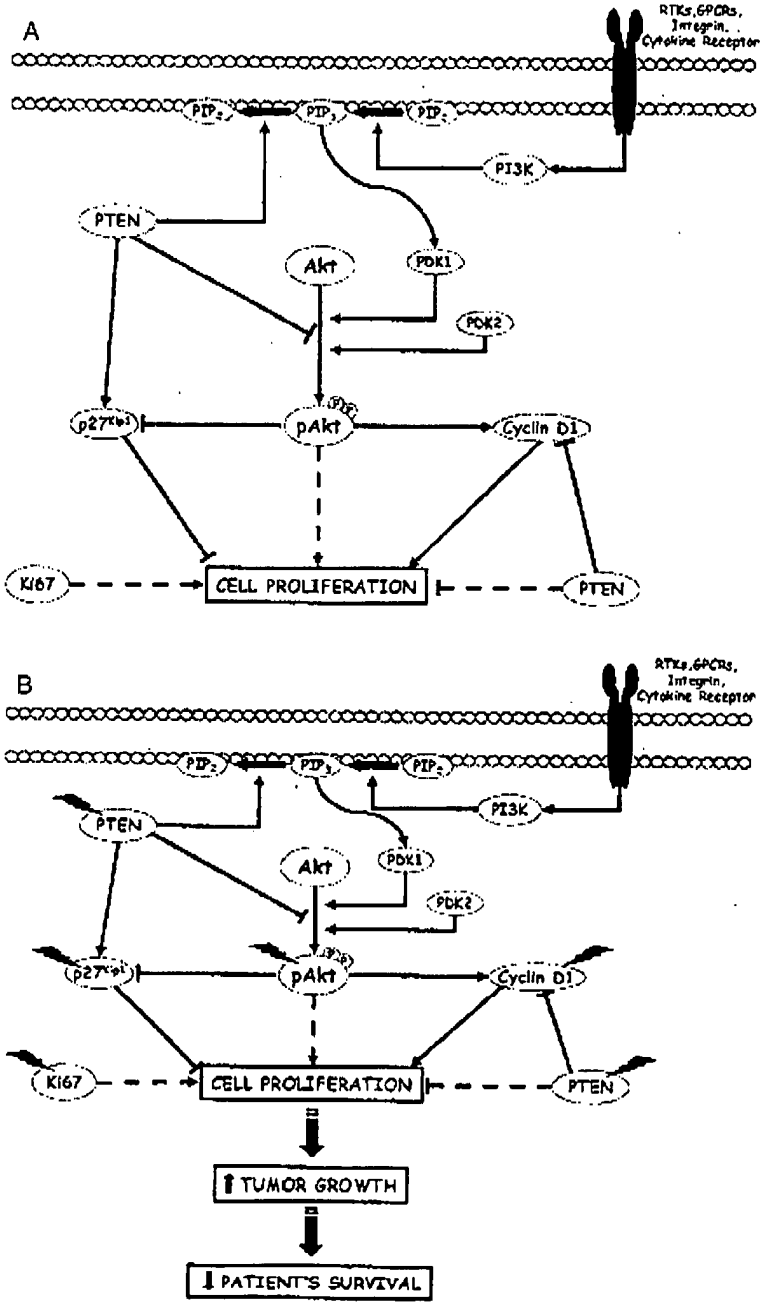

Fig. 2 Schematic representation of the role of pAkt, PTEN, cyclin D1, $p27^{Kip1}$, and Ki67 in the regulation of cell proliferation in (A) normal and (B) cancer cells, where their dysregulation (arrowhead) leads to an increased tumor cell proliferation and growth, and eventually to a decrease in the patient's outcome.

49 patients with PTEN$^+$ tumors did not show evidence of disease at the end of the 10-year follow-up observation (Table 1).

3.3. PTEN and pAkt status association with proteins involved in regulation of cell proliferation

To investigate the relationship between the PTEN or pAkt status and the mechanisms involved in the regulation of cell proliferation, we evaluated the expression of the $p27^{Kip1}$ and cyclin D1 proteins (Fig. 1C and D), whose expression is tightly regulated by pAkt and PTEN (Fig. 2A).

PTEN status was significantly associated with $p27^{Kip1}$ ($P = .0001$) and cyclin D1 expression ($P = .003$). A higher percentage of $p27^{Kip1}$-positive cells (22.9 ± 1.9) and a lower percentage of cyclin D1–positive cells (12.6 ± 2.1) were observed in PTEN$^+$ tumors compared to the PTEN$^-$ ones (7.4 ± 2.6 and 24.3 ± 3.4, respectively).

On the other hand, a significant inverse relationship was found between pAkt and $p27^{Kip1}$ expression ($P = .04$). In fact, pAkt$^+$ tumors showed a lower percentage of $p27^{Kip1}$-positive cells (16.6 ± 1.9) compared to the pAkt$^-$ ones (27.8 ± 2.5). As expected (Fig. 2A), pAkt$^+$ tumors showed a higher percentage of cyclin D1–positive cells (16.9 ± 2.0) than the pAkt$^-$ ones (11.7 ± 5.0), although this correlation was not statistically significant ($P = .36$).

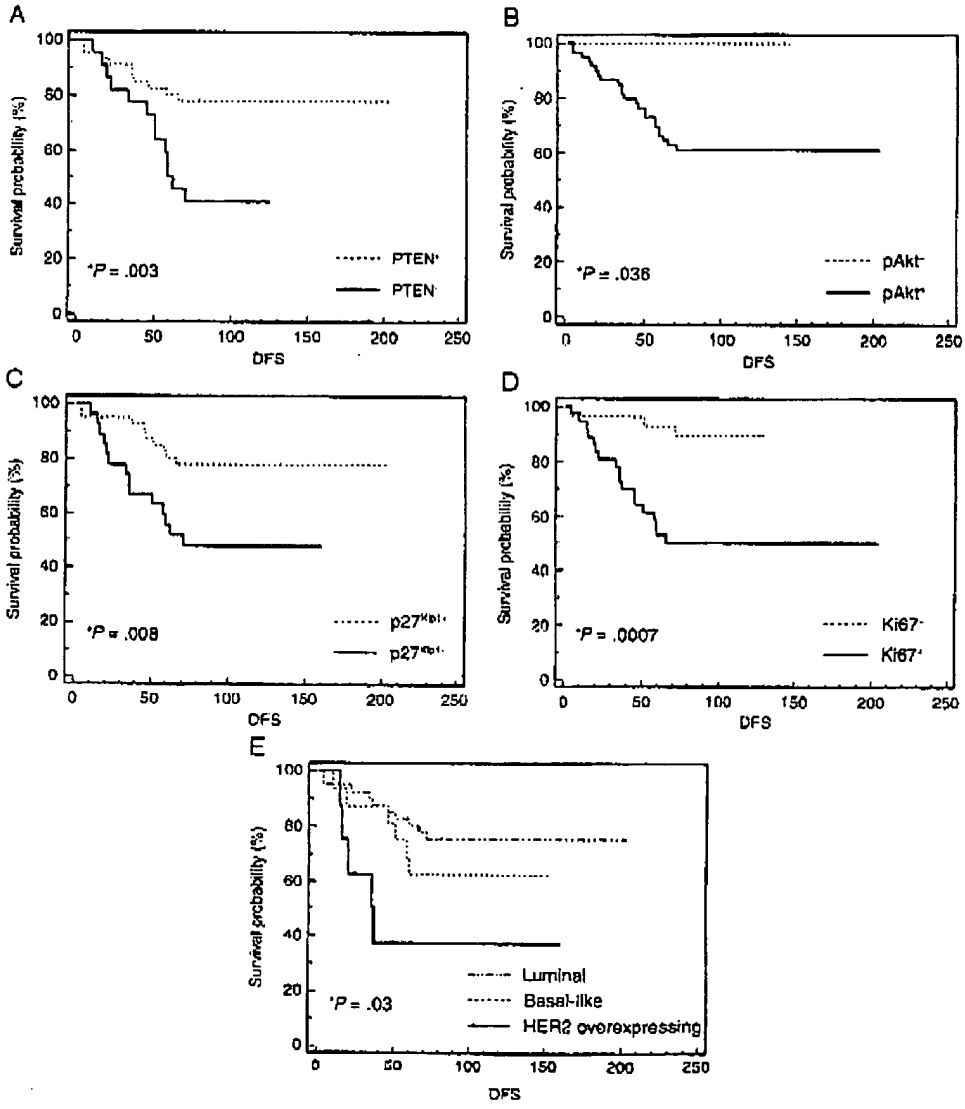

Fig. 3 Kaplan-Meier curves comparing survival in patients with node-negative breast cancer in relation to (A) PTEN, (B) pAkt, (C) $p27^{Kip1}$, and (D) Ki67 status, and in relation to (E) the new molecular classification of breast cancer. *P value assessed using the log-rank test.

Table 2 Relationship between the DFS and the clinical and molecular parameters in patients with node-negative breast cancer

Parameter	DFS (mo)	*P* value[a]
Age		
≤50 y	102 (82-122)	.67
>50 y	94 (80-107)	
Tumor size		
pT1 ≤ 2 cm	98 (85-111)	.47
pT2 > 2 cm	90 (69-110)	
Histology		
Ductal	97 (85-108)	.77
Lobular	105 (21-188)	
ER status[b]		
ER^+	105 (92-118)	.12
ER^-	87 (66-108)	
Ki67 status[b]		
$Ki67^+$	85 (67-103)	*.012*
$Ki67^-$	113 (103-124)	
Molecular classification[c]		
Luminal	105 (92-118)	.38[d]
HER2 overexpressing	67 (17-117)	*.034*[e]
Basal-like	94 (70-118)	.23[f]
pAkt status[b]		
$pAkt^+$	92 (80-105)	*.035*
$pAkt^-$	127 (121-132)	
PTEN status[b]		
$PTEN^+$	107 (94-120)	*.007*
$PTEN^-$	76 (57-95)	
Cyclin D1 status[b]		
Cyclin $D1^+$	100 (88-112)	.50
Cyclin $D1^-$	93 (71-114)	
$p27^{Kip1}$ status[b]		
$p27^{Kip1+}$	108 (95-120)	*.015*
$p27^{Kip1-}$	80 (61-100)	

NOTE. Values are shown as mean (95% CI).

[a] *P* value assessed using the Student *t* test. Significant *P* values are in italics.

[b] Cut-off ≥ 10% positive cells or nuclei.

[c] *P* value assessed between [d]luminal and basal-like, [e]luminal and HER2 overexpressing, and [f]HER2 overexpressing and basal-like.

3.4. Survival analysis

Twenty-three (32%) of the 72 patients relapsed within 5 years from diagnosis. To assess the prognostic value of the PI3K/Akt/PTEN pathway, we performed a survival analysis using the Kaplan-Meier method and the log-rank test to compare the survival curves.

PTEN, pAkt, $p27^{Kip1}$, and Ki67 status, as well as the new molecular breast cancer classification, were related to the DFS of the patients. In fact, the patients with $PTEN^-$ (*P* = .003), $pAkt^+$ (*P* = .036), $p27^{Kip1-}$ (*P* = .008), and $Ki67^+$ (*P* = .0007) tumors showed worse recurrence rates compared to the patients with $PTEN^+$, $pAkt^-$, $p27^{Kip1+}$, and $Ki67^-$ tumors (Fig. 3A-D). Similarly, the Kaplan-Meier curves showed a significant separation between the patients with the HER2 overexpressing breast cancer subtype compared to the luminal or basal-like ones (*P* = .03; Fig. 3E).

Consistent with these results, the patients with $PTEN^-$ (*P* = .007), $pAkt^+$ (*P* = .035), $p27^{Kip1-}$ (*P* = .015), or $Ki67^+$ (*P* = .012) tumors showed significantly shorter mean DFS compared to those with $PTEN^+$, $pAkt^-$, $p27^{Kip1+}$, or $Ki67^-$ tumors, as shown in Table 2. In addition, the most aggressive HER2 overexpressing breast cancer subtype showed a significantly shorter mean DFS compared to the luminal one (*P* = .034), whereas no significant difference in the mean DFS was observed between the basal-like subtype and the luminal or the HER2 overexpressing subtypes of breast cancer (Table 2).

3.5. Multivariate Cox proportional-hazards regression analysis

To investigate the effect on survival of those factors that were found to be strongly relevant to prognosis (Ki67, PTEN, and $p27^{Kip1}$), a Cox proportional-hazards regression model was designed including the age at diagnosis, tumor size, ER, Ki67, PTEN, and $p27^{Kip1}$ status as covariates.

The multivariate analysis by the Cox proportional-hazards regression model showed that PTEN and Ki67 were independent predictive factors of disease recurrence. In fact, HR in $PTEN^-$ and $Ki67^+$ patients was significantly higher compared to the $PTEN^+$ and $Ki67^-$ ones, whereas no significant difference in HR was observed in relation to the $p27^{Kip1}$ status (Table 3).

Table 3 Multivariate Cox proportional-hazards regression analysis of different potential prognostic factors in relation to DFS in node-negative breast cancers

Variable	Hazards ratio*	95% CI	*P* value[†]
Age[‡]	0.76	0.26-2.22	.62
Tumor size[§]	0.77	0.25-2.31	.64
ER[‖]	2.24	0.66-7.59	.19
Ki67[¶]	7.78	2.18-27.84	*.0017*
PTEN[‖]	4.63	1.55-13.80	*.006*
$p27^{Kip1}$[‖]	0.97	0.35-2.68	.95
Deregulated Ki67 and PTEN **	38.30	4.12-355.75	*.0014*
Deregulated Ki67 and $p27^{Kip1}$ ††	15.44	1.74-136.88	*.014*
Deregulated PTEN and $p27^{Kip1}$ ‡‡	4.31	1.43-12.98	*.009*
Deregulated Ki67, PTEN and $p27^{Kip1}$ §§	23.81	2.52-225.21	*.006*

*HR assessed as: [‡]>50 *vs* ≤50 years; [§]pT2 > 2 cm *vs* pT1 ≤ 2 cm; [‖]negative tumors *vs* positive tumors; [¶]positive tumors *vs* negative tumors; **$Ki67^-/PTEN^-$ tumors *vs* $Ki67^-/PTEN^+$ tumors; ††$Ki67^+/p27^{Kip1-}$ tumors *vs* $Ki67^-/p27^{Kip1+}$ tumors; ‡‡ $PTEN^-/p27^{Kip1-}$ tumors *vs* $PTEN^+/p27^{Kip1+}$ tumors; §§$Ki67^+/PTEN^-/p27^{Kip1-}$ tumors *vs* $Ki67^-/PTEN^+/p27^{Kip1+}$ tumors.

To identify a subgroup of patients with a higher risk of relapse, we performed a multivariate analysis taking into account the simultaneous deregulation of 2 risk factors (Ki67 and PTEN, Ki67 and $p27^{Kip1}$, or PTEN and $p27^{Kip1}$) or all the 3 risk factors (Ki67, PTEN, and $p27^{Kip1}$).

A significant increase in HR was observed in patients who showed a deregulated expression of both Ki67/PTEN, Ki67/$p27^{Kip1}$, or PTEN/$p27^{Kip1}$ proteins (Fig. 2B and Table 3). In fact, the risk of disease recurrence of the $Ki67^+/PTEN^-$, $Ki67^+/p27^{Kip1-}$, and $PTEN^-/p27^{Kip1-}$ patients increased by 38.30-, 15.44-, and 4.31-fold in comparison with the HR of the $Ki67^-/PTEN^+$, $Ki67^-/p27^{Kip1+}$, and $PTEN^+/p27^{Kip1+}$ patients, respectively (Table 3). Similarly, the simultaneous deregulation of all the 3 variables significantly increased the HR of disease recurrence (HR, 23.81; $P = .006$) (Table 3). Moreover, survival analysis by the Kaplan-Meier method showed a significant separation among the DFS curves of the above-described different phenotypes (Fig. 4).

4. Discussion

About 30% of the patients with node-negative breast cancer develop distant metastases and die within 10 years from diagnosis. New clinicopathologic guidelines based on reliable prognostic markers are required to identify those patients at high risk of disease recurrence who would benefit from more aggressive adjuvant therapy and/or a closer follow-up. The present study was aimed to explore the clinical and prognostic significance of the PI3K/Akt/PTEN pathway in the patients with node-negative breast cancer.

The dysregulation of the PI3K/Akt pathway has been recently involved in the pathogenesis of several human cancers [1-3] and a large number of findings have highlighted a critical role of this pathway in the initiation and progression of primary mammary epithelial tumor cells to a metastatic phenotype [24,25]. Recent studies have shown that Akt and PTEN are associated with breast cancer malignancy and a poor prognosis [19,26-29].

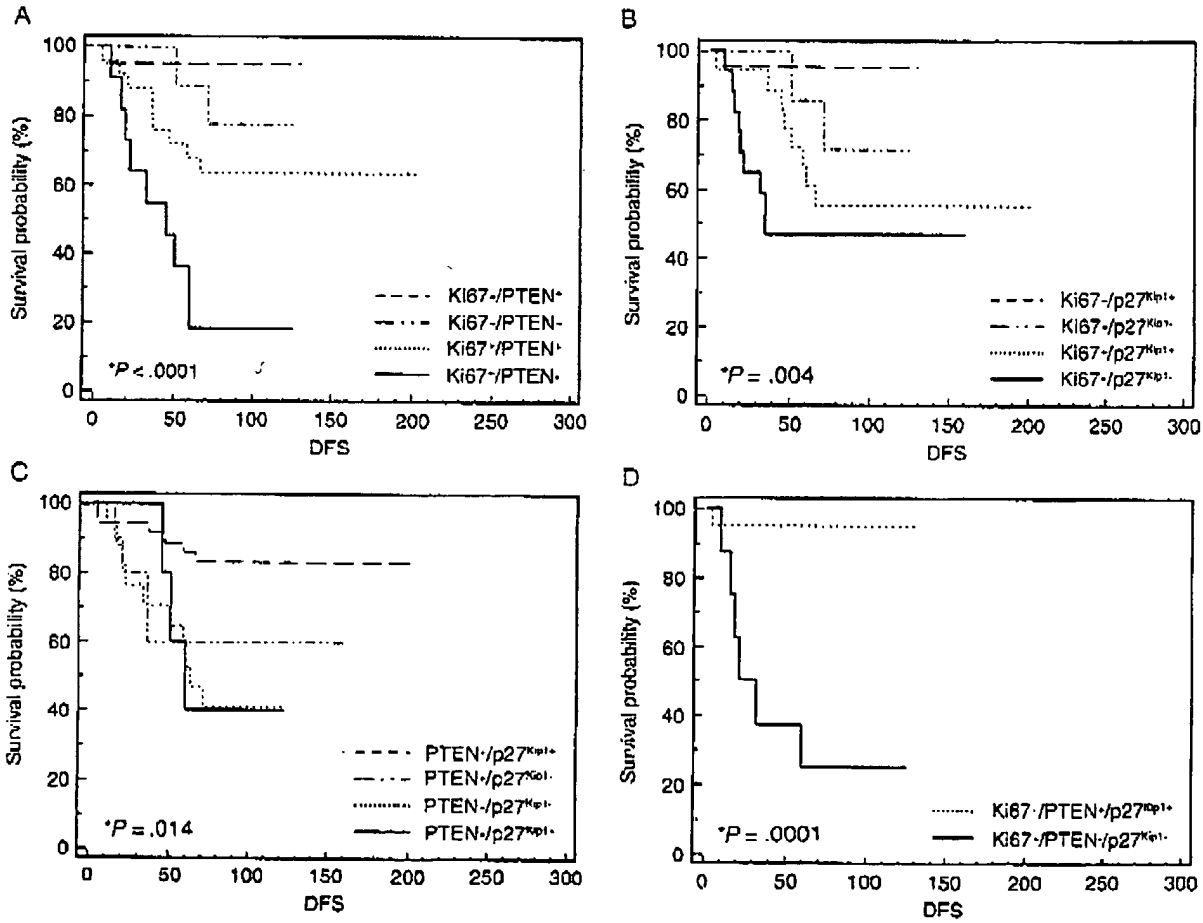

Fig. 4 Kaplan-Meier curves in a series of 72 patients with node-negative breast cancer stratified according to the deregulated expression of (A) Ki67/PTEN, (B) Ki67/$p27^{Kip1}$, (C) PTEN/$p27^{Kip1}$, (D) and Ki67/PTEN/$p27^{Kip1}$. *P value assessed using the log-rank test.

In our study, the overexpression of PTEN was significantly associated with the absence of disease recurrence ($P = .005$), suggesting an important role of the *PTEN* gene as a tumor suppressor gene in malignant breast cancer progression. Moreover, our data showed a highly significant association between a shorter DFS of the patients with node-negative breast cancer and the dysregulation of the PI3K/Akt pathway.

Univariate analysis revealed that the pAkt overexpression or the reduced PTEN and $p27^{Kip1}$ expression identifies a subgroup of patients with node-negative breast cancer with a poor prognosis. In addition, the patients with the HER2 overexpressing subtype and high Ki67 expression showed a worse prognosis compared to those with the luminal and basal-like subtypes of breast cancer and low Ki67 expression, respectively.

Moreover, multivariate analysis by the Cox proportional-hazards regression model showed that PTEN and Ki67 were independent prognostic factors of disease recurrence. In fact, the patients with node-negative breast cancer with high Ki67 or reduced PTEN expression had a significantly higher HR compared to those with low Ki67 or high PTEN expression. Furthermore, the combined analysis revealed that the simultaneous deregulation of Ki67 and PTEN strongly increases the risk of disease recurrence. Interestingly, the absence of PTEN expression identifies a phenotype at poorer prognosis in the subset of patients with $Ki67^+$ tumors. Similarly, the deregulation of $p27^{Kip1}$ expression seems to differentiate the patients at high risk of disease recurrence in the subset of patients with $Ki67^-$ and $PTEN^+$ tumors that have a good prognosis.

In agreement with the literature data, activated Akt kinase has been found in 87.5% of the node-negative breast tumors [30,31], whereas PTEN expression was absent or reduced in 32% of the analyzed tumors [16,17,26,32]. The expected inverse relationship between the loss of PTEN expression and pAkt overexpression was not observed in our group of tumors, although all the $pAkt^-$ tumors were $PTEN^-$ tumors, indicating that the main upstream regulator of Akt in most early breast cancers could be the ER, rather than PTEN, HER2, or EGFR, as suggested by Panhigrahi et al [30].

Despite their strong relationship with the patient's clinical outcome, we did not find any significant association between pAkt or PTEN status and the main clinicopathologic and biological markers, such as the age, size, histologic subtype, tumor grade, Ki67 expression, and ER status, or the new molecular breast cancer classification. Although other authors did not show any correlation between pAkt or PTEN status and the main clinicopathologic parameters [17,26,32], the histologic subtype and in particular the grade have a clear prognostic value in breast cancer, and the expression of pAkt and PTEN would be expected to vary accordingly. The possible explanation for the lack of correlation between the analyzed markers and the histologic subtype or grade is dual. Firstly, the lack of correlation could be biased by the relatively small number of the patients. Secondly, the lack of correlation between pAkt or PTEN expression and the histologic subtype could be due to the fact that, in our cohort of patients with node-negative breast carcinoma, only 3 had a lobular carcinoma. However, we suppose that these markers are more likely to identify more aggressive tumors in a group of cancers instead of being over/underexpressed in a single histotype. As to the grade, the evaluation of the pAkt or PTEN markers gives us a functional portrait of the tumor cells that are more tightly related to the clinical aggressiveness, whereas the grade derives from the direct observation of physical characteristics of the tumor cells that usually correlate with the biological behavior of the whole tumor population. Therefore, the lack of correlation is probably due to the fact that the identification of more aggressive tumors based on the physical characteristics does not perfectly overlap with that made on the basis of the functional characteristics by pAkt or PTEN markers.

In the present study, we also explored the relationship between pAkt or PTEN status and the mechanisms involved in cell proliferation control.

According to their key role in the regulation of the cell proliferation [9,11], pAkt and PTEN status was significantly associated with the cyclin-dependent kinase inhibitor $p27^{Kip1}$. The expression of $p27^{Kip1}$ has been shown to be inversely related to pAkt expression ($P = .04$) and directly related to PTEN expression ($P = .0001$). Moreover, we observed a significant inverse relationship ($P = .003$) between PTEN and cyclin D1 expression. These results are in agreement with the role of pAkt and PTEN in $p27^{Kip1}$ and cyclin D1 regulation through the protein stabilization and transcriptional activation of the *cyclin D1* and *$p27^{Kip1}$* genes [10,11,33]. Despite their striking relationship with the cyclin D1 expression, PTEN and pAkt expression was not related to the tumor proliferation assessed by the Ki67 expression. This lack of correlation could be explained by the fact that Ki67 overexpression, which is the result of a plethora of cellular events involved in cell proliferation, is not directly related to cyclin D1 expression in agreement with our previous data [34]. Furthermore, Schmitz et al [31] have recently shown that node-negative breast tumors with activated Akt exhibit a lower apoptotic rate rather than an increase in cell proliferation compared to pAkt-negative tumors. Therefore, the activation of the PI3K/Akt pathway in node-negative breast cancers may promote cell survival rather than cell proliferation.

In conclusion, our data show that the deregulation of the PI3K/Akt pathway contributes to a more aggressive phenotype in node-negative breast cancer and identifies a subgroup of patients at poor prognosis characterized by a high expression of activated Akt kinase and a loss of PTEN and $p27^{Kip1}$ expression, suggesting that their evaluation together with the classical prognostic markers could improve the prognostic signature of the patients with node-negative breast cancer at high-risk of disease recurrence.

References

[1] Testa JR, Bellacosa A. Akt plays a central role in tumorigenesis. Proc Natl Acad Sci USA 2001;98:10983-5.

[2] Nicholson KM, Anderson NG. The protein kinase B/Akt signalling pathway in human malignancy. Cell Signal 2002;14:381-95.

[3] Vivanco I, Sawyers CL. The phosphatidylinositol 3-kinase/AKT pathway in human cancer. Nat Rev Cancer 2002;2:489-501.

[4] Datta SR, Brunet A, Greenberg ME. Cellular survival: a play in three Akts. Genes Dev 1999;13:2905-27.

[5] Brazil DP, Yang Z, Hemmings BA. Advances in protein kinase B signalling: AKTion on multiple fronts. Trends Biochem Sci 2004;29: 233-42.

[6] Vazquez F, Sellers WR. The PTEN tumor suppressor protein: an antagonist of phosphoinositide 3-kinase signalling. Biochim Biophys Acta 2000;1470:M21-M35.

[7] Di Cristofano A, Pandolfi PP. The multiple roles of PTEN in tumor suppression. Cell 2000;100:387-90.

[8] Weng LP, Brown JL, Eng C. PTEN coordinates G(1) arrest by down-regulating cyclin D1 via its protein phosphatase activity and up-regulating p27 via its lipid phosphatase activity in a breast cancer model. Hum Mol Genet 2001;10:599-604.

[9] Chung JH, Eng C. Nuclear-cytoplasmic partitioning of phosphatase and tensin homologue deleted on chromosome 10 (PTEN) differentially regulates the cell cycle and apoptosis. Cancer Res 2005;65: 8096-100.

[10] Mamillapalli R, Gavrilova N, Mihaylova VT, et al. PTEN regulates the ubiquitin-dependent degradation of the CDK inhibitor p27(KIP1) through the ubiquitin E3 ligase SCF(SKP2). Curr Biol 2001;11: 263-7.

[11] Radu A, Neubauer V, Akagi T, Hanafusa H, Georgescu MM. PTEN induces cell cycle arrest by decreasing the level and nuclear localization of cyclin D1. Mol Cell Biol 2003;23:6139-49.

[12] Li J, Yen C, Liaw D, et al. PTEN, A putative protein tyrosine phosphatase gene mutated in human brain, breast and prostate cancer. Science 1997;275:1943-7.

[13] Steck PA, Pershouse MA, Jasser SA, et al. Identification of a candidate tumour suppressor gene, MMAC1, at chromosome 10q23.3 that is mutated in multiple advanced cancers. Nat Genet 1997;15:356-62.

[14] Khan S, Kumagai T, Vora J, et al. PTEN promoter is methylated in a proportion of invasive breast cancers. Int J Cancer 2004;112: 407-10.

[15] Suzuki H, Freije D, Nusskern DR, et al. Interfocal heterogeneity of PTEN/MMAC gene alteration in multiple metastatic prostate cancer tissues. Cancer Res 1998;58:204-9.

[16] Shi W, Zhang X, Pintilie M, et al. Dysregulated PTEN-PKB and negative receptor status in human breast cancer. Int J Cancer 2003;104:195-203.

[17] Perren A, Weng PL, Boag AH, et al. Immunohistochemical evidence of loss of PTEN expression in primary ductal adenocarcinomas of the breast. Am J Pathol 1999;155:1253-60.

[18] Kurose K, Zhou XP, Araki T, Cannistra SA, Maher ER, Eng C. Frequent loss of PTEN expression is linked to elevated phosphorylated Akt levels, but not associated with p27 and cyclin D1 expression, in primary epithelial ovarian carcinomas. Am J Pathol 2001;158: 2097-106.

[19] Stål O, Pérez-Tenorio G, Akerberg L, et al. Akt kinases in breast cancer and the results of adjuvant therapy. Breast Cancer Res 2003;5:R37-R44.

[20] Nielsen TO, Hsu FD, Jensen K, et al. Immunohistochemical and clinical characterization of the basal-like subtype of invasive breast carcinoma. Clin Cancer Res 2004;10:5367-74.

[21] Perou CM, Sørlie T, Eisen MB, et al. Molecular portraits of human breast tumours. Nature 2000;406:747-52.

[22] Sørlie T. Molecular portraits of breast cancer: tumour subtypes as distinct disease entities. Eur J Cancer 2004;40:2667-75.

[23] Livasy CA, Karaca G, Nanda R, et al. Phenotypic evaluation of the basal-like subtype of invasive breast carcinoma. Mod Pathol 2006;19:264-71.

[24] Dillon RL, White DE, Muller WJ. The phosphatidylinositol 3-kinase signalling network: implications for human breast cancer. Oncogene 2007;26:1338-45.

[25] Liu W, Bagaitkar J, Watabe K. Roles of AKT signal in breast cancer. Front Biosci 2007;12:4011-9.

[26] Depowski PL, Rosenthal SI, Ross JE. Loss of expression of PTEN gene protein product is associated with poor outcome in breast cancer. Mod Pathol 2001;14:672-6.

[27] Pérez-Tenorio G, Stål O, Southeast Sweden Breast Cancer Group. Activation of AKT/PKB in breast cancer predicts a worse outcome among endocrine treated patients. Br J Cancer 2002;86:540-5.

[28] Shoman N, Klassen S, McFadden A, Bickis MG, Torlakovic E, Chibbar R. Reduced PTEN expression predicts relapse in patients with breast carcinoma treated by tamoxifen. Mod Pathol 2005;18: 250-9.

[29] Tsutsui S, Inoue H, Yasuda K, et al. Reduced expression of PTEN protein and its prognostic implications in invasive ductal carcinoma of the breast. Oncology 2005;68:398-404.

[30] Panhigrahi AR, Pinder SE, Chan SY, Paish EC, Robertson JF, Ellis IO. The role of PTEN and its signalling pathways, including AKT, in breast cancer; an assessment of relationships with other prognostic factors and with outcome. J Pathol 2004; 204:93-100.

[31] Schmitz KJ, Otterbach F, Callies R, et al. Prognostic relevance of activated Akt kinase in node-negative breast cancer: a clinicopathological study of 99 cases. Mod Pathol 2004;17:15-21.

[32] Bose S, Crane A, Hibshoosh H, Mansukhani M, Sandweis L, Parsons R. Reduced expression of PTEN correlates with breast cancer progression. Hum Pathol 2002;33:405-9.

[33] Diehl JA, Cheng M, Roussel MF, Sherr CJ. Glycogen synthase kinase-3β regulates cyclin D1 proteolysis and subcellular localization. Genes Dev 1998;12:3499-511.

[34] Collecchi P, Santoni T, Gnesi E, et al. Cyclins of phases G1, S and G2/M are overexpressed in aneuploid mammary carcinomas. Cytometry 2000;42:254-60.

Akt Phosphorylation and Gefitinib Efficacy in Patients With Advanced Non–Small-Cell Lung Cancer

Federico Cappuzzo, Elisabetta Magrini, Giovanni Luca Ceresoli, Stefania Bartolini, Elisa Rossi, Vienna Ludovini, Vanesa Gregorc, Claudia Ligorio, Alessandra Cancellieri, Stefania Damiani, Anna Spreafico, Carlo Terenzio Paties, Laura Lombardo, Cesare Calandri, Guido Bellezza, Maurizio Tonato, Lucio Crinò

Background: **Gefitinib, a specific epidermal growth factor receptor (EGFR) tyrosine kinase inhibitor, has activity against approximately 10% of unselected non–small-cell lung cancer (NSCLC) patients. Phosphatidylinositol 3′-kinase (PI3K)/Akt and Ras/Raf/mitogen-activated protein kinase (MAPK), the two main EGFR-signaling pathways, mediate EGFR effects on proliferation and survival. Because activation of these pathways is dependent on the phosphorylation status of the components, we evaluated the association between phosphorylation status of Akt (P-Akt) and MAPK (P-MAPK) and gefitinib activity in patients with advanced NSCLC.** ***Methods:*** **Consecutive patients (n = 106) with NSCLC who had progressed or relapsed on standard therapy received gefitinib (250 mg/day) until disease progression, unacceptable toxicity, or patient refusal. P-Akt and P-MAPK positivity was determined with immunohistochemistry using tumor tissues obtained before any anticancer treatment. Association of P-Akt and time to progression was determined by univariable and multivariable analyses. All statistical tests were two-sided.** ***Results:*** **Of the 103 evaluable patients, 51 (49.5%) had tumors that were positive for P-Akt, and 23 (22.3%) had tumors that were positive for P-MAPK. P-Akt–positivity status was statistically significantly associated with being female ($P<.001$), with never-smoking history ($P = .004$), and with bronchioloalveolar carcinoma histology ($P = .034$). Compared with patients whose tumors were negative for P-Akt, patients whose tumors were positive for P-Akt had a better response rate (26.1% versus 3.9%; $P = .003$), disease control rate (60.9% versus 23.5%; $P<.001$), and time to progression (5.5 versus 2.8 months; $P = .004$). Response rate, disease control rate, and time to progression did not differ according to P-MAPK status. The multivariable analysis showed that P-Akt positivity was associated with a reduced risk of disease progression (hazard ratio = 0.58, 95% confidence interval = 0.35 to 0.94).** ***Conclusions:*** **Patients with P-Akt–positive tumors who received gefitinib had a better response rate, disease control rate, and time to progression than patients with P-Akt–negative tumors, suggesting that gefitinib may be most effective in patients with basal Akt activation. [J Natl Cancer Inst 2004;96:1133–41]**

Lung cancer is the leading cause of cancer death among men and women in Europe and North America *(1)*. Despite aggressive surgical and chemotherapeutic intervention, the prognosis of patients with non–small-cell lung cancer (NSCLC) remains poor, with an overall cure rate of less than 15% *(2)*. Given the rapid advances in the molecular and biological understanding of the tumorigenic process, several new strategies, including those that involve specific molecular targets, have been developed for the treatment of various cancers.

One potential family of therapeutic targets is the epidermal growth factor receptor (EGFR) superfamily. These cell membrane receptors have been implicated in the development and progression of cancer through their effects on cell cycle progression, apoptosis, angiogenesis, and metastasis *(3–6)*. The EGFR superfamily includes four distinct receptors: EGFR/ErbB-1, HER2/ErbB-2, HER3/ErbB-3, and HER4/ErbB-4. Although specific soluble ligands that bind to the extracellular domains of EGFR, HER3, and HER4 have been identified, no ligand has been identified for the HER2 receptor. Several ligands can bind to EGFR, including EGF and transforming growth factor α (TGF-α). After the ligand binds the receptor, the receptor dimerizes—either as a homodimer or as a heterodimer with other members of the EGFR family, but preferentially with HER2—and undergoes autophosphorylation at specific tyrosine residues within the intracellular domain. These autophosphorylation events in turn activate downstream signaling pathways, including the Ras/Raf/mitogen-activated protein kinase (MAPK) pathway and the phosphatidylinositol 3′-kinase (PI3K)–Akt pathway. Activation of Ras initiates a multistep phosphorylation cascade that leads to the activation of MAPKs. The MAPKs ERK1 and ERK2 subsequently regulate gene transcription and have been linked to cell proliferation, survival, and transformation in laboratory studies *(7)*. Akt also plays a critical role in controlling the balance between cell survival and apoptosis *(8)*. Phosphorylation of Akt is required for its activation; once activated, Akt inactivates proapoptotic proteins, including the Bcl-2 family member Bad and caspase-9, and cell cycle–regulatory molecules *(9–10)*. Akt function is also important for cell survival when cells are exposed to different apoptotic stimuli, such as growth factor withdrawal, ultraviolet radiation, and DNA damage *(11–15)*. Given its association with cell survival, it is not

Affiliations of authors: Department of Oncologic Sciences, Bellaria-Maggiore Hospital, Bologna, Italy (FC, EM, SB, CL, AC, SD, LL, CC, LC); Division of Radiochemotherapy, Scientific Institute University Hospital San Raffaele-Milano, Italy (GLC, VG, AS, CTP); CINECA—Interuniversity Consortium, Bologna, Italy (ER); Policlinico Monteluce, Division of Medical Oncology, Perugia, Italy (VL, GB, MT).

Correspondence to: Federico Cappuzzo, MD, Bellaria Hospital, Division of Medical Oncology, Via Altura 3, 40139-Bologna, Italy (e-mail: federico.cappuzzo@ausl.bo.it).

See "Notes" following "References."

DOI: 10.1093/jnci/djh217

surprising that Akt has been found to be overexpressed in several cancers, including lung *(15)*, pancreatic *(16)*, thyroid *(17)*, and ovarian *(18–19)* cancers. Recently, Akt phosphorylation has been observed in more than 60% of patients with NSCLC *(20)*.

Drugs interfering with EGFR pathways are thought to be of potential therapeutic benefit in tumors expressing or overexpressing EGFR, and during the last decade, several molecules have been synthesized to inhibit the tyrosine kinase domain of EGFR *(21,22)*. Among the more promising new drugs is ZD-1839 (gefitinib or Iressa; AstraZeneca, London, U.K.), an orally active, selective EGFR tyrosine kinase inhibitor with antitumor activity against a variety of human cancer cell lines expressing EGFR *(23)*. After objective responses were observed in 11% of study participants in phase I trails *(24–27)*, two large phase II trials (IDEAL 1 and 2) *(28,29)* were conducted. The results of the IDEAL trials confirmed that gefitinib is active in approximately 10% of patients with NSCLC in whom standard therapy failed *(28,29)*. Although these results were considered encouraging because they were obtained from patients in whom standard therapies were largely ineffective, only a small percentage of patients responded to single-agent gefitinib. Preclinical data have suggested that EGFR expression is not the critical factor in determining whether a patient will respond to gefitinib *(30)*, although tumors that overexpress HER2 are highly sensitive to gefitinib *(31)*. In our previous trial *(32)*, conducted on 63 patients with NSCLC who gave their consent for EGFR and HER2 analysis, we examined the association between efficacy and tolerability of gefitinib and EGFR and HER2 expression. In that small study *(32)*, in which HER2 status was determined with immunohistochemistry, there was no association between HER2 expression and gefitinib activity.

Although the degree of EGFR expression does not affect response to gefitinib, clinical responses to EGFR-blocking agents suggest that, in some patients with NSCLC, the EGFR signaling pathway may be the critical pathway for tumor growth. It is possible that patients who respond to EGFR-blocking agents such as gefitinib are those patients in whom tumor cell survival is maintained by activated EGFR-dependent pathways. To test this hypothesis and to determine if it is possible to identify which patients may respond to gefitinib therapy, we evaluated the association between the phosphorylation status of MAPK and Akt in patients with advanced NSCLC before starting gefitinib therapy and evaluated their response to gefitinib therapy. This trial was designed to evaluate possible associations between the phosphorylation status of Akt and of MAPK and gefitinib activity in terms of response rate and time to progression.

Patients and Methods

Patients

Study enrollment began in February 2001, and the last patients were enrolled in August 2003. In the period, February 2001–June 2002, because of the ongoing HER2 study *(32)*, patients were asked to give their consent for inclusion in the HER2 study (N = 55), the Akt/MAPK study (N = 22) (the results of which are described in this article), or both studies (N = 8).

Patients included in the present study had histologically confirmed, measurable, locally advanced or metastatic NSCLC and had progressed or relapsed after standard therapy. Patients who had not received any previous chemotherapy were included in the study if they were considered not eligible for systemic therapy because of age, poor performance status, or any medical condition contraindicating chemotherapy. To be eligible for the study, patients had to be aged older than 18 years, have an ECOG performance status of 2 or less, have a white blood cell count of at least 3.5×10^9/L, have a platelet count of at least 100×10^9/L, have a hemoglobin level of at least 9 g/dL, have an absolute granulocyte count of more than 2.0×10^9/L, have a bilirubin level that was less than 1.5-fold the upper limit of normal, have a prothrombin time or activated partial thromboplastin time of less than 1.5 times that of control, have an alanine aminotransferase (ALT) or aspartate aminotransferase (AST) levels of less than threefold the upper limits of normal (this level was increased to fivefold for patients with known hepatic metastases), and have a calculated creatinine clearance rate of more than 45 mL/min. Patients were ineligible for the study if they had evidence of prior or concurrent malignancy, with the exception of *in situ* carcinoma of the cervix, adequately treated basal cell carcinoma of the skin, or no evidence of recurrence of a malignancy treated 5 or more years ago.

Before patients were included in the trial, all patients were asked about their smoking history and classified as nonsmoker (never smoker), former smoker (stopped smoking more than 6 months before enrollment onto the trial), or current smoker (stopped smoking less than 6 months before enrollment onto the trial or still an active smoker). Lung cancer histology was defined according to the World Health Organization pathology classification *(33)*. Written informed consent was obtained from each patient entering the study. The study was approved by the appropriate ethics review boards and followed the recommendations of the Declaration of Helsinki for biomedical research involving human subjects and the guidelines for good clinical practice.

Study Design and Treatment

In this study, 106 consecutive patients with NSCLC who progressed or relapsed after standard therapy failed received gefitinib daily at a dose of 250 mg. Patients received the drug until their disease progressed (n = 77), they experienced unacceptable toxicity (n = 1), or they refused to comply further (n = 1). The drug was provided by AstraZeneca on a compassionate-use basis.

Before the time of entry on the trial, a baseline evaluation was performed for each patient that included a complete history and physical examination, a complete blood cell count and serum chemistry analysis, urinalysis, an electrocardiogram, chest x-ray, and a total-body computed tomography (CT) scan. Other imaging modalities, such as magnetic resonance imaging and bone scintigraphy, were performed according to specific clinical indications. All baseline imaging procedures were performed within 4 weeks before study entry. Biochemical screening, which was performed every 4 weeks, included assessments of serum levels of creatinine, electrolytes, alkaline phosphatase, bilirubin, AST, ALT, calcium, magnesium, and total protein. Patients were evaluated for response according to the RECIST (response evaluation criteria in solid tumors) criteria (36). Tumor response was assessed by CT scan every 2 months, with a confirmatory evaluation that was repeated in patients who had

not progressed to therapy at least 4 weeks after the initial determination of response.

Immunohistochemical Staining

Tumor specimens obtained at the time of primary diagnosis or at the time of study entry were collected for P-Akt and P-MAPK immunohistochemistry. Paraffin-embedded tissue sections were stained with antibodies against phospho-Akt (P-Akt; Cell Signaling Technology, Beverly, MA) and phospho-MAPK (P-MAPK; Cell Signaling Technology), according to the manufacturer's recommended protocol. Briefly, 4-μm–thick tissue sections were placed on glass slides and deparaffinized. The tissue sections were incubated in 1× Microstain Unmasker Buffer (pH 8) (Ventana, Tucson, AZ) for 40 minutes at 98 °C to unmask the antigens. The reaction was quenched with 1% hydrogen peroxide. Nonspecific binding sites were blocked with 5% goat serum in phosphate-buffered saline (PBS) for 1 hour at room temperature. The sections were then incubated with P-Akt (Ser 473) rabbit polyclonal antibody (1:50 diluted in phosphate buffer) or P-p44/42 Map Kinase (Thr202/Tyr204) polyclonal antibody (1:100 diluted in phosphate buffer) overnight at 4 °C. The sections were developed by using a two-step method involving a large-volume biotinylated goat polyvalent antibody and a large-volume streptavidin peroxidase reagent (Lab Vision, Fremont, CA). The negative controls were incubated with nonimmune solution in place of primary antibody.

Immunohistochemically stained sections were interpreted independently by two pathologists who were blinded to all patient information. The intensity of staining seen in different areas of the same slide was analyzed according to criteria described previously for p53 *(34)*. Immunohistochemical analyses were centralized, and all were performed at the Bellaria Hospital Pathology Department. Immunohistochemical results were blinded, and the referring physician was informed of the results only at the end of the trial or when the patient was withdrawn from the study.

At present, there are no validated scoring systems for interpreting immunohistochemical staining for P-MAPK or P-Akt. We used a system for interpreting P-MAPK staining that was based on staining intensity. If none of the tumor cells stained, the intensity was coded as 0; if more than 10% of the tumor cells stained weakly, the intensity was coded as 1+; if more than 10% of the tumor cells stained moderately, the intensity was coded as 2+; and if more than 10% of the tumor cells stained strongly, the intensity was coded as 3+. Specimens having a score of 0 or 1+ were considered negative, whereas a score of 2+ or 3+ was considered positive. We used a system for interpreting P-Akt staining that was based on subcellular staining localization. Activation of Akt by phosphorylation results in its translocation from the cytoplasm to the nucleus *(35)*. Thus, staining was considered positive if nuclear staining was present and negative if nuclear staining was absent.

Statistical Analysis

Intent-to-treat analyses were performed on data from all patients who entered the study and received treatment. The trial was designed to detect a difference in response rate between the patients whose tumors were P-Akt positive and patients whose tumors were P-Akt negative. A sample size of 94 patients, with 47 patients in each group, was considered adequate to detect a difference of 25% (5%–30%) between the two groups, with a two-sided significance level (α) of 5% and a power of 90%. Sample size was calculated using SPSS version 11.5.1 (SPSS Italia srl, Bologna, Italy).

Statistical analyses were performed with respect to clinical characteristics and response to therapy. For both proteins, differences between the two groups (positive and negative) were compared by Fisher's exact test or chi-square test for nominal variables and the Mann–Whitney test or Student's t test for continuous variables. Normality of the distribution of continuous variables was assessed with the Kolmogorov–Smirnov test. Time to progression, overall survival, and 95% confidence intervals (CIs) were evaluated with the Kaplan–Meier method *(37)*, and differences between the two groups were evaluated with the log-rank test. Risk factors associated with time to progression were evaluated using Cox's proportional hazards regression model with a step-down procedure *(38)*. Proportional hazard assumptions were checked and satisfied. Only those variables with statistically significant results in univariate analysis were included in the multivariable analysis. The criterion for removing a variable was the likelihood ratio statistic, which was based on the maximum partial likelihood estimate (default P value of .10 for removal from the model). Data analysis was planned for 3 months after the enrollment of the last patient. This time was selected because standard therapies had failed in our cohort, and the patients therefore had a poor prognosis. The degree of agreement between the two pathologists involved in the study (EM and SD) was assessed by a weighted κ statistic *(39)*. All statistical analyses were performed using SPSS version 11.5.1 (SPSS Italia srl).

Results

Patient Characteristics

From February 2001 through August 2003, 106 consecutive patients from three Italian institutions fulfilled the selection criteria and received gefitinib daily at a dose of 250 mg. The majority of patients (76 patients) were enrolled after June 2002. Tumor tissue specimens were not suitable for immunohistochemistry from four patients: sections from two patients could not be stained for P-Akt and P-MAPK, sections from one patient could not be stained for P-Akt, and sections from one patient could not be stained for P-MAPK. Thus, 103 patients contributed immunohistochemistry results for either P-Akt or P-MAPK. Patient characteristics are listed in Table 1. The majority of the patients were male (63.1%), with a median age of 63 years (range = 25–83 years) and with a good ECOG (Eastern Cooperative Oncology Group) performance status (86.4% had a performance status of 0 or 1). Among the patient cohort, 55.3% had adenocarcinoma, 12.6% had bronchioloalveolar carcinoma, 20.4% had squamous-cell carcinoma, 9.8% had undifferentiated carcinoma, and 1.9% had large-cell carcinoma. Seven patients (6.8%) received gefitinib as first-line therapy: One patient was aged older than 80 years, and six patients had comorbidities contraindicating chemotherapy. The remaining 96 patients had all received chemotherapy before gefitinib, and of these patients, 74.7% had received chemotherapy that included a platinum salt. At the time of study entry, the majority of patients were current (50.5%) or former (31.1%) smokers.

Table 1. Patient characteristics and association with the phosphorylation status of Akt and MAPK determined by immunohistochemistry in evaluable patients*

Characteristic	P-Akt status				P-MAPK status			
	Total n = 103	P-Akt–positive (%) n = 51 (49.5)	P-Akt–negative (%) n = 52 (50.5)	P	Total n = 103	MAPK 2+/3+ (%) n = 23 (22.3)	MAPK 0/1+ (%) n = 80 (77.7)	P
Sex								
Male	65 (63.1)	24 (47.1)	41 (78.8)	<.001	65 (63.1)	14 (60.9)	51 (63.8)	.811
Female	38 (36.9)	27 (52.9)	11 (21.2)		38 (36.9)	9 (39.1)	29 (36.3)	
Age, y								
Median	62.6	62	63			62	63	
Range	25–83	25–83	33–77			25–80	33–83	
Disease stage								
III	14 (13.6)	7 (13.7)	7 (13.5)	.969	14 (13.6)	4 (17.4)	10 (12.5)	.509
IV	89 (86.4)	44 (86.3)	45 (86.5)		89 (86.4)	19 (82.6)	70 (87.5)	
Histology								
ADC	57 (55.3)	24 (47.1)	33 (63.5)	.034†	58 (56.3)	10 (43.5)	48 (60.0)	.480†
SCC	21 (20.4)	12 (23.5)	9 (17.3)		20 (19.4)	6 (26.1)	14 (17.5)	
BAC	13 (12.6)	10 (19.6)	3 (5.8)		13 (12.6)	4 (17.4)	9 (11.3)	
UndiffT	10 (9.8)	5 (9.8)	5 (9.6)		10 (7.7)	3 (13.0)	7 (8.8)	
LCC	2 (1.9)	0 (0.0)	2 (3.8)		2 (1.9)	0 (0.0)	2 (2.5)	
ECOG performance status								
0	47 (45.6)	24 (47.1)	23 (44.2)	.539‡	46 (44.7)	9 (39.1)	37 (46.3)	.297‡
1	42 (40.8)	19 (37.3)	23 (44.2)		43 (41.7)	9 (39.1)	34 (42.5)	
2	14 (13.6)	8 (15.7)	6 (11.5)		14 (13.6)	5 (21.7)	9 (11.3)	
Previous chemotherapy courses								
0	7 (6.8)	2 (3.9)	5 (9.6)	NA	7 (6.8)	2 (8.7)	5 (6.31)	NA
1	44 (42.7)	25 (49.0)	19 (36.5)		43 (41.7)	12 (52.2)	31 (38.8)	
2	41 (39.8)	19 (37.3)	22 (42.3)		42 (40.6)	7 (30.4)	35 (43.8)	
3+	11 (10.7)	5 (9.8)	6 (11.5)		11 (10.7)	2 (8.7)	9 (11.3)	
Previous cisplatin								
Yes	77 (74.7)	35 (68.6)	42 (80.8)	NA	77 (76.2)	17 (73.9)	61 (76.2)	NA
No	25 (25.3)	16 (31.4)	10 (19.2)		24 (23.8)	6 (26.1)	19 (23.8)	
Smoking history								
No	19 (18.4)	15 (29.4)	4 (7.7)	.004§	19 (18.4)	4 (17.4)	15 (18.8)	1.000§
Former	32 (31.1)	16 (31.4)	16 (30.8)		31 (30.1)	8 (34.8)	23 (28.8)	
Current	52 (50.5)	20 (39.2)	32 (61.5)		53 (51.5)	11 (47.8)	42 (52.5)	

*Phospho-Akt (P-Akt) and phospho-MAPK (P-MAPK) status was determined by immunohistochemistry on tumor sections. Tumors that had nuclear P-Akt staining, a measure of Akt activation, were considered positive. For P-MAPK staining, if none of the tumor cells stained, the intensity was 0 (considered negative); if more than 10% of the tumor cells stained weakly, the intensity was 1+ (considered negative); if more than 10% of the tumor cells stained moderately, the intensity was 2+ (considered positive); and if more than 10% of the tumor cells stained strongly, the intensity was 3+ (considered positive). ADC = adenocarcinoma; SCC = squamous-cell carcinoma; BAC = bronchioloalveolar carcinoma; UndiffT = undifferentiated; LCC = large-cell carcinoma; ECOG = Eastern Cooperative Oncology Group; NA = not assessable.

†BAC versus other histology.

‡Performance status 0–1 versus 2.

§No smoker versus former plus current smoker.

Immunohistochemistry was performed on primary lung tumor specimens obtained before any anticancer therapy. Tumor tissue specimens were obtained at the time of surgery for 26 patients, at the time of original diagnosis of advanced disease for 73 patients, and immediately before starting gefitinib therapy for seven patients. Among the 103 patients evaluated for P-Akt and P-MAPK status, 52 (50.5%) had tumors that were negative for P-Akt and 51 (49.5%) had tumors that were positive for P-Akt, 80 (77.7%) had tumors that were negative (0–1+) for P-MAPK, 14 (13.6%) had tumors that were moderately positive (2+) for P-MAPK, and nine (8.7%) had tumors that were strongly positive (3+) for P-MAPK. The agreement between the two pathologists who reviewed all immunohistochemical staining was very strong, with a weighted κ statistic of 0.973 for P-Akt ($P<.001$) and 0.966 for P-MAPK ($P<.001$).

We next evaluated the association between P-Akt and P-MAPK status and clinical variables. P-Akt status was statistically significantly associated with being female ($P<.001$), never-smoking history ($P = .004$), and a bronchioloalveolar carcinoma histology ($P = .034$). No association was found between P-Akt status and other tumor histologies. P-MAPK status was not statistically significantly related to any clinical variable.

Response to Therapy

One hundred patients were evaluable for response. Six patients were considered not evaluable for response because of the absence of any measurable lesion (one patient) or because the patient was lost to follow-up after the baseline visit (five patients). Gefitinib was administered orally, with a median treat-

Table 2. Response to gefitinib therapy in patients with advanced non–small-cell lung cancer according to the phosphorylation status of Akt and MAPK

Tumor phosphorylation status*	Total No. of evaluable tumors	No. of complete and partial responses (%)†	P	No. with stable disease (%)	No. of complete and partial responses and stable disease (%)	P
Total = 103	97	14 (14.4)		26 (26.8)	40 (41.2)	
P-AKT+	46	12 (26.1)	.003	16 (34.8)	28 (60.9)	<.001
P-AKT−	51	2 (3.9)		10 (19.6)	12 (23.5)	
MAPK 0/1+	75	9 (12.0)	.298	20 (27.8)	29 (38.7)	.461
MAPK 2+/3+	22	5 (22.7)		6 (27.3)	11 (50.0)	

*Phospho-Akt (P-Akt) and phospho-MAPK (P-MAPK) status was determined by immunohistochemistry on tumor sections. Tumors that had nuclear P-Akt staining, a measure of Akt activation, were considered positive. For P-MAPK staining, if none of the tumor cells stained, the intensity was 0 (considered negative); if more than 10% of the tumor cells stained weakly, the intensity was 1+ (considered negative); if more than 10% of the tumor cells stained moderately, the intensity was 2+ (considered positive); and if more than 10% of the tumor cells stained strongly, the intensity was 3+ (considered positive).

†Complete response was defined as the disappearance of all target lesions; partial response was defined as at least a 30% decrease in the sum of the longest diameter of target lesions (RECIST [response evaluation criteria in solid tumors] criteria).

ment duration of 3.6 months (range = 0.6–23.5 months). One (1%) patient had a complete response, 13 (13%) patients had a partial response, and 26 (26%) patients had stable disease, for an overall response rate of 14% (95% CI = 7.9% to 22.4%). The overall response rate, including complete responses and partial responses, was 26.1% for patients with P-Akt–positive tumors and 3.9% for patients with P-Akt–negative tumors (mean difference = 22.2%, 95% CI = 14.0 to 30.4; $P = .003$). The disease control rate, which includes complete responses, partial responses, and stable disease, was 60.9% for patients with P-Akt–positive tumors and 23.5% for patients with P-Akt–negative tumors (mean difference = 37.4%, 95% CI = 27.9 to 46.9; $P < .001$). There was no difference in terms of response rate and disease control rate among patients with P-MAPK–negative tumors and patients with P-MAPK–positive tumors (response rates = 12% versus 22.7%, respectively; $P = .298$; disease control rate = 38.7% versus 50%, respectively; $P = .461$) (Table 2). Eighteen patients had tumors that were positive for both P-Akt and P-MAPK. In this subgroup of patients, the response rate was 29.4% and disease control rate was 58.8%, values that were not statistically significantly different from those observed for patients with tumors positive for P-Akt and negative for P-MAPK (response rate = 24.1%, disease control rate = 62.1%) but statistically significantly better than those observed for patients whose tumors were negative for both P-Akt and P-MAPK (response rate = 4.4%; $P = .014$; and disease control rate = 24.4%; $P = .011$) (Table 3). No comparisons were made with six patients whose tumors were negative for P-Akt but positive for P-MAPK because of the small sample size.

Time to Progression and Survival Analysis

Final analysis was performed in November 2003, after more than 3 months since the enrollment of the last patient. With a median follow-up time of 6.6 months (range = 0.6–24.1 months), the median time to progression for the entire cohort was 3.4 months (range = 0.6–24.1 months), and median overall survival time was 9.4 months (range = 0.6–24.1 months). At the time of the final analysis, 33 patients with P-Akt–positive tumors and 44 patients with P-Akt–negative tumors had radiologically confirmed disease progression, whereas 27 patients with P-Akt–positive tumors and 41 patients with P-Akt–negative tumors had symptomatic progression (onset of new symptoms or worsening of existing disease-related symptoms). Median time to progression was statistically significantly longer for patients with P-Akt–positive tumors than for patients with P-Akt–negative tumors (5.5 versus 2.8 months, mean difference = 2.7 months, 95% CI = 1.5 to 3.9 months; $P = .004$) (Fig. 1). Time to progression did not differ on the basis of P-MAPK status (3.2 months for patients with P-MAPK–negative tumors versus 4.8 months for patients with P-MAPK–negative tumors; $P = .29$). Median time to progression was 6.2 months for patients with tumors that were positive for both P-Akt and P-MAPK, which was not statistically significantly different from the median time to progression of patients with tumors that were negative for P-Akt and P-MAPK (2.8 months; $P = .05$) or from that of patients with tumors that were positive for P-Akt and negative for P-MAPK (0/1+) (5.3 months; $P = .63$).

To define which variables were predictive of improved time to progression, we evaluated prespecified prognostic factors at

Table 3. Association between response to gefitinib therapy and phosphorylation status of Akt and MAPK in patients with advanced non–small-cell lung cancer

Tumor phosphorylation status*	Total No. of evaluable tumors	No. of complete and partial responses (%)	P	No. of complete, partial, and stable disease responses (%)	P
P-Akt−/MAPK 2+/3+	18	5 (29.4)	.737	10 (58.8)	.828
P-Akt+/MAPK 0/1+	33	7 (24.1)		18 (62.1)	
P-Akt−/MAPK 0/1+	46	2 (4.4)	.014	11 (24.4)	.011

*Phospho-Akt (P-Akt) and phospho-MAPK (P-MAPK) status was determined by immunohistochemistry on tumor sections. Tumors that had nuclear P-Akt staining, a measure of Akt activation, were considered positive. For P-MAPK staining, if none of the tumor cells stained, the intensity was 0 (considered negative); if more than 10% of the tumor cells stained weakly, the intensity was 1+ (considered negative); if more than 10% of the tumor cells stained moderately, the intensity was 2+ (considered positive); and if more than 10% of the tumor cells stained strongly, the intensity was 3+ (considered positive).

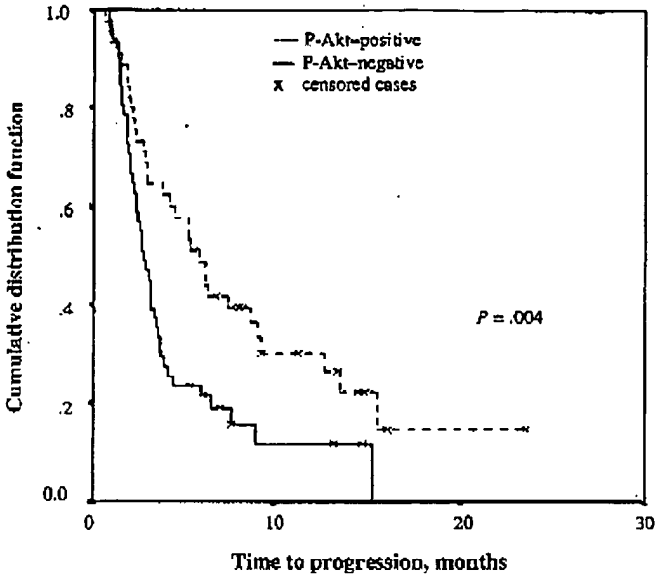

No. at risk		
P-Akt–positive		
45	9	1
P-Akt–negative		
51	3	0

Fig. 1. Time to progression in patients with advanced non–small-cell lung cancer who received gefitinib therapy according to the phosphorylation status of Akt. Phosphorylation status was determined on the basis of immunohistochemistry on tumor sections stained before the patients received gefitinib therapy. Median time to progression was 5.5 months (95% CI = 3.8 to 7.2 months) for patients with P-Akt–positive tumors and 2.8 months (95% CI = 2.3 to 3.3 months) for patients with P-Akt–negative tumors. Differences between the two groups were evaluated with the log-rank test.

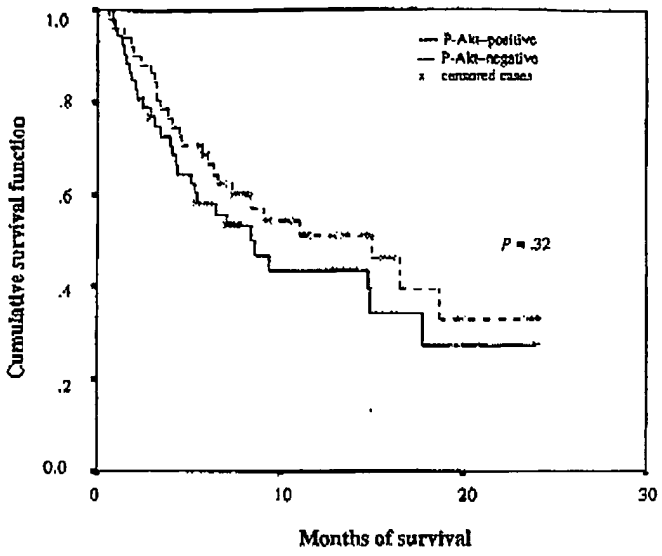

No. at risk		
P-Akt–positive		
51	18	4
P-Akt–negative		
52	13	2

Fig. 2. Survival in patients with advanced non–small-cell lung cancer who received gefitinib therapy according to the phosphorylation status of Akt. Phosphorylation status was determined on the basis of immunohistochemistry on tumor sections stained before the patients received gefitinib therapy. Median survival was 15.0 months (95% CI = 7.4 to 22.6 months) for patients with P-Akt–positive tumors and 8.3 months (95% CI = 4.8 to 11.8 months) for patients with P-Akt–negative tumors. Differences between the two groups were evaluated with the log-rank test.

study entry, such as age, sex (male versus female), performance status (0/1 versus 2), disease stage (III versus IV), smoking history (current and former smoker versus never smoker), histology (adenocarcinoma including bronchioloalveolar versus other histotypes), P-MAPK status (P-MAPK 0/1+ versus P-MAPK 2+/3+), P-Akt status (P-Akt positive versus P-Akt negative) in a univariate analysis, and those variables associated with statistically significant relationships (sex, performance status, smoking history, and P-Akt status) were included in the multivariable model. P-Akt status, smoking history, and performance status were statistically significantly associated with risk of progression. Patients with P-Akt–positive tumors had a statistically significantly lower risk of disease progression than patients with P-Akt–negative tumors (hazard ratio [HR] = 0.58, 95% CI = 0.35 to 0.94), whereas patients with a performance status of 2 or patients who smoked (current or former) had a statistically significantly higher risk of disease progression (HR = 2.65, 95% CI = 1.33 to 5.27; and HR = 1.75, 95% CI = 1.08 to 2.85, respectively). Median survival time was 15.0 months (95% CI = 7.4 to 22.6 months) for patients with P-Akt–positive tumors and 8.3 months (95% CI = 4.8 to 11.8 months) for patients with P-Akt–negative tumors (P = .32) (Fig. 2). Median survival times were similar among patients whose tumors differed on the basis of P-MAPK status (P = .96).

Discussion

We evaluated the relationship between the efficacy of gefitinib therapy and P-Akt/P-MAPK status in patients with advanced NSCLC, and we found that patients whose tumors showed activation of the PI3K–Akt pathway (i.e., whose tumors were positive for P-Akt) had statistically significantly better response rates, disease control rates, and times to progression. Gefitinib is a synthetic anilinoquinazoline tyrosine kinase inhibitor that is selective for the EGFR. Although it could be hypothesized that EGFR expression is a prerequisite for a response to the drug, EGFR expression has not turned out to be useful in the selection of patients who respond to gefitinib. Indeed, preclinical data suggest that gefitinib sensitivity is not related to EGFR expression *(30)*—a finding that is supported by the fact that patients with squamous-cell carcinomas had lower response rates than patients with adenocarcinoma, despite their higher levels of EGFR expression. Because EGFR preferentially dimerizes with HER2, and because preclinical data suggested that HER2-overexpressing tumors are more sensitive to gefitinib therapy *(31)*, we previously analyzed the association between HER2 status and gefitinib activity *(32)*. Although in that small study no association was found between gefitinib activity and HER2 expression, the results confirmed that a small subgroup of patients are still particularly sensitive to gefitinib.

On the basis of previous findings, we hypothesized that response to gefitinib would occur only in patients whose

tumors were dependent on sustained activation of the EGFR signaling pathways, and only in those in whom these pathways were suppressed by the drug. In this study, we evaluated the two major EGFR signaling pathways (PI3K–Akt and Ras/Raf/MAPK). Only the PI3K–Akt pathway was statistically significantly associated with gefitinib activity. Compared with patients whose tumors were negative for P-Akt, patients whose tumors were positive for P-Akt had a better response rate (26.1% versus 3.9%; $P = .003$) and disease control rate (60.9% versus 23.5%; $P<.001$). No difference in response and disease control rate was observed between patients with P-MAPK–negative and P-MAPK–positive tumors. Patients whose tumors were positive for both P-Akt and P-MAPK had better response and disease control rates only in comparison with patients whose tumors were negative for both markers ($P = .01$) and not in comparison with patients whose tumors were positive for P-Akt but negative for P-MAPK. These findings are consistent with preclinical data suggesting that the PI3K–Akt pathway plays a critical role in the antitumor effects of gefitinib and that inhibition of the MAPK pathway is not sufficient to mediate response to the drug *(40)*.

In two large phase II studies evaluating gefitinib, only being female and having an adenocarcinoma histology were associated with a clinical response *(28,29)*. More recently, Shah et al. *(41)* also reported that, in a multivariable analysis of 140 patients, those patients who had never smoked cigarettes and those with bronchioloalveolar carcinoma histology were more likely to respond to gefitinib. These findings are in agreement with those of our study, in which P-Akt status was statistically significantly associated with being female ($P<.001$), never smoking history ($P = .004$), and bronchioloalveolar carcinoma histology ($P = .034$). Results from analyses of the time-to-progression data support the central role of Akt activation in gefitinib activity. Compared with patients whose tumors were negative for P-Akt, patients whose tumors were positive for P-Akt had a statistically significantly longer time to progression (5.5 versus 2.8 months; $P = .004$). We found no difference in the time to progression among patients grouped on the basis of P-MAPK status ($P = .29$), although we noted slight, albeit not statistically significant, evidence of a longer time to progression among patients whose tumors were positive for both markers compared with patients whose tumors were negative for both markers ($P = .05$).

To further investigate the difference in time to progression observed among patients whose tumors were positive or negative for P-Akt, we performed a planned multivariable analysis, and only those variables that were statistically significant in the univariate analysis (sex, performance status, smoking history, and P-Akt status) were included in the model. To ensure that only relevant factors were retained in the multivariable model, the backward regression technique was used at the 10% significance level. In the multivariable analysis, P-Akt status was statistically significantly associated with a reduced risk of disease progression (HR = 0.58, 95% CI = 0.35 to 0.94). Importantly, after being adjusted for P-Akt status, performance status and smoking history remained statistically significantly associated with an increased risk of disease progression (HR = 2.65 [95% CI = 1.33 to 5.27] and 1.75 [95% CI = 1.08 to 2.85], respectively), and female sex was immediately removed at the first step of the backward elimination. These data indicate that P-Akt status, performance status, and smoking history are independent factors for disease progression but that being female is not when Akt status is considered. These findings do not represent a variation in respect to the IDEAL trial results because in those studies *(28,29)*, sex was related to response rate and not to time to progression. Moreover, the impact of P-Akt was not evaluated in the multivariable model used in the IDEAL trials.

Although response rate, disease control rate, and time to progression were better for 51 patients whose tumors were positive for P-Akt than for 52 patients whose tumors were negative, two patients among the latter group had major responses and 10 patients had stable disease. This finding may be explained by the fact that the tumor specimens used for the immunohistochemical assays were generally obtained at the time of primary diagnosis and not immediately before starting the trial. Preclinical data showed that NSCLC tumors may become more dependent on the EGFR signaling pathway, and therefore more sensitive to EGFR blocking strategies, as they are exposed to different chemotherapies *(42,43)*. This finding may also explain the negative results of the INTACT trials, in which standard chemotherapy plus gefitinib was compared with standard chemotherapy alone in previously untreated patients with NSCLC *(44,45)*. In our study, only 6.6% of individuals received gefitinib as first-line therapy, and in five of those patients, the PI3K–Akt pathway was not activated (i.e., their tumors were P-Akt negative). Another important finding is that almost 40% of patients with P-Akt–positive tumors did not benefit from gefitinib therapy. Recent data indicate that sensitivity to gefitinib therapy requires intact EGFR-stimulated Akt signaling activity and that loss of PTEN, a phosphatase that negatively regulates Akt by dephosphorylating it, can lead to aberrant Akt activation and, finally, to gefitinib resistance *(40,46,47)*. In this study, PTEN status was not determined, but a retrospective analysis of PTEN status in all patients included in this trial is ongoing.

No difference in survival was found among any group of patients separated on the basis of Akt or MAPK phosphorylation status, but survival was not the primary end point of the study, and at the time of this analysis, median follow-up was too short and the number of censored cases too high to detect any difference. Analysis of survival curves does show a trend that favors patients whose tumors are positive for P-Akt, and it is possible that with longer follow-up a difference in survival outcome could be detected.

Recent reports *(48,49)* showed that specific missense and deletion mutations in the tyrosine kinase domain of the EGFR gene are statistically significantly associated with gefitinib sensitivity. However, although objective responses were reported in up to 18%, and symptomatic improvement in 40%, of the unselected gefitinib-treated NSCLC patients *(28,29)*, the low frequency of these mutations in unselected U.S. patients *(49)* suggests that other mechanisms could be involved in the response to gefitinib, such as Akt activation. Further studies should evaluate the association between Akt activation and EGFR gene status.

Finally, this trial showed that Akt is activated in approximately 50% of patients with NSCLC. Our findings are in agreement with the results of Brognard et al. *(15)*, who showed that Akt is constitutively active in many cases of NSCLC, and our findings confirm the recent report by Lee et al. *(20)*, who showed that tumors in patients with NSCLC frequently express phosphorylated Akt. Despite the observation that many patients with

NSCLC express activated Akt, the relationship between Akt activation and lung carcinogenesis remains unclear.

In conclusion, our findings suggest that gefitinib therapy is more active in patients with tumors that are positive for P-Akt than in those with tumors that are negative for P-Akt. Further prospective studies are needed to evaluate the role of other associated markers such as PTEN and to assess the impact of previous therapies on Akt signaling pathway.

REFERENCES

(1) Greenlee RT, Hill-Harmon MB, Murray T, Thun M. Cancer statistics, 2001. CA Cancer J Clin 2001;51:15–36.

(2) Jemal A, Thomas A, Murray T, Thun M. Cancer statistics, 2002. CA Cancer J Clin 2002;52:23–47.

(3) Salomon D, Gullick W. The erbB family of receptors and their ligands: multiple targets for therapy. Signal 2001;2:4–11.

(4) Ciardello F, Tortora G. A novel approach in the treatment of cancer: targeting the epidermal growth factor receptor. Clin Cancer Res 2001;7: 2958–70.

(5) Arteaga CL. Overview of epidermal growth factor receptor biology and its role as a therapeutic target in human neoplasia. Semin Oncol 2002;29(5 Suppl 14):3–9.

(6) Bunn PA Jr, Franklin W. Epidermal growth factor receptor expression, signal pathway, and inhibition in non-small cell lung cancer. Semin Oncol 2002;29(5 Suppl 14):38–44.

(7) Lewis TS, Shapiro PS, Ahn NG. Signal transduction through MAP kinase cascades. Adv Cancer Res 1998;74:49–139.

(8) Franke TF, Kaplan DR, Cantley LC. PI3K: downstream AKTion blocks apoptosis. Cell 1997;88:435–7.

(9) Datta SR, Dudek H, Tao X, Masters S, Fu H, Gotoh Y, et al. Akt phosphorylation of BAD couples survival signals to the cell-intrinsic death machinery. Cell 1997;91:231–41.

(10) Cardone MH, Roy N, Stennicke HR, Salvesen GS, Franke TF, Stanbridge E, et al. Regulation of cell death protease caspase-9 by phosphorylation. Science 1998;282:1318–21.

(11) Hemmings BA. AKT signaling: linking membrane events to life and death decision. Science 1997;275:628–30.

(12) Kulik G, Weber MJ. Akt-dependent and -independent survival signaling pathways utilized by insulin-like growth factor I. Mol Cell Biol 1998;18: 6711–8.

(13) Kulik G, Klippel A, Weber MJ. Antiapoptotic signalling by the insulin-like growth factor I receptor, phosphatidylinositol 3-kinase, and Akt. Mol Cell Biol 1997;17:1595–606.

(14) Ng SSW, Tsao MS, Chow S, Hedley DW. Inhibition of phosphatidylinositide 3-kinase enhances gemcitabine-induced apoptosis in human pancreatic cancer cells. Cancer Res 2000;60:5451–5.

(15) Brognard J, Clark AS, Ni Y, Dennis PA. Akt/protein kinase B is constitutively active in non-small cell lung cancer cells and promotes cellular survival and resistance to chemotherapy and radiation. Cancer Res 2001; 61:3986–97.

(16) Cheng JQ, Ruggeri B, Klein WM, Sonoda G, Altomare DA, Watson DK, et al. Amplification of AKT2 in human pancreatic cells and inhibition of AKT2 expression and tumorigenicity by antisense RNA. Proc Natl Acad Sci U S A 1996;93:3636–41.

(17) Vasko V, Saji M, Hardy E, Kruhlak M, Larin A, Savchenko V, et al. Akt activation and localisation correlate with tumour invasion and oncogene expression in thyroid cancer. J Med Genet 2004;41:161–70.

(18) Yuan ZQ, Sun M, Feldman RI, Wang G, Ma X, Jiang C, et al. Frequent activation of AKT2 and induction of apoptosis by inhibition of phosphoinositide-3-OH kinase/Akt pathway in human ovarian cancer. Oncogene 2000;19:2324–30.

(19) Cheng JQ, Godwin AK, Bellacosa A, Taguchi T, Franke TF, Hamilton TC, et al. AKT2, a putative oncogene encoding a member of a subfamily of protein-serine/threonine kinases, is amplified in human ovarian carcinomas. Proc Natl Acad Sci U S A 1992;89:9267–71.

(20) Lee SH, Kim HS, Park WS, Kim SY, Lee KY, Kim SH, et al. Non-small cell lung cancer frequently express phosphorylated Akt: an immunohistochemical study. APMIS 2002;110:587–92.

(21) Levitzki A, Gazit A. Tyrosine kinase inhibition: an approach to drug development. Science 1995;267:1782–8.

(22) Levitt ML, Koty PP. Tyrosine kinase inhibitors in preclinical development. Invest New Drugs 1999;7:213–26.

(23) Ciardiello F, Caputo R, Bianco R, Damiano V, Pomatico G, De Placido S, et al. Antitumour effect and potentiation of cytotoxic drug activity in human cancer cells by ZD1839 (Iressa), an epidermal growth factor receptor-selective tyrosine kinase inhibitor. Clin Cancer Res 2000;6: 2053–63.

(24) Kris MG, Herbst R, Rischin D, LoRusso P, Baselga J, Hammond L, et al. Objective regression in non-small cell lung cancer patients treated in phase I trials of oral ZD 1839 (Iressa), a selective tyrosine kinase inhibitor that blocks the epidermal growth factor receptor (EGFR) [abstract 233]. Lung Cancer 2000;29(Suppl 1):72.

(25) Baselga J, Rischin D, Ranson M, Calvert H, Raymond E, Kieback DG, et al. Phase I safety, pharmacokinetic, and pharmacodynamic trial of ZD1839, a selective oral epidermal growth factor receptor tyrosine kinase inhibitor, in patients with five selected solid tumor types. J Clin Oncol. 2002;20:4292–302.

(26) Herbst RS, Maddox AM, Rothenberg ML, Small EJ, Rubin EH, Baselga J, et al. Selective oral epidermal growth factor receptor tyrosine kinase inhibitor ZD1839 is generally well-tolerated and has activity in non-small-cell lung cancer and other solid tumors: results of a phase I trial. J Clin Oncol 2002;20:3815–25.

(27) Ranson M, Hammond LA, Ferry D, Kris M, Tullo A, Murray PI, et al. ZD1839, a selective oral epidermal growth factor receptor-tyrosine kinase inhibitor, is well tolerated and active in patients with solid, malignant tumors: results of a phase I trial. J Clin Oncol 2002;20:2240–50.

(28) Fukuoka M, Yano S, Giaccone G, Tamura T, Nakagawa K, Douillard JY, et al. Multi-institutional randomized phase II trial of gefitinib for previously treated patients with advanced non-small-cell lung cancer. J Clin Oncol 2003;21:2237–46.

(29) Kris MG, Natale RB, Herbst RS, Lynch TJ Jr, Prager D, Belani CP, et al. Efficacy of gefitinib, an inhibitor of the epidermal growth factor receptor tyrosine kinase, in symptomatic patients with non-small cell lung cancer: a randomized trial. JAMA 2003;290:2149–58.

(30) Sirotnak FM, Zakowski MF, Miller VA, Scher HI, Kris MG. Efficacy of cytotoxic agents against human tumor xenografts is markedly enhanced by coadministration of ZD1839 (Iressa), an inhibitor of EGFR tyrosine kinase. Clin Cancer Res 2000;6:4885–92.

(31) Moasser MM, Basso A, Averbuch SD, Rosen N. The tyrosine kinase inhibitor ZD1839 ("Iressa") inhibits HER2-driven signaling and suppresses the growth of HER2-overexpressing tumor cells. Cancer Res 2001;61:7184–8.

(32) Cappuzzo F, Gregorc V, Rossi E, Cancellieri A, Magrini E, Paties CT, et al. Gefitinib in pretreated non-small-cell lung cancer (NSCLC): analysis of efficacy and correlation with HER2 and epidermal growth factor receptor expression in locally advanced or metastatic NSCLC. J Clin Oncol 2003: 21:2658–63.

(33) Travis WD, Colby TV, Corrin B, Shimosato Y, Brambilla E. Histological typing of lung and pleural tumors. 3rd ed. Berlin (Germany): Springer; 1999.

(34) Allred DC, Clark GM, Elledge R, Fuqua SA, Brown RW, Chamness GC, et al. Association of p53 protein expression with tumor cell proliferation rate and clinical outcome in node-negative breast cancer. J Natl Cancer Inst 1993;85:200–6.

(35) Meier R, Alessi DR, Cron P, Andjelkovic M, Hemmings BA. Mitogenic activation, phosphorylation, and nuclear translocation of protein kinase Bbeta. J Biol Chem 1997;272:30491–7.

(36) Therasse P. New guidelines to evaluate the response to treatment in solid tumors. J Natl Cancer Inst 2000;92:205–16.

(37) Kaplan EL, Meier P: Nonparametric estimation from incomplete observations. J Am Stat Assoc 1985;53:457–81.

(38) Cox DR. Regression models and life tables. J R Stat Soc B 1972;34:187–220.

(39) Agresti A. Categorical data analysis. New York (NY): John Wiley & Sons; 1990.

(40) She QB, Solit D, Basso A, Moasser MM. Resistance to gefitinib in PTEN-null HER-overexpressing tumor cells can be overcome through restoration of PTEN function or pharmacologic modulation of constitutive phosphatidylinositol 3'-kinase/Akt pathway signaling. Clin Cancer Res 2003;9:4340–6.

(41) Shah NT, Miller VA, Kris MG, Patel J, Venkatraman E, Benporat L, et al. Bronchioloalveolar histology and smoking history predict response to gefitinib [abstract 2524]. Proc ASCO 2003;22:628.

(42) Sato JD, Kawamoto T, Le AD, Mendelsohn J, Polikoff J, Sato GH. Biological effects in vitro of monoclonal antibodies to human epidermal growth factor receptors. Mol Biol Med 1983;1:511–29.

(43) Perez-Soler R, Dai Q, Ling YH, Zou Y, Lin M, Kroog G, et al. Molecular mechanisms of sensitivity and resistance to the HER1/EGFR tyrosine Kinase inhibitor erlotinib [abstract O-247]. Lung Cancer 2003;41:s72.

(44) Giaccone G, Herbst RS, Manegold C, Scagliotti G, Rosell R, Miller V, et al. Gefitinib in combination with gemcitabine and cisplatin in advanced non-small-cell lung cancer: a phase III trial—INTACT 1. J Clin Oncol 2004;22:777–84.

(45) Herbst RS, Giaccone G, Schiller JH, Natale RB, Miller V, et al. Gefitinib in combination with paclitaxel and carboplatin in advanced non-small-cell lung cancer: a phase III trial—INTACT 2. J Clin Oncol 2004;22:785–94.

(46) Bianco R, Shin I, Ritter CA, Yakes FM, Basso A, Rosen N, et al. Loss of PTEN/MMAC1/TEP in EGF receptor-expressing tumor cells counteracts the antitumor action of EGFR tyrosine kinase inhibitors. Oncogene 2003;22:2812–22.

(47) Jammal ML, Kruyt FA, Rodriguez JA, Giaccone G. Response to epidermal growth factor receptor inhibitors in non-small cell lung cancer cells: limited antiproliferative effects and absence of apoptosis associated with persistent activity of extracellular signal-regulated kinase or Akt kinase pathways. Clin Cancer Res 2003;9:2316–26.

(48) Lynch TJ, Bell DW, Sordella R, Gurubhagavatula S, Okimoto RA, Brannigan BW, et al. Activating mutations in the epidermal growth factor receptor underlying responsiveness of non-small-cell lung cancer to gefitinib. N Engl J Med 2004;350:2129–39.

(49) Paez JG, Janne PA, Lee JC, Tracy S, Greulich H, Gabriel S, et al. EGFR mutations in lung cancer: correlation with clinical response to gefitinib therapy. Science 2004;304:1497–500.

NOTES

We thank Katherine Brandt Tomato and Dr. Thomas Chanin for their editorial assistance and Dr. Fred Hirsch for his useful comments on the manuscript.

Manuscript received January 8, 2004; revised May 28, 2004; accepted June 4, 2004.

Pathol. Oncol. Res. (2011) 17:257–261
DOI 10.1007/s12253-010-9307-1

RESEARCH

Activation of the PI3K/Akt Pathway Mediates Bone Morphogenetic Protein 2-Induced Invasion of Pancreatic Cancer Cells Panc-1

Xiong Chen · Jie Liao · YeBin Lu · XiaoHui Duan · WeiJia Sun

Received: 22 May 2010 / Accepted: 1 September 2010 / Published online: 17 September 2010

Abstract Bone morphogenetic proteins (BMPs) signaling has an emerging role in pancreatic cancer. However, because of the multiple effects of different BMPs, no final conclusions have been made as to the role of BMPs in pancreatic cancer. In our studies, we have focused on bone morphogenetic protein 2(BMP-2) because it induces an epithelial to mesenchymal transition (EMT) and accelerates invasion in the human pancreatic cancer cell line Panc-1. It has been reported that the phosphatidylinositol 3-kinase (PI3K)/Akt pathway mediates invasion of gastric and colon cancer cells, which is unrevealed in pancreatic cancer cells. The objective of our study was to investigate whether BMP-2 mediated invasion might pass through the PI3K/Akt pathway. Our results show that expression of phosphorylation of Akt was increased by treatment with BMP-2, but not Noggin, a BMP-2 antagonist. Then pretreatment of Panc-1 cells with LY294002, an inhibitor of the PI3K/AKT pathway, significantly inhibited BMP-2-induced EMT and invasiveness. The data suggest that BMP-2 accelerates invasion of panc-1 cells via the PI3K/AKT pathway in panc-1 cells, which gives clues to searching new therapy targets in advanced pancreatic cancer.

X. Chen · Y. Lu · X. Duan
Department of General Surgery, XiangYa Hospital,
Central South University,
Changsha 410008 Hunan, People's Republic of China

J. Liao
Department of Endocrinology, XiangYa Hospital,
Central South University,
Changsha 410008 Hunan, People's Republic of China

W. Sun (✉)
Institute of Pancreatic Diseases, Central South University,
Changsha 410008 Hunan, People's Republic of China
e-mail: sunweijiays@hotmail.com

Keywords PI3K/Akt · Bone morphogenetic protein-2 (BMP-2) · Invasion · Epithelial to mesenchymal transition (EMT)

Introduction

Although the management and treatment of patients with pancreatic cancer have improved in the last few decades, the overall 5-year survival rate remains at less than 5%. Patients rarely exhibit symptoms before the cancer has become locally advanced or metastatic [1, 2]. BMPs have an emerging role in pancreatic cancer. BMPs belong to the transforming growth factor β (TGF-β) superfamily. BMPs exert their effects via two different types of serine/threonine kinase receptors, BMP type I (BMPR-IA and BMPR-IB) and type II (BMPR-II) receptors. BMP receptor type I is activated upon ligand binding and subsequently phosphorylates receptor -activated Smad proteins (Smad-1, Smad-5 and Smad-8). The phosphorylated Smads then bind to a common mediator Smad (Co-smad, Smad-4), translocate into the nucleus and activate transcription of target genes [3, 4]. BMPs have broad functions including the regulation of many types of normal tissue patterning [5–7] and epithelial-mesenchymal interaction in the developmental process [8]. More recently, it has been reported that BMPs induced EMT and invasion of Panc-1 cells, which was related to activation of Smad1, 5, 8 pathway [9].

Although Smads are critical for BMP family signaling, recent data have implicated multiple non-Smad pathways, including PI3K/Akt, NF-κB, or RAS/ERK pathways, in mediating BMP signaling [10]. It has been found that the PI3K/Akt pathway plays an important role in maintaining the neoplastic phenotype of pancreatic cancer cells. Inhibition of the pathway significantly improved the

survival of nude mice bearing pancreatic tumor xenografts [11, 12]. Increased expression of the PI3K catalytic subunit genes and an increase in Akt activity has been observed in pancreatic cancer cells [13]. Interestingly, which may lead to activation of Akt, was shown to be correlated with metastatic pancreatic cancer [11, 14]. Furthermore, activation of Akt has been suggested to be associated with chemoresistance of aggressive pancreatic cancer [15, 16].

It has been reported that BMP-2 causes EMT and accelerates invasion of Panc-1 cells, and more recently, two studies observed that BMP-2 accelerates the motility and invasiveness of gastric and colon cancer cells via activation of the PI3K/Akt pathway [17, 18], but the role of the PI3K/Akt pathway in invasiveness of pancreatic cancer cells induced by BMP-2 has not been fully investigated. In the present study, we explored the role of the PI3K/Akt pathway in BMP-2-induced EMT and cellular invasiveness. Our results suggest that the BMP-2 signaling pathway induces metastatic functions of pancreatic cancer through the recruitment of the PI3K/Akt pathway.

Materials and Methods

Cell Culture

Human pancreatic cancer cell line Panc-1 was purchased from the Institute of Cell Biology, Shanghai, China, and cultured in Dulbecco's modified Eagle's medium. The medium was supplemented with 4.5 g/L glucose and L-glutamine, 100 IU penicillin, 100 mg/ml streptomycin and 10% fetal bovine serum.

Reagents and Antibodies

Recombinant human BMP-2 and noggin were purchased from R&D Systems (Minneapolis, MN). LY294002 were purchased from Calbiochem (San Diego, CA). Antibodies specific for Akt and phospho-Akt, were obtained from Cell Signaling Technology (Beverly, MA). Antibodies specific for E-cadherin, Slug and β-actin were purchased from Santa Cruz Biotechnology (Santa Cruz, CA).

Western Blotting

Cells were lysed by the addition of lysis buffer containing150 mM NaCl,50 mM Tris-HCl, 1% Nonidet P40, and 0.5% sodium deoxycholate. Cell lysates were cleared by centrifugation at 16,000 rpm, 4°C for 15 min. Cleared lysates were boiled for 5 min at 100 C after the addition of 5× sample loading buffer containing 1 M Tris-HCl (pH 6.8), sodium dodecylsulphate, glycerol, and bromphenolblue. The samples were electrophoresed at 200 V on 12.5% polyacrylamide gels and transferred to nitrocellulose membranes (Bio-Rad, Hercules, CA), blocked with 5% non-fat dry milk, and incubated with the primary antibody. The primary antibodies used in this study were as follows: The primary antibodies were as follows: anti-Akt (Cell Signaling Technology), anti-phospho-Akt (Ser 473: Cell Signaling Technology), anti-E-cadherin (Santa Cruz Biotechnology, Inc.), anti-Slug (Santa Cruz Biotechnology, Inc.), anti-β-actin (Santa Cruz Biotechnology, Inc.).

Matrigel Invasion Assay

In vitro invasion assays were performed using 24-well Matrigel-coated transwells (BD Biosciences). 1×10^5 cells/well were seeded in the upper chamber, serum-free medium containing BMP-2 or control vehicle was added to the lower chamber. After 24 h of incubation, non-migrating cells were removed from the upper chamber with a cotton swab and migrating cells on the underside were fixed and stained with crystal violet. The invasing cells were then counted by microscopy. All experiments were repeated three times.

Statistical Analysis

Statistical comparisons were performed by two-tailed Student's t test. Data are given as the mean ± SEM. Significance was established when $P<0.05$.

Results

BMP-2 Up-Regulates Protein Level of the PI3K/Akt Pathway in Panc-1 Cells

To determine whether the PI3K/Akt pathway was involved in the BMP-2-mediated cellular response in panc-1 cells, we first compared levels of phosphorylated and non-phosphorylated Akt in Panc-1 cells treated with BMP-2 or control vehicle by using Western blotting. Stimulation with BMP-2 led to a significant increase in phosphorylation of ser473 in Akt (Fig. 1a). However, there was no change observed in the expression of total Akt, irrespective of the presence of BMP-2. To further confirm the effect of BMP-2 on the expression or kinase activation of Akt, we inhibited the BMP-2 pathway by treating cells with Noggin and then performed Western blot analysis for phosphorylated Akt. As expected, phosphorylation of Akt was markedly reduced in cells that were treated with Noggin when compared with cells treated with control vehicle (Fig. 1a), suggesting that BMP-2 signaling plays a critical role in Akt activation. LY294002,an inhibitor of the PI3K/Akt pathway, attenuated the effect of BMP-2 on the PI3K/Akt pathway. In spite of

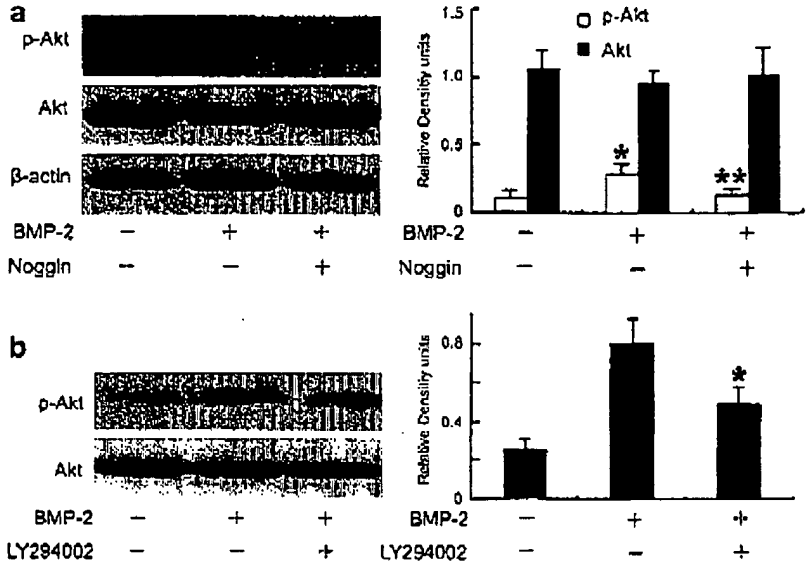

Fig. 1 BMP-2 up-regulates protein level of the PI3K/Akt pathway in Panc-1 cells. (a) Panc-1 cells were pretreated with Noggin (5 μg/ml) for 60 min, and then stimulated with BMP-2(100 ng/ml) for 60 min. The total protein was harvested for Western blot analysis using specific antibodies against p-Akt, Akt, and β-actin. *P<0.01, compared with cells that were treated with control vehicle. **P<0.01, compared with cells that were treated with BMP-2. (b) Cells were pretreated with 20 μM LY294002 + DMSO for 30 min followed by stimulation with BMP-2 for 60 min. Protein extracts were prepared for Western blot analysis using specific antibodies against p-Akt and Akt. *P<0.01, compared with cells that were treated with BMP-2 + DMSO

the presence of added BMP-2, treatment with LY294002 significantly decreased phosphorylation of Akt (Fig. 1b).

Inhibition of the PI3K/Akt Pathway Decreases BMP-2-Induced Invasion in Panc-1 Cells

BMP-2 has recently been demonstrated to increase the invasiveness of pancreatic cancer cells, BMP-2 treatment of Panc-1 cells dramatically increased the invasion compared with untreated cells through Matrigel [9].To determine the roles of the PI3K/Akt pathway during BMP-2-induced invasion in Panc-1 cells, we examined the effects of blocking the PI3K/Akt pathway on BMP-2-induced invasion. Treatment with LY294002 of Panc-1cells before BMP-2 stimulation significantly decreased invasion than that compared with cells treated with BMP-2 alone. Taken together, these findings show that the BMP-2 signaling pathway modulates the invasion of Panc-1 cells through PI3K/Akt signals. In addition, invasive activity in response to LY294002 by Panc-1 cells treated with BMP-2 was blocked (Fig. 2).

Inhibition of the PI3K/Akt Pathway Attenuates EMT Induced by BMP-2 in Panc-1 Cells

Recent studies have reported that BMP-2 induces EMT, a crucial step for cancer invasion and metastasis, in pancreatic cancer cells. To determine the roles of the PI3K/Akt

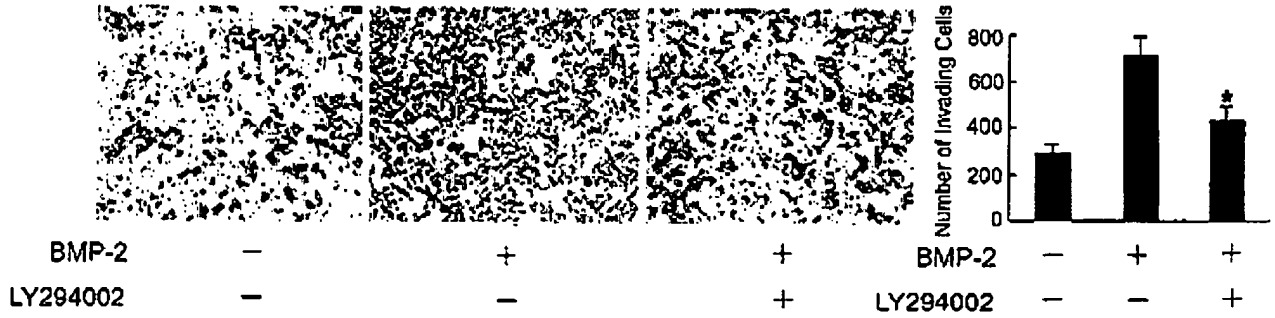

Fig. 2 Invasive activity in response to LY294002 by Panc-1 cells treated with BMP-2 was blocked. Panc-1 cells treated with LY294002 (20 μM) in the presence of BMP-2 (100 ng/ml) were then evaluated in a performance invasion assay.*P<0.01, compared with cells that were treated with BMP-2 plus DMSO

pathway during BMP-2-induced EMT in Panc-1 cells, we examined the effects of blocking the PI3K/Akt pathway on BMP-2-induced EMT. Panc-1 cells were pretreated with LY294002 before BMP-2 stimulation and Western blotting for E-cadherin and Slug was performed. We found that decreasing levels of expression of E-cadherin protein by BMP- 4 was completely reverted in Panc-1 cells when the PI3K/Akt pathway was blocked by LY294002 (Fig. 3). Similarly, pretreatment with LY294002 also blocked Slug expression that results from BMP-2 stimulation (Fig. 3). Collectively, these findings strongly suggest that the PI3K/Akt pathway is involved in the EMT response to BMP-2.

Discussion

Recently, several studies have suggested that BMP signaling plays a role in the control of the invasiveness of pancreatic cancer cells. For example, Gordon et al. [9] reported that BMP-2 and BMP-4 is highly overexpressed in human pancreatic cancer and stimulates tumor growth and motility in Panc-1 cells. Hamada et al. [19] also demonstrated that the BMP signaling pathway modulates EMT, resulting in enhancement of invasion in Panc-1 cells. Although these reports demonstrated the role that Smad pathway plays in invasion of pancreatic cancer cells, little is known about that PI3K/Akt pathway regulation plays on BMP-2 induced metastatic behavior of pancreatic cancer cells. The PI3K/Akt pathway is a major cascade stimulating cell migration and invasion in various human cancers [20–22]. Moreover, the PI3K/Akt pathway has been shown to be activated by BMP-2 [23]. Several groups have found that the PI3K/Akt pathway is correlated with the acquisition of migratory and invasive capabilities by BMP-2 [17, 18]. To better understand the molecular mechanism by which BMP-2 promotes invasion of Panc-1 cells. Firstly, we examined that in this study using recombinant human BMP-2 to activate the PI3K/Akt pathway in panc-1 cells. Our results showed that Stimulation with BMP-2 led to a significant increase in phosphorylation of ser473 in Akt, which was blocked by LY294002. Then, using matrigel invasion assay, we observed that increasing invasive capability of Panc-1 induced by BMP-2 was recovered. These findings suggesting that the PI3K/Akt pathway is involved in the invasion response to BMP-2.

EMT, a complex process that leads to loss of epithelial morphology and gain of an invasive fibroblast-like mesenchymal phenotype, is a crucial step for cancer invasion and metastasis in various cancer cell [24–27].EMT is often associated with a decrease or loss of epithelial markers, E-cadherin, and a gain of mesenchymal markers, Slug, which is known to repress expression of the E-cadherin gene. Recent studies have reported that BMPs induces EMT in pancreatic cancer cells and this contributes to increased invasiveness [19].To further confirm the role of the PI3K/Akt pathway in BMP-2 induced invasion of Panc-1 cells, we demonstrated that blockage of the PI3K/Akt pathway by the PI3K inhibitor, LY294002, attenuates Panc-1cells responsive to BMP-2 mediated EMT, indicating that the PI3K/Akt pathway modulates BMP-2 signaling in pancreatic cancer invasion. Interestingly, It has been founded that the activation of PI3K signaling pathways was not detected in BMP-4 treated panc-1 cells. Therefore, to understand this difference of BMP-2 and BMP-4 in pancreatic cancer, further studies will be needed. More recently, Kang MH et al. [17, 18] demonstrated that BMP2 promotes the invasiveness of gastric and colon cancer cells via activation of the PI3K/Akt pathway, which is highly in accordance with our findings.

In summary, BMPs signaling has an important role in pancreatic cancer. Based on our data, we suggest that BMP-2-induced EMT and invasiveness of Panc-1 cells is accomplished by activation of the PI3K/Akt pathway and the precise mechanism is yet to be further defined, which is relevant to our investigation of therapeutic molecular targets to Pancreatic cancer.

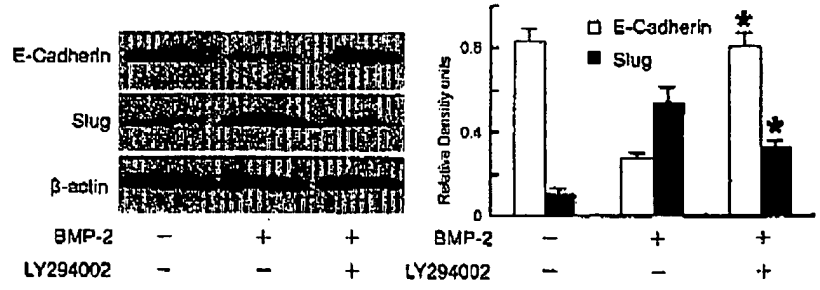

Fig. 3 Inhibition of the PI3K/Akt pathway attenuates EMT induced by BMP-2 in Panc-1 cells. Panc-1 cells were pretreated for 30 min with LY294002 (20 μM) followed by stimulation with BMP-2 (100 ng/ml). Western blotting with anti-E-cadherin, anti-Slug, or anti-β-actin was carried out. *P<0.01, compared with cells that were treated with BMP-2 plus DMSO

Acknowledgements This study was supported, in part, by the Chinese Key Basic Research Development Program (973 Program) Project.

References

1. Ganslcr T, Brawley OW (2010) Cancer statistics, 2010. CA Cancer J Clin 60(1):1
2. Li DH, Xie KP, Wolff R, Abbruzzese JL (2004) Pancreatic cancer. Lancet 363(9414):1049–1057
3. ten Dijke P, Korchynskyi E, Valdimarsdottir G, Goumans MJ (2003) Controlling cell fate by bone morphogenetic protein receptors. Mol Cell Endocrinol 211(1–2):105–113
4. Yamamoto Y, Oelgeschlager M (2004) Regulation of bone morphogenetic proteins in early embryonic development. Naturwissenschaften 91(11):519–534
5. Mukhopadhyay A, McGuire T, Peng CY, Kessler JA (2009) Differential effects of BMP signaling on parvalbumin and somatostatin interneuron differentiation. Development 136(15): 2633–2642
6. Mukhopadhyay P, Webb CL, Warner DR, Greene RM, Pisano MM (2008) BMP signaling dynamics in embryonic orofacial tissue. J Cell Physiol 216(3):771–779
7. Shimizu T, Tanaka T, Iso T, Kawai-Kowase K, Kurabayashi M (2009) Bone morphogenetic protein-2 (BMP-2) and BMP-7 act as instructive factors to specify notch signaling controlling smooth muscle cell phenotype. Circulation 120(18):S1114
8. Gong SG, Guo C (2003) Bmp4 gene is expressed at the putative site of fusion in the midfacial region. Differentiation 71(3):228–236
9. Gordon KJ, Kirkbride KC, How T, Blobe GC (2009) Bone morphogenetic proteins induce pancreatic cancer cell invasiveness through a Smad1-dependent mechanism that involves matrix metalloproteinase-2. Carcinogenesis 30(2):238–248
10. Beck SE, Carethers JM (2007) BMP suppresses PTEN expression via RAS/ERK signaling. Cancer Biol Ther 6(8):1313–1317
11. Ma J, Sawai H, Matsuo Y, Ochi N, Yasuda A, Takahashi H, Wakasugi T, Funahashi H, Sato M, Takeyama H (2008) IGF-1 mediates PTEN suppression and enhances cell invasion and proliferation via activation of the IGF-1/PI3K/Akt signaling pathway in pancreatic cancer cells. J Surg Res
12. Stoll V, Calleja V, Vassaux G, Downward J, Lemoine NR (2005) Dominant negative inhibitors of signalling through the phosphoinositol 3-kinase pathway for gene therapy of pancreatic cancer. Gut 54(1):109–116
13. Reichert M, Saur D, Hamacher R, Schmid RM, Schneider G (2007) Phosphoinositide-3-kinase signaling controls S-phase kinase-associated protein 2 transcription via E2F1 in pancreatic ductal adenocarcinoma cells. Cancer Res 67(9):4149–4156
14. Chen PH, Yang CR (2008) Decoy receptor 3 expression in AsPC-1 human pancreatic adenocarcinoma cells via the phosphatidylinositol 3-kinase-, Akt-, and NF-kappa B-dependent pathway. J Immunol 181(12):8441–8449
15. Liu DP, Zhang Y, Dang CX, Ma QY, Lee W, Chen W (2007) siRNA directed against TrkA sensitizes human pancreatic cancer cells to apoptosis induced by gemcitabine through an inactivation of PI3K/Akt-dependent pathway. Oncol Rep 18(3):673–677
16. Yip-Schneider MT, Wiesenauer CA, Schmidt CM (2003) Inhibition of the phosphatidylinositol 3′-kinase signaling pathway increases the responsiveness of pancreatic carcinoma cells to sulindac. J Gastrointest Surg 7(3):354–363
17. Kang MH, Kang HN, Kim JL, Kim JS, Oh SC, Yoo YA (2009) Inhibition of PI3 kinase/Akt pathway is required for BMP2-induced EMT and invasion. Oncol Rep 22(3):525–534
18. Kang MH, Kim JS, Seo JE, Oh SC, Yoo YA (2010) BMP2 accelerates the motility and invasiveness of gastric cancer cells via activation of the phosphatidylinositol 3-kinase (PI3K)/Akt pathway. Exp Cell Res 316(1):24–37
19. Hamada S, Satoh K, Hirota M, Kimura K, Kanno A, Masamune A, Shimosegawa T (2007) Bone morphogenetic protein 4 induces epithelial-mesenchymal transition through MSX2 induction on pancreatic cancer cell line. J Cell Physiol 213(3):768–774
20. Amiri A, Noei F, Jeganathan S, Kulkarni G, Pinke DE, Lee JM (2007) eEF1A2 activates Akt and stimulates Akt-dependent actin remodeling, invasion and migration. Oncogene 26(21):3027–3040
21. Liu H, Radisky DC, Nelson CM, Zhang H, Fata JE, Roth RA, Bissell MJ (2006) Mechanism of Akt1 inhibition of breast cancer cell invasion reveals a protumorigenic role for TSC2. Proc Natl Acad Sci USA 103(11):4134–4139
22. Meng Q, Xia C, Fang J, Rojanasakul Y, Jiang BH (2006) Role of PI3K and AKT specific isoforms in ovarian cancer cell migration, invasion and proliferation through the p70S6K1 pathway. Cell Signal 18(12):2262–2271
23. Sugimori K, Matsui K, Motomura H, Tokoro T, Wang JY, Higa S, Kimura T, Kitajima I (2005) BMP-2 prevents apoptosis of the N1511 chondrocytic cell line through PI3K/Akt-mediated NF-kappa B activation. J Bone Miner Metab 23(6):411–419
24. Gilmartin B, Fox E, Mcardle E, Daly P, Hopkins A, Harrison M, Kay E, Fitzpatrick J, Dervan P, Mccann A (2006) EMT in human bladder cancer: the fundamental role of snail transcriptional repression. BJU Int 97:7
25. Maddipatla S, Khoury T, Gibbs JF, Nusser E, Rutledge P, Iwata K, Black J, Javle M (2007) Epithelial-mesenchymal transition (EMT) and role of p-Erk in surgically resected pancreatic cancer. Ann Surg Oncol 14(2):4
26. Roskelley CD, Somasiri AM, Tognon C, Sorensen P, Nielsen J, McNagny K, Huntsman D, Dedhar S (2004) On the road to EMT: Genes and phenes that regulate tumor subtype-specific breast cancer progression. FASEB J 18(5):A761–A762
27. Spaderna S, Schmalhofer O, Hlubek F, Berx G, Eger A, Merkel S, Jung A, Kirchner T, Brabletz T (2006) A transient, EMT-linked loss of basement membranes indicates metastasis and poor survival in colorectal cancer. Gastroenterology 131(3):830–840

Published in final edited form as:
Cancer Res. 2009 May 15; 69(10): 4116–4124. doi:10.1158/0008-5472.CAN-08-3441.

Characterization of a Naturally Occurring Breast Cancer Subset Enriched in Epithelial-to-Mesenchymal Transition and Stem Cell Characteristics

Bryan T. Hennessy[1,2,6], **Ana-Maria Gonzalez-Angulo**[2,3,6], **Katherine Stemke-Hale**[2,6], **Michael Z. Gilcrease**[4], **Savitri Krishnamurthy**[4], **Ju-Seog Lee**[2], **Jane Fridlyand**[7], **Aysegul Sahin**[4], **Roshan Agarwal**[2], **Corwin Joy**[5], **Wenbin Liu**[5], **David Stivers**[5], **Keith Baggerly**[5], **Mark Carey**[2,6], **Ana Lluch**[8], **Carlos Monteagudo**[9], **Xiaping He**[10], **Victor Weigman**[10], **Cheng Fan**[10], **Juan Palazzo**[11], **Gabriel N. Hortobagyi**[3], **Laura K. Nolden**[2], **Nicholas J. Wang**[7], **Vicente Valero**[3], **Joe W. Gray**[7], **Charles M. Perou**[10], and **Gordon B. Mills**[2,6]

[1]Department of Gynecologic Medical Oncology, The University of Texas M. D. Anderson Cancer Center, Houston, Texas

[2]Department of Systems Biology, The University of Texas M. D. Anderson Cancer Center, Houston, Texas

[3]Department of Breast Medical Oncology, The University of Texas M. D. Anderson Cancer Center, Houston, Texas

[4]Department of Pathology, The University of Texas M. D. Anderson Cancer Center, Houston, Texas

[5]Department of Bioinformatics and Computational Biology, The University of Texas M. D. Anderson Cancer Center, Houston, Texas

[6]Department of Kleberg Center for Molecular Markers, The University of Texas M. D. Anderson Cancer Center, Houston, Texas

[7]Lawrence Berkeley National Laboratory, Berkeley, California

[8]Clinic Hospital, Valencia, Spain

[9]University of Valencia, Valencia, Spain

[10]Lineberger Comprehensive Cancer Center, Chapel Hill, North Carolina

[11]Department of Pathology, Thomas Jefferson University, Philadelphia, Pennsylvania

Abstract

Metaplastic breast cancers (MBC) are aggressive, chemoresistant tumors characterized by lineage plasticity. To advance understanding of their pathogenesis and relatedness to other breast cancer subtypes, 28 MBCs were compared with common breast cancers using comparative genomic hybridization, transcriptional profiling, and reverse-phase protein arrays and by sequencing for

Requests for reprints: Bryan T. Hennessy, Department of Gynecologic Medical Oncology, The University of Texas M. D. Anderson Cancer Center, 1515 Holcombe Boulevard, Houston, TX 77030. Phone: 713-563-1792; Fax: 713-745-1541; E-mail: bhennessy@mdanderson.org.
B.T. Hennessy and A-M. Gonzalez-Angulo are co-first authors. C.M. Perou and G.B. Mills are co-senior authors.

Note: Supplementary data for this article are available at Cancer Research Online (http://cancerres.aacrjournals.org/).

Disclosure of Potential Conflicts of Interest
No potential conflicts of interest were disclosed.

common breast cancer mutations. MBCs showed unique DNA copy number aberrations compared with common breast cancers. *PIK3CA* mutations were detected in 9 of 19 MBCs (47.4%) versus 80 of 232 hormone receptor–positive cancers (34.5%; $P = 0.32$), 17 of 75 *HER-2*–positive samples (22.7%; $P = 0.04$), 20 of 240 basal-like cancers (8.3%; $P < 0.0001$), and 0 of 14 claudin-low tumors ($P = 0.004$). Of 7 phosphatidylinositol 3-kinase/AKT pathway phosphorylation sites, 6 were more highly phosphorylated in MBCs than in other breast tumor subtypes. The majority of MBCs displayed mRNA profiles different from those of the most common, including basal-like cancers. By transcriptional profiling, MBCs and the recently identified claudin-low breast cancer subset constitute related receptor-negative subgroups characterized by low expression of GATA3-regulated genes and of genes responsible for cell-cell adhesion with enrichment for markers linked to stem cell function and epithelial-to-mesenchymal transition (EMT). In contrast to other breast cancers, claudin-low tumors and most MBCs showed a significant similarity to a "tumorigenic" signature defined using $CD44^+/CD24^-$ breast tumor–initiating stem cell–like cells. MBCs and claudin-low tumors are thus enriched in EMT and stem cell–like features, and may arise from an earlier, more chemoresistant breast epithelial precursor than basal-like or luminal cancers. *PIK3CA* mutations, EMT, and stem cell-like characteristics likely contribute to the poor outcomes of MBC and suggest novel therapeutic targets.

Introduction

Metaplastic breast cancers (MBC) are aggressive estrogen receptor-α–negative, progesterone receptor-negative, HER-2–negative (triple-negative) tumors characterized by mesenchymal/sarcomatoid and/or squamous metaplasia of malignant breast epithelium (1–7). Because of limited understanding of their pathogenesis, MBCs are treated in the same fashion as basal-like or triple receptor-negative ductal cancers. However, whereas neoadjuvant chemotherapy is associated with high pathologic complete response rates in basal-like carcinomas, MBCs are usually chemoresistant (2).

Transcriptional profiling has defined breast cancer subtypes (8,9). The origin of luminal A and B tumors appears to be the mammary duct luminal epithelium with concomitant hormone receptor expression. Elevated HER-2 expression defines a subgroup with a poor prognosis; however, the responsiveness of this subgroup to trastuzumab improves outcomes (10). In contrast, basal-like cancers likely represent multiple different subtypes arising from distinct precursor cells from those of other cancers. Some basal-like breast cancers likely arise from mammary myoepithelial cells. To date, basal-like cancers have not presented specific therapy targets.

As MBCs are triple-negative, they are distinct from luminal and *HER-2*-amplified cancers. As they express some markers associated with basal-like cancers (e.g., epidermal growth factor receptor and cytokeratins 5/6), MBCs are proposed to represent a form of basal-like breast cancer. However, distinct clinical features such as chemoresistance suggest that MBCs may represent a unique subtype (2,3).

We applied an integrated genomic-proteomic approach to determine mechanisms underlying metaplastic carcinogenesis and MBC chemoresistance along with the relatedness of MBCs to known breast cancer subtypes. Most MBCs showed a unique molecular profile and form a distinct subtype most closely related to a novel subset of receptor-negative breast cancers (claudin-low) characterized by loss of genes involved in cell-cell adhesion. An enrichment for stem cell-like and epithelial-to-mesenchymal transition (EMT) markers in MBCs (and claudin-low tumors) along with frequent genomic aberrations that activate the phosphatidylinositol 3-kinase (PI3K)/AKT pathway suggest reasons for MBC chemoresistance and that MBCs and claudin-low tumors may arise from more immature precursor cells than other breast cancers.

Materials and Methods

Human tumors

Twenty-eight frozen grade 3 MBCs with sarcomatoid (19) or squamous (9) metaplasia were obtained from the Breast Tumor Bank at The University of Texas M. D. Anderson Cancer Center (MDACC) and from a collaborator in Valencia (A.L.). The diagnosis was reconfirmed by pathologists at MDACC (M.Z.G. and S.K.; refs. 2,3). Frozen tissue was used for DNA extraction (28 tumors) and, where adequate frozen tumor tissue remained, for RNA and protein extraction (16 MDACC tumors; ref. 11).

Three tumor cohorts were used for comparison with MBCs (Supplementary Fig. S1). The first cohort, used for comparison of mutation frequency (547 tumors) and functional proteomic profiles (693), was composed of 693 frozen primary breast tumors obtained under institutional review board-approved protocols from MDACC. These tumors were subdivided into clinically defined subtypes as described previously (Table 1; ref. 12).

A second cohort of 145 primary breast tumors was used for comparison with MBC gene copy number profiles herein (13,14). A third cohort (Lineberger Comprehensive Cancer Center) of 184 breast tumors and 9 normal breast tissues was used for comparison with MBC transcriptional profiles (8,9,15). There were no statistically significant differences in the proportion of patients with tumors of different stages between the cohorts.

Comparative genomic hybridization

Comparative genomic hybridization profiles from the 28 MBCs were generated at Lawrence Berkeley National Laboratory using single nucleotide polymorphism (SNP)-based GeneChip Human Mapping 50K Sty arrays (Affymetrix) and compared with BAC-comparative genomic hybridization profiles of primary breast tumors previously generated and processed (J.F.) at Lawrence Berkeley National Laboratory using HumArray1.14/HumArray2.0 (13,14,16–18). MBC 50K data are available.[12]

For comparison with Lawrence Berkeley National Laboratory tumors, the 28 MBC SNP chips were mapped to BAC resolution. This approach has been validated by comparing data derived using both platforms to analyze breast cancer cell lines (data not shown). Lawrence Berkeley National Laboratory tumors were remapped to the May04 freeze from University of California-Santa Cruz and regions around each BAC clone were defined as within a half distance to each neighboring clone or to the beginning or end of the chromosome if telomeric. A median expression value was then obtained for SNPs in each BAC region. Missing values were assigned if <5 SNPs mapped to a particular region. Each array was recentered to have a median of 0. The resulting values were segmented using circular binary segmentation (CBS) followed by a merge-level procedure to combine segmented levels across the genome. Each missing value was assigned the value of its corresponding segment. Gain/loss events and fraction of genome altered were calculated. After this resolution reduction (median, 18 SNPs/BAC; mean, 30), the mean variability estimate was 0.25. Similar analyses beginning with the CBS steps were done on the original dChip processed data. We used a Fisher's test to measure the difference in copy number at probes on each side of genes encoding PI3K/AKT pathway components. These *P* values were used to fit a β-uniform mixture model to determine significance at a given false discovery rate.

[12] ftp://bcarrish.lbl.gov/njwang/

To directly compare the 50K SNP and older BAC platforms, DNA extracted from five MBCs was also run using the BAC platform. This confirmed a high concordance for the matched data derived from the two platforms (data not shown).

Detection of mutations

DNA was extracted from 547 MDACC breast tumors along with 14 Lineberger Comprehensive Cancer Center claudin-low breast tumors and 19 MBCs with sufficient remaining DNA for mutation detection (9,11,12). Following whole-genome amplification, *p53/PTEN* genes were resequenced (19). *CTNNB1* exon 3 (the most common site of mutations) was amplified from genomic DNA using a forward primer located at the 5′ portion and a reverse primer at the 3′ end of the exon. A tumor sample with a known *CTNNB1* mutation was amplified and sequenced in parallel with tumor samples as a positive control. A SNP-based approach (Sequenom MassArray) was used to detect mutations in *PIK3CA, KRAS*, and E17K mutations in the *AKT1/2/3* genes (12,20). This approach is unsuitable for detection of mutations that are not "hotspot" mutations but is particularly suitable to mutation detection in breast cancer where stromal "contamination" is prevalent (21).

Reverse-phase protein array

Reverse-phase protein array was applied with the antibodies in Supplementary Table S1 to compare PI3K/AKT and mitogen-activated protein kinase (MAPK) pathway activation in protein lysates derived from 16 MBCs versus 693 common breast cancers (Supplementary Table S2; refs. 22–25). The expression of each antibody in a sample was corrected for protein loading using the average expression levels of all probed proteins. Antibodies were obtained from SDI (YB1), Epitomics, Inc. (p70S6K, PR), Lab Vision Corporation (ERα), Santa Cruz Biotechnology (CCND1, CCNE1, EGFR, GSK3, p27), Upstate Biotechnology (Src) and Cell Signaling Technology, Inc.

Transcriptional profiling

Total RNA was isolated by phenol-chloroform extraction (Trizol, Life Technologies), and mRNA was purified by either magnetic separation using Dynabeads (Dynal) or the Invitrogen FastTrack 2.0 Kit. Twelve of 16 MBC RNA samples with RNA integrity numbers > 6 were assayed on Agilent oligomicroarrays at Lineberger Comprehensive Cancer Center and compared with a published Agilent microarray data set also previously assayed and processed (C.M.P.) at Lineberger Comprehensive Cancer Center (8,9,15). The microarray and clinical data are available at University of North Carolina Microarray Database and in the Gene Expression Omnibus (GSE10885). Expression Analysis Systematic Explorer was applied to perform functional analysis of gene lists.

Mapping gene expression onto regions of MBC copy number change

Using a Significance Analysis of Microarray (SAM)-defined list of MBC-defining genes, we determined the chromosomal location of each gene to link with the comparative genomic hybridization data. Probes with an undefined chromosomal position were discarded from further analyses. CBS was applied to the preprocessed MBC copy number data to determine breakpoints for aberrations (26). The CBS calls made were as follows: class.segment <- segment (class.cna, α = 0.05, p.method = "perm," nperm = 1,000, trim = 0.05, undo.splits = "sdundo," undo.SD = 2, verbose = 2). Using CBS output, a plot of segment intensities versus segment markers was used to determine an intensity boundary threshold of 0.12. Segments with intensity values beyond this threshold were flagged as gained or lost based on the sign of intensity and parsed from the original CBS output. By applying a customized R script to this output, segments from each sample were collated and regions were assigned that had varying levels of overlap between the MBC patients. Cutoffs were made for regions with aberrations

in ≥1 of 3 of MBCs tested. SAM genes with chromosomal locations that were contained within these gains and losses were determined and plotted.

Comparison of the MBC and claudin-low transcriptional profiles with a CD44$^+$/CD24$^{-/low}$ breast cancer cell profile

We compared breast tumor transcriptional signatures with a "tumorigenic" signature[13] that was derived by comparing gene expression profiles of flow-sorted CD44$^+$/CD24$^{-/low}$ cancer cells with profiles of all other sorted cells (CD44$^-$/CD24$^+$ and CD44$^-$/CD24$^-$ combined). For each tumor, a "R value" was derived in relation to the "tumorigenic" signature, which was defined as the Pearson's correlation between the "tumorigenic" gene signature pattern (using "1" and "−1" for up and down, respectively) and tumor expression values. Tumors with high R values would tend to have both high expression of many of the genes high in "tumorigenic" cells and low expression of many of the genes low in "tumorigenic" cells (and vice versa for tumors with low R values).

Statistical analysis

R[14] and NCSS/PASS software were used. Reported *P* values are two sided. ANOVA and *t* tests for gene expression data were done using SAS. For clustering, we used CLUSTER and TREEVIEW (University of Glasgow) softwares.

Results

MBCs possess patterns of DNA copy number gains and losses that are distinct from those in common breast cancers

MBCs showed a high level of genomic instability based on fraction of the genome altered and number of transitions. However, MBCs showed a unique set of aberrations compared with common breast cancers (Fig. 1; refs. 13,14). Specifically, gains of distal chromosome 1p/5p and loss of 3q were common in MBCs but rare in other breast cancers (13,14). Conversely, alterations that occur in most breast cancers, such as gain of chromosome 1q and loss of 16q, were uncommon in MBC (13,14). In particular, compared with basal-like tumors, MBCs exhibited more frequent amplification of 1p/11q/12q/14q/19p/19q/22q and increased frequency of loss at 1q/2p/3q/8q. There was retention of 5q/9q/15q/16p/17p/17q/19p/19q/20q/22q compared with basal-like tumors. Overall, MBCs did not display similar alterations to basal-like cancers and showed substantial differences from common breast cancers, compatible with MBCs representing a distinct subgroup.

MBCs possess distinct patterns of somatic mutations from basal-like breast cancers

PIK3CA mutations were detected in 9 of 19 (47.4%) MBCs compared with 80 of 232 (34.5%) hormone receptor-positive cancers ($P = 0.32$), 17 of 75 (22.7%) *HER-2*-amplified samples ($P = 0.04$), 20 of 240 (8.3%) triple-negative cancers ($P < 0.0001$), and 0 of 14 claudin-low tumors ($P = 0.004$; Table 1; ref. 12). The *PIK3CA* mutation frequencies in the common subtypes are compatible with those frequencies reported in the literature, with the exception of that in claudin-low tumors, which has not been reported (27). One *PTEN* mutation was detected in a MBC (5%) that did not have a *PIK3CA* mutation. *p53* mutations were detected in 6 of 19 (32%) MBCs. No mutation in exon 3 of *CTNNB1* was detected in 19 MBCs.

Strikingly, therefore, 10 of 19 (53%) MBCs showed PI3K/AKT pathway mutations. This was significantly different from the mutation rate in triple-negative/basal-like cancers in particular.

[13]Creighton et al., submitted for publication.
[14]http://cran.r-project.org

Further, other PI3K/AKT pathway genomic aberrations were more frequent in MBCs. Based on two SNP probes closest to each end of genes encoding PI3K/AKT components, *AKT1* (chromosome 14), *AKT2* (chromosome 19), and *RPS6KB2* (p70S6K, chromosome 11) showed more frequent copy number gain (Fisher's exact test, $P < 0.05$ at a 1% false discovery rate) in MBCs compared with other subtypes. This was also supported at the protein level using reverse-phase protein array data (Supplementary Table S2). Thus, PI3K/AKT pathway aberrations likely play a major role in MBC pathophysiology, further suggesting that MBCs and basal-like tumors are distinct.

PI3K pathway activation in MBC

The high frequency of genomic aberrations in PI3K/AKT pathway genes implicates this pathway in MBC pathogenesis. This pathway has already been implicated in breast cancer resistance to multiple therapies (28–30). Using reverse-phase protein array, phosphorylation of most core PI3K/AKT pathway proteins was elevated in MBCs compared with at least one other breast tumor subtype (Fig. 2), with the exception of phosphorylated p70S6K. The most likely explanation for the latter discrepancy is phosphorylation of p70S6K by kinases other than core PI3K/AKT pathway kinases (31,32). Overall, however, key PI3K/AKT pathway components are generally more highly phosphorylated in MBCs than in most other breast tumors, which parallels the results of the genomic analyses and could contribute to the poor outcomes associated with MBC (Supplementary Fig. S2).

Only glycogen synthase kinase 3 phosphorylation was higher in MBCs possessing mutant versus wild-type *PIK3CA/PTEN* genes ($P = 0.01$). The failure to show an association between PI3K/AKT pathway mutations and activation is potentially due to the small number of tumors analyzed. However, alterations in PI3K/AKT pathway activation by processes independent of mutations, by other interacting pathways, or by signaling modulation through feedback loops may have prevented identification of statistically significant associations (33). Compatible with the latter contention, we have shown previously that *PIK3CA* mutational status is not correlated with AKT phosphorylation in hormone receptor-positive breast cancers or cell lines (12).

We also quantified expression and phosphorylation of several PI3K/AKT pathway-activating and pathway-related proteins (Supplementary Table S2). Epidermal growth factor receptor expression was lower in MBCs compared with other breast cancer subtypes. HER-2 levels were also significantly decreased in MBCs relative to hormone receptor-positive, triple-negative, and, in particular, HER-2–positive tumors. Cyclin E1, a PI3K/AKT pathway target, was present at higher levels in MBCs compared with hormone receptor-positive and HER-2–positive tumors ($P = 0.0005$ and 0.02, respectively; refs. 34,35). The Y box–binding protein 1 (YB1) has been implicated in chemoresistance and is located in the chromosome 1p amplicon in MBC (Fig. 1; ref. 36). Indeed, *YB1* was more frequently amplified (at 1% false discovery rate) in MBCs than in other tumors, and YB1 protein expression was also higher in MBCs.

MBC transcriptional profiles are distinct from those of basal-like breast cancers and related to those of claudin-low breast tumors

On unsupervised hierarchical clustering, the majority of MBCs displayed markedly different mRNA profiles from those of most common breast cancers including basal-like cancers (data not shown). To explore the relationships between MBCs and the intrinsic breast cancer subtypes, 12 MDACC MBCs were compared with 184 breast tumors and 9 normal breast samples by hierarchical clustering using a combination of four intrinsic gene lists (8,9,15,37). MBCs were somewhat heterogeneous in this analysis (Supplementary Fig. S3). Two MBCs clustered with basal-like tumors, two with a novel subtype of receptor-negative tumors that is characterized by loss of a cluster of genes that encode proteins involved in cell-cell adhesion (claudin-low tumors), two clustered within the normal-like group, and six formed a novel

subgroup with characteristics intermediate between those of basal-like and claudin-low tumors (Supplementary Fig. S3).

To assess the significance of this clustering pattern, we applied "SigClust" to test the null hypothesis that any group of samples contained within a common dendrogram branch constitutes a single group (38). This analysis showed that the dendrogram branch containing six MBCs, along with some previously assayed tumors, represents a distinct group. On reanalysis of the histology of the latter tumors, four showed metaplastic and/or spindloid features compatible with the tumors representing MBCs (Supplementary Fig. S4). Further, mouse mammary tumors that are similar to human claudin-low tumors show a spindloid morphology (9).

The gene set that defines claudin-low and MBC tumors (Supplementary Fig. S3*C*) was determined by Gene Ontology analysis to be enriched for the terms tight junction, intercellular junction, apicolateral plasma membrane, and cell junction. Of 29 claudin-low cluster genes, 13 are positively regulated by GATA3 and none by estrogen receptor-α (hypergeometic mean analysis, $P < 0.01$; ref. 39). In addition to lacking genes involved in cell-cell adhesion and polarity, MBCs and claudin-low tumors lack luminal genes including *GATA3* (Supplementary Fig. S3*F*) and *HER-2* and show inconsistent expression of genes associated with basal-like tumors (Supplementary Fig. S3*D*). *t* tests confirmed that the expression of the claudin-low cluster of genes (Supplementary Fig. S3*C*) was lower in MBCs versus other breast cancers (Supplementary Table S3).

MBCs and claudin-low tumors express high levels of stem cell and EMT markers

SAM was used to identify a MBC versus common breast tumor expression signature (40,41). This analyses resulted in 556 up and 373 down genes, with a false discovery rate of <1 gene (Supplementary Table S4). Almost 33% of the "SAM up" and 50% of the SAM down genes mapped to regions of copy number aberration (see below). In a Gene Ontology analysis using Expression Analysis Systematic Explorer, the top six enriched biological processes in the "up" gene list were cell communication, cell adhesion, signal transduction, cellular process, cell-cell adhesion, and intracellular protein transport, whereas protein transport, intracellular transport, transport, male meiosis, and ubiquitin-dependent protein catabolism were enriched in the "down" gene list (40). The claudin-low gene cluster showed a statistically significant overlap with the SAM-defined "down" genes (15 of 29 genes; hypergeometic mean analysis, $P < 0.001$). Genes near the top of the MBC "up" list that have been previously implicated in carcinogenesis included *ALK*, crystallin γ, and the master regulator of EMT, *TWIST1* (42–45).

Breast cancers are thought to contain a minority population of tumor initiating/stem cell-like cells with high CD44 but low or undetectable levels of CD24 ($CD44^+/CD24^-$); these cells have higher "tumorigenic" capacity than other purified populations of tumor-derived cells (46). Their phenotype and the low responsiveness of MBCs to chemotherapy suggest that MBCs might possess stem cell-like characteristics. Indeed, MBCs had markedly elevated CD44/CD24 and CD29/CD24 ratios compared with other breast cancers, with the exception of claudin-low tumors (Fig. 3). This "electronic stem cell signature" is also differentially expressed between fluorescence-activated cell-sorted human breast tumor-initiating cells and normal breast epithelial cells (Supplementary Fig. S5; refs. 46,47).

EMT is characterized by the up-regulation of vimentin and of E-cadherin repressor molecules (snail/slug/twist) with down-regulation of E-cadherin and other cell adhesion molecules (45, 48,49). These events occur in MBCs and claudin-low tumors (Fig. 3; Supplementary Table S3). In MBCs, *TWIST1* and snail homologue 2 (*SNAI2/SLUG*) were expressed at high levels, whereas *SNAI3* was overexpressed in claudin-low tumors. Thus, claudin-low tumors and

MBCs may be enriched for stem cell-like and EMT markers, features that may contribute to poor patient outcomes (Supplementary Fig. S2; refs. 2,3).

Genes that are altered at the genomic and transcriptional levels in MBC

Three hundred six genes (Supplementary Table S5) in the SAM-derived MBC transcriptome localized to areas of chromosomal gain and loss in at least 33% of MBCs (Supplementary Fig. S6*A* and *B*). Thus, these genes show coordinate changes at the DNA and RNA levels in MBC. Functional analysis of these genes (Supplementary Tables S6 and S7) showed that, among genes that are amplified and overexpressed in MBCs, components of three major branches (JNK, MAPK, and p38) that compose the MAPK signaling pathway are significantly overrepresented in MBCs. Compatible with this finding, phosphorylation of three of four assessed protein components of these pathways [JNK ($P = 0.06$), MEK ($P = 0.003$), and p38 ($P = 0.0008$) but not ERK1/2 (P = NS)] was higher in MBCs versus all other breast cancers.

Comparison of the MBC and claudin-low transcriptional profiles with a $CD44^+/CD24^{-/low}$ breast cancer cell profile

Given their enrichment for stem cell markers, we compared the transcriptional signatures of MBCs and other breast cancers with a "tumorigenic" signature[13] that was derived by comparing gene expression profiles of flow-sorted $CD44^+/CD24^{-/low}$ breast tumor cells with profiles of all other sorted cells ($CD44^-/CD24^+$ and $CD44^-/CD24^-$). In contrast to other breast cancers, except for tumors of the "claudin-low" subtype, most of the MBCs showed a clear association with the "tumorigenic" signature (Fig. 4). Further, of 373 and 217 down-regulated genes in the MBC and "tumorigenic" signatures, respectively, there were 29 shared genes (Supplementary Table S8; $P = 1 \times 10^{-13}$ for the overlap); 5 of these 29 genes were components of the claudin-low gene cluster. In addition, as has been shown with the claudin-low signature,[13] the MBC signature is enriched in post-docetaxel and post-letrozole treatment specimens (Supplementary Fig. S7). These data collectively suggest that, at diagnosis, MBCs and claudin-low tumors possess transcriptional features that are enriched in highly purified breast tumor-initiating and chemoresistant breast cancer cell fractions (50), the latter also compatible with an enrichment for stem cell-like activity.

Discussion

MBCs are aggressive, chemoresistant tumors associated with poor outcomes (2,3). Although uncommon, MBCs account for several hundred new breast cancer cases every year in the United States, thus representing a therapeutic dilemma for oncologists. With only retrospective case reviews as a basis for making recommendations, it has not been possible to define therapy guidelines. Thus, we sought to determine the relationship of MBCs to common breast cancers, particularly basal-like breast cancers given the common assumption that MBCs are basal-like cancers. We also sought to determine whether the underlying pathophysiology of MBCs would result in the identification of new drug targets.

Supplementary Fig. S8 summarizes the features of MBC defined in this study that have potential clinical and therapeutic utility. Due to low expression of hormone receptors and HER-2 as well as expression of some basal epithelial markers, MBCs have been proposed to represent a form of basal-like breast cancer (4). However, based on the integrated analyses herein, most MBCs likely represent an independent subtype that is distinct from basal-like cancers. Their transcriptional profiles are most closely related to claudin-low cancers, a novel subgroup of receptor-negative breast cancers that are clearly different from basal-like cancers (Supplementary Fig. S3). Comparative genomic hybridization profiles, their enrichment for stem cell-like markers, and their PI3K/AKT pathway activation status also differentiate MBCs from basal-like cancers. MBCs, like claudin-low cancers, express high levels of EMT markers

and show elevated CD44/CD24 and CD29/CD24 ratios, which have been proposed to represent breast cancer stem cell-like markers (46). Indeed, a recent study detected a direct and causative link between EMT and the gain of epithelial stem cell properties (51). These features likely contribute to the lineage plasticity of MBCs on light microscopy and to their limited chemoresponsiveness (2,3). Claudin-low features, including EMT and stem cell-like properties, also potentially contribute to the aggressive phenotype of MBCs. This is supported by the significant overlap between the MBC signature and the "tumorigenic" signature,[13] with overlapping genes including five of the claudin-low genes (Supplementary Fig. S3C). The MBC, the "tumorigenic," and the claudin-low signatures are all enriched in residual post-treatment chemoresistant breast tumors. Thus, MBCs and claudin-low breast tumors may arise from a more primitive and chemoresistant "stem" cell than luminal or basal-like tumors.

The pattern of chromosomal gains and losses in MBCs is distinct from that in other breast cancers including basal-like cancers. This unique pattern suggests that the processes underlying metaplastic carcinogenesis are distinct from those associated with other breast cancer subtypes. MBCs show a high frequency of mutation, amplification, and activation of PI3K/AKT pathway components. This is markedly different from basal-like breast cancers, where we and others have shown that PI3K/AKT pathway genomic mutations are uncommon (12,27).[15] We also did not detect *PIK3CA* mutations in 14 claudin-low breast cancers pointing to differences between claudin-low breast cancers and MBCs. The frequency of *PIK3CA* and *PTEN* mutations combined with amplification of *AKT* and *p70S6K* suggests that PI3K/AKT pathway activation is critical to metaplastic carcinogenesis. Activation of this pathway, along with enrichment for tumor-initiating/stem cells, may underlie the chemoresistance and poor outcomes associated with MBC (28–30). MBCs also show a high frequency of amplification, overexpression, and activation of MAPK pathway components. As particularly important genes and targets in cancer are likely to be aberrant at the level of the genome, transcriptome, and proteome, the PI3K/AKT and MAPK pathways are therefore potentially attractive therapy targets in MBC. As inhibitors of the PI3K/AKT and MAPK pathways are now in clinical trials, it will be of interest to determine whether these inhibitors will sensitize MBCs to cytotoxic drugs (52). As there are no MBC cell lines or animal models available, it will be necessary to develop a consortium approach to test this hypothesis in patients.

In contrast to a recently published study, mutations in exon 3 of *CTNNB1* were not identified in 19 MBCs in our study (53). This may in part relate to the fact that our study was restricted to high-grade MBCs, whereas the previous study included a significant proportion of lower-grade MBCs, tumors that behave in a less aggressive fashion than high-grade MBCs.

This study has several potential limitations. Although a subset (6 of 12, 50%) of MBCs constitute a significantly related group of tumors as defined by SigClust, it is clear that MBCs form a somewhat heterogeneous group of receptor-negative breast cancers in terms of their molecular characteristics. Just as breast tumors that are defined as ductal are clearly heterogeneous based on receptor status and transcriptional profiling, it is not surprising that MBCs represent a molecularly heterogeneous group. MBCs are microscopically heterogeneous, with this study being limited to tumors with squamous and sarcomatoid metaplasia (1–7). The rarity of MBC precluded analysis of other histologic variants. In addition, it is possible that MBC represents multiple different diseases. However, there were no clear correlation between the pattern of gene copy number change and the histologic appearance of the tumors analyzed.

The major conclusions of this article are (*a*) MBCs are molecularly distinct from other breast cancers; (*b*) despite their relative histologic uniformity, MBCs are molecularly heterogeneous;

[15] www.sanger.ac.uk

and (*c*) claudin-low breast cancers are likely the most closely related ductal breast cancer subset to MBCs. The molecular mechanisms underlying metaplastic carcinogenesis are likely different from those associated with other breast cancer subtypes including basal-like cancers. By gene expression analysis, MBCs and claudin-low tumors share common features that suggest related cellular origins, potentially from a more primitive cell than that implicated as a precursor to luminal or basal-like tumors. It is likely that MBCs, and potentially claudin-low tumors, define a novel chemoresistant triple-negative breast cancer subgroup that exhibits a signature similar to that of breast tumor-initiating cells and of residual common breast tumor cells isolated after patient treatment. The frequency of PI3K/AKT pathway aberrations argues that this pathway should be explored as a therapeutic target in MBC. A challenge to advancing therapy for MBC patients is the infrequency of this disease. However, a centralized clinical trial effort is a feasible venture that will improve patient outcomes.

Acknowledgments

Grant support: Kleberg Center for Molecular Markers at MDACC, Cancer Center Support Grant CA16672 at MDACC, and MDACC Physician Scientist Program and The McNair Scholars Program supported by The Robert and Janice McNair Foundation (B.T. Hennessy); National Cancer Institute grants K23-CA121994 and R21-CA120248 and National Cancer Institute Breast Specialized Program for Research Excellence grant P50-CA116199 (A-M. Gonzalez-Angulo); National Cancer Institute grants CA116199 and CA099031 (G.B. Mills); Komen Foundation grant FAS0703849 (G.B. Mills, A-M. Gonzalez-Angulo, and B.T. Hennessy); National Cancer Institute Breast Specialized Program for Research Excellence grants P50-CA58223-09A1 and RO1-CA-101227-01, V Foundation for Cancer Research, and Breast Cancer Research Foundation (C.M. Perou); and Director, Office of Science, Office of Biological & Environmental Research, U.S. Department of Energy contract DE-AC02-05CH11231 and NIH/National Cancer Institute grants P50 CA58207 and U54 CA112970 (J.W. Gray).

We thank Len Pennacchio and Jan-Fang Cheng (Lawrence Berkeley National Laboratory) for Sanger sequencing and Jenny Chang and Chad Creighton for sharing data and providing analysis concerning their "tumorigenic" signature in Creighton et al. (submitted for publication).

References

1. Tavassoli, FA. Pathology of the breast. Vol. 2nd ed., Hong Kong: Appleton and Lange; 1999. 1999
2. Hennessy BT, Giordano S, Broglio K, et al. Biphasic metaplastic sarcomatoid carcinoma of the breast. Ann Oncol 2006;17:605–613. [PubMed: 16469754]
3. Hennessy BT, Krishnamurthy S, Giordano S, et al. Squamous cell carcinoma of the breast. J Clin Oncol 2005;23:7827–7835. [PubMed: 16258085]
4. Reis-Filho JS, Milanezi F, Steele D, et al. Metaplastic breast carcinomas are basal-like tumours. Histopathology 2006;49:10–21. [PubMed: 16842242]
5. Wargotz ES, Deos PH, Norris HJ. Metaplastic carcinomas of the breast. II. Spindle cell carcinoma. Hum Pathol 1989;20:732–740. [PubMed: 2473024]
6. Foschini MP, Dina RE, Eusebi V. Sarcomatoid neoplasms of the breast: proposed definitions for biphasic and monophasic sarcomatoid mammary carcinomas. Semin Diagn Pathol 1993;10:128–136. [PubMed: 8367622]
7. Gutman H, Pollock RE, Janjan NA, Johnston DA. Biologic distinctions and therapeutic implications of sarcomatoid metaplasia of epithelial carcinoma of the breast. J Am Coll Surg 1995;180:193–199. [PubMed: 7850054]
8. Sorlie T, Perou CM, Tibshirani R, et al. Gene expression patterns of breast carcinomas distinguish tumor subclasses with clinical implications. Proc Natl Acad Sci U S A 2001;98:10869–10874. [PubMed: 11553815]
9. Herschkowitz JI, Simin K, Weigman VJ, et al. Identification of conserved gene expression features between murine mammary carcinoma models and human breast tumors. Genome Biol 2007;8:R76. [PubMed: 17493263]
10. Romond EH, Perez EA, Bryant J, et al. Trastuzumab plus adjuvant chemotherapy for operable HER2-positive breast cancer. N Engl J Med 2005;353:1673–1684. [PubMed: 16236738]

11. Pinkel D, Segraves R, Sudar D, et al. High resolution analysis of DNA copy number variation using comparative genomic hybridization to microarrays. Nat Genet 1998;20:207–211. [PubMed: 9771718]
12. Stemke-Hale K, Gonzalez-Angulo AM, Lluch A, et al. An integrative genomic and proteomic analysis of PIK3CA, PTEN and AKT mutations in breast cancer. Cancer Res 2008;68:6084–6091. [PubMed: 18676830]
13. Chin K, DeVries S, Fridlyand J, et al. Genomic and transcriptional aberrations linked to breast cancer pathophysiologies. Cancer Cell 2006;10:529–541. [PubMed: 17157792]
14. Fridlyand J, Snijders AM, Ylstra B, et al. Breast tumor copy number aberration phenotypes and genomic instability. BMC Cancer 2006;6:96. [PubMed: 16620391]
15. Hu Z, Fan C, Oh DS, et al. The molecular portraits of breast tumors are conserved across microarray platforms. BMC Genomics 2006;7:96. [PubMed: 16643655]
16. Snijders AM, Schmidt BL, Fridlyand J, et al. Rare amplicons implicate frequent deregulation of cell fate specification pathways in oral squamous cell carcinoma. Oncogene 2005;24:4232–4242. [PubMed: 15824737]
17. Snijders AM, Nowak N, Segraves R, et al. Assembly of microarrays for genome-wide measurement of DNA copy number. Nat Genet 2001;29:263–264. [PubMed: 11687795]
18. Janne PA, Li C, Zhao X, et al. High-resolution single-nucleotide polymorphism array and clustering analysis of loss of heterozygosity in human lung cancer cell lines. Oncogene 2004;23:2716–2726. [PubMed: 15048096]
19. Tartaglia M, Pennacchio LA, Zhao C, et al. Gain-of-function SOS1 mutations cause a distinctive form of Noonan syndrome. Nat Genet 2007;39:75–79. [PubMed: 17143282]
20. Thomas RK, Baker AC, Debiasi RM, et al. High-throughput oncogene mutation profiling in human cancer. Nat Genet 2007;39:347–351. [PubMed: 17293865]
21. West RB, Nuyten DS, Subramanian S, et al. Determination of stromal signatures in breast carcinoma. PLoS Biol 2005;3:e187. [PubMed: 15869330]
22. Tibes R, Qiu Y, Lu Y, Hennessy B, Mills GB, Kornblau S. Reverse phase protein array (RPPA): validation of a novel proteomic technology and utility for analysis of primary leukemia specimens and hematopoietic stem cells. Mol Cancer Ther 2006;5:2512–2521. [PubMed: 17041095]
23. Liang J, Shao SH, Xu ZX, et al. The energy sensing LKB1-AMPK pathway regulates $p27^{kip1}$ phosphorylation mediating the decision to enter autophagy or apoptosis. Nat Cell Biol 2007;9:218–224. [PubMed: 17237771]
24. Hu J, He X, Baggerly KA, Coombes KR, Hennessy BT, Mills GB. Non-parametric quantification of protein lysate arrays. Bioinformatics 2007;23:1986–1994. [PubMed: 17599930]
25. Hennessy BT, Lu Y, Poradosu E, et al. Quantified pathway inhibition as a pharmacodynamic marker facilitating optimal targeted therapy dosing: Proof of principle with the AKT inhibitor perifosine. Clin Cancer Res 2007;13:7421–7431. [PubMed: 18094426]
26. Venkatraman ES, Olshen AB. A faster circular binary segmentation algorithm for the analysis of array CGH data. Bioinformatics 2007;23:657–663. [PubMed: 17234643]
27. Saal LH, Holm K, Maurer M, et al. PIK3CA mutations correlate with hormone receptors, node metastasis, and ERBB2, and are mutually exclusive with PTEN loss in human breast carcinoma. Cancer Res 2005;65:2554–2559. [PubMed: 15805248]
28. Stassi G, Garofalo M, Zerilli M, et al. PED mediates AKT-dependent chemoresistance in human breast cancer cells. Cancer Res 2005;65:6668–6675. [PubMed: 16061647]
29. Mondesire WH, Jian W, Zhang H, Ensor J, Hung MC, Mills GB. Targeting mammalian target of rapamycin synergistically enhances chemotherapy-induced cytotoxicity in breast cancer cells. Clin Cancer Res 2004;10:7031–7042. [PubMed: 15501983]
30. Knuefermann C, Lu Y, Liu B, et al. HER2/PI-3K/Akt activation leads to a multidrug resistance in human breast adenocarcinoma cells. Oncogene 2002;22:3205–3212. [PubMed: 12761490]
31. Le Pabic H, L'Helgouale'h A, Coutant A, et al. Involvement of the serine/threonine p70S6 kinase in TGF-β1-induced ADAM12 expression in cultured human hepatic stellate cells. J Hepatol 2005;43:1038–1044. [PubMed: 16139919]

32. Grove JR, Price DJ, Banerjee P, Balasubramanyam A, Ahmad MF, Avruch J. Regulation of an epitope-tagged recombinant Rsk-1 S6 kinase by phorbol ester and ERK/MAP kinase. Biochemistry 1993;32:7727–7738. [PubMed: 7688567]

33. Wan X, Harkavy B, Shen N, Grohar P, Helman LJ. Rapamycin induces feedback activation of Akt signaling through an IGF-1R-dependent mechanism. Oncogene 2007;26:1932–1940. [PubMed: 17001314]

34. Lee SR, Park JH, Park EK, Chung CH, Kang SS, Bang OS. Akt-induced promotion of cell-cycle progression at G_2/M phase involves upregulation of NF-Y binding activity in PC12 cells. J Cell Physiol 2005;205:270–277. [PubMed: 15887249]

35. Reichert M, Saur D, Hamacher R, Schmid RM, Schneider G. Phosphoinositide-3-kinase signaling controls S-phase kinase-associated protein 2 transcription via E2F1 in pancreatic ductal adenocarcinoma cells. Cancer Res 2007;67:4149–4156. [PubMed: 17483325]

36. Huang J, Tan PH, Li KB, Matsumoto K, Tsujimoto M, Bay BH. Y-box binding protein, YB-1, as a marker of tumor aggressiveness and response to adjuvant chemotherapy in breast cancer. Int J Oncol 2005;26:607–613. [PubMed: 15703814]

37. Perreard L, Fan C, Quackenbush JF, et al. Classification and risk stratification of invasive breast carcinomas using a real-time quantitative RT-PCR assay. Breast Cancer Res 2006;8:R23. [PubMed: 16626501]

38. Liu Y, Hayes DN, Nobel A, Marron JS. Statistical significance of clustering for high dimension low sample size data. J Am Stat Assoc 2008;103:1281–1293.

39. Oh DS, Troester MA, Usary J, et al. Estrogen-regulated genes predict survival in hormone receptor-positive breast cancers. J Clin Oncol 2006;24:1656–1664. [PubMed: 16505416]

40. Tusher VG, Tibshirani R, Chu G. Significance analysis of microarrays applied to the ionizing radiation response. Proc Natl Acad Sci U S A 2001;98:5116–5121. [PubMed: 11309499]

41. Dennis G Jr, Sherman BT, Hosack DA, et al. DAVID: Database for Annotation, Visualization, and Integrated Discovery. Genome Biol 2003;4:P3. [PubMed: 12734009]

42. Chiarle R, Voena C, Ambrogio C, Piva R, Inghirami G. The anaplastic lymphoma kinase in the pathogenesis of cancer. Nat Rev Cancer 2008;8:11–23. [PubMed: 18097461]

43. Sun H, Ma Z, Li Y, et al. γ-S crystallin gene (CRYGS) mutation causes dominant progressive cortical cataract in humans. J Med Genet 2005;42:706–710. [PubMed: 16141006]

44. Moyano JV, Evans JR, Chen F, et al. αB-crystallin is a novel oncoprotein that predicts poor clinical outcome in breast cancer. J Clin Invest 2006;116:261–270. [PubMed: 16395408]

45. Yang J, Mani SA, Donaher JL, et al. Twist, a master regulator of morphogenesis, plays an essential role in tumor metastasis. Cell 2004;117:927–939. [PubMed: 15210113]

46. Liu R, Wang X, Chen GY, et al. The prognostic role of a gene signature from tumorigenic breast-cancer cells. N Engl J Med 2007;356:217–226. [PubMed: 17229949]

47. Takahashi K, Tanabe K, Ohnuki M, et al. Induction of pluripotent stem cells from adult human fibroblasts by defined factors. Cell 2007;131:861–872. [PubMed: 18035408]

48. Shipitsin M, Campbell LL, Argani P, et al. Molecular definition of breast tumor heterogeneity. Cancer Cell 2007;11:259–273. [PubMed: 17349583]

49. Lien HC, Hsiao YH, Lin YS, et al. Molecular signatures of metaplastic carcinoma of the breast by large-scale transcriptional profiling: identification of genes potentially related to epithelial-mesenchymal transition. Oncogene 2007;26:7859–7871. [PubMed: 17603561]

50. Li X, Lewis MT, Huang J, et al. Intrinsic resistance of tumorigenic breast cancer cells to chemotherapy. J Natl Cancer Inst 2008;100:672–679. [PubMed: 18445819]

51. Mani SA, Guo W, Liao MJ, et al. The epithelial-mesenchymal transition generates cells with properties of stem cells. Cell 2008;133:704–715. [PubMed: 18485877]

52. Hennessy BT, Smith DL, Ram PT, Lu Y, Mills GB. Exploiting the PI3K/AKT pathway for cancer drug discovery. Nat Rev Drug Discov 2005;4:988–1004. [PubMed: 16341064]

53. Hayes MJ, Thomas D, Emmons A, Giordano TJ, Kleer CG. Genetic changes of Wnt pathway genes are common events in metaplastic carcinomas of the breast. Clin Cancer Res 2008;14:4038–4044. [PubMed: 18593979]

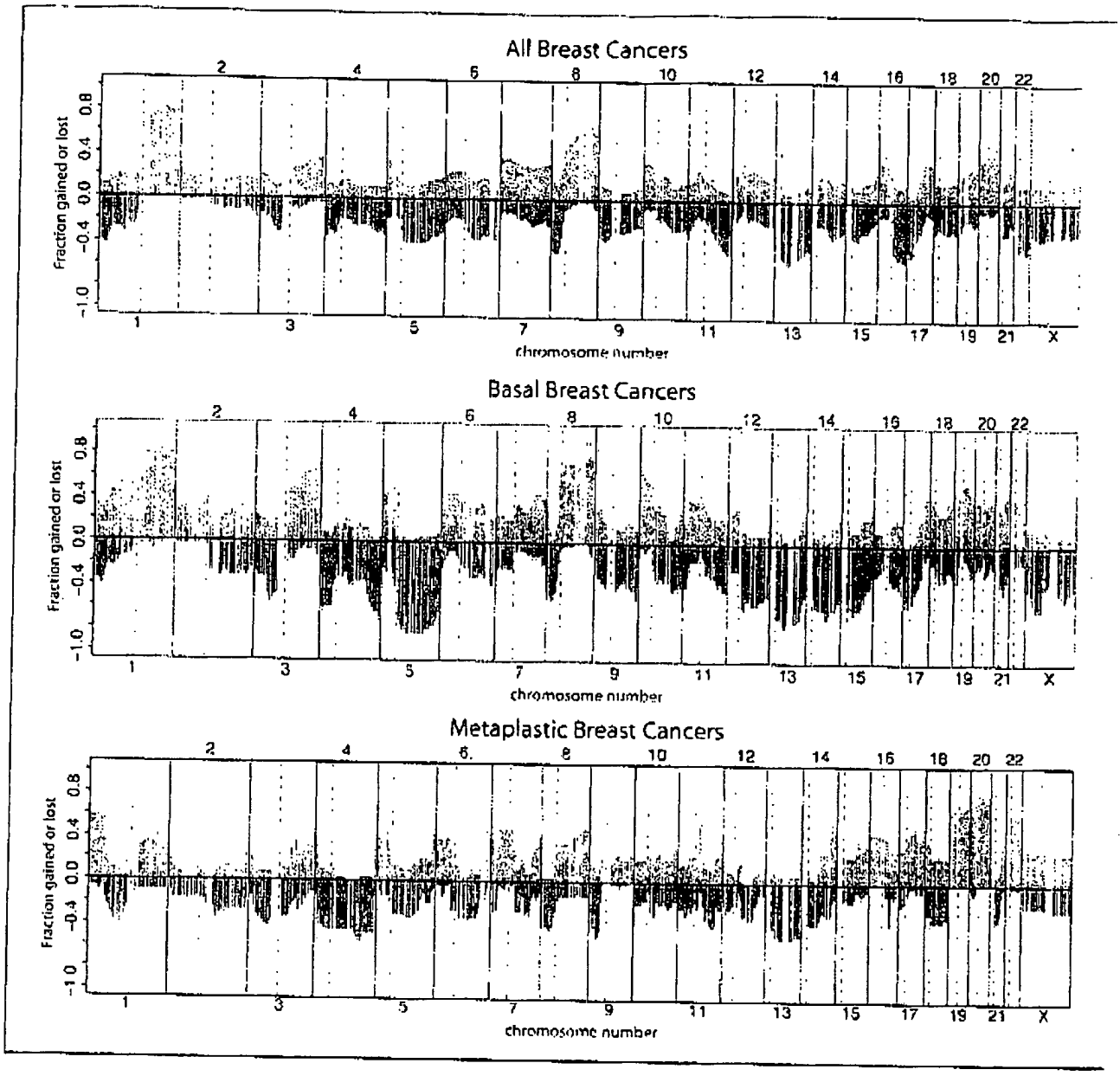

Figure 1.

Gene copy number changes. Gains and losses in all common breast cancers (including luminal, *HER-2*–amplified, and basal-like cancers) and basal-like cancers alone versus metaplastic breast tumors were determined. Chromosomes are subdivided into arms and ordered from left to right, beginning with 1p, 1q and ending with X.

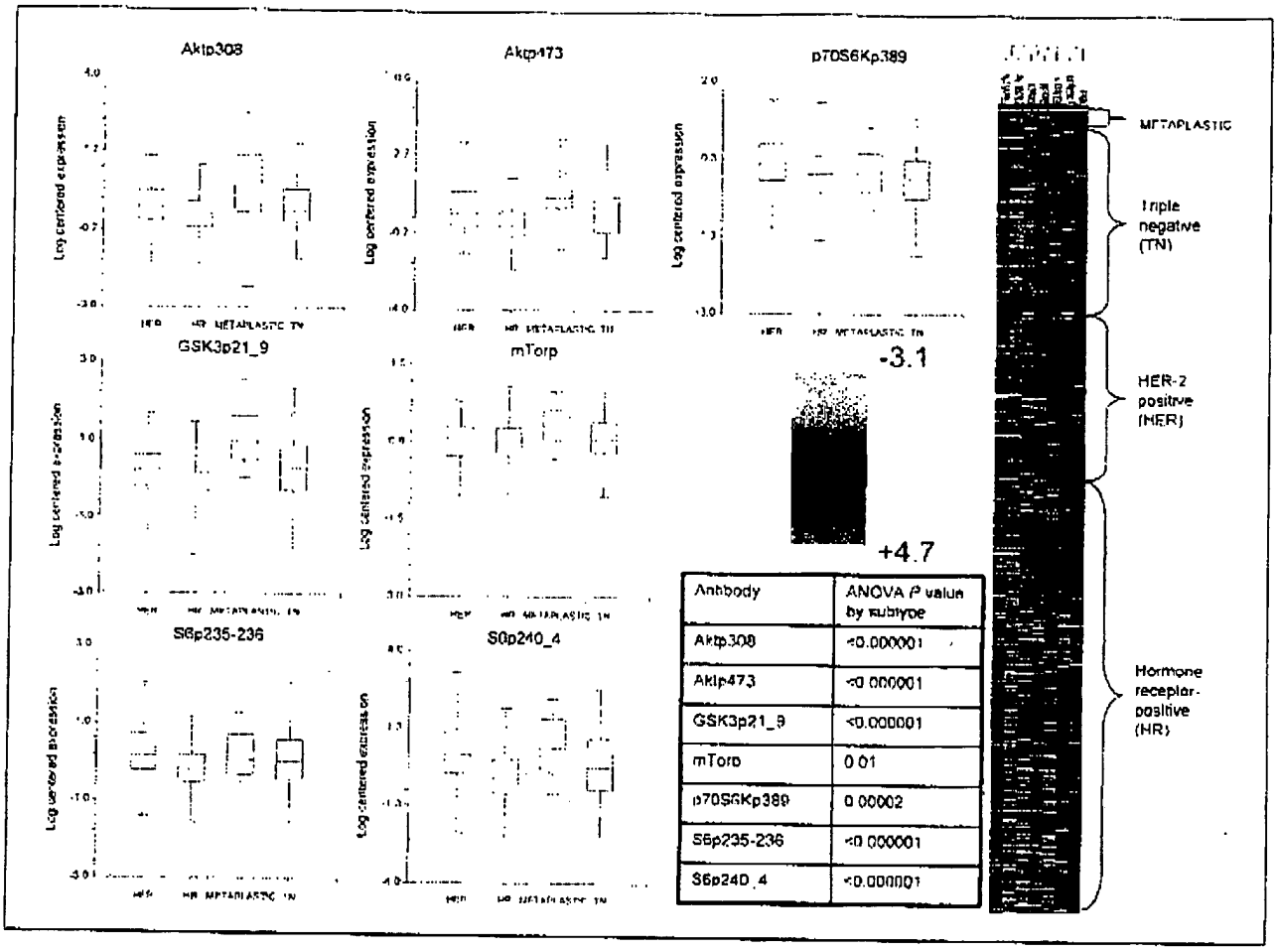

Figure 2.
Functional proteomics of MBC. Comparative expression of seven core PI3K/AKT pathway phosphoproteins in 383 hormone receptor–positive (*HR*), 142 HER-2–positive (*HER*), and 168 triple-negative (*TN*) breast tumors and 16 MBCs was determined. *GSK3*, glycogen synthase kinase 3; *XpY*, phosphorylation of protein X at amino acid(s) Y.

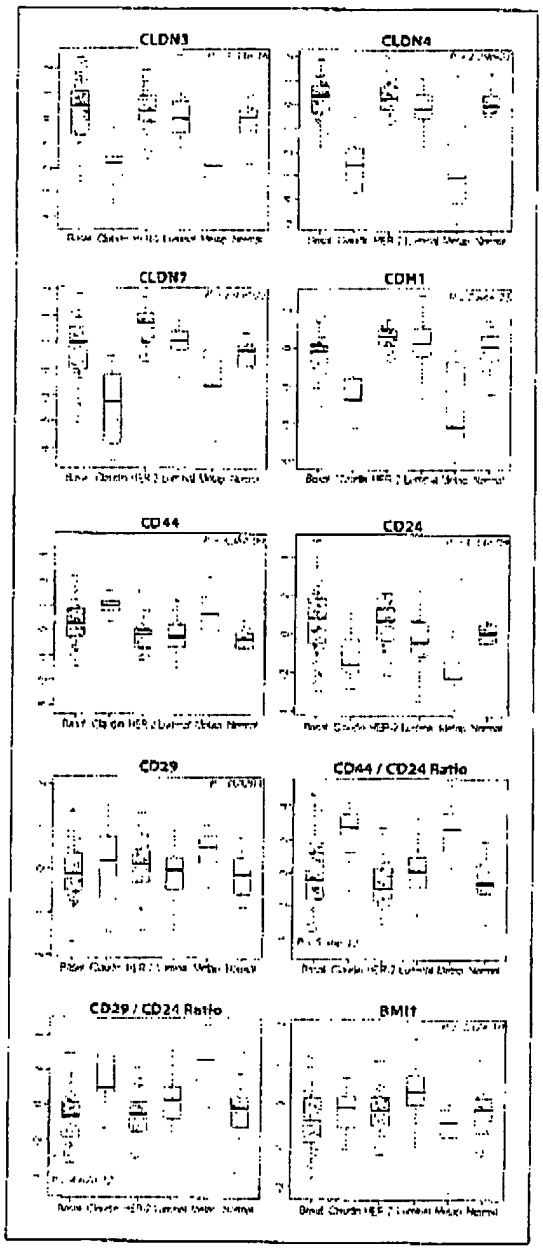

Figure 3.

Expression of claudin-low and stem cell markers in breast cancer subgroups. Using data from transcriptional profiling, metaplastic (*Metap*) and claudin-low tumors express low levels of claudins CLDN3, CLDN4, and CLDN7 of CDH1 (E-cadherin) and high CD44/CD24 and CD29/CD24 ratios. *P* values (ANOVA). *P* values for the metaplastic-basal comparison of stem cell markers were 0.41 (BMI1), 0.19 (CD44), 0.004 (CD29), 0.00009 (CD24), 0.00006 (CD44/CD24 ratio), and 0.00007 (CD29/CD24 ratio).

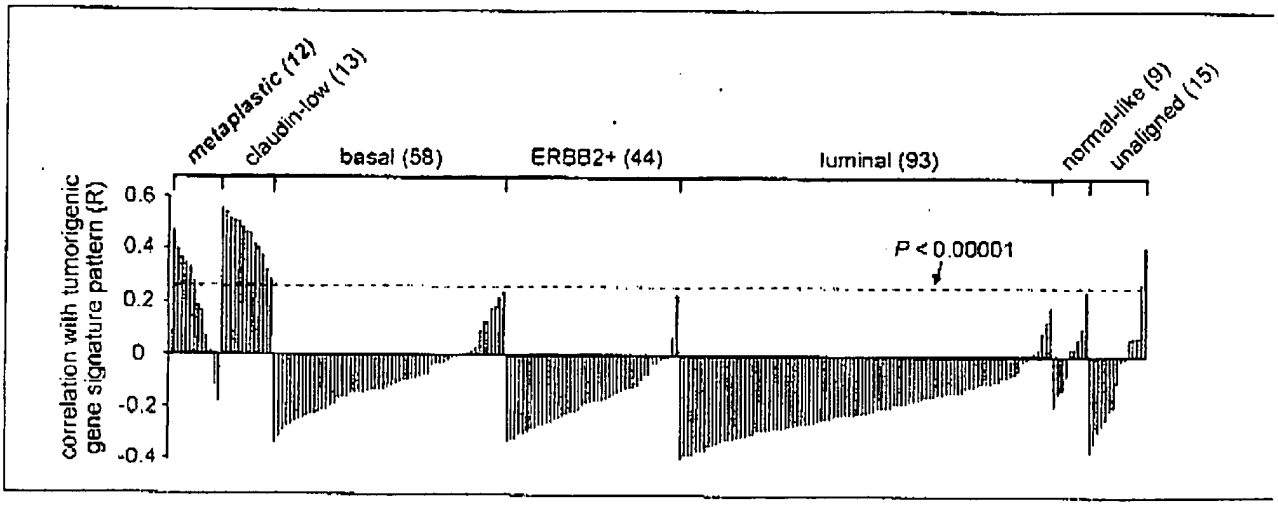

Figure 4.

A $CD44^{+}/CD24^{-/low}$ "tumorigenic" gene signature is enriched in human breast tumors of the "claudin-low" and metaplastic (MBC) subtypes. The correlation shown is between the "tumorigenic" signature pattern (Creighton and colleagues, submitted for publication; using "1" and "−1," for up and down genes, respectively) and each MBC as well an each tumor in the gene expression profile dataset by Herschkowitz and colleagues (9). R values above red dotted line are significant ($P < 0.00001$).

Table 1

Frequency of mutations in the *PIK3CA*, *AKT1/2/3*, *PTEN*, and *KRAS* genes in human breast cancers

Tumor subtype	*PIK3CA* catalytic domain (%)	*PIK3CA* other (%)	*PIK3CA* total (%)	*PTEN* (%)	*AKT1* E17K (%)	*AKT2/3* E17K (%)	*KRAS* (%)
All human breast tumors, excluding metaplastic and claudin-low cancers	73/547 (13.3)	44/547 (8.0)	117/547 (21.4)	2/88 (2.3)	6/418 (1.4)	0/418 (0)	0/418 (0)
Human breast HR+	48/232 (20.7)	32/232 (13.8)	80/232 (34.5)	2/58 (3.4)	6/232 (2.6)	0/232 (0)	0/232 (0)
Human breast HER-2+	13/75 (17.3)	4/75 (5.3)	17/75 (22.7)	0/10 (0)	0/75 (0)	0/75 (0)	0/75 (0)
Human breast TN	12/240 (5.0)	8/240 (3.3)	20/240 (8.3)	0/20 (0)	0/111 (0)	0/111 (0)	0/111 (0)
Human breast claudin-low	0/14 (0)	0/14 (0)	0/14 (0)	-	0/14 (0)	0/14 (0)	0/14 (0)
Human breast metaplastic	4/19 (21.1)	5/19 (26.3)	9/19 (47.4)	1/19 (5.3)	0/19 (0)	0/19 (0)	1/19 (5.3)

NOTE: *PIK3CA*, *AKT1/2/3*, and *PTEN* mutation frequency in hormone receptor–positive (HR+), HER-2–positive, and triple-negative (TN) cancers, used herein as a comparator for metaplastic and claudin-low tumors, has been published (12).

ORIGINAL ARTICLE

The Phosphotidyl Inositol 3-Kinase/Akt Signal Pathway Is Involved in Interleukin-6-mediated Mcl-1 Upregulation and Anti-apoptosis Activity in Basal Cell Carcinoma Cells

S. H. Jee,*† H. C. Chiu,*† T. F. Tsai,* W. L. Tsai,* Y. H. Liao,* C. Y. Chu,* and M. L. Kuo‡

*Department of Dermatology, National Taiwan University Hospital, Taiwan; †Department of Dermatology and ‡Institute of Toxicology, College of Medicine, National Taiwan University, Taipei, Taiwan

Dysregulation of interleukin-6 has been reported to be associated with various types of tumors, and interleukin-6 plays an important part in regulating apoptosis in many types of cells. Previously, Mcl-1 was shown to be significantly increased in interleukin-6-overexpressed basal cell carcinoma cells and conferred on them anti-apoptotic activity. The aim of this study was to investigate which signaling pathway is involved in the anti-apoptotic effect of interleukin-6 on basal cell carcinoma cells. Here we show that the addition of recombinant 100 ng per ml interleukin-6 to basal cell carcinoma cells induced a 2.3-fold increase in the level of Mcl-1 protein in basal cell carcinoma cells. Transfection with dominant-negative STAT3 (STAT3F) into interleukin-6-treated basal cell carcinoma cells caused a decrease of phosphotyrosyl STAT3 but did not alter Mcl-1 protein levels; however, AG490, a Janus tyrosine kinase inhibitor, was capable of inhibiting the interleukin-6-induced elevation of Mcl-1 protein. Next, interleukin-6 stimulation elicited extracellular signal-regulated kinase activation in basal cell carcinoma cells, and the mitogen-activated protein kinase inhibitor, PD98059, could affect this response without affecting the interleukin-6-medi-ated Mcl-1 upregulation. Use of the two phosphotidyl inositol 3-kinase inhibitors, LY294002 and wortmannin, to check whether this pathway is involved in Mcl-1 upregulation by interleukin-6, we found that the phosphotidyl inositol 3-kinase inhibitors completely attenuated the interleukin-6-induced Mcl-1 upregulation. Furthermore, in the interleukin-6-overexpressing basal cell carcinoma cell clone, dominant-negative Akt also significantly reduced the increased level of Mcl-1. Interestingly, Janus tyrosine kinase inhibitor, AG490, treatment strongly blocked the phosphotidyl inositol 3-kinase pathway activation, as evidenced by the decrease in phospho-Akt level. Blockage of phosphotidyl inositol 3-kinase/Akt pathway abolished the interleukin-6-mediated anti-apoptotic activity in ultraviolet B treated cells. Unexpectedly, without ultraviolet B irradiation, STAT3F transfection also induced a significant apoptosis in basal cell carcinoma/interleukin-6 cells. Taken together, our data suggest that both the phosphotidyl inositol 3-kinase/Akt and STAT3 pathways are potentially involved in interleukin-6-mediated cell survival activity in basal cell carcinoma cells; however, the upregulation of the anti-apoptotic Mcl-1 protein by interleukin-6 is mainly through the Janus tyrosine kinase/phosphotidyl inositol 3-kinase/Akt, but not the STAT3 pathway. *Key words: Akt/anti-apoptosis/basal cell carcinoma/interleukin-6/Mcl-1/phosphotidyl inositol 3-kinase/STAT3/ultraviolet B. J Invest Dermatol 119:1121–1127, 2002*

Interleukin (IL)-6 is a multifunctional cytokine acting on various types of cells. This cytokine was able to induce acute phase plasma protein synthesis in hepatocytes (Gauldie *et al*, 1987) and to enhance the proliferation and/or differentiation of a wide array of cells (Hirano *et al*, 1986; Garman *et al*, 1987; Van Damme *et al*, 1987; Lotz *et al*, 1988; Tosato *et al*, 1988; Grossman *et al*, 1989; Gilhar *et al*, 1995). IL-6 has been implicated in the pathogenesis of psoriasis (Yoshinaga *et al*, 1995; Ameglio *et al*, 1997), which is an idiopathic skin disease that is histopathologically characterized by accelerated epidermal pro-liferation, absence of apoptosis in epidermis, and infiltration of inflammatory cells. The IL-6 level is rapidly elevated in human keratinocytes when exposed to ultraviolet (UV) irradiation (Petit-Frere *et al*, 1998); however, the role of IL-6 in skin cells in response to UV remains unclear. An interesting study showed that IL-6 treatment caused growth arrest in human primary melanoma cells but failed to induce the same effect in more aggressively growing melanoma cells (Florenes *et al*, 1999). This indicates that IL-6 may act as a negative regulator in the development of human melanoma. In contrast, it has been reported that IL-6 is a mitogen for basal cell carcinoma (BCC) cells (Jee *et al*, 2001). These findings suggest that IL-6 may have different effects on different types of

Manuscript received February 28, 2002; revised May 7, 2002; accepted for publication August 5, 2002

Reprint requests to: Min-Liang Kuo, PhD, Laboratory of Molecular & Cellular Toxicology, Institute of Toxicology, No. 1, Sec. 1, Jen-Ai Road, Taipei, Taiwan. Email: toxkml@ha.mc.ntu.edu.tw

Abbreviations: dnAkt, dominant-negative mutant of an Akt; PI 3-kinase, phosphotidyl inositol 3-kinase; IL-6, interleukin 6; STAT3, signal transducer and activator of transcription 3; STAT3F, dominant-negative STAT3; JAK, Janus tyrosine kinases; MEK, mitogen activated protein kinase kinase; BCC, basal cell carcinoma; BCC/IL-6, IL-6-overexpressing BCC cells; LY, LY294002; WM, wortmannin.

skin cells and its effects are certainly associated with the pathogenesis of human skin cancer.

BCC is one of the most commonly encountered neoplasms in the world and is characterized as locally aggressive with little metastatic potential (Lear *et al*, 1998). UV irradiation is considered to be a major etiologic factor for the pathogenesis of BCC (Kricker *et al*, 1994). Interestingly, UV irradiation can trigger the release of IL-6 and tumor necrosis factor-α from human epidermal keratinocytes (Chung *et al*, 1996; Avalos-Diaz *et al*, 1999). Cultured BCC cells stained with specific cytokine antibodies showed significant expression of IL-6 (Yen *et al*, 1996). These findings suggest the possible involvement of IL-6 in the pathologic process of BCC. To answer this question, a previous study has shown that ectopic overexpression of IL-6 in BCC cells resulted in enhancement of tumorigenicity in nude mice as compared with vector control cells (Jee *et al*, 2001). Besides, the IL-6-mediated enhancement of tumor potency of BCC cells was at least in part due to its anti-apoptotic activity (Jee *et al*, 2001). The Mcl-1 gene has further been identified as a critical downstream effector of IL-6-elicited anti-apoptotic signaling. Furthermore, IL-6 has recently been shown to function as a key player in the apoptosis of several human cancer cells, such as multiple myeloma, renal cell carcinoma, prostate cancer, Kaposi's sarcoma, colorectal cancer, and hepatoma (Akira and Kishimoto, 1992; Aoyagi *et al*, 1996; Adler *et al*, 1999; Aoki *et al*, 1999; Kinoshita *et al*, 1999; Kuo *et al*, 2001).

This step in the mechanism of deregulation of apoptosis has emerged as a central feature in human cancer development (Hanahan and Weinberg, 2000). The cell survival signaling pathways elicited by IL-6 have been investigated but mostly in hematopoietic cells. In general, three major signaling pathways, including the STAT3 pathway (Puthier *et al*, 1999), phosphotidyl inositol 3-kinase (PI 3-kinase)/Akt pathway (Qiu *et al*, 1998; Chen *et al*, 1999; Kuo *et al*, 2001; Wei *et al*, 2001), and mitogen-activated protein kinase pathway (Thabard *et al*, 2001) have been reported to be involved in the IL-6-mediated cellular functions. Which signaling pathway is active after IL-6 treatment depends upon the cell context. In this study, we sought to determine the role of IL-6 in UVB-induced apoptosis in BCC cells and identify which signal transduction mediators would be involved in IL-6-induced Mcl-1 expression.

MATERIALS AND METHODS

Cell origin and cell culture The BCC cell line originally named BCC-1/KMC was established from human BCC derived from the undifferentiated type of BCC tumor arising on a thermal traumatic scar. Cytokeratin K8.13 was demonstrated in the cytoplasm (Yen *et al*, 1996). The BCC cell line was cultured in RPMI-1640 medium supplemented with 10% fetal bovine serum, streptomycin (100 mg per liter), and penicillin (60 mg per liter). The vector clone (BCC/neo) and IL-6 overexpression clone (BCC/IL-6) were cultured in the same medium as described above, but with the addition of 500 μg G418 per ml (Jee *et al*, 2001).

Antibodies and reagents Affinity-purified monoclonal mouse anti-Akt, anti-Mcl-1, anti-ERK1/2, and anti-phospho-ERK1/2 antibodies, and rabbit polyclonal anti-IL-6Rα IgG were purchased from Santa Cruz Biotechnology (Santa Cruz, CA). The anti-phospho-Akt was from Promega (Madison, WI). The anti-phospho-STAT3 was from Upstate Biotechnology (Lake Placid, NY). The PI 3-kinase inhibitors wortmannin (WM), LY294002 (LY), Janus tyrosine kinase (JAK) inhibitor, AG490 and MEK inhibitor, PD98059 were obtained from Calbiochem (San Diego, CA).

Western blot analysis The cellular lysates were prepared as described previously (Kuo *et al*, 1998). A 50 μg sample of each lysate was subjected to electrophoresis on 10% sodium dodecyl sulfate–polyacrylamide gels, and for detection of Mcl-1, STAT3, phospho-STAT3 (p-STAT3), Akt, phospho-Akt (p-Akt), ERK1/2, and phospho-ERK1/2 (p-ERK1/2). The samples were then electroblotted on nitrocellulose paper. After blocking, blots were incubated with anti-Mcl-1, anti-STAT3, anti-p-STAT3, anti-Akt, anti-p-Akt, anti-ERK1/2, and anti-p-ERK1/2 antibodies in phosphate-buffered saline (PBS) containing Triton X-100) for 1 h followed by three washes (15 min each) in PBS Triton X-100, and then incubated with horseradish peroxidase-conjugated goat anti-mouse IgG (for the primary monoclonal antibodies) and with horseradish peroxidase-conjugated goat anti-rabbit IgG (for the primary polyclonal antibodies; Amersham), respectively, for 30 min. After washing, blots were incubated for 1 min with the western blotting reagent ECL (Amersham (Buckinghamshire, UK)) and chemi-luminescence from the blots was detected by exposure of Kodak-BioMax films to the blots for 30 s to 10 min. The intensity of bands on auto-radiograms were quantified by scanning laser densitometry.

Reverse transcriptase–polymerase chain reaction (reverse transcriptase–PCR) RNA from BCC cells treated with IL-6 were isolated using commercial kits (BIOTECX Laboratory Inc. (Houston, TX)). The total RNA was subjected to first-strand synthesis using Random Hexamer (Amersham, Pharmacia Biotec (Buckinghamshire, UK)) and M-MLV Reverse Transcriptase (RNase H Minus) (Promega) at 37°C for 3 h. The cDNA was then diluted to a final volume of 50 μl and quantified. Five micrograms of cDNA was amplified in the presence of 0.5 U Taq polymerase per μl (Protech Technology, Taipei, Taiwan) and 25 pmol of both the sense and the anti-sense Mcl-1 or β-actin oligonucleotides in PCR buffer (10 mM Tris pH 9, 50 mM KCl, 1.5 mM $MgCl_2$, 0.01% gelatin, and 0.1% Triton X-100):

Mcl-1 sense, 5′-GCGGATCCACCATGTTTGGCCTCAAAAGA-3′
Mcl-1 anti-sense, 5′-GCGTCGACAGGCTATCTTATTAGATATGC-3′
β-actin sense, 5′-CGTCTGGACCTGGCTGGCCGGGACC-3′
β-actin anti-sense, 5′-CTAGAAGCATTTGCGGTGGACGATG-3′

The reaction mixture was incubated for 5 min at 94°C and then amplified by 25 PCR cycles (denaturation for 1 min at 94°C, annealing for 1 min at 55°C for Mcl-1 and 56°C for β-actin, and extension for 1 min at 72°C). Each PCR product was then analyzed on a 2% agarose gel, stained with 1 μg ethidium bromide per ml, viewed and photographed. The intensity of bands on photographs was quantified by scanning laser densitometry.

DNA construct and transient transfection To construct a hemagglutinin epitope-tagged dominant-negative mutant of an Akt (dnAkt) expression plasmid, an hemagglutinin epitope tag was inserted into dnAKT cDNA and cloned into a pcDNA3 vector (GIBCO, Invitrogen; Grand Island, NY; Chen *et al*, 1999). IL-6–overexpressing BCC cells (BCC/IL-6) were plated 24 h before transfection at a density of 1×10^5 cells in 35 mm Petri dish. Cells were transfected with 1 μg of dnAkt plasmid using, according to the manufacturer's instructions, the Transfast™ Transfection Reagent (Promega). For assay of JAK/STAT3 signal pathway, 1 μg of the hemagglutinin-tagged dominant-negative mutant of STAT3F plasmid (Nakajima *et al*, 1996) or control plasmid (pcDNA3) was constructed using the same method described above. The amount of hemagglutinin was concomitantly measured to confirm the transfection efficiency.

Flow cytometry for apoptosis assay Cell cultures grown to about 70–80% confluence and serum-starved for 24 h were irradiated with UVB at 25 mJ per cm^2. Twenty-four hours later, the floating cells were collected from culture medium, centrifuged, and then washed once with PBS. Cells that adhered to the culture dish were trypsinized with 0.5 ml of trypsin (0.05% trypsin and 0.02% ethylenediamine tetraacetic acid) for 5 min and then collected. The floating cells and the collected adherent cells were pooled and centrifuged at $1500 \times g$ for 5 min. Pellets were washed with PBS twice, followed by adding 200 μl of PBS and 800 μl of absolute ethanol (i.e., 80% EtOH) and incubated at −20°C for at least 3 h. Then, 0.5% Triton X-100 (in PBS) was added and mixed well, followed by RNase (final volume 0.05% v/v), and the mixture was incubated at 37°C for 20–30 min. An equal volume of propidium iodide (50 μg per ml in PBS) was added to the samples, which were then analyzed by flow cytometry (FACSCalibur, Becton Dickinson, Le Pont de Claix, France) using CELLQuest software (Becton Dickinson).

RESULTS

IL-6 upregulates Mcl-1 in human BCC cells Previous data demonstrated that the Mcl-1 protein level, but not other Bcl-2 family members, was obviously increased in BCC/IL-6 (Jee *et al*, 2001). Here we show that exposure to human recombinant IL-6 also increased the Mcl-1 protein level in BCC cells. Western blotting revealed that upon IL-6 stimulation with a dose of 100 ng per ml, the level of Mcl-1 protein initially increased at 2 h, and peaked at 6–8 h, then declined to basal level (**Fig 1*A***). In contrast, the level of Bcl-2 protein was little changed (Fig 1*A*). A 2.3-fold increase of Mcl-1 protein occurred in BCC

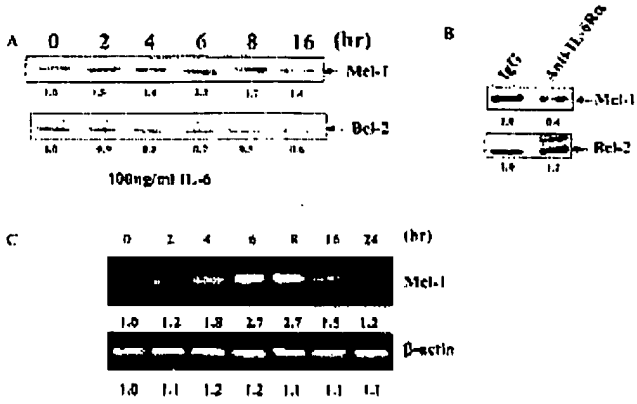

Figure 1. IL-6 regulates the expression of Mcl-1 in human BCC cells in a time-dependent manner. (*a*) Twenty-four hour serum-starved BCC cells (5×10^5 per ml) were treated with 50 ng per ml or 100 ng per ml of IL-6 for different amounts of time (0, 2, 4, 6, 8, or 16 h). (*b*) Serum-starved BCC cells (5×10^5 per ml) were treated 1 μg of anti-IL-6Rα antibody for 12 h. After treatment, cell lysates were prepared and analyzed by western blotting as described in *Materials and Methods*. (*c*) The number below each lane indicate the relative intensity to control (defined as 1.0). This is one representative experiment of three.

cells after exposure to 100 ng per ml, respectively. We previously reported that the BCC/IL-6 cells displayed an elevated level of Mcl-1 (Jee *et al*, 2001). Here we found that the increased level of Mcl-1 in BCC/IL-6 cells was effectively diminished by treatment with specific anti-IL-6Rα antibody but not by control IgG (**Fig 1B**). The above findings suggest that both paracrine and autocrine IL-6 can induce endogenous Mcl-1 upregulation in BCC cells. In addition, reverse transcriptase–PCR analysis showed that *mcl-1* mRNA was significantly elevated and peaked at 6–8 h after IL-6 treatment (**Fig 1C**), suggesting that the IL-6-mediated increased in *mcl-1* gene expression is possibly through transcriptional regulation.

STAT3 and ERK1/2 activation are not required for Mcl-1 upregulation mediated by IL-6 Determining which signaling pathways are involved in IL-6-mediated Mcl-1 upregulation in human BCC cells was the next topic of interest. First, possible involvement of the STAT3 pathway in IL-6-mediated Mcl-1 upregulation was examined. To address this issue, either control vector or STAT3 dominant-negative mutant (STAT3F), in which Tyr-705, a phosphoacceptor site of STAT3, was mutated to phenylalanine (Nakajima *et al*, 1996), was transiently transfected into BCC/IL-6 cells. Transient transfectants and pcDNA3 control cells were analyzed for their effect on STAT3 activity by determining the tyrosine-phosphorylation status of STAT3 (p-STAT3) in the IL-6 overexpressing BCC cells.

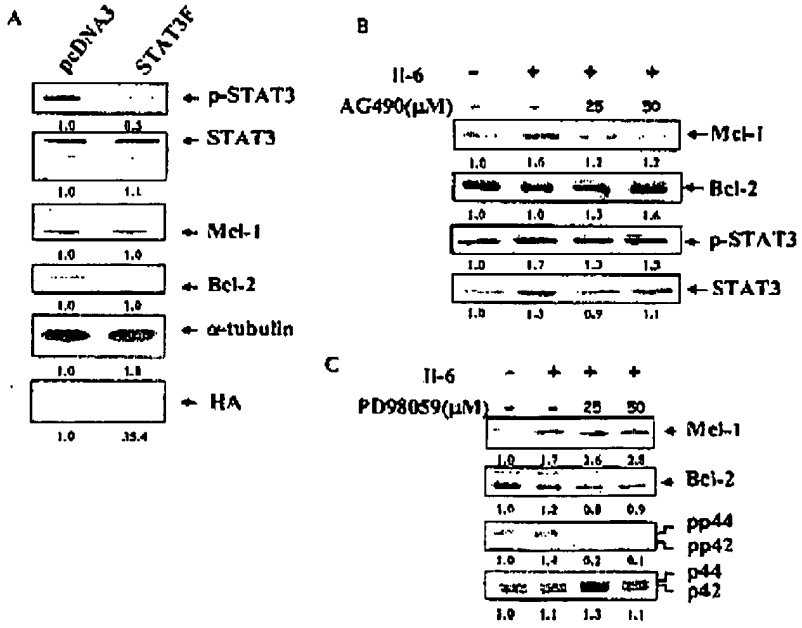

Figure 2. STAT3 pathway and ERK pathway are not involved in IL-6 upregulation of Mcl-1. (*a*) Dominant-negative STAT3 (dnSTAT3, STAT3F) reduces IL-6-induced tyrosine phosphorylation of STAT3. After transient transfection of BCC/IL-6 with control vector (pcDNA3) and hemagglutinin-tagged dominant-negative STAT3 (STAT3F) for 48 h, the cell lysates with an equal amount of proteins were subjected to western blotting with anti-phospho-STAT3 antibody, which specifically recognizes the phosphotyrosine at Tyr 705 of the STAT3 protein, was performed to check their STAT3 function. Dominant-negative STAT3 failed to inhibit IL-6-induced Mcl-1 expression. Lysates from cells (as indicated above) were analyzed by western blotting using anti-Mcl-1 antibody. (*b,c*) JAK inhibitors (AG490) reduced IL-6-induced tyrosine phosphorylation of STAT3 and serine phosphorylation of Akt and Mcl-1 expression; MEK inhibitor (PD98059) abolished the IL-6-induced activation of ERK, but not Mcl-1 expression. Forty-eight hour serum-starved BCC cells (5×10^5 per ml) pretreated with IL-6 (100 ng per ml) for 15 min were then incubated with 25 μM and 50 μM of AG490 for a further 1 h. Lysates from cells as indicated were used for western blotting with anti-phospho-STAT3 antibody (*c, lower panel*) and anti-phospho-Akt antibody (*c, lower panel*). For assessment of Mcl-1, the incubation time of AG490 was 6 h. Lysates were used for western blotting with anti-Mcl-1 antibody (*b*). To investigate the involvement of RAS/MEK/ERK pathway, serum-starved BCC cells (5×10^5 per ml) pretreated with IL-6 (100 ng per ml) for 15 min were incubated with 25 μM and 50 μM of PD98059 for a further 1 and 6 h for assessment of ERK1/2 (*c, upper panel*) and Mcl-1, respectively (*b*). Cell lysates were prepared and used for western blotting with antibody specific to phosphorylated ERK1/2 (*c, upper panel*) or anti-Mcl-1 antibody (*b*). The number below each lane indicate the relative intensity to control (defined as 1.0). This is one representative experiment of three.

Expression of STAT3F resulted in inhibition of STAT3 function, as evidenced by the decrease in p-STAT3 with addition of a specific anti-p-STAT3 antibody (**Fig 2*A***); however, Mcl-1 and other internal control proteins such as Bcl-2 and α-tubulin, were all not significantly attenuated by transfection with STAT3F. The high expression of hemagglutinin and marked decrease of p-STAT3 after transfection of hemagglutinin-tagged STAT3F indicated that a high transfection efficiency was achieved and allowed for detecting the inhibitory effect of STAT3F on the level of Mcl-1 (**Fig 2*A***). To confirm further that the JAK, an upstream kinase of STAT3, is not involved in the IL-6-induced Mcl-1 upregulation, a specific inhibitor for the JAK family of kinases, the tyrphostin AG490, was utilized. As **Fig 2(*B*)** illustrates, pretreating BCC cells with AG490 significantly reduced the tyrosine-phosphorylated state of STAT3 and Mcl-1 in the presence of IL-6, suggesting that JAK is necessary for Mcl-1 expression induced by IL-6; however, according to **Fig 2(*A*)**, activation of STAT3 pathway is not required for IL-6-induced Mcl-1 upregulation. Therefore, we strongly suggest that JAK induces Mcl-1, possibly through another downstream mediator.

Next, we examined whether ERK1/2 could be activated by IL-6 and be involved in Mcl-1 upregulation in this cell context. **Figure 2(*C*)** shows that IL-6 apparently activated the ERK pathway in BCC cells, as evidenced by the increased phosphorylated form of p42 and p44. The IL-6-induced increase of phosphorylated ERK, as expected, was greatly reduced by treatment with PD98059, a highly specific inhibitor of MEK; however, PD98059 failed to inhibit the IL-6-induced Mcl-1 expression. These findings indicate that in BCC cells, the ERK pathway is not involved in IL-6-induced Mcl-1 upregulation.

The PI 3-kinase/Akt pathway is involved in the IL-6-induced Mcl-1 expression Previous investigations on different cell modes have demonstrated that IL-6 could activate PI 3-kinase and Akt pathways, which mediate the anti-apoptotic signal of IL-6 in human hepatoma Hep3B cells (Chen *et al*, 1999; Kuo *et al*, 2001) and human cervical cancer C33A cells (Wei *et al*, 2001). We thus examined whether PI 3-kinase/Akt pathway is involved in IL-6-induced Mcl-1 upregulation in BCC cells. To address this, two specific inhibitors of PI 3-kinase, WM and LY, were used. As **Fig 3(*A*)** reveals, 12.5 or 25 μM of LY or 50 or 100 nM of WM significantly decreased the elevated level of Mcl-1 induced by IL-6. Under identical circumstances, IL-6-stimulated PI 3-kinase activity was blocked by both LY and WM, as indicated by the decrease of the phosphorylated form of the Akt protein (p-Akt), which was recognized by a specific antibody (**Fig 3*B***). The serine/threonine protein kinase Akt is a downstream effector of PI 3-kinase and can be activated by IL-6 in Hep3B cells (Chen *et al*, 1999; Kuo *et al*, 2001) and C33A cells (Wei *et al*, 2001). To assess the role of Akt in the IL-6-induced Mcl-1 increase in BCC cells, the effect of dnAkt was investigated. A hemagglutinin-tagged kinase-defective dnAkt (Chen *et al*, 1999) was transiently transfected into BCC/IL-6 cells herein to examine its influence on IL-6-mediated Mcl-1 upregulation. **Figure 3(*C*)** reveals that the increased Mcl-1 protein level in BCC/IL-6 cells was significantly diminished by transfection with dnAkt but not with pcDNA3 control vector. The successful expression of dnAkt in BCC/IL-6 cells was determined by the hemagglutinin level using western blotting (**Fig 3*C***). Above findings indicate that PI 3-kinase and its downstream Akt are activated by IL-6 and mediate the signaling to upregulate the level of Mcl-1.

In **Fig 2(*B*)**, we have clearly demonstrated that JAK is critical for IL-6-mediated Mcl-1 upregulation. Besides, it is known that JAK is recruited immediately by gp130 upon IL-6 treatment (Puthier *et al*, 1999). We thus propose that JAK may act upstream to transduce signaling to PI 3-kinase/Akt pathway and finally activate the Mcl-1 expression. To clarify this hypothesis, we checked whether AG490 treatment would affect the level of p-Akt in BCC cells treated with IL-6. **Figure 3(*D*)** shows that the IL-6-induced increase in phosphorylated Akt levels in BCC cells was markedly diminished by 25 and 50 μM of AG490. These data suggest that the signaling pathway responsible for IL-6 mediation

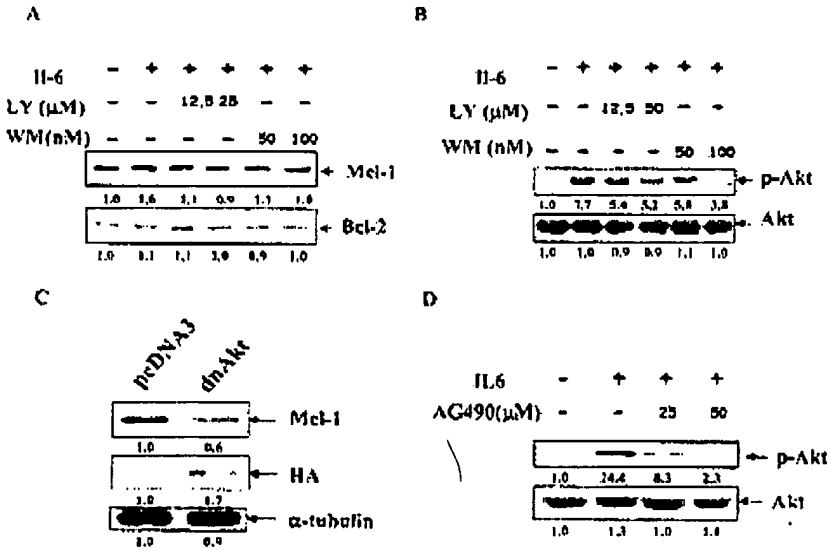

Figure 3. PI 3-kinase/Akt pathways are involved in the IL-6 upregulation of Mcl-1. (*a*) PI 3-kinase inhibitors reduced IL-6-induced Mcl-1 expression. Twenty-four hour serum-starved BCC cells (5×10^5 per ml) were pretreated with IL-6 (100 ng per ml) for 15 min followed by incubation with PI 3-kinase inhibitors, LY (12.5 and 25 μM) or WM (50 and 100 nM) for six more hours. The cell lysates with an equal amount of protein were subjected to western blotting with anti-Mcl-1 antibody. (*b*) PI 3-kinase inhibitors attenuated IL-6 elicited serine phosphorylation of Akt. The cells were treated (as indicated above), except incubation time with IL-6 was for 1 h. Anti-pAkt antibody was used for western blotting analysis. (*c*) dnAkt inhibits IL-6-regulated Mcl-1 upregulation. BCC/IL-6 cells were transfected with hemagglutinin-tagged dnAkt or control vector (pcDNA3) for 48 h. Cell lysates were analyzed by western blotting using anti-Mcl-1 antibody (*upper panel*) and anti-hemagglutinin antibody (*lower panel*). (*d*) AG490 attenuates activation of Akt in a concentration-dependent manner. The cells were treated as (*b*), except AG490 (25 and 50 μM) was used instead of LY and WM. The number below each lane indicate the relative intensity to control (defined as 1.0). This is one representative experiment of three.

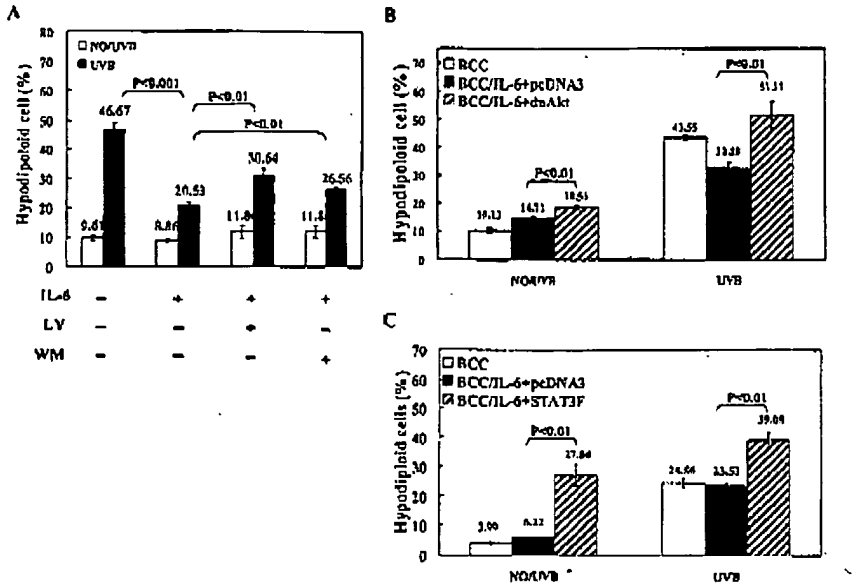

Figure 4. *(a,b)* **PI 3-kinase/Akt and** *(c)* **STAT3 are involved in anti-apoptotic activity regulated by IL-6.** *(a)* PI 3-kinase inhibitors blocked the anti-apoptotic activity of IL-6. Serum-starved BCC cells (5×10^5 per ml) were pretreated with PI 3-kinase inhibitors, LY (25 and 50 μM) or WM (50 and 100 nM), followed by IL-6 (100 ng per ml) for an additional hour. Cells were then irradiated with 25 mJ per cm^2 of UVB. Twenty-four hours after UVB irradiation, the cells were harvested for flow cytometric analysis. *(b)* dnAkt blocks the anti-apoptotic effect of IL-6. Forty-eight hours after transient transfection of BCC/IL-6 with control vector (pcDNA3) and hemagglutinin-tagged dnAkt, BCC/IL-6 cells (5×10^5 per ml) were irradiated with 25 mJ per cm^2 of UVB or not irradiated. Twenty-four hours after UVB irradiation or no irradiation, cells were harvested for flow cytometric analysis. *(c)* Dominant-negative STAT3 (STAT3F) blocks the anti-apoptotic effect of IL-6. Control vector (pcDNA3) and hemagglutinin-tagged dominant-negative STAT3 (STAT3F) were transiently transfected into BCC/IL-6 cells followed by the same procedure as *(b)*. Parental BCC cells plus and minus UV served as controls in *(b)* and *(c)*. Percentages of hypodiploid cells are expressed as mean ± SD of three experiments. Student's t test was used for comparison.

of Mcl-1 upregulation in human BCC cells may be a novel JAK/PI 3-kinase/Akt pathway.

PI 3-kinase/Akt and STAT3 pathways are involved in the anti-apoptotic activity of IL-6 It has previously been demonstrated that IL-6-upregulated Mcl-1 confers resistance to UVB-induced apoptosis in BCC cells, as evidenced by transient transfection of anti-sense Mcl-1 (Jee *et al*, 2001). In this study, we further demonstrated that the PI 3-kinase/Akt, but not STAT3, pathway is critically involved in IL-6-mediated upregulation of Mcl-1 in BCC cells. We thus examined whether PI 3-kinase/Akt is involved in IL-6-regulated anti-apoptotic activity against UVB irradiation. Exposure of BCC cells with recombinant IL-6 resulted in a protection against UVB-induced apoptosis (Student's t test, $p < 0.001$, **Fig 4*A***). The IL-6-mediated anti-apoptotic activity against UVB was diminished by treatment with LY or WM (**Fig 4*A***). Supportive of this finding, transfection of dnAkt vector into BCC/IL-6 cells also lead to a dramatic attenuation of their anti-apoptotic activity against UVB irradiation (**Fig 4*B***). These results strongly suggest an important role of the PI 3-kinase/Akt signaling pathway in IL-6-mediated cell survival. On the other hand, a previous study showed that the STAT3 signaling pathway also contributes the anti-apoptotic activity of IL-6 in human hepatoma cells (Chen *et al*, 1999). Thus we transfected dominant-negative STAT3 (STAT3F) into BCC/IL-6 cells to see its effect on cell death. Interestingly, STAT3F transfection caused a significant increase of apoptotic cell death in BCC/IL-6 cells with or without concomitant treatment with UVB, when compared with control vector (**Fig 4*C***). This observation suggests that STAT3 pathway was involved in IL-6-induced cell survival activity but not in Mcl-1 upregulation. It is possible that activation of STAT3 and PI 3-kinase/Akt pathways may lead to different downstream effectors to protect cell death.

Taken together, our findings suggest that the anti-apoptotic activity of IL-6 against UVB irradiation is mediated though the activation of PI 3-kinase/Akt followed by upregulation of Mcl-1 in BCC cells. Without apoptotic stimuli, however, the STAT3 pathway provides a fundamental survival mechanism of IL-6 and this mechanism is independent of Mcl-1 upregulation.

DISCUSSION

IL-6 has been reported to be associated with various types of tumors. Emerging evidence has demonstrated that IL-6 plays an important part in regulating apoptosis in many types of cells. This anti-apoptotic effect may be attributed to the malignant progression of tumors. UVB has been the important etiologic factor of skin cancer. Nucleotide excision repair, apoptosis, and cell cycle regulation are major defense mechanisms against the carcinogenic effect of UVB; however, the anti-apoptotic effect of UVB mediated by IL-6 in skin cells has not been well documented.

We previously demonstrated that ectopic expression of IL-6 in BCC cells resulted in an increment in Mcl-1 protein level (Jee *et al*, 2001). Here we show addition of recombinant IL-6 also evidently elevates the level of Mcl-1 protein. These findings indicate either an autocrine or paracrine loop of IL-6 synthesis can stimulate endogenous Mcl-1 expression in BCC cells. (Yang *et al*, 1996) reported that unlike Bcl-2, Mcl-1 contains a PEST sequence; Rogers *et al* (1986) found the amino acid sequences of ten proteins with intracellular half-lives less than 2 hours contain one or more regions rich in proline (P) glutamic acid (E), serine (S) and threonine (T). They renamed these regions PEST regions. This probably accounts for the lability of Mcl-1 (half-life of 1–3 h). In a previous study using a hepatoma cell model, we observed this same property of Mcl-1 protein (Kuo *et al*, 2001); however,

in this study, upon IL-6 stimulation, the level of Mcl-1 reached a maximum at 6 h and was sustained for 16 h. It seems that Mcl-1 has a longer half-life in BCC cells. The reason for the more delayed induction and more prolonged half-life of Mcl-1 in BCC cells is unknown and needs to be further investigated.

The signaling pathways leading to the Mcl-1 expression have been investigated and varied according to the type of cell models or stimuli employed. For example, activation of protein kinase C/ERK pathway was necessary for TPA (12-o-tetradecanoylphorbol-13-acetate) or the microtubule-disrupting agent-induced Mcl-1 expression in ML-1 human myeloblastic leukemia cells (Townsend *et al*, 1998). IL-6 has been reported to induce Mcl-1 expression in multiple myeloma cells through the JAK/STAT3 pathway, but not the Ras/ERK pathway (Puthier *et al*, 1999). A previous study showed that granulocyte-macrophage colony-stimulating factor and IL-3 activated Mcl-1 expression in TF-1 leukemia and Ba/F3 pro-B cells, respectively, and the Mcl-1 induction in both cells was mediated through the PI 3-kinase/Akt pathway (Wang *et al*, 1999). The above investigations have almost focused on the cell systems that are of hematopoietic origin. Recently, we and others began to study the regulatory mechanism of Mcl-1 by IL-6 in cells of epithelial origin. Interestingly, unlike the situation in the hematopoietic cells, the PI 3-kinase pathway is commonly activated and necessary for Mcl-1 upregulation in a wide array of epithelial cancer cells, including hepatoma cells (Kuo *et al*, 2001), prostatic cancer cells (Chung *et al*, 2000), and cervical cancer cells (Wei *et al*, 2001). In agreement with those who experimented in these cancer cell lines, we also find that the PI 3-kinase and its downstream effector Akt is activated by IL-6 in BCC cells. The PI 3-kinase/Akt signaling pathway is important for cell survival activity and Mcl-1 expression in BCC cells.

Upon IL-6 binding, its receptor triggers the recruitment of the signal-transducing protein gp130, subsequently leading to the activation of the gp130-associated Janus kinases (JAK) (Murakami *et al*, 1993; Luttticken *et al*, 1994; Narazaki *et al*, 1994). JAK phosphorylate gp130 at several tyrosine residues and these phosphotyrosines recruit various SH2 domain-containing proteins, such as STAT and SHP-2 (Akira *et al*, 1994; Boulton *et al*, 1994). These events led to the activation of multiple signal transduction pathways, such as the STAT, Ras/ERK and PI 3-kinase pathway (Hibi *et al*, 1996; Heinrich *et al*, 1998). Although the STAT3 pathway was not involved in IL-6-induced Mcl-1 upregulation, blockage of the STAT3 pathway leads to cell death in IL-6-overexpressed BCC cells. This indicates that certain anti-apoptotic genes located downstream of the STAT3 pathway in IL-6-overexpressed BCC cells have not been identified yet. Consistently, the STAT3 pathway has already been reported to participate in anti-apoptosis of multiple myeloma cells (Fukada *et al*, 1996; Catlett-Falcone *et al*, 1999). Bcl-xL was found to be elevated in human multiple myeloma cells by IL-6 through the STAT3 pathway (Puthier *et al*, 1999); however, a previous study showed that the level of many Bcl-2 family proteins, including Bcl-xL and Bcl-2 was not altered in IL-6-overexpressed BCC cells (Jee *et al*, 2001). This result excludes the possible involvement of some well-known Bcl-2 family proteins in the STAT3 pathway-mediated anti-apoptotic activity in IL-6-overexpressed BCC cells. Bellido *et al* (1998) demonstrated that p21 is a downstream effector of gp130/stat3 activation and a critical mediator of the pro-differentiating and anti-apoptotic effects of IL-6 type cytokines on human osteoblastic cells. In our system, increased expression of p21 protein was observed upon IL-6 stimulation (data not shown). How p21 promotes survival and any other anti-apoptotic factors regulated by STAT3 remains elusive and requires further investigation.

The PI 3-kinase/Akt signaling pathway is involved in the survival effect of many growth factors and some transforming oncogenes (Skorski *et al*, 1997; Songyang *et al*, 1997). Recent findings demonstrate that the pro-apoptotic protein Bad (Datta *et al*, 1997) and procaspase 9 (Cardone *et al*, 1998) were the downstream targets of Akt, which protects cells from apoptosis; however, Bad has a restricted tissue distribution, and not every survival signal that activates Akt stimulates Bad phosphorylation (Scheid and Durono, 1998). The phosphorylation inactivation of procaspase 9 by Akt is not generally observed in all cell types. It is possible that Akt may exert its anti-apoptotic effect via the activation or inactivation of other cellular targets. Our studies in hepatoma cells, cervical cancer cells, and BCC cells provide evidence that Mcl-1, the survival factor activated by IL-6, is another cellular target of the PI 3-kinase/Akt signaling pathway. Unlike the phosphorylation of Bad or procaspase 9, the PI 3-kinase/Akt pathway upregulates the Mcl-1 expression at the level of transcription (data not shown).

Although IL-6 exerts an anti-apoptotic activity in a wide variety of cells, the cell survival signaling pathways activated by the cytokine is varied. Greater understanding of the specific anti-apoptotic signal pathways activated by IL-6 in skin cancer cells may enable the development of effective preventive measures or therapies for human skin cancers.

This work was supported by grants from National Science Council, Taiwan (NSC-88-2314-B002-254 and NSC-89-2314-B002-254).

REFERENCES

Adler HL, McCurdy MA, Kattan MW, Timme TL, Scardino PT, Thompson TC: Elevated levels of circulating interleukin-6 and transforming growth factor-beta1 in patients with metastatic prostatic carcinoma. *J Urol* 161:182–187, 1999

Akira S, Kishimoto T: IL-6 and NF-IL6 in acute-phase response and viral infection. [Review] *Immunol Rev* 127:25–50, 1992

Akira S, Nishio Y, Inoue M, *et al*: Molecular cloning of APRF, a novel IFN-stimulated gene factor 3 p91-related transcription factor involved in the gp130-mediated signaling pathway. *Cell* 77:63–71, 1994

Ameglio F, Bonifati C, Fazio M, *et al*: Interleukin-11 production is increased in organ cultures of lesional skin of patients with active plaque-type psoriasis as compared with nonlesional and normal skin. Similarity to interleukin-1 beta, interleukin-6 and interleukin-8. *Arch Dermatol Res* 289:399–403, 1997

Aoki Y, Jaffe ES, Chang Y, *et al*: Angiogenesis and hematopoiesis induced by Kaposi's sarcoma-associated herpesvirus-encoded interleukin-6. *Blood* 93:4034–4043, 1999

Aoyagi T, Takishima K, Hayakawa M, Nakamura H: Gene expression of TGF-alpha, EGF and IL-6 in cultured renal tubular cells and renal cell carcinoma. *Int J Urol* 3:392–396, 1996

Avalos-Diaz E, Alvarado-Flores E, Herrera-Esparza R: UV-A irradiation induces transcription of IL-6 and TNF alpha genes in human keratinocytes and dermal fibroblasts. *Rev Rhoum* 66:13–19, 1999

Bellido T, O'Brien CA, Roberson PK, Manolagas SC: Transcriptional activation of the p21 (WAF1,CIP1,SDI1) gene by interleukin-6 type cytokines. A prerequisite for their pro-differentiating and anti-apoptotic effects on human osteoblastic cells. *J Biol Chem* 273:21137–21144, 1998

Boulton TG, Stahl N, Yancopoulos GD: Ciliary neurotrophic factor/leukemia inhibitory factor/interleukin 6/oncostatin M family of cytokines induces tyrosine phosphorylation of a common set of proteins overlapping those induced by other cytokines and growth factors. *J Biol Chem* 269:11648–11655, 1994

Cardone MH, Roy N, Stennicke H, *et al*: Regulation of cell death protease caspase-9 by phosphorylation. [see comments] *Science* 282:1318–1321, 1998

Catlett-Falcone R, Landowski TH, Oshiro MM, *et al*: Constitutive activation of Stat3 signaling confers resistance to apoptosis in human U266 myeloma cells. *Immunity* 10:105–115, 1999

Chen RH, Chang MC, Su YH, Tsai YT, Kuo ML: Interleukin-6 inhibits transforming growth factor-beta-induced apoptosis through the phosphatidylinositol 3-kinase/Akt and signal transducers and activators of transcription 3 pathways. *J Biol Chem* 274:23013–23019, 1999

Chung JH, Youn SH, Kwh WS, *et al*: Ultraviolet B irradiation-enhanced interleukin (IL)-6 production and mRNA expression are mediated by IL-1 alpha in cultured human keratinocytes. *J Invest Dermatol* 106:715–720, 1996

Chung TD, Yu JJ, Kong TA, Spiotto MT, Lin JM: Interleukin-6 activates phosphatidylinositol-3 kinase, which inhibits apoptosis in human prostate cancer cell lines. *Prostate* 42:1–7, 2000

Datta SR, Dudek H, Tao X, *et al*: Akt phosphorylation of BAD couples survival signals to the cell-intrinsic death machinery. *Cell* 91:231–241, 1997

Florenes VA, Lu C, Bhattacharya N, *et al*: Interleukin-6 dependent induction of the cyclin-dependent kinase inhibitor p21WAF1/CIP1 is lost during progression of human malignant melanoma. *Oncogene* 18:1023–1032, 1999

Fukada T, Hibi M, Yamanaka Y, *et al*: Two signals are necessary for cell proliferation induced by a cytokine receptor gp130: involvement of STAT 3 in anti-apoptosis. *Immunity* 5:449–460, 1996

Garman RD, Jacobs KA, Clark SC, Raulet DH: B-cell-stimulatory factor 2 (beta 2 interferon) functions as a second signal for interleukin 2 production by mature murine T cells. *Proc Natl Acad Sci USA* 84:7629–7633, 1987

Gauldie J, Richards C, Harnish D, Lansdorp P, Baumann H: Interferon beta 2/B-cell stimulatory factor type 2 shares identity with monocyte-derived hepatocyte-stimulating factor and regulates the major acute phase protein response in liver cells. *Proc Natl Acad Sci USA* 84:7251–7255, 1987

Gilhar A, Pillar T, Etzioni A: Possible role of cytokines in cellular proliferation of the skin transplanted onto nude mice. *Arch Dermatol* 131:38–42, 1995

Grossman RM, Krueger J, Yourish D, *et al*: Interleukin-6 is expressed in high levels in psoriatic skin and stimulates proliferation of cultured human keratinocytes. *Proc Natl Acad Sci USA* 86:6367–6371, 1989

Hanahan D, Weinberg RA: The hallmarks of cancer. [Review] *Cell* 100:57–70, 2000

Heinrich PC, Behrmann I, Muller-Newen G, Schaper F, Graeve L: Interleukin-6-type cytokine signalling through the gp130/Jak/STAT pathway. [Review] *Biochem J* 334:297–314, 1998

Hibi M, Nakajima K, Hirano T: IL-6 cytokine family and signal transduction: a model of the cytokine system. [Review] *J Mol Med* 74:1–12, 1996

Hirano T, Yasukawa K, Harada H, *et al*: Complementary DNA for a novel human interleukin (BSF-2) that induces B lymphocytes to produce immunoglobulin. *Nature* 324:73–76, 1986

Jee SH, Shen SC, Chiu HC, Tsai WL, Kuo ML: Overexpression of interleukin-6 in human basal cell carcinoma cell lines increases anti-apoptotic activity and tumorigenic potency. *Oncogene* 20:198–208, 2001

Kinoshita T, Ito H, Miki C: Serum interleukin-6 level reflects the tumor proliferative activity in patients with colorectal carcinoma. *Cancer* 85:2526–2531, 1999

Kricker A, Armstrong BK, English DR: Sun exposure and non-melanocytic skin cancer. [Review] *Cancer Causes Control* 5:367–392, 1994

Kuo ML, Chuang SE, Lin MT, Yang SY: The involvement of PI 3-kinase/Akt-dependent up-regulation of Mcl-1 in the prevention of apoptosis of Hep3B cells by interleukin-6. *Oncogene* 20:677–685, 2001

Kuo ML, Shen SC, Yang CH, Chuang SE, Cheng AL, Huang TS: Bcl-2 prevents topoisomerase II inhibitor GL331-induced apoptosis is mediated by down-regulation of poly (ADP-ribose) polymerase activity. *Oncogene* 17:2225–2234, 1998

Lear JT, Harvey I, de Berker D, Strange RC, Fryer AA: Basal cell carcinoma. [Review] *J R Soc Med* 91:585–588, 1998

Lotz M, Jirik F, Kabouridis P, *et al*: B cell stimulating factor 2/interleukin 6 is a costimulant for human thymocytes and T lymphocytes. *J Exp Med* 167:1253–1258, 1988

Lutticken C, Wegenka UM, Yuan J, *et al*: Association of transcription factor APRF and protein kinase Jak1 with the interleukin-6 signal transducer gp130. *Science* 263:89–92, 1994

Murakami M, Hibi M, Nakagawa N, *et al*: IL-6-induced homodimerization of gp130 and associated activation of a tyrosine kinase. *Science* 260:1808–1810, 1993

Nakajima K, Yamanaka Y, Nakae K, *et al*: A central role for Stat3 in IL-6-induced regulation of growth and differentiation in M1 leukemia cells. *EMBO J* 15:3651–3658, 1996

Namzaki M, Wittbuhn BA, Yoshida K, *et al*: Activation of JAK2 kinase mediated by the interleukin 6 signal transducer gp130. *Proc Natl Acad Sci USA* 91:2285–2289, 1994

Petit-Frere C, Clingen PH, Grewe M, *et al*: Induction of interleukin-6 production by ultraviolet radiation in normal human epidermal keratinocytes and in a human keratinocyte cell line is mediated by DNA damage. *J Invest Dermatol* 111: 354–359, 1998

Puthier D, Bataille R, Amiot M: IL-6 up-regulates mcl-1 in human myeloma cells through JAK/STAT rather than ras/MAP kinase pathway. *Eur J Immunol* 29: 3945–3950, 1999

Qiu Y, Robinson D, Pretlow TG, Kung HJ: Etk/Bmx, a tyrosine kinase with a pleckstrin-homology domain, is an effector of phosphatidylinositol 3′-kinase and is involved in interleukin 6-induced neuroendocrine differentiation of prostate cancer cells. *Proc Natl Acad Sci USA* 95:3644–3649, 1998

Rogers S, Wells R, Rechsteiner M: Amino acid sequences common to rapidly degraded proteins: the PEST hypothesis. *Science* 234:364–368, 1986

Scheid MP, Durnio V: Dissociation of cytokine-induced phosphorylation of Bad and activation of PKB/akt: involvement of MEK upstream of BAD phosphorylation. *Proc Nat'l Acad Sci USA* 95:7439–7444, 1998

Skorski T, Bellacosa A, Nieborowski-Skorska M, *et al*: Transformation of hematopoietic cells by BCR/ABL requires activation of a Pi-3k/AKT-dependent pathway. *Embo J* 16:6151–6161, 1997

Songyang Z, Baltimore D, Cantley LC, Kaplan DR, Franke TF: Interleukin 3-dependent survival by the Akt protein kinase. *Proc Natl Acad Sci USA* 94:11345–11350, 1997

Thabard W, Collette M, Mellerin MP, *et al*: IL-6 upregulates its own receptor on some human myeloma cell lines. *Cytokine* 14:252–256, 2001

Tosato G, Seamon KB, Goldman ND, *et al*: Monocyte-derived human B-cell growth factor identified as interferon-beta 2 (BSF-2, IL-6). *Science* 239: 502–504, 1988

Townsend KJ, Trusty JL, Traupman MA, Eastman A, Craig RW: Expression of the antiapoptotic MCL1 gene product is regulated by a Mitogen activated protein kinase-mediated pathway triggered through microtubule disruption and protein kinase C. *Oncogene* 17:1223–1234, 1998

Van Damme J, Opdenakker G, Simpson RJ, *et al*: Identification of the human 26-kD protein, interferon beta 2 (IFN-beta 2), as a B cell hybridoma/plasmacytoma growth factor induced by interleukin 1 and tumor necrosis factor. *J Exp Med* 165:914–919, 1987

Wang JM, Chao JR, Chen W, Kuo HL, Yen JJ, Yang-Hsin HF: The antiapoptotic gene MCL-1 is up-regulated by the phosphatidylinositol 3-kinase/Akt signaling pathway through a transcription factor complex containing CREB. *Mol Cell Biol* 19:6195–6206, 1999

Wei LH, Kuo ML, Chen CA, *et al*: The anti-apoptotic role of interleukin-6 in human cervical cancer is mediated by up-regulation of Mcl-1 through a PI 3-kinase/Akt pathway. *Oncogene* 20:5799–5809, 2001

Yang T, Buchan HL, Townsend KJ, Craig RW: MCL-1, a member of the BCL-2 family, is induced rapidly in response to signals for cell differentiation or death, but not to signals for cell proliferation. *J Cell Physiol* 166:523–536, 1996

Yen HT, Chiang LC, Wen KH, Tsai CC, Yu CL, Yu H: The expression of cytokines by an established basal cell carcinoma cell line (BCC-1/KMC) compared with cultured normal keratinocytes. *Arch Dermatol Res* 288:157–161, 1996

Yoshinaga Y, Higaki M, Terajima S, *et al*: Detection of inflammatory cytokines in psoriatic skin. *Arch Dermatol Res* 287:158–164, 1995

REVIEW

PTEN: New Insights into Its Regulation and Function in Skin Cancer

Mei Ming[1] and Yu-Ying He[1]

Skin cancer is the most common cancer in the United States. UV radiation in sunlight is the major environmental factor causing skin cancer development. PTEN (phosphatase and tensin homolog deleted on chromosome 10), a recently discovered tumor suppressor gene, is frequently mutated, deleted, or epigenetically silenced in various human cancers. PTEN negatively regulates the oncogenic phosphatidylinositol 3-kinase (PI3K)/protein kinase B (AKT) signaling pathways. PTEN is clearly a critical tumor suppressor for skin cancer in humans and in mice. This review summarizes the recent progress in the function of PTEN in the development of skin cancer, including basal-cell carcinoma, squamous-cell carcinoma, and melanoma. The regulation of PTEN by UV radiation is also discussed in association with skin carcinogenesis. Understanding the fundamental mechanisms that lead to the reduction of PTEN function in skin carcinogenesis and the essential association with UV radiation opens up new opportunities for molecular chemoprevention and therapy of skin cancer by targeting PTEN pathways.

Journal of Investigative Dermatology (2009) **129**, 2109–2112; doi:10.1038/jid.2009.79; published online 2 April 2009

INTRODUCTION

Skin cancer is the most common type of cancer in the United States. Each year more than one million new cases are diagnosed, accounting for more than 40% of all cancers diagnosed. Skin cancers include basal-cell carcinoma (BCC), squamous-cell carcinoma (SCC), known as non-melanoma skin cancer, and melanoma. BCCs and SCCs account for ~80 and 16% of all skin cancers, respectively, whereas malignant melanomas account for only 4% of all skin cancers (Bowden, 2004). BCCs and SCCs are both derived from the basal layer of the epidermis of the skin. BCCs are slow growing and rarely metastasize, whereas SCCs can be highly invasive and may metastasize (Bowden, 2004). In contrast, melanoma is derived from melanocytes and the mortality associated with melanoma is high. UV irradiation in sunlight (Ramos *et al.*, 2004; Erb *et al.*, 2008) is the major environmental factor causing skin cancer. The rising incidence rates of BCC, SCC, and melanoma are highly associated with increased exposure to UV radiation because of increased sun exposure caused by sunbed tanning for cosmetic purposes, increased outdoor activities, changes in clothing style, increased longevity, and/or ozone depletion (Rigel, 2008).

PTEN (phosphatase and tensin homolog deleted on chromosome 10) functions as a highly effective tumor suppressor in a wide variety of tumor tissues (Suzuki *et al.*, 2008) by negatively regulating the phosphatidylinositol 3-kinase (PI3K)/protein kinase B (AKT) pathway (Maehama and Dixon, 1998). Loss of PTEN function through deletion, mutation, and/or decreased expression, has been found both in human sporadic cancers (Steck *et al.*, 1997; Kohno *et al.*, 1998; Birck *et al.*, 2000; Harima *et al.*, 2001; Byun *et al.*, 2003) and in hereditary cancer syndromes (Liaw *et al.*, 1997; Marsh *et al.*, 1997; Harima *et al.*, 2001). This ubiquitous and evolutionarily conserved signaling cascade influences many functions, including cell growth, survival, proliferation, migration, and metabolism (Endersby and Baker, 2008). Although largely unknown, similar or distinct PTEN involvement may exist in skin carcinogenesis.

The review here is to provide a new perspective of PTEN regulation and function in skin carcinogenesis, its interaction with other critical signaling pathways involved in skin cancer, and its regulation by environmental UV radiation. Furthermore, the possibility of selectively targeting PTEN chemoprevention and therapy of skin cancer is also discussed.

PTEN IN SKIN CANCER

Functional studies supported the hypothesis that PTEN is a critical tumor suppressor in skin cancer. Loss of PTEN activity through mutation, deletion, or reduced expression has been shown to play an important role in skin tumor development. Germline mutations in PTEN, detected in patients with Cowden's disease and Bannayan–Riley–Ruvalcaba syndrome (Bonneau and Longy, 2000), lead to the loss of PTEN function, which increases the risk of tumorigenesis in skin as well as in other organs (Liaw *et al.*, 1997; Trojan *et al.*, 2001).

[1]Section of Dermatology, Department of Medicine, University of Chicago, Chicago, Illinois, USA

Correspondence: Dr Yu-Ying He, Section of Dermatology, Department of Medicine, University of Chicago, Chicago, Illinois 60637, USA. E-mail: yyhe@medicine.bsd.uchicago.edu

Abbreviations: AKT, protein kinase B; BCC, basal-cell carcinoma; PI3K, phosphoinositide 3-kinase; PTEN, phosphatase and tensin homolog deleted on chromosome 10; SCC, squamous-cell carcinoma; Shh, sonic Hedgehog

Received 2 October 2008; revised 3 February 2009; accepted 24 February 2009; published online 2 April 2009

PTEN in BCC

Loss of PTEN function may be critical for BCC formation through activating Sonic Hedgehog (Shh) signaling. BCC, at the molecular level, is characterized by aberrant activation of Shh signaling, usually because of mutations either in the *patched (Ptc)* or *smoothened (Smo)* genes (Reifenberger, 2007), or because of hyperactivation of this pathway. It is interesting that PTEN may be critical for Shh signaling. Recent studies have shown that PI3K/AKT activation is essential for Shh signaling by controlling PKA-mediated Gli inactivation (Riobo *et al.*, 2006). Although little is known regarding PTEN function in BCC, loss of PTEN function in BCC would upregulate the PI3K/AKT pathway to stimulate even low-level ligand-dependent or ligand-independent Shh signaling caused by mutations in Hedgehog pathway components. Although deletions of 10q23, where PTEN is located, were found to be an infrequent event in BCC (Quinn *et al.*, 1994), the inactivation of PTEN by other mechanisms may play an important role in BCC development.

PTEN in SCC

The critical role of genetic PTEN suppression in SCC has been shown in humans and in mice. The tumor suppressing function of PTEN in SCC has been shown in patients with Cowden's disease, *in vitro* in human keratinocytes, and *in vivo*, using a chemical skin carcinogenesis model. The association of cutaneous SCC with Cowden's disease has also been reported (Nuss *et al.*, 1978; Camisa *et al.*, 1984). The decreasing levels of PTEN expression are correlated with a malignant transformation of the skin induced by UVA (315–400 nm), as shown by the formation of SCC in nude mice (He *et al.*, 2006).

Mice with PTEN deletion and mutation are highly susceptible to tumor induction (Suzuki *et al.*, 1998). Conditional knockout of PTEN in skin leads to neoplasia in skin (Li *et al.*, 2002; Suzuki *et al.*, 2003; Backman *et al.*, 2004), thereby showing the pivotal role of PTEN in skin cancer development. PTEN deficiency in mice causes increases in cell proliferation, apoptotic resistance, stem-cell renewal/maintenance, centromeric instability, and DNA double-strand breaks (Groszer *et al.*, 2001; Kimura *et al.*, 2003; Wang *et al.*, 2006; He *et al.*, 2007; Shen *et al.*, 2007; Yanagi *et al.*, 2007), which can enhance susceptibility to carcinogens and the occurrence of secondary genetic or epigenetic alterations that can lead to skin cancer development.

Complex mechanisms may mediate the inactivation of PTEN. Somatic mutations, deletion, or promoter hypermethylation of PTEN have not been detected in SCCs of human skin (Quinn *et al.*, 1994; Kubo *et al.*, 1999; Murao *et al.*, 2006). Thus, the inactivation of PTEN by other mechanisms may be involved in SCC pathogenesis, including inactivation of the protein and/or epigenetic silencing, and the mechanism(s) by which its function and activity are regulated remain to be established.

Loss of PTEN function may occur as an early or late event, and PTEN loss has contributed to skin cancer development. Immunohistochemical studies have shown that, in mouse skin tumors, PTEN immunoreactivity was clearly confined to differentiating areas of the papillomas, and to the most differentiating areas in SCC samples, whereas PTEN staining is lost in non-differentiating infiltrative areas of SCCs, suggesting the expression and localization of PTEN in tumor sections that represent the different stages of mouse skin carcinogenesis (Segrelles *et al.*, 2002).

PTEN in melanoma

Loss of PTEN function has been implicated in the development of melanoma (Wu *et al.*, 2003). A high frequency of PTEN mutations has also been detected in malignant melanomas (Bonneau and Longy, 2000). On the basis of melanoma cell lines and mainly metastatic tumors, many studies also showed that PTEN played a significant role in sporadic cutaneous melanomas (Tsao *et al.*, 1998). PTEN inactivation was a late event likely related to melanoma progression rather than to initiation, and the translocation of PTEN expression from nuclear predominance to cytoplasmic predominance occurs from melanocyte to primary melanoma to metastasis melanoma. The potential genetic interaction among *NRAS*, *BRAF*, and *PTEN* may play a critical role in melanoma development (Tsao *et al.*, 2004).

Loss of PTEN function also increases AKT3 activation in melanoma. AKT3 protein, but not AKT1 or AKT2 protein, was found to be increased in melanoma cell lines when compared with normal melanocytes. Mechanisms of AKT3 deregulation occurred through a combination of overexpression of AKT3, accompanying copy number increases of the gene, and decreased PTEN protein function, occurring through loss or haploinsufficiency of the PTEN gene (Stahl *et al.*, 2004; Robertson, 2005).

PTEN REGULATION BY UV RADIATION

Recent studies show that UV radiation regulates PTEN function in skin cells. UV exposure causes gene alteration of PTEN (Hocker and Tsao, 2007). Inducing Egr-1 by exposing cells to acute UVC (100–280 nm) upregulates the expression of the PTEN messenger RNA and protein, and leads to apoptosis. Loss of Egr-1 expression, which often occurs in human cancers, could deregulate the PTEN gene and contribute to the radiation resistance of some cancer cells (Virolle *et al.*, 2001).

Our recent evidence shows that chronic UVA radiation decreased PTEN expression, and this decrease is required for enhanced cell survival in the transformed human keratinocytes, suggesting that PTEN might be critical for skin carcinogenesis induced by UVA (He *et al.*, 2006). PTEN increases sensitivity to cell death in response to several apoptotic stimuli, including UV irradiation and treatment with tumor necrosis factor α, by negatively regulating the PI3K/AKT pathway (Stambolic *et al.*, 1998), implying that PTEN alterations might be involved in UV-induced skin cancer. UVB (280–315 nm) was also reported to inhibit PTEN by increasing PTEN phosphorylation in human dermal fibroblasts, as phosphorylation of PTEN downregulates its lipid phosphatase and protein stability (Oh *et al.*, 2006). Thus

UV-mediated inhibition of PTEN function may further enhance AKT activation induced by UV radiation.

It is likely that multiple complex interactions at the transcriptional, post-transcriptional, and/or post-translational levels are involved. Systematic characterization of PTEN regulation by UV radiation will not only advance our knowledge of the fundamental mechanisms of PTEN involvement in skin cancer, but also facilitate the development of feasible approaches to prevent PTEN suppression because of chronic UV exposure.

Furthermore, UV-induced production of reactive oxygen species and the resultant oxidative stress exposure plays an important role in photocarcinogenesis caused by UV, and reactive oxygen species are believed to be involved in many inflammatory skin disorders, skin cancer formation, phototoxicity, and skin aging. PTEN activity can be inhibited by reactive oxygen species (Gimm *et al.*, 2000), implying that reduced PTEN activity by UV-induced reactive oxygen species formation might be involved in UV-induced skin tumorigenesis.

CONCLUSIONS AND FUTURE DIRECTIONS

PTEN plays a critical role in skin homeostasis and is a critical tumor suppressor in the prevention of skin carcinogenesis, as shown in humans and in mice. This has positioned PTEN in a central role of tumor suppression by antagonizing PI3K/AKT pathways in skin carcinogenesis. Proper function of PTEN is essential for maintaining the balance in cell proliferation and survival in epidermal cells, including keratinocytes and melanocytes in skin, to prevent transformation.

In addition, UV radiation, the major risk factor causing skin cancer, suppresses PTEN expression, indicating that PTEN may be the critical target for UV-induced skin tumorigenesis. As skin cancer is the most common malignancy in the United States, elucidating the mechanisms of PTEN function, and its regulation and function in the pathogenesis of BCC, SCC, and melanoma will have a broad impact in improving patients' quality of life and reduce the high morbidity associated with these cancers. Targeted PTEN, directly or by interfering with upstream proteins regulating PTEN activity, presents a new and more effective preventive and therapeutic approach in reducing skin cancer burden, as suggested in other cancers. Recently, the protective nature of phytoestrogens has been shown to be partially mediated by increasing PTEN expression, indicating that PTEN may be one of the critical molecular targets for skin cancer prevention and treatment.

CONFLICT OF INTEREST

The authors state no conflict of interest.

ACKNOWLEDGMENTS

We apologize to those investigators whose work could not be directly referenced owing to space limitations. Work in the authors' laboratory was supported by the Department of Medicine and the Section of Dermatology at the University of Chicago, the American Skin Association, and the University of Chicago Cancer Research Center (P30 CA014599). The authors are grateful for Dr Ann Motten for her critical reading of this manuscript.

REFERENCES

Backman SA, Ghazarian D, So K, Sanchez O, Wagner KU, Hennighausen L *et al.* (2004) Early onset of neoplasia in the prostate and skin of mice with tissue-specific deletion of Pten. *Proc Natl Acad Sci USA* 101:1725–30

Birck A, Ahrenkiel V, Zeuthen J, Hou-Jensen K, Guldberg P (2000) Mutation and allelic loss of the PTEN/MMAC1 gene in primary and metastatic melanoma biopsies. *J Invest Dermatol* 114:277–80

Bonneau D, Longy M (2000) Mutations of the human PTEN gene. *Hum Mutat* 16:109–22

Bowden GT (2004) Prevention of non-melanoma skin cancer by targeting ultraviolet-B-light signalling. *Nat Rev Cancer* 4:23–35

Byun DS, Cho K, Ryu BK, Lee MG, Park JI, Chae KS *et al.* (2003) Frequent monoallelic deletion of PTEN and its reciprocal associatioin with PIK3CA amplification in gastric carcinoma. *Int J Cancer* 104:318–27

Camisa C, Bikowski JB, McDonald SC (1984) Cowden's disease. Association with squamous cell carcinoma of the tongue and perianal basal cell carcinoma. *Arch Dermatol* 120:677–8

Endersby R, Baker SJ (2008) PTEN signaling in brain: neuropathology and tumorigenesis. *Oncogene* 27:5416–30

Erb P, Ji J, Kump E, Mielgo A, Wernli M (2008) Apoptosis and pathogenesis of melanoma and nonmelanoma skin cancer. *Adv Exp Med Biol* 624:283–95

Gimm O, Perren A, Weng LP, Marsh DJ, Yeh JJ, Ziebold U *et al.* (2000) Differential nuclear and cytoplasmic expression of PTEN in normal thyroid tissue, and benign and malignant epithelial thyroid tumors. *Am J Pathol* 156:1693–700

Groszer M, Erickson R, Scripture-Adams DD, Lesche R, Trumpp A, Zack JA *et al.* (2001) Negative regulation of neural stem/progenitor cell proliferation by the Pten tumor suppressor gene *in vivo*. *Science* 294:2186–9

Harima Y, Sawada S, Nagata K, Sougawa M, Ostapenko V, Ohnishi T (2001) Mutation of the PTEN gene in advanced cervical cancer correlated with tumor progression and poor outcome after radiotherapy. *Int J Oncol* 18:493–7

He XC, Yin T, Grindley JC, Tian Q, Sato T, Tao WA *et al.* (2007) PTEN-deficient intestinal stem cells initiate intestinal polyposis. *Nat Genet* 39:189–98

He YY, Pi J, Huang JL, Diwan BA, Waalkes MP, Chignell CF (2006) Chronic UVA irradiation of human HaCaT keratinocytes induces malignant transformation associated with acquired apoptotic resistance. *Oncogene* 25:3680–8

Hocker T, Tsao H (2007) Ultraviolet radiation and melanoma: a systematic review and analysis of reported sequence variants. *Hum Mutat* 28:578–88

Kimura T, Suzuki A, Fujita Y, Yomogida K, Lomeli H, Asada N *et al.* (2003) Conditional loss of PTEN leads to testicular teratoma and enhances embryonic germ cell production. *Development* 130:1691–700

Kohno T, Takahashi M, Manda R, Yokota J (1998) Inactivation of the PTEN/MMAC1/TEP1 gene in human lung cancers. *Genes Chromosomes Cancer* 22:152–6

Kubo Y, Urano Y, Hida Y, Arase S (1999) Lack of somatic mutation in the PTEN gene in squamous cell carcinomas of human skin. *J Dermatol Sci* 19:199–201

Li G, Robinson GW, Lesche R, Martinez-Diaz H, Jiang Z, Rozengurt N *et al.* (2002) Conditional loss of PTEN leads to precocious development and neoplasia in the mammary gland. *Development* 129:4159–70

Liaw D, Marsh DJ, Li J, Dahia PL, Wang SI, Zheng Z *et al.* (1997) Germline mutations of the PTEN gene in Cowden disease, an inherited breast and thyroid cancer syndrome. *Nat Genet* 16:64–7

Maehama T, Dixon JE (1998) The tumor suppressor, PTEN/MMAC1, dephosphorylates the lipid second messenger, phosphatidylinositol 3,4,5-trisphosphate. *J Biol Chem* 273:13375–8

Marsh DJ, Dahia PL, Zheng Z, Liaw D, Parsons R, Gorlin RJ *et al.* (1997) Germline mutations in PTEN are present in Bannayan-Zonana syndrome. *Nat Genet* 16:333–4

Murao K, Kubo Y, Ohtani N, Hara E, Arase S (2006) Epigenetic abnormalities in cutaneous squamous cell carcinomas: frequent inactivation of the RB1/p16 and p53 pathways. *Br J Dermatol* 155:999–1005

Nuss DD, Aeling JL, Clemons DE, Weber WN (1978) Multiple hamartoma syndrome (Cowden's disease). *Arch Dermatol* 114:743–6

Oh JH, Kim A, Park JM, Kim SH, Chung AS (2006) Ultraviolet B-induced matrix metalloproteinase-1 and -3 secretions are mediated via PTEN/Akt pathway in human dermal fibroblasts. *J Cell Physiol* 209:775–85

Quinn AG, Sikkink S, Rees JL (1994) Basal cell carcinomas and squamous cell carcinomas of human skin show distinct patterns of chromosome loss. *Cancer Res* 54:4756–9

Ramos J, Villa J, Ruiz A, Armstrong R, Matta J (2004) UV dose determines key characteristics of nonmelanoma skin cancer. *Cancer Epidemiol Biomarkers Prev* 13:2006–11

Reifenberger J (2007) [Basal cell carcinoma. Molecular genetics and unusual clinical features]. *Hautarzt* 58:406–11

Rigel DS (2008) Cutaneous ultraviolet exposure and its relationship to the development of skin cancer. *J Am Acad Dermatol* 58:S129–32

Riobo NA, Lu K, Ai X, Haines GM, Emerson CP Jr (2006) Phosphoinositide 3-kinase and Akt are essential for Sonic Hedgehog signaling. *Proc Natl Acad Sci USA* 103:4505–10

Robertson GP (2005) Functional and therapeutic significance of Akt deregulation in malignant melanoma. *Cancer Metastasis Rev* 24:273–85

Segrelles C, Ruiz S, Perez P, Murga C, Santos M, Budunova IV *et al.* (2002) Functional roles of Akt signaling in mouse skin tumorigenesis. *Oncogene* 21:53–64

Shen WH, Balajee AS, Wang J, Wu H, Eng C, Pandolfi PP *et al.* (2007) Essential role for nuclear PTEN in maintaining chromosomal integrity. *Cell* 128:157–70

Stahl JM, Sharma A, Cheung M, Zimmerman M, Cheng JQ, Bosenberg MW *et al.* (2004) Deregulated Akt3 activity promotes development of malignant melanoma. *Cancer Res* 64:7002–10

Stambolic V, Suzuki A, de la Pompa JL, Brothers GM, Mirtsos C, Sasaki T *et al.* (1998) Negative regulation of PKB/Akt-dependent cell survival by the tumor suppressor PTEN. *Cell* 95:29–39

Steck PA, Pershouse MA, Jasser SA, Yung WK, Lin H, Ligon AH *et al.* (1997) Identification of a candidate tumour suppressor gene, MMAC1, at chromosome 10q23.3 that is mutated in multiple advanced cancers. *Nat Genet* 15:356–62

Suzuki A, de la Pompa JL, Stambolic V, Elia AJ, Sasaki T, del Barco Barrantes I *et al.* (1998) High cancer susceptibility and embryonic lethality associated with mutation of the PTEN tumor suppressor gene in mice. *Curr Biol* 8:1169–78

Suzuki A, Itami S, Ohishi M, Hamada K, Inoue T, Komazawa N *et al.* (2003) Keratinocyte-specific Pten deficiency results in epidermal hyperplasia, accelerated hair follicle morphogenesis and tumor formation. *Cancer Res* 63:674–81

Suzuki A, Nakano T, Mak TW, Sasaki T (2008) Portrait of PTEN: messages from mutant mice. *Cancer Sci* 99:209–13

Trojan J, Plotz G, Brieger A, Raedle J, Meltzer SJ, Wolter M *et al.* (2001) Activation of a cryptic splice site of PTEN and loss of heterozygosity in benign skin lesions in Cowden disease. *J Invest Dermatol* 117:1650–3

Tsao H, Goel V, Wu H, Yang G, Haluska FG (2004) Genetic interaction between NRAS and BRAF mutations and PTEN/MMAC1 inactivation in melanoma. *J Invest Dermatol* 122:337–41

Tsao H, Zhang X, Benoit E, Haluska FG (1998) Identification of PTEN/MMAC1 alterations in uncultured melanomas and melanoma cell lines. *Oncogene* 16:3397–402

Virolle T, Adamson ED, Baron V, Birle D, Mercola D, Mustelin T *et al.* (2001) The Egr-1 transcription factor directly activates PTEN during irradiation-induced signalling. *Nat Cell Biol* 3:1124–8

Wang S, Garcia AJ, Wu M, Lawson DA, Witte ON, Wu H (2006) Pten deletion leads to the expansion of a prostatic stem/progenitor cell subpopulation and tumor initiation. *Proc Natl Acad Sci USA* 103:1480–5

Wu H, Goel V, Haluska FG (2003) PTEN signaling pathways in melanoma. *Oncogene* 22:3113–22

Yanagi S, Kishimoto H, Kawahara K, Sasaki T, Sasaki M, Nishio M *et al.* (2007) Pten controls lung morphogenesis, bronchioalveolar stem cells, and onset of lung adenocarcinomas in mice. *J Clin Invest* 117:2929–40

Neurofibromatosis 2 (NF2) tumor suppressor merlin inhibits phosphatidylinositol 3-kinase through binding to PIKE-L

Rong Rong*, Xiaoling Tang*, David H. Gutmann†, and Keqiang Ye*‡

*Department of Pathology and Laboratory Medicine, Emory University School of Medicine, 615 Michael Street, Atlanta, GA 30322; and †Department of Neurology, Washington University School of Medicine, 660 South Euclid Avenue, Box 8111, St. Louis, MO 63110

Edited by Solomon H. Snyder, Johns Hopkins University School of Medicine, Baltimore, MD, and approved November 12, 2004 (received for review August 13, 2004)

Neurofibromatosis 2 (NF2) is a tumor suppressor, although the molecular mechanism accounting for this effect remains unknown. Here, we show that merlin exerts its activity by inhibiting phosphatidylinositol 3-kinase (PI3-kinase), through binding to PIKE-L. Wild-type merlin, but not patient-derived mutant (L64P), binds PIKE-L and inhibits PI3-kinase activity. This suppression of PI3-kinase activity results from merlin disrupting the binding of PIKE-L to PI3-kinase. In addition, merlin suppression of PI3-kinase activity as well as schwannoma cell growth is abrogated by a single PIKE-L point mutation (P187L) that cannot bind merlin but can still activate PI3-kinase. Knocking down PIKE-L with RNA interference abolishes merlin's tumor-suppressive activity. Our data support the hypothesis that PIKE-L is an important mediator of merlin growth suppression.

Neurofibromatosis 2 (NF2) is a dominantly inherited disorder characterized by bilateral occurrence of vestibular schwannomas and other brain tumors, including meningiomas and ependymomas (1). The *NF2* tumor suppressor gene encodes an intracellular membrane-associated protein, called merlin or schwannomin, which belongs to the band 4.1 family of cytoskeleton-associated proteins (2, 3). Inactivation of the *NF2* gene and consequent lack of gene expression are the primary cause of this disease, although the molecular mechanism accounting for the tumor-suppressive activity remains unknown (4).

Merlin, like other ERM (ezrin/radix/moesin) proteins, is highly enriched in microvilli and filopodia as well as the ruffling edges of motile cells (5, 6). Overexpression of merlin results in dramatic changes in the actin cytoskeleton and impairs cell attachment and motility (7). Moreover, it can effectively suppress the growth of rat schwannoma cells, both *in vitro* and *in vivo* (4, 8). Knocking down merlin leads to alterations in actin cytoskeleton-mediated events and increases cell proliferation (9). merlin exists in "open" (inactive) and "closed" (growth-suppressive) conformations dictated by the ability of merlin to form an intramolecular association between the N and C termini of the protein (10–13). The full-length merlin I containing exon 17 exists in a closed conformation, whereas merlin II with exon 16 or disease-oriented mutants display open conformation. merlin cycles between open and closed conformations *in vivo* that differentially determine whether it forms heterooligomers with ERM proteins or other binding targets to transduce its growth-regulatory signal (14). Numerous merlin-binding partners have been identified, but none of these molecules provides substantial clues as to the tumor-suppressive activity of merlin.

PIKE [phosphatidylinositol 3-kinase (PI3-kinase) enhancer] is a brain-specific GTPase that binds to PI3-kinase and stimulates its lipid kinase activity (15). It exists in three isoforms, PIKE-S (short form), PIKE-L (long form), and PIKE-A, as the result of alternative splicing (PIKE-L and -S) or a differential transcription initiation site (PIKE-A). PIKE-S originally was identified in a yeast two-hybrid screen searching for binding partners of protein 4.1N, a neuronal member of the band 4.1 superfamily. Nerve growth factor treatment leads to PIKE-S activation by triggering the nuclear translocation of phospholipase C γ1, which acts as a physiological guanine-nucleotide-exchange factor for PIKE through its SH3 domain (16). Nerve growth factor treatment also elicits translocation of membrane-associated 4.1N to the nucleus, where it binds to PIKE-S. We showed previously that the PIKE-S/PI3-kinase signaling pathway is negatively regulated by protein 4.1N (15). PIKE-L occurs in both the cytoplasm and the nucleus. Recently, we showed that it forms a complex with Homer 1 and couples PI3-kinase to the metabotropic glutamate receptor, preventing neuronal apoptosis (17).

Here, we report that merlin specifically binds to PIKE-L and abolishes its stimulatory effect on PI3-kinase by blocking the association between PIKE-L and PI3-kinase. Patient-derived mutant L64P merlin does not interact with PIKE-L and has no effect on PI3-kinase activity. Moreover, P187L mutation on PIKE-L disrupts its interaction with merlin, leading to its failure to inhibit PI3-kinase.

Materials and Methods

Plasmids and Reagents. GST-tagged merlin, merlin N-terminal domain (NTD; residues 1–332), and merlin C-terminal domain (residues 342–595) in pGex vector were kindly provided by Vijaya Ramesh (Massachusetts General Hospital, Harvard Medical School, Boston). Mouse monoclonal anti-hemagglutinin (HA)-horseradish peroxidase, anti-Myc-horseradish peroxidase, anti-Flag, and anti-GST antibodies were from Sigma. Mouse monoclonal anti-Ser-473, anti-Thr-308, and anti-Akt antibodies were from Cell Signaling Technology (Beverly, MA). Rabbit polyclonal anti-NF2, anti-p85, and anti-p110 antibodies were from Santa Cruz Biotechnology. Protein A/G-conjugated agarose beads were from Calbiochem. Glutathione sepharose 4B was supplied by Amersham Pharmacia. Adenovirus expressing short hairpin (sh)-PIKE RNA was supplied by Welgene (Worcester, MA). All chemicals not listed above were purchased from Sigma.

Coimmunoprecipitation and *in Vitro* Binding and PI3-Kinase Assays. The experimental procedures for coimmunoprecipitation and *in vitro* binding and *in vitro* PI3-kinase assays are described in ref. 18.

Immunofluorescent Staining of Schwannoma Cells. Induced and uninduced cells were fixed with cold (−20°C) methanol for 5 min and then rehydrated by PBS for 1 min. Nonspecific sites were blocked by incubating with 200 μl of 1% BSA in PBS at 37°C for 15 min. PIKE-L was stained with mouse anti-PIKE antibody (1:300 dilution in PBS containing 1% BSA) and incubated (200

This paper was submitted directly (Track II) to the PNAS office.

Freely available online through the PNAS open access option.

Abbreviations: ERM, ezrin/radix/moesin; HA, hemagglutinin; HRS, hepatocyte growth factor-regulated tyrosine kinase substrate; MTT, 3-(4,5-dimethylthiazol-2-yl)-2,5-diphenyl tetrazolium bromide; NF2, neurofibromatosis 2; NTD, N-terminal domain; PI3-kinase, phosphatidylinositol 3-kinase.

‡To whom correspondence should be addressed. E-mail: kye@emory.edu.

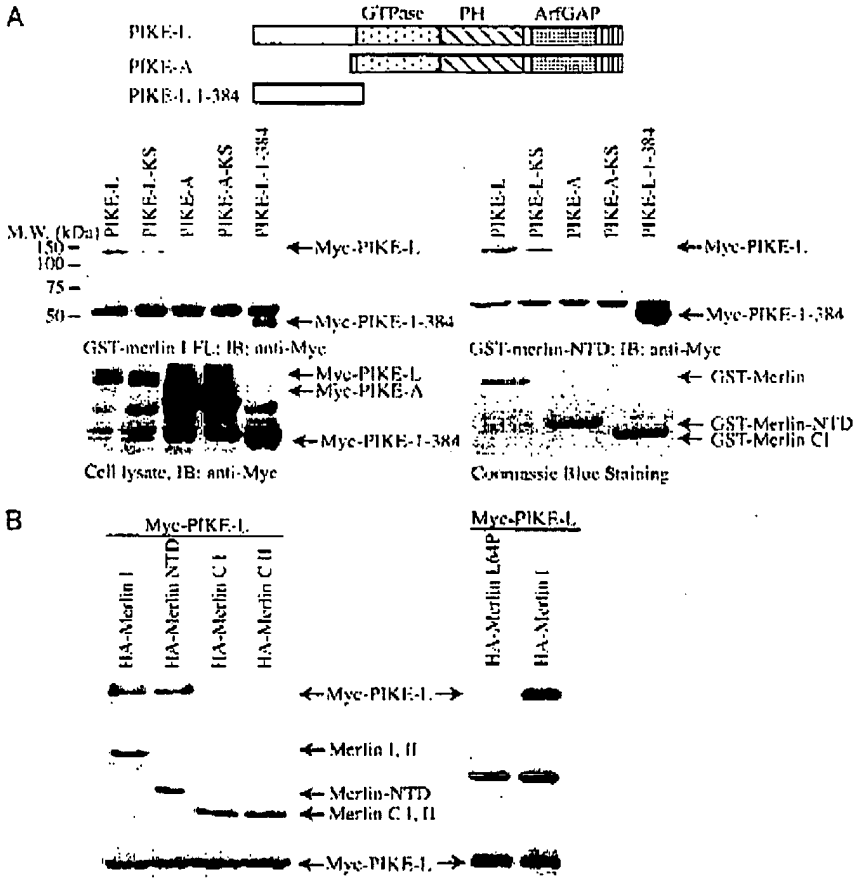

Fig. 1. PIKE-L interacts with merlin. (*A*) The FERM domain of merlin binds to the N terminus of PIKE-L *in vitro*. (*Top*) Illustration of the PIKE constructs used. GST-merlin and GST-FERM domain of merlin bind to PIKE-L but not PIKE-A. (*Middle*) Purified GST-merlin and GST-merlin-NTD were incubated with HEK293 cell lysates transfected with various myc-tagged PIKE constructs. After 3-h incubation at 4°C, the associated proteins were analyzed by Western blotting with anti-myc antibody. PIKE-L and PIKE-L N terminus (amino acid residues1–384) robustly binds to both merlin and merlin-NTD. The dominant-negative PIKE-L-KS displayed reduced binding activity to merlin. (*Left Bottom*) Protein expression of transfected constructs was confirmed by myc immunoblotting. (*Right Bottom*) Levels of GST-merlin recombinant proteins were verified by Coomassie blue staining. (*B*) PIKE-L interacts with merlin *in vivo*. Various HA-merlin constructs and myc-PIKE-L were cotransfected into HEK293 cells. PIKE-L was immunoprecipitated with anti-myc antibody, and bound proteins were visualized by Western blot with anti-HA antibody. Both full-length merlin and merlin NTD interacted with PIKE-L (*Left Top*, lanes 1 and 2). Patient-derived L64P mutant did not bind to PIKE-L (*Right Top*). Similar levels of all HA-merlin and myc-PIKE constructs were expressed in all experiments (*Middle* and *Bottom*).

μl), and merlin was stained with rabbit polyclonal anti-NF2 antibody (1:250 dilution). The secondary antibodies are Texas red-labeled goat anti-rabbit and FITC-conjugated goat anti-mouse antibodies, respectively. The staining was performed as described in ref. 19.

Subcellular Fractionation from Schwannoma Cells. For membrane extracts, cells were lysed by mechanical disruption in cold hypotonic buffer (10 mM Hepes, pH 7.4/1 mM EDTA/protease inhibitors). The nuclei were pelleted by centrifugation at 750 × *g* for 10 min. Further centrifugation of the resulting supernatant at $1 \times 10^5 \times g$ for 1 h led to recovery of the cytosolic fraction (C). The pellet was extracted with a membrane extraction buffer (50 mM Tris, pH 7.4/1% Triton X-100/150 mM NaCl/1 mM EDTA/1 mM Na_3VO_4/protease inhibitors) and centrifuged at $1 \times 10^5 \times g$ for 1 h. This supernatant corresponded to the Triton X-100 soluble membrane extract (S). The final pellet was extracted with modified RIPA buffer (pH 7.5) and centrifuged at $1 \times 10^5 \times g$ for 5 min; this supernatant corresponded to the Triton X-100 insoluble fraction (I).

Infection of Schwannoma Cells with Adenovirus. Adenovirus-expressing WT dominant-negative (K413AS414N) or P187L point mutant PIKE-L was prepared as described in ref. 20. The virus was purified by CsCl banding with 10^{11} to 10^{12} plaque-forming units, introduced into doxycycline-induced or uninduced schwannoma cells, and cultured overnight. The GFP was monitored with an immunofluorescence microscope.

Assay with 3-(4,5-Dimethylthiazol-2-yl)-2,5-Diphenyl Tetrazolium Bromide (MTT). The same number of rat RT4-D6P2T schwannoma cells were induced with doxycycline for 1 day and infected with adenovirus expressing WT PIKE-L, dominant-negative PIKE-L-KS, or PIKE-L-P187L. Cells were incubated 48 h after infection with 0.5 mg of MTT per ml of fresh medium at 37°C for 1 h. The formazan products were dissolved in DMSO and quantified by measurement of the absorbance at 562 nm, which represents the number of proliferating cells.

Statistical Analysis. The results were expressed as means ± SEM calculated from the specified numbers of determination. Student's *t* test was used to compare individual data with control value.

Results

merlin Binds to PIKE-L. The homology between protein 4.1N and merlin suggests that merlin might have similar inhibitory effects on PI3-kinase activity. To explore this possibility, we conducted affinity chromatography interaction experiments to investigate the association between PIKE and full-length merlin and detected a robust interaction with PIKE-L. This interaction maps to the N terminus of PIKE-L (amino acid residues 1–384), consistent with the failure of the PIKE-A isoform, which lacks the N terminus of PIKE-L (21), to bind merlin *in vitro* (Fig. 1*A Left Lower*). Protein 4.1N binding to PIKE-L involves residues in the C terminus of protein 4.1N; thus, we examined the ability of the merlin NTD and C-terminal domain fragments to bind PIKE-L. We showed that merlin binding to PIKE-L requires residues in the FERM-containing NTD *in vitro* (Fig. 1*A Right Lower*). In contrast, we observed no binding with the C-terminal domain of merlin (Fig. 1*B*). We have demonstrated previously that the association between PIKE-S and PI3-kinase is GTP-dependent and can be abolished by mutations of K413 and S414 in the PIKE-L GTPase domain. The

NEUROSCIENCE

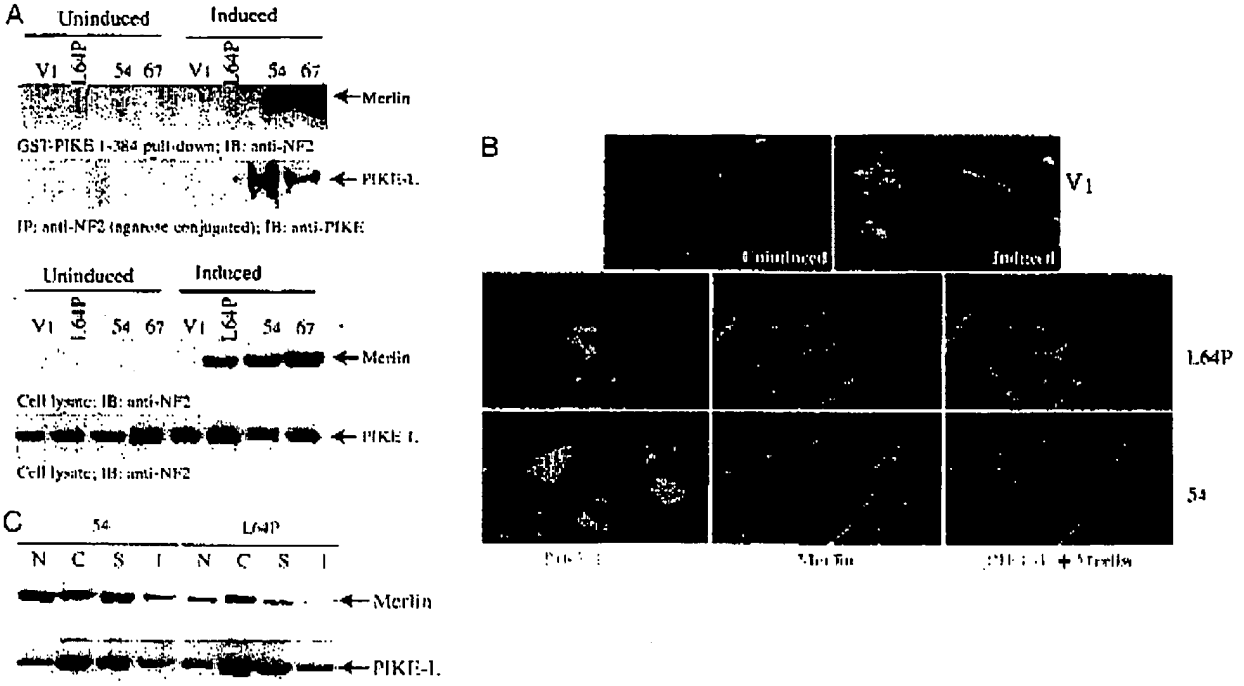

Fig. 2. PIKE-L interacts with WT merlin in schwannoma cells. (*A*) Rat RT4-D6P2T schwannoma cells stably transfected with empty vector (V_1), merlin mutant L64P, or WT merlin (5_4 and 6_7, two clones) were either uninduced or induced with doxycycline for 1 day. One milligram of cell lysate was incubated with purified GST-PIKE-L-1–384. After 3-h incubation at 4°C, the associated proteins were analyzed by Western blotting with anti-NF2. (*Top Upper*) WT merlin, but not merlin mutant L64P, selectively binds to the N terminus of PIKE-L. (*Top Lower*) Coimmunoprecipitation with anti-NF2 reveals that PIKE-L specifically associates with WT merlin but not L64P mutant. (*Bottom*) The induced merlin was verified with anti-NF2 antibody. (*B*) PIKE-L colocalizes with WT merlin in schwannoma cells. Uninduced and induced schwannoma cells were stained with mouse anti-PIKE antibody and rabbit polyclonal anti-merlin antibody. (*Top*) PIKE-L resides in both the cytoplasm and the nucleus. (*Middle* and *Bottom*) Merlin L64P exclusively distributes in the cytoplasm, whereas WT merlin occurs in both compartments, colocalizing with PIKE-L in 5_4 cell line. (*C*) Subcellular fractionation of 5_4 and L64P cells. The cytosolic (C), membrane soluble (S), membrane insoluble (I), and nuclear (N) fractions were prepared. Immunoblotting analysis was performed with anti-PIKE and anti-merlin antibodies. (*Upper*) Both WT and mutant merlin display similar distribution patterns in C, S, and I fractions; by contrast, a very faint amount of L64P was observed in the nucleus compared to counterpart in the WT cells. (*Lower*) PIKE-L reveals identical subcellular distribution.

dominant inhibitory PIKE-L-KS mutant (K413AS414N) has been shown to prevent PIKE-L activation of PI3-kinase by binding to, but not activating, PI3-kinase (15, 17). We showed that the PIKE-L-KS mutant exhibits moderately reduced binding to merlin, suggesting that PIKE-L GTPase activity might be important in regulating the association between PIKE-L and merlin (Fig. 1*A Left Lower*).

To demonstrate the interaction between merlin and PIKE-L *in vivo*, we performed coimmunoprecipitation binding assays in HEK293 cells. In these experiments, both full-length merlin and the merlin NTD strongly bound to PIKE-L. In addition, merlin containing the patient-derived missense mutation (L64P) within the NTD, previously shown to lack growth-suppressor properties (8, 12), did not bind to PIKE-L (Fig. 1*B Right*).

To determine whether the interaction between merlin and PIKE-L occurs in schwannoma cells, we used the RT4-D6P2T rat schwannoma cell line with inducible expression of either WT or L64P mutant merlin. Incubation of RT4 cell lysates with GST-PIKE-1–384 confirmed this interaction with WT, but not L64P mutant, merlin (Fig. 2*A*). We observed identical results by coimmunoprecipitation with agarose-conjugated anti-NF2 antibody *in vivo* (Fig. 2*A*). The induction of merlin in L64P, 5_4, and 6_7 cells was verified (Fig. 2*A*). An equal amount of PIKE-L was confirmed in both induced and uninduced cells (Fig. 2*A*).

To investigate whether PIKE-L and merlin colocalize in intact cells, we conducted immunofluorescent staining with schwannoma cells. Before merlin induction, PIKE-L occurs in both the cytoplasm and the nucleus in V_1 control cells (Fig. 2*B Top*). Similar subcellular distribution occurs in L64P, 5_4, and 6_7 cells (data not shown). The induced merlin L64P exclusively resides in the cytoplasm, whereas demonstrable PIKE-L locates in the nucleus (Fig. 2*B Middle*). By contrast, WT merlin (5_4 cell line) colocalizes with PIKE-L in the whole cell (Fig. 2*B Bottom*). To further evaluate these two proteins' colocalization, we performed subcellular fractionation with induced L64P and 5_4 cell lines. Both WT merlin and L64P display similar distribution in cytosolic (C), membrane soluble (S), and insoluble (I) fractions. However, compared with robust nuclear distribution of WT merlin in 5_4 cells, a faint amount of mutant merlin disperses in the nuclear fraction of L64P cells (Fig. 2*C Upper*), fitting with immunohistochemistry staining results. The modest level of L64P in the nuclear fraction might be due to unbroken cells. By contrast, the same distribution pattern of PIKE-L was detected in both cells (Fig. 2*C Lower*). Collectively, these results demonstrate that merlin and PIKE-L interact *in vitro* and *in vivo* and that this association requires residues in the N terminus of PIKE-L and the FERM (NTD) of merlin.

Pro-187 → Leu Mutation in PIKE-L Disrupts Its Interaction with merlin. To identify the region of PIKE-L required for merlin binding, we examined the binding of various truncations of PIKE-L to merlin *in vitro*, by using equal amounts of GST-PIKE truncation constructs and merlin (Fig. 5*A*, which is published as supporting information on the PNAS web site). *In vitro* binding assay revealed that amino acid residues 180–225 of PIKE-L appear to mediate binding to merlin (Fig. 5*B Lower*). The expression of purified recombinant

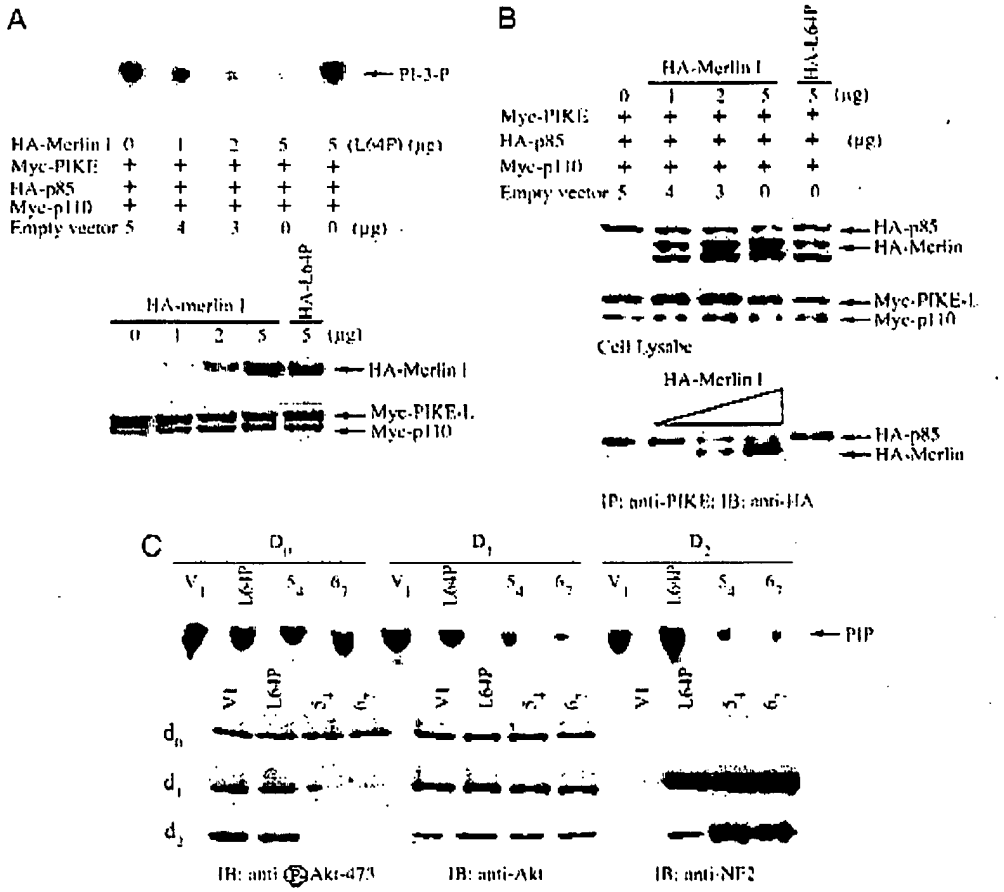

Fig. 3. merlin blocks the stimulatory effect of PIKE-L on PI3-kinase. (*A*) TLC was used to assay PI3-kinase activity. HEK293 cells were transfected with the indicated expression constructs. PI3-kinase was immunoprecipitated by anti-p110 antibody and assayed for *In vitro* lipid kinase activity. (*Top*) Increasing amount of merlin progressively diminished PI3-kinase activity, but L64P failed to do so. (*Middle*) Gradually increasing levels of HA-merlin was expressed in transfected cells. (*Bottom*) Equal amount of Myc-p110 and Myc-PIKE-L was confirmed by anti-myc immunoblotting. (*B*) merlin competes with PI3-kinase for binding to PIKE-L. (*Bottom*) Myc-PIKE-L was immunoprecipitated by anti-PIKE antibody, and the coprecipitated HA-p85 and HA-merlin were visualized by Western blot with anti-HA antibody. (*Middle*) Equal amounts of Myc-p110 and PIKE-L were confirmed with anti-Myc antibody. (*Top*) Increased expression of merlin was confirmed. (*C*) Merlin mediates PI3-kinase in schwannoma cells. TLC was used to assay PI3-kinase activity. Rat RT4-D6P2T schwannoma cells stably transfected with empty vector, merlin mutant L64P, or WT merlin (5_4 or 6_7) were uninduced or induced with doxycycline for 0, 1, or 2 days. (First blot from top) PI3-kinase activity is abolished by induced WT merlin, but not merlin mutant L64P. Akt and its phosphorylation in the lysate of schwannoma cells were analyzed. (*Left*, lower three blots) WT, but not patient-derived L64P, merlin blocks Akt phosphorylation. (*Center* and *Right*, lower three blots) The expression of Akt and induced merlin was verified.

GST proteins was verified (Fig. 5*B Upper*). Previously, we demonstrated that PIKE-L binds to Homer, an adaptor protein known to link metabotropic glutamate receptors to multiple intracellular targets including the inositol-1,4,5-trisphosphate receptor. Binding of Homer to PIKE-L mapped to a similar region in PIKE-L, and the PIKE-L P187L mutation disrupted the interaction between PIKE-L and Homer 1c (17). In this study, we found that this same amino acid substitution also abolished the binding of full-length PIKE-L to merlin (Fig. 5*C*, lane 2). Therefore, P187L mutation in PIKE-L abrogates its interactions with merlin.

merlin Competes with PI3-Kinase for Binding to PIKE-L. Studies in our laboratory have shown that overexpression of protein 4.1N abolishes the ability of PIKE-S to stimulate PI3-kinase (15). To determine whether merlin similarly could inhibit PIKE activation of PI3-kinase, we cotransfected increasing amounts of merlin with PIKE-L and PI3-kinase into HEK293 cells. Cotransfected merlin significantly reduced PIKE-L-induced activation of PI3-kinase activity in a dose-dependent manner; by contrast, merlin L64P failed to inhibit PI3-kinase activity at the same concentration (Fig. 3*A*). To evaluate whether merlin competes with PI3-kinase for binding to PIKE-L, we transfected increasing amounts of merlin along with p110, p85, and PIKE-L into HEK293 cells (Fig. 5*B*). Binding of p85 to PIKE-L was dramatically reduced in proportion to the level of merlin expression. However, merlin (L64P) was unable to block PI3-kinase for binding to PIKE-L (Fig. 3*B*), suggesting that merlin competes with PI3-kinase for binding to PIKE-L, thus inhibiting PIKE-L activation of PI-3 kinase. In this model, if merlin impairs PI3-kinase binding to PIKE-L, merlin expression should result in reduced PI3-kinase activity *in vivo*. As predicted, we observed markedly reduced PI3-kinase activity in RT4-D6P2T rat schwannoma cells upon induction of WT merlin expression. High levels of PI3-kinase activity were observed in all cells before merlin induction. After induction of WT merlin expression, PI3-kinase activity was diminished substantially in both the WT merlin-inducible 5_4 and 6_7 cell lines. In contrast, PI3-kinase activity was not altered in RT4 cells induced to express mutant L64P merlin (Fig. 3*C*), consistent with the failure of this mutant to bind to PIKE-L. The inhibition of PI3-kinase activity in these cells is further demonstrated by significant reductions in the phosphorylation status of Akt, a downstream effector of PI3-kinase (Fig. 3*C*). As seen before, no effect of mutant L64P merlin on Akt activation was observed. Therefore, merlin inhibits PI3-kinase activity by competing with PI3-kinase for binding to PIKE-L.

merlin Inhibits PI3-Kinase and Schwannoma Proliferation Through PIKE-L. We showed previously that PIKE-L containing the P187L mutation stimulates PI3-kinase as effectively as WT PIKE-L. In contrast, the dominant-negative PIKE-L-KS mutant prevents stimulation of PI3-kinase (17). To determine whether merlin suppresses PI3-kinase activity through PIKE-L, we infected RT4-D6P2T schwannoma cells with control adenovirus or adenovirus expressing WT PIKE-L, PIKE-L-KS, or PIKE-L-P187L and monitored PI3-kinase activity upon merlin induction. Compared with control (V_1)

NEUROSCIENCE

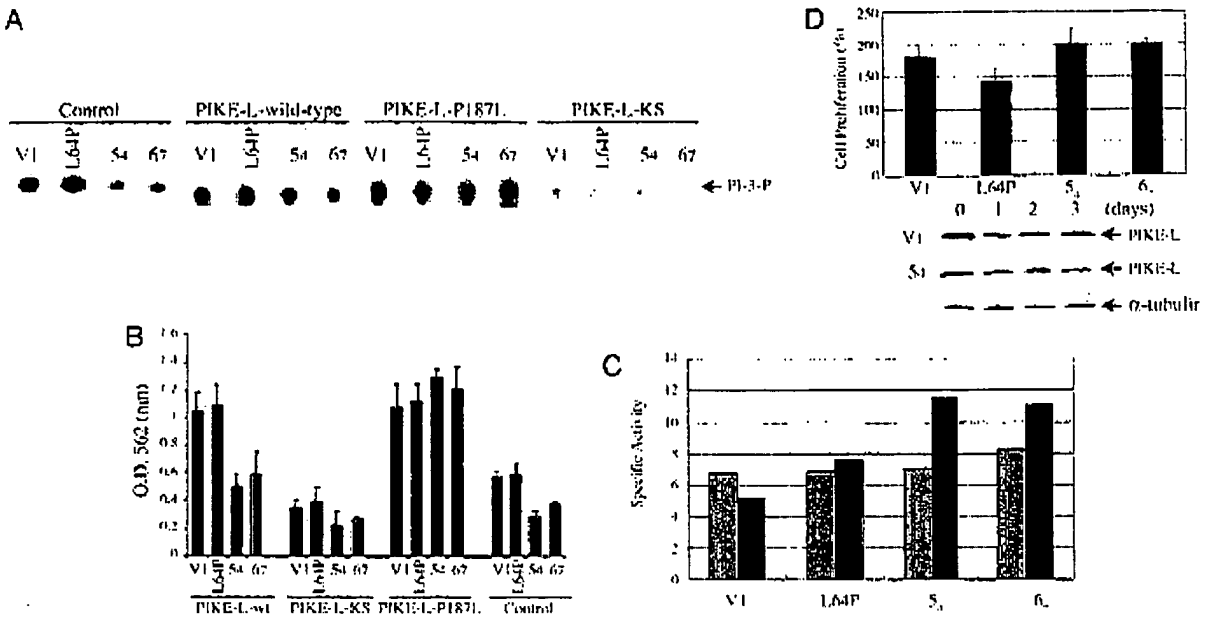

Fig. 4. merlin suppresses PI3-kinase activity through PIKE-L. (*A*) TLC was used to assay PI3-kinase activity in rat RT4-D6P2T schwannoma cells, which were infected with control adenovirus or adenovirus expressing WT PIKE-L, PIKE-L-KS, or PIKE-L-P187L. Infection with WT PIKE-L or PIKE-L-P187L resulted in an increase in PI3-kinase activity compared with control infected. This effect was suppressed in the merlin-expressing clones 5_4 and 6_7. PI3-kinase activity was unaffected in merlin clones infected with PIKE-L-P187L or merlin mutant L64P infected with either WT or P187L PIKE-L, presumably because of the inability of merlin or PIKE-L to cointeract. As expected, the dominant-negative mutant, PIKE-L-KS, inhibited PI3-kinase. (*B*) The number of proliferating rat RT4-D6P2T schwannoma cells was measured by MTT assay. Cellular proliferation paralleled PI3-kinase activity. (*C*) Caspase-3 activity assay. Empty vector (V_1), merlin mutant L64P, and WT merlin (5_4 and 6_7) cells were induced for 3 days. Caspase-3 activity assay was conducted with 30 μg of protein from day 0 (gray bar) and 3 (black bar) samples. Induction of WT merlin substantially increases apoptosis compared with control or L64P mutant. (*D*) Knocking down PIKE-L abolishes the tumor-suppressive activity of merlin. The cells was induced and infected with adenovirus expressing sh-PIKE RNA. The expression of PIKE-L in both L64P and 5_4 cells was decreased substantially upon infection of PIKE RNA interference (blots). Surprisingly, knocking down PIKE-L robustly increases cell proliferation in 5_4 and 6_7 cells compared with control and L64P cells (graph). The results were expressed as means ± SEM calculated from five times of determination ($P < 0.05$).

or mutant L64P merlin-expressing cells, WT merlin-expressing cells (5_4 and 6_7) exhibited markedly reduced levels of PI3-kinase activity (Fig. 4*A*). Infection with WT PIKE-L resulted in an increase in PI3-kinase activity compared with control infected cells, presumably due to PIKE-L enhancement of PI3-kinase activity. This effect on PI3-kinase activity was reduced in the merlin-expressing 5_4 and 6_7 cell lines, but the magnitude of reduction was identical to that observed in control-infected cells. In striking contrast, we observed a reversal of the merlin-induced reduction in PI3-kinase activity in the 5_4 and 6_7 cell lines infected with PIKE-L-P187L, consistent with the fact that this mutant is incapable of binding to merlin but can still stimulate PI3-kinase activity. As previously shown for the dominant inhibitory PIKE-L-KS mutant, expression resulted in a dramatic decrease in PI3-kinase activity in all cell lines. These results suggest that merlin inhibition of PI3-kinase activity operates through PIKE-L binding.

To provide a functional link between merlin regulation of PI3-kinase and merlin growth suppression, we analyzed cell growth upon expression of PIKE-L in inducible merlin-expressing confluent RT4 cells in parallel experiments. In control adenovirus-infected cells, substantial cell proliferation occurs in V_1 and L64P cells but not in 5_4 and 6_7 cells. Expression of PIKE-L escalates cell growth in four cell lines with smaller increases in 5_4 and 6_7 cells than in V_1 and L64P cells. Consistent with the PI3-kinase regulation results, we observed a reversal of merlin growth suppression in the WT merlin-expressing RT4 cells upon the introduction of PIKE-L-P187L. Infection of dominant-negative PIKE-L-KS substantially inhibits all cell growth (Fig. 4*B*).

To explore whether increased cell proliferation after the introduction of PIKE-L is related to enhanced cell survival, we monitored the basal rate of cell survival upon induction of merlin. Caspase-3 activity assay demonstrated that expression of WT merlin triggers an ≈40–70% apoptotic activity increase in 6_7 and 5_4 cells at day 3 after induction vs. day 0, whereas no significant increase was observed in control (V_1) or L64P cells (Fig. 4*C*). These observations are consistent with previous reports that merlin expression results in increased cell death (22, 23).

Induction of WT, but not mutant, merlin suppresses cell proliferation (Fig. 4*B*). If PIKE-L plays a critical role in mediating merlin's tumor-suppressive activity, then knocking down PIKE-L expression in schwannoma cells should compromise this effect. Accordingly, we prepared an adenovirus expressing sh-PIKE RNA to inhibit PIKE-L expression. As expected, PIKE-L was successfully decreased upon infection in both 5_4 and L64P cells; by contrast, α-tubulin was not affected (Fig. 4*D*). Strikingly, cell proliferation assay showed that both WT merlin cells present ≈200% growth at day 3 compared with day 0, whereas ≈175% and 145% increases were observed on control and L64P cells, respectively (Fig. 4*D*), indicating that WT merlin, instead of suppressing cell growth, provokes cell proliferation in the absence of PIKE-L. Collectively, these observations demonstrate that merlin growth suppression is mediated in part by binding to PIKE-L and its inhibitory effects on PI3-kinase activation.

Discussion

Our findings that PIKE-L mediates the tumor-suppressive activity of merlin through PI3-kinase provide a molecular mechanism that may account for the negative growth regulatory function of merlin. WT PIKE-L robustly binds to merlin. By contrast, GTPase mutated dominant-negative PIKE-L-KS faintly associates with merlin (Fig.

1), suggesting that the interaction between merlin and PIKE-L is mediated by the GTPase activity. Our previous study revealed that PIKE-L-KS binds to PI3-kinase but prevents its activation (17). WT PIKE-L-triggered PI3-kinase activity was decreased substantially in WT merlin-induced cells compared with L64P and control cells (Fig. 4*A*), indicating that PI3-kinase activity is regulated by merlin/PIKE-L interaction. However, expression of PIKE-L-KS in schwannoma cells potently inhibited PI3-kinase activity in all cells, regardless of WT or mutant merlin induction (Fig. 4*A*), suggesting that merlin does not interrupt the effect of PIKE-L-KS on PI3-kinase. This effect correlates with its crippled binding activity to merlin (Fig. 1).

The FERM domain of merlin binds to the N terminus of PIKE-L (Fig. 1). Both PIKE-L and -S isoforms share the same N-terminal region, suggesting that PIKE-S also might bind to merlin. As predicted, our *in vitro* binding assay with GST-PIKE-S revealed that these two proteins interact with each other. Moreover, this interaction also was observed in coimmunoprecipitation assays in transfected HEK293 cells (data not shown). However, PIKE-S was not detected in schwannoma cells, fitting with the previous finding that PIKE-S predominantly occurs in neuronal tissue (15). Given the high sequence conservation between merlin and ERM proteins in the FERM domain, it is possible that PIKE-L also might bind to other ERM proteins. merlin is directly phosphorylated on Ser-518 by members of the p21-activated kinase (PAK) family of kinases, including PAK1 and PAK2 (24, 25). Recently, we showed that a merlin mutant that mimics Ser-518 phosphorylation (S518D) cannot suppress cell growth or motility in RT4 rat schwannoma cells and results in dramatic changes in cell morphology and actin cytoskeleton organization (26). Consistently, S518D mutation attenuated the interaction between merlin and PIKE-L compared with WT and S518A merlin (data not shown).

To determine how merlin functions as a growth suppressor, several groups have used yeast two-hybrid cloning to identify novel merlin partners, including CD44 (27, 28), βII-spectrin (29), SCHIP-1 (30), hepatocyte growth factor-regulated tyrosine kinase substrate (HRS) (31), NHE-RF (32), and β1-integrin (33). Among the merlin-associated proteins, CD44 and HRS are the potential candidates mediating the growth suppressive activity of merlin. At high cell density, merlin becomes hypophosphorylated and associates with the cytoplasmic tail of CD44 and inhibits cell growth in response to HA. At low cell density, merlin is phosphorylated, is growth permissive, and exists in a complex with ezrin, moesin, and CD44 (28). Hepatocyte growth factor is one of the most potent mitogens for Schwann cells and also promotes cell motility (34). HRS specifically interacts with the C-terminal domain of merlin. Merlin interacts with HRS in the unfolded, or open, conformation. However, merlin binding to HRS does not negatively regulate HRS growth suppressor activity (14).

In addition to cell-growth regulation, merlin regulates actin cytoskeleton-mediated functions, such as spreading, motility, and attachment. Accordingly, merlin has been implicated in Rac/Cdc42 signaling (25, 35). Recently, merlin has been shown to inhibit directly the Rac/CDC42-dependent Ser/Thr kinase PAK1, which is essential for both Ras transformation and neurofibromatosis type 1 (36, 37). Moreover, merlin also has been suggested to inhibit Ras/mitogen-activated protein kinase cascade (38). Our findings that merlin specifically binds to PIKE-L and abrogates PIKE's effects on PI3-kinase provides further evidence that merlin acts as a tumor suppressor by antagonizing the PIKE/PI3-kinase pathway. The discovery that merlin regulates cell growth through PI3-kinase/Akt-mediated signaling pathways is intriguing in light of the established relationship between other FERM-containing proteins and apoptosis (39, 40). Although most previous studies of merlin function have focused on the ability of merlin to reduce cell proliferation, merlin expression also can result in increased cell death (22). Transduction of merlin into human schwannoma cells was found to decrease cell growth by inducing apoptosis (23). The PI3-kinase/Akt pathway plays an essential role in promoting cell survival in various cell types. In this fashion, merlin expression would result in decreased PIKE-induced PI3-kinase activity and decreased Akt activation, culminating in increased cell death. Thus, our studies, to our knowledge, provide the first mechanistic insights into how merlin might regulate cell growth by modulating PI3-kinase/Akt pathway.

We thank Drs. Helen Morrison and Peter Herrlich (Karlsruhe, Germany) for the WT merlin inducible RT4 schwannoma cell lines. This work was supported by Department of Defense New Investigator Award NF020013 (to K.Y.) and National Institutes of Health Grant R01-NS35848 (to D.H.G.).

1. Eldridge, R. (1981) *Adv. Neurol.* **29**, 57–65.
2. Rouleau, G. A., Merel, P., Lutchman, M., Sanson, M., Zucman, J., Marineau, C., Hoang-Xuan, K., Demczuk, S., Desmaze, C., Plougastel, B., *et al.* (1993) *Nature* **363**, 515–521.
3. Trofatter, J. A., MacCollin, M. M., Rutter, J. L., Murrell, J. R., Duyao, M. P., Parry, D. M., Eldridge, R., Kley, N., Menon, A. G., Pulaski, K., *et al.* (1993) *Cell* **72**, 791–800.
4. Gutmann, D. H. (1997) *Neurobiol. Dis.* **3**, 247–261.
5. Gonzalez-Agosti, C., Xu, L., Pinney, D., Beauchamp, R., Hobbs, W., Gusella, J. & Ramesh, V. (1996) *Oncogene* **13**, 1239–1247.
6. Scherer, S. S. & Gutmann, D. H. (1996) *J. Neurosci. Res.* **46**, 595–605.
7. Gutmann, D. H., Sherman, L., Seftor, L., Haipek, C., Hoang Lu, K. & Hendrix, M. (1999) *Hum. Mol. Genet.* **8**, 267–275.
8. Sherman, L., Xu, H. M., Geist, R. T., Saporito-Irwin, S., Howells, N., Ponta, H., Herrlich, P. & Gutmann, D. H. (1997) *Oncogene* **15**, 2505–2509.
9. Huynh, D. P. & Pulst, S. M. (1996) *Oncogene* **13**, 73–84.
10. Gonzalez-Agosti, C., Wiederhold, T., Herndon, M. E., Gusella, J. & Ramesh, V. (1999) *J. Biol. Chem.* **274**, 34438–34442.
11. Gutmann, D. H., Geist, R. T., Xu, H., Kim, J. S. & Saporito-Irwin, S. (1998) *Hum. Mol. Genet.* **7**, 335–345.
12. Gutmann, D. H., Haipek, C. A. & Hoang Lu, K. (1999) *J. Neurosci. Res.* **58**, 706–716.
13. Meng, J. J., Lowrie, D. J., Sun, H., Dorsey, E., Pelton, P. D., Bashour, A. M., Groden, J., Ratner, N. & Ip, W. (2000) *J. Neurosci. Res.* **62**, 491–502.
14. Gutmann, D. H. (2001) *Hum. Mol. Genet.* **10**, 747–755.
15. Ye, K., Hurt, K. J., Wu, F. Y., Fang, M., Luo, H. R., Hong, J. J., Blackshaw, S., Ferris, C. D. & Snyder, S. H. (2000) *Cell* **103**, 919–930.
16. Ye, K., Aghajani, B., Luo, H. R., Moriarity, J. L., Wu, F. Y., Hong, J. J., Hurt, K. J., Bae, S. S., Suh, P. G. & Snyder, S. H. (2002) *Nature* **415**, 541–544.
17. Rong, R., Ahn, J. Y., Huang, H., Nagata, E., Kalman, D., Kapp, J. A., Tu, J., Worley, P. F., Snyder, S. H. & Ye, K. (2003) *Nat. Neurosci.* **6**, 1153–1161.
18. Ye, K., Compton, D. A., Lai, M. M., Walensky, L. D. & Snyder, S. H. (1999) *J. Neurosci.* **19**, 10747–10756.
19. Ye, K., Ke, Y., Keshava, N., Shanks, J., Kapp, J. A., Tekmal, R. R., Petros, J. & Joshi, H. C. (1998) *Proc. Natl. Acad. Sci. USA* **95**, 1601–1606.
20. He, T. C., Zhou, S., da Costa, L. T., Yu, J., Kinzler, K. W. & Vogelstein, B. (1998) *Proc. Natl. Acad. Sci. USA* **95**, 2509–2514.
21. Ahn, J. Y., Rong, R., Kroll, T. G., Van Meir, E. G., Snyder, S. H. & Ye, K. (2004) *J. Biol. Chem.* **279**, 16461–16471.
22. Shaw, R. J., McClatchey, A. I. & Jacks, T. (1998) *J. Biol. Chem.* **273**, 7757–7764.
23. Schulze, K. M., Hanemann, C. O., Muller, H. W. & Hanenberg, H. (2002) *Hum. Mol. Genet.* **11**, 69–76.
24. Kissil, J. L., Johnson, K. C., Eckman, M. S. & Jacks, T. (2002) *J. Biol. Chem.* **277**, 10394–10399.
25. Xiao, G. H., Beeser, A., Chernoff, J. & Testa, J. R. (2002) *J. Biol. Chem.* **277**, 883–886.
26. Surace, E. I., Haipek, C. A. & Gutmann, D. H. (2004) *Oncogene* **23**, 580–587.
27. Sainio, M., Zhao, F., Heiska, L., Turunen, O., den Bakker, M., Zwarthoff, E., Lutchman, M., Rouleau, G. A., Jaskelainen, J., Vaheri, A. & Carpen, O. (1997) *J. Cell. Sci.* **110**, 2249–2260.
28. Morrison, H., Sherman, L. S., Legg, J., Banine, F., Isacke, C., Haipek, C. A., Gutmann, D. H., Ponta, H. & Herrlich, P. (2001) *Genes Dev.* **15**, 968–980.
29. Scoles, D. R., Huynh, D. P., Morcos, P. A., Coulsell, E. R., Robinson, N. G., Tamanoi, F. & Pulst, S. M. (1998) *Nat. Genet.* **18**, 354–359.
30. Goutebrize, L., Brault, E., Muchardt, C., Camonis, J. & Thomas, G. (2000) *Mol. Cell. Biol.* **20**, 1699–1712.
31. Scoles, D. R., Huynh, D. P., Chen, M. S., Burke, S. P., Gutmann, D. H. & Pulst, S. M. (2000) *Hum. Mol. Genet.* **9**, 1567–1574.
32. Murthy, A., Gonzalez-Agosti, C., Cordero, E., Pinney, D., Candia, C., Solomon, F., Gusella, J. & Ramesh, V. (1998) *J. Biol. Chem.* **273**, 1273–1276.
33. Obremski, V. J., Hall, A. M. & Fernandez-Valle, C. (1998) *J. Neurobiol.* **37**, 487–501.
34. Krasnoselsky, A., Massay, M. J., DeFrances, M. C., Michalopoulos, G., Zarnegar, R. & Ratner, N. (1994) *J. Neurosci.* **14**, 7284–7290.
35. Shaw, R. J., Paez, J. G., Curto, M., Yaktine, A., Pruitt, W. M., Saotome, I., O'Bryan, J. P., Gupta, V., Ratner, N., Der, C. J., *et al.* (2001) *Dev. Cell* **1**, 63–72.
36. Kissil, J. L., Wilker, E. W., Johnson, K. C., Eckman, M. S., Yaffe, M. B. & Jacks, T. (2003) *Mol. Cell* **12**, 841–849.
37. Hirokawa, Y., Tikoo, A., Huynh, J., Utermark, T., Hanemann, C. O., Giovannini, M., Xiao, G. H., Testa, J. R., Wood, J. & Maruta, H. (2004) *Cancer J.* **10**, 21–26.
38. Lim, J. Y., Kim, H., Kim, Y. H., Kim, S. W., Huh, P. W., Lee, K. H., Jeun, S. S., Rha, H. K. & Kang, J. K. (2002) *Biochem. Biophys. Res. Commun.* **302**, 238–245.
39. Gautreau, A., Poullet, P., Louvard, D. & Arpin, M. (1999) *Proc. Natl. Acad. Sci. USA* **96**, 7300–7305.
40. Kondo, T., Takeuchi, K., Doi, Y., Yonemura, S., Nagata, S. & Tsukita, S. (1997) *J. Cell Biol.* **139**, 749–758.

Oncogene (2005) 24, 3574–3582

www.nature.com/onc

Positive feedback regulation between AKT activation and fatty acid synthase expression in ovarian carcinoma cells

Hui Qin Wang[1], Deborah A Altomare[1], Kristine L Skele[1], Poulikos I Poulikakos[1], Francis P Kuhajda[2], Antonio Di Cristofano[1] and Joseph R Testa*[,1]

[1]*Human Genetics Program, Fox Chase Cancer Center, 333 Cottman Avenue, Philadelphia, PA 19111-2497, USA;* [2]*Department of Pathology, The Johns Hopkins University School of Medicine, Baltimore, MD 21224, USA*

Activation of AKT and overexpression of fatty acid synthase (FAS) are frequently observed in human ovarian cancer. To explore a possible connection between AKT and FAS, immunohistochemical analyses were conducted on an ovarian cancer tissue microarray, which revealed a significant correlation between phosphorylated AKT (phospho-AKT) and expression of FAS. To investigate the relationship between phospho-AKT and FAS *in vitro*, a variety of experiments employing a specific phosphatidylinositol 3-OH kinase (PI3K) inhibitor (LY294002), inducible PTEN expression in *PTEN*-null cells, or *AKT1* siRNA demonstrated that phosphatidylinositol-3 kinase (PI3K)/AKT signaling modulates FAS expression. In contrast, inhibition of FAS activity by the drug C75 resulted in downregulation of phospho-AKT and increased cell death. To explore the functional relationship between phospho-AKT and FAS, we used SKOV3, C200, and OVCAR10 ovarian carcinoma cells, which have constitutively active AKT, and OVCAR5 cells, which have very low basal phospho-AKT levels. Treatment with LY294002 abolished AKT activity and potentiated apoptosis induced by FAS inhibitors cerulenin or C75 only in cells with constitutively active AKT, suggesting that constitutive activation of AKT protects against FAS inhibitor-induced cell death. Furthermore, inhibition of FAS activity by cerulenin or C75 resulted in downregulation of phospho-AKT, which preceded the induction of apoptosis. To investigate the relationship between phospho-AKT and FAS *in vivo*, severe combined immunodeficient mice injected intraperitoneally with SKOV3 cells were treated with C75. Growth of SKOV3 xenografts was markedly inhibited by C75. Analysis of the levels of phospho-AKT and FAS in C75-treated tumors revealed concordant downregulation of phospho-AKT and FAS. Collectively, our findings are consistent with a working model in which AKT activation regulates FAS expression, at least in part, whereas FAS activity modulates AKT activation.
Oncogene (2005) **24**, 3574–3582. doi:10.1038/sj.onc.1208463
Published online 4 April 2005

Keywords: apoptosis; AKT/protein kinase B; fatty acid synthase; ovarian cancer

*Correspondence: JR Testa; E-mail: joseph.testa@fccc.edu
Received 11 August 2004; revised 15 December 2004; accepted 15 December 2004; published online 4 April 2005

Introduction

Ovarian cancer is the most common cause of death from gynecologic cancer among women in the United States. Recurrent molecular genetic alterations seen in ovarian cancer include *MYC* amplification, *TP53* and *KRAS* mutations, overexpression of *HER2/neu*, and germline mutations of *BRCA1* and *BRCA2* (Aunoble *et al.*, 2000). In addition, phosphatidylinositol 3-OH kinase (PI3K) amplification has been reported in some ovarian carcinomas and ovarian cancer cell lines and is accompanied by increased PI3K activity (Shayesteh *et al.*, 1999; Philp *et al.*, 2001). We previously demonstrated amplification and/or overexpression of the *AKT2* oncogene in human ovarian cancers (Cheng *et al.*, 1992), and AKT2 and AKT1 kinases are frequently activated in primary ovarian carcinomas (Yuan *et al.*, 2000; Sun *et al.*, 2001). Numerous studies have established that AKT activation promotes cell survival and enhances tumor cell growth and invasiveness (Datta *et al.*, 1999; Testa and Bellacosa, 2001). Moreover, active AKT has been shown to confer resistance to chemotherapy and radiation in cell lines derived from a variety of tumor types (Ng *et al.*, 2000; Page *et al.*, 2000; Hu *et al.*, 2002), and LY294002, a potent inhibitor of the PI3K/AKT pathway, inhibits growth of ovarian carcinoma cells in culture or as xenografts in nude mice (Hu *et al.*, 2002).

Fatty acid synthase (FAS) is a multifunctional metabolic enzyme that catalyses the terminal steps in the synthesis of long-chain saturated fatty acids. The production of fatty acids supports membrane synthesis in proliferating cells (Jackowski *et al.*, 2000). In normal cells, FAS is expressed at low levels due to the presence of abundant amounts of dietary lipids. However, increased levels of FAS are found in a wide array of solid tumors including carcinomas of the breast (Alo *et al.*, 1996), prostate (Epstein *et al.*, 1995), ovary (Gansler *et al.*, 1997; Alo *et al.*, 2000), stomach (Kusakabe *et al.*, 2002), and lung (Piyathilake *et al.*, 2000), as well as in mesotheliomas (Gabrielson *et al.*, 2001), retinoblastomas (Camassei *et al.*, 2003a) and nephroblastomas (Camassei *et al.*, 2003b). Overexpression of FAS appears to occur very early in cancer development and is more pronounced in clinically aggressive cancers (Gansler *et al.*, 1997). Inhibition of

FAS activity preferentially inhibits tumor cell growth and induces apoptosis in breast cancer (Pizer *et al.*, 1996a; Pizer *et al.*, 1998), prostate cancer (Pizer *et al.*, 2001; De Schrijver *et al.*, 2003), and mesothelioma cells (Gabrielson *et al.*, 2001). FAS appears to provide a selective proliferative advantage; thus, FAS has become a promising target for anticancer drug development.

PI3K/AKT signaling has been implicated in the regulation of FAS expression in breast cancer cells (Yang *et al.*, 2002), prostate cancer cells (Van de Sande *et al.*, 2002), and adipocyte/3T3 cells (Wang and Sul, 1998). However, to date, a connection between downregulation of AKT expression and decreased FAS protein has not been documented, nor has it been shown that inhibition of FAS activity can inhibit AKT activation. In this report, we address the relationship between AKT and FAS in human cancer cells. We show that PI3K/AKT signaling regulates FAS expression, based on *in vitro* studies employing a variety of experimental tools including a specific PI3K inhibitor, a *PTEN*-deficient cell line stably transfected with an inducible *PTEN* construct, and *AKT1* siRNA. In addition, inhibition of FAS activity by the drug C75 resulted in downregulation of phospho (active)-AKT and increased apoptosis. Based on these findings, we propose a positive feedback loop between AKT activation and FAS expression.

Results

To investigate the relationship between increased AKT activity and overexpression of FAS in human ovarian carcinomas, we performed immunohistochemical analyses of phosphorylated AKT (phospho-AKT) (Ser473) and FAS on an ovarian cancer tissue microarray. We found that 21 of 31 (68%) tumor specimens expressed elevated levels of phospho-AKT, and 25 of 31 (80%) expressed FAS (Table 1). All 21 cases with elevated phospho-AKT also expressed FAS ($P<0.001$, Fisher's exact test; $P<0.0001$, Jonckheere–Terpstra test). Among these, six with highest FAS staining also stained most intensely for phospho-AKT. Four tumors that expressed FAS did not show elevated staining for phospho-AKT. Six tumors were negative for both phospho-AKT and FAS protein. Figure 1 depicts serial sections of two representative tumors with intense staining for both phospho-AKT and FAS in tumor cells but not in adjacent stromal tissues. Collectively, these data indicate a significant correlation between AKT activation and FAS expression in this series of ovarian carcinomas.

Table 1 Expression of FAS is significantly correlated with that of phospho-AKT in a series of ovarian carcinomas[a]

	FAS positive	*FAS negative*	*Total*
AKT positive	21	0	21
AKT negative	4	6	10
Total	25	6	31

Immunohistochemical staining was performed on an ovarian cancer tissue microarray with antibodies against phospho-AKT and FAS. Based on the scoring system described in Materials and methods, scores of 2 or 3 were considered positive for phospho-AKT and FAS, and scores of 0 or 1 were considered negative. [a]$P<0.01$ as determined by Fisher's exact test; $P<0.0001$ as determined by the Jonckheere–Terpstra test

Since phospho-AKT was present in most FAS-positive ovarian carcinoma specimens, the presence of phospho-AKT may contribute to the expression of FAS in this subset of tumors. To test this hypothesis, we used several ovarian cancer cell lines that, under serum starvation conditions, exhibit constitutively active AKT (phospho-AKT), to determine if phospho-AKT affects FAS expression. First, serum-starved SKOV3 cells were treated with different concentrations of LY294002. As shown in Figure 2a, FAS protein levels as well as phospho-AKT levels decreased significantly after treatment with LY294002 in a dose-dependent manner. Similar to SKOV3 cells, FAS protein levels in

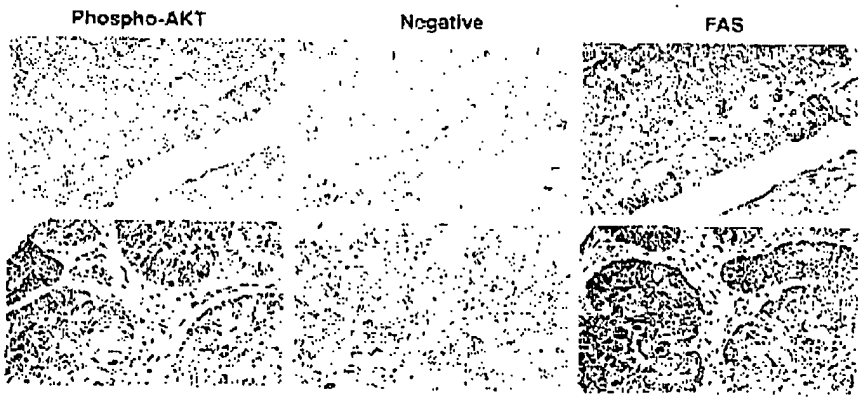

Figure 1 FAS expression correlates with AKT activation in human ovarian carcinomas. Immunohistochemical staining of two representative human ovarian tumors from an ovarian cancer tissue microarray. Serial sections of an ovarian cancer tissue microarray were stained with phospho-AKT (Ser473) antibody (1 : 50) and FAS antibody (5 μg/ml). Negative controls were incubated with phospho-AKT (Ser473) antibody preabsorbed with a phospho-AKT (Ser473) blocking peptide. Magnification, × 200

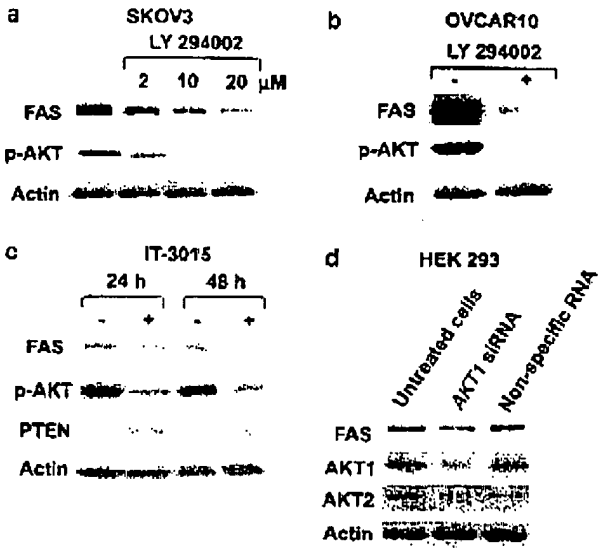

Figure 2 FAS expression is dependent on PI3K/AKT signaling. (a, b) Inhibition of PI3K/AKT by LY294002 resulted in a significant decrease of FAS protein in SKOV3 cells (a) and OVCAR10 cells (b). SKOV3 and OVCAR10 cells were treated with the indicated concentrations of LY294002 or with DMSO as a vehicle control. After 48 h, total cellular extracts were prepared. Equal amounts of protein were subjected to Western blot analysis. (c) PTEN induction resulted in decreased phospho-AKT and FAS protein levels in IT-3015 cells. IT-3015 cells were cultured with or without doxycycline (2 μg/ml) for 24 or 48 h. Whole cell lysates were prepared and subjected to Western blot analysis. (d) *AKT1* siRNA transfection of HEK293 cells resulted in decreased AKT1 and FAS protein levels, but not AKT2 protein levels. HEK293 cells were transfected with *AKT1* siRNA or control siRNA. At 60 h after transfection, whole cell lysates were prepared and subjected to Western blot analysis

OVCAR10 cells also decreased after treatment with LY294002 (Figure 2b). However, LY294002 treatment did not result in a significant decrease of FAS protein levels in OVCAR4 and OVCAR5 cells, which do not exhibit constitutively active AKT under serum starvation conditions (data not shown). Next, we used an endometrial carcinoma cell line (IT-3015) derived from *PTEN*-null Ishikawa cells. IT-3015 is engineered to express PTEN in a tetracycline-dependent manner. When PTEN expression was induced by the tetracycline analog doxycycline, both phospho-AKT and FAS levels decreased (Figure 2c). To confirm that the effects of doxycycline on FAS expression are due to PTEN induction and not doxycycline treatment alone, parental Ishikawa cells were treated with doxycycline for 24 and 48 h, and no changes in phospho-AKT and FAS levels were observed at either time point (data not shown). To further explore the role of AKT in regulating FAS expression, we used HEK293 cells, which have constitutively active AKT and high transfection efficiency. By using AKT1 and AKT2 isoform-specific antibodies, we found that AKT1 is the predominant AKT isoform in 293 cells (data not shown). *AKT1* siRNA was introduced into HEK293 cells, which resulted in a 60% reduction in AKT1 protein expression levels and a 50% reduction in FAS expression at 60 h post-transfection (Figure 2d). AKT2 levels were not affected by *AKT1* siRNA (Figure 2d). To our knowledge, this is the first demonstration that downregulation of AKT1 leads to decreased expression of FAS. Collectively, the data summarized above indicate that PI3K/AKT signaling regulates FAS expression, and that AKT is a regulator of FAS expression.

Since the mitogen-activated protein kinase (MAPK) pathway has been shown to be involved in H-*ras*-mediated upregulation of FAS expression in breast carcinoma cells (Yang *et al.*, 2002), we tested whether the MAPK pathway is also involved in the regulation of FAS expression in SKOV3 cells. Treatment of SKOV3 cells with the MAPK inhibitor PD 98059 did not alter FAS protein levels (data not shown), which indicates that the MAPK pathway is not involved in the regulation of FAS expression in this cell line.

To determine if FAS inhibition induces cell death in ovarian cancer cells, SKOV3, C200, and OVCAR10, each of which exhibits constitutively active AKT under serum starvation conditions, were treated with cerulenin, a naturally occurring FAS inhibitor (D'Agnolo *et al.*, 1973). Cerulenin at a concentration of 3 μg/ml induced cell death in SKOV3, C200, and OVCAR10 cells, but the amount of cell death differed among the cell lines (Figure 3a, d, and e). SKOV3 cells, which have the highest phospho-AKT levels, were the most sensitive to cerulenin, suggesting that endogenous AKT activity may be predictive of sensitivity to FAS inhibition. Similarly, Brognard *et al.* (2001) have demonstrated that lung cancer cell lines with constitutively active AKT are highly sensitive to chemotherapeutic drugs and radiation. As expected, treatment of ovarian carcinoma cells with the PI3K inhibitor LY294002 abolished AKT activity, consistent with AKT activation being PI3K-dependent. A marked increase in cerulenin-induced apoptosis was observed when LY294002 and cerulenin were added simultaneously in ovarian carcinoma cells with constitutively active AKT (SKOV3, C200, and OVCAR10) (Figure 3a, d, and e). In contrast, cerulenin at 3 μg/ml did not induce apoptosis in ovarian carcinoma cells without constitutively active AKT (OVCAR5), and no increase in cerulenin-induced apoptosis was observed when combining cerulenin with LY294002 in OVCAR5 cells (Figure 4a). To exclude the possibility that the additive effects of LY294002 and cerulenin correlate with additive decrease in FAS level, we examined the levels of FAS expression after treatment of SKOV3 cells for 48 h with cerulenin or LY294002 alone, or with a combination of cerulenin and LY294002. As shown in Figure 3b, cerulenin alone did not decrease FAS protein levels. In contrast, LY294002 treatment resulted in decreased FAS expression, but no further decrease was observed when cerulenin and LY294002 were combined. In addition, to confirm that apoptosis occurred in SKOV3 cells treated with cerulenin or LY294002 alone, or with a combination of cerulenin and LY294002, immunoblot analysis was performed to determine the levels of active caspase-3. As shown in Figure 3c, active caspase-3 was induced by

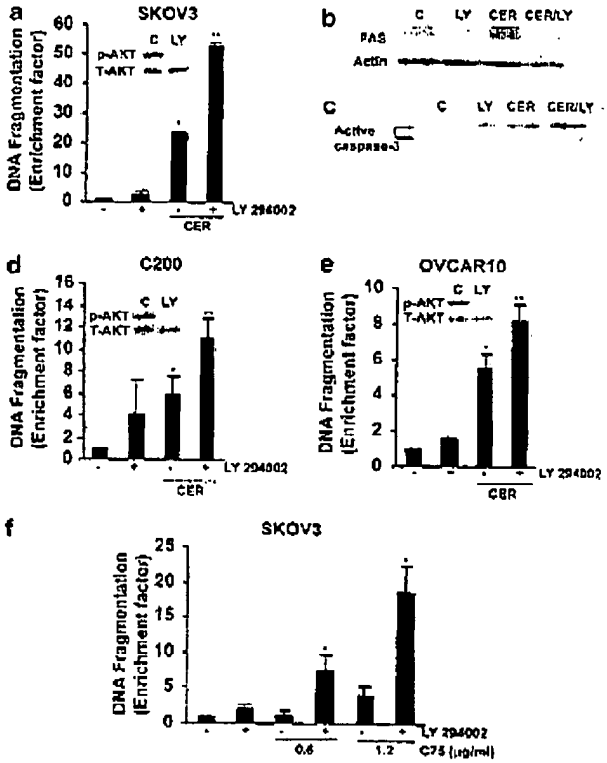

Figure 3 Inhibition of PI3K/AKT signaling potentiates apoptosis induced by the FAS inhibitors in ovarian carcinoma cells with constitutively active AKT. (a) ELISA analysis of cerulenin-induced apoptosis in the presence or absence of LY294002 in SKOV3. Cells were treated with cerulenin (CER, 3 μg/ml) with or without LY294002 for 48 h in serum-free medium. The cells were lysed and the supernatant was used for ELISA analysis of DNA fragmentation. Data are shown as mean $\pm$ s.d. ($n=4$). $^{*}P<0.05$ *versus* control treated cells; $^{**}P<0.05$ *versus* cerulenin-treated cells by Student's *t*-test. The inset shows representative Western blots for phospho-AKT and total AKT (C represents DMSO as a vehicle control and LY represents LY294002). For Western blot analysis, cells were starved for 20 h in serum-free medium in the absence or presence of LY294002 (LY, 20 μM); whole cell homogenates were prepared and Western blot analyses of phospho-AKT and total AKT (T-AKT) were performed as described in Materials and methods. (b) Western blot analysis of FAS protein after treatment with LY294002 (LY) and cerulenin (CER) for 48 h. (c) Western blot analysis of active caspase-3 protein after treatment with LY294002 (LY) and cerulenin (CER) for 48 h. (d, e) ELISA analysis of cerulenin-induced apoptosis in the presence or absence of LY294002 in C200 (d) and OVCAR10 (e) cells. (f) ELISA analysis of FAS inhibitor C75-induced apoptosis in the presence or absence of LY294002 in SKOV3 cells. Cells were treated with C75 at concentrations of 0.6 or 1.2 μg/ml, with or without LY294002 for 48 h in serum-free medium, and the cells were lysed and the supernatant was used for ELISA analysis of DNA fragmentation. Data are shown as mean $\pm$ s.d. ($n=3$). $^{*}P<0.05$ *versus* C75-treated cells by Student's *t*-test

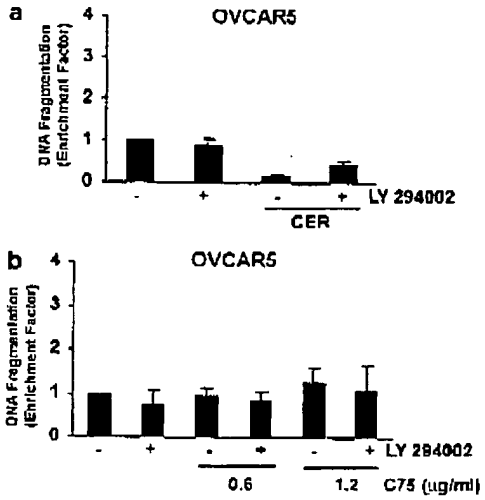

Figure 4 Ovarian carcinoma cells without constitutively active AKT are resistant to FAS and PI3K/AKT inhibitor-induced apoptosis. (a) ELISA analysis of cerulenin-induced apoptosis in the presence or absence of LY294002 in OVCAR5 cells. Cells were treated with cerulenin (CER, 3 μg/ml) with or without LY294002 for 48 h in serum-free medium. The cells were lysed and the supernatant was used for ELISA analysis of DNA fragmentation. Data are shown as mean $\pm$ s.d. ($n=4$). (b) ELISA analysis of FAS inhibitor C75-induced apoptosis in the presence or absence of LY294002 in OVCAR5 cells. Cells were treated with C75 at concentrations of 0.6 or 1.2 μg/ml, with or without LY294002 for 48 h in serum-free medium, and the cells were lysed and the supernatant was used for ELISA analysis of DNA fragmentation. Data are shown as mean $\pm$ s.d. ($n=3$)

treatment with either cerulenin or LY294002 and was further increased when LY294002 and cerulenin were combined.

Next, we tested the effect of C75, a synthetic, chemically stable FAS inhibitor (Kuhajda *et al*., 2000), on SKOV3 and OVCAR5 cells. We found that C75-induced apoptosis was significantly increased by inhibition of PI3K/AKT signaling in SKOV3 cells (Figure 3f), but not in OVCAR5 cells (Figure 4b). These results indicate that PI3K/AKT inhibition increases FAS inhibitor-induced apoptosis in cells with constitutively active AKT.

Fatty acids synthesized by FAS are incorporated into membrane phospholipids. Inhibition of FAS by C75 or *FAS* siRNA results in decreased phospholipid content in the membrane (Swinnen *et al*., 2003). Since activation of AKT relies on membrane phospholipids, we next tested if inhibition of FAS activity affects AKT activation. SKOV3 cells were serum-starved overnight and treated with C75 for 6, 12, and 24 h. C75 treatment resulted in markedly decreased levels of phospho-AKT at 12 h, and this was sustained to 24 h (Figure 5a). Total AKT levels remained unchanged following treatment with C75. Phospho-AKT levels could also be downregulated by cerulenin treatment (Figure 5b). In order to show that the decrease of phospho-AKT is not due to cytotoxicity of C75, we counted viable cells by Trypan blue exclusion assay. The percentage of viable cells at 12 h (93% $\pm$ 1.83) and 24 h (95% $\pm$ 0.95) post-C75 treatment did not differ from that observed in control cells (94% $\pm$ 1.93). In addition, we did not observe any active caspase-3 or cleaved PARP product at 12 or 24 h post-treatment with C75 (data not shown). Collectively, these findings indicate that the C75-induced decrease in phospho-AKT is not due to general cytotoxicity.

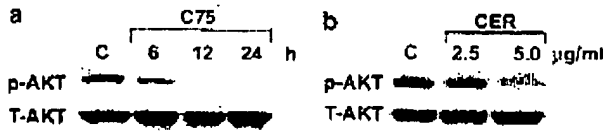

Figure 5 FAS inhibitors downregulate phospho-AKT levels in SKOV3 cells *in vitro*. (a) SKOV3 cells were starved in serum-free McCoy's 5A medium overnight and treated with 5 μg/ml C75 for 6, 12, and 24 h. (b) SKOV3 cells were starved in serum-free McCoy's 5A medium overnight and treated with cerulenin (CER) at 2.5 and 5.0 μg/ml for 24 h. Whole cell lysates were prepared and Western blot analyses of phospho-AKT and total AKT were carried out as indicated in Materials and methods

Cerulenin has previously been shown to inhibit tumor progression, including formation of ascites in an ovarian cancer xenograft model (Pizer *et al*., 1996b). To test the effect of the newer synthetic FAS inhibitor C75 on SKOV3 xenografts in female severe combined immunodeficient (SCID) mice, individual animals were injected intraperitoneally (i.p.) with 5×10^6 SKOV3 cells. After 1 week, mice were treated with C75 at a weekly dose of 20 mg/kg, or with 5% DMSO in PBS as a vehicle control. After 4 weeks of treatment, mice were killed and the tumors were collected. In addition to a large primary tumor, each vehicle-treated mouse developed multiple tumor nodules attached to the spleen, liver, or pancreas (mean number, 4.6 ± 1.6 tumors per mouse). However, most of the C75-treated mice developed only a single visible tumor (Figure 6a), which was usually located immediately below the stomach. C75-treated mice exhibited a 50% reduction in total tumor weight compared to vehicle-treated mice (Figure 6b).

Since C75 treatment induced a reduction in phospho-AKT levels in SKOV3 cells *in vitro*, we tested whether treatment with C75 resulted in reduced phospho-AKT levels *in vivo*. We analysed phospho-AKT and FAS levels in primary tumors derived from vehicle-treated mice and tumors from C75-treated mice by Western blot analysis. Markedly decreased levels of both phospho-AKT and FAS were observed in four of six C75-treated tumors (Figure 6c). Densitometric analysis revealed that the overall phospho-AKT and FAS expression levels observed in the six C75-treated tumors were significantly lower than in the control tumors. In two tumors, phospho-AKT and FAS levels did not decrease. We speculate that these two tumors acquired additional genetic or epigenetic changes during the numerous generations required for tumor formation, which may have rendered them insensitive to C75. Despite this discrepancy, it is notable that the amount of phospho-AKT was concordant with the level of FAS expression in all six tumors. In order to show that the decrease in phospho-AKT and FAS levels was not due to loss of tumor tissue through necrosis, all tumors were evaluated histologically. We did not observe any difference in the extent of necrosis between control and C75-treated tumors.

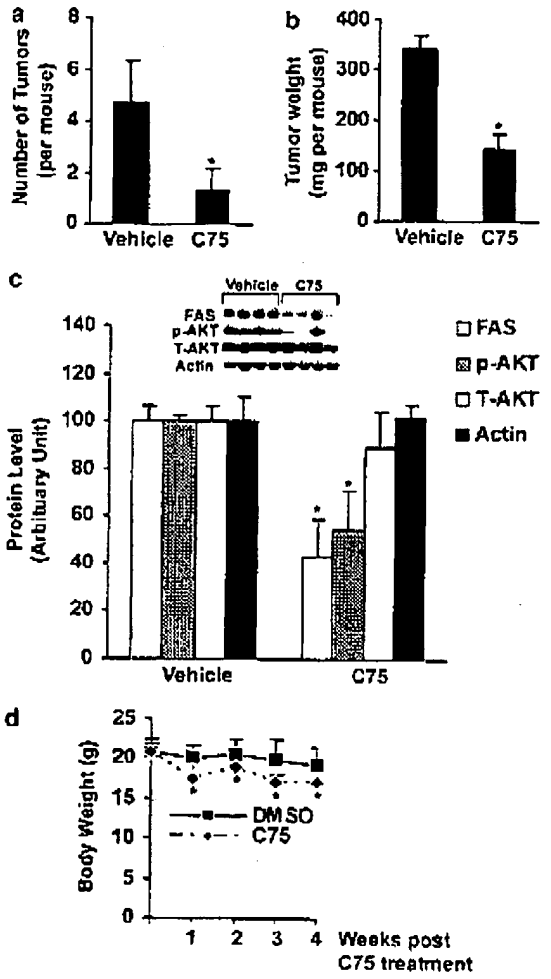

Figure 6 C75 inhibits SKOV3 tumor growth in a mouse xenograft model and downregulates phospho-AKT levels *in vivo*. (a) C75 treatment results in decreased tumor numbers. (b) C75 treatment results in decreased tumor weight. SCID mice at 6 weeks of age were injected i.p. with 5×10^6 SKOV3 cells. After 1 week, mice were treated with C75 at 20 mg/kg/dose or with 5% DMSO in PBS as a vehicle control. After 4 weeks of treatment, mice were killed and tumor numbers (a) and tumor weights (b) were determined. $^*P<0.05$ compared to vehicle-treated mice by Student's *t*-test. (c) C75 treatment results in decreased phospho-AKT and FAS protein levels *in vivo*. Whole cell homogenates of individual tumor were prepared, and Western blot analyses of FAS, phospho-AKT, total AKT, and actin were carried out as described in Materials and methods. The inset shows representative findings by Western blot analysis. The band intensities were quantified by densitometric scanning, and the data are expressed as mean ± s.e. ($n = 6$ each for C75- and vehicle-treated control groups). $^*P<0.05$ compared to tumors derived from vehicle-treated mice by Student's *t*-test. (d) C75 treatment results in decreased body weight. The body weight of each mouse was measured before and weekly after treatment with C75 or vehicle control (DMSO). $^*P<0.05$ compared to vehicle-treated mice by Student's *t*-test

Finally, it is noteworthy that animals treated with C75 did exhibit weight loss. Similar to previous studies with other xenograft models, roughly a 15% reduction in body weight was observed in C75-treated mice (Figure 6d).

Discussion

Our studies indicate that there is a positive feedback regulation between AKT activation and FAS expression in ovarian carcinoma cells grown *in vitro*, and this is supported by a high correlation between AKT activation and FAS expression in primary ovarian carcinoma specimens. AKT activation appears to regulate FAS expression, at least in part, whereas fatty acids synthesized by FAS are incorporated into membrane phospholipids, which are mediators of AKT activation. Overexpression of FAS has been previously reported in a wide variety of human tumors. The close correlation between FAS expression and AKT activation in our series of ovarian carcinomas suggests that AKT plays an important role in regulating FAS expression in ovarian cancer. Our *in vitro* experiments with SKOV3 and OVCAR10 cells indicate that inhibition of PI3K/AKT signaling results in decreased expression of FAS. When PTEN expression was induced in *PTEN*-null IT-3015 cells, FAS and phospho-AKT levels decreased coordinately; in addition, when expression of AKT1 was knocked down about 60% in HEK293 cells after *AKT1* siRNA transfection, we observed a 50% decrease in FAS levels. These several lines of evidence indicate that AKT activity modulates FAS expression. The data are consistent with previous reports showing that PI3K signaling regulates FAS expression in prostate cancer cells, breast cancer cells, and 3T3 adipocytes (Wang and Sul, 1998; Van de Sande *et al*., 2002; Yang *et al*., 2002). AKT has been studied extensively during the past decade, and one of its main functions is to promote cell survival (Datta *et al*., 1999). Cancer cells with constitutively active AKT may have a dependence on AKT activity for survival, and recent studies have demonstrated that inhibition of PI3K/AKT signaling can sensitize cancer cells to apoptosis induced by chemotherapeutic drugs or radiation (Ng *et al*., 2000; Page *et al*., 2000; Brognard *et al*., 2001; Clark *et al*., 2002; Hu *et al*., 2002; Schmidt *et al*., 2002; Jin *et al*., 2003; Knuefermann *et al*., 2003). We found that LY294002 enhances C75- and cerulenin-induced apoptosis in cell lines exhibiting constitutively active AKT. FAS inhibition results in downregulation of phospho-AKT levels (Figure 4), and LY294002 treatment may further decrease the levels of phospho-AKT, thus increasing FAS inhibitor-induced cell death in cells with constitutively active AKT.

Inhibition of FAS activity by either cerulenin or C75 downregulates phospho-AKT production. Regarding the specificity of C75 as a FAS inhibitor, recent work has shown that C75 affects two cellular processes. First, it inhibits fatty acid synthesis through slow-binding inhibition of FAS. Second, it increases fatty acid oxidation through increasing the activity of carnitine palmitoyltransferase-1 (CPT-1). Two recent publications (Thupari *et al*., 2002; Zhou *et al*., 2003) showed that FAS inhibition, not increased fatty acid oxidation, is responsible for C75's proapoptotic effects in human cancer cells. Etomoxir, an irreversible inhibitor of CPT-1, was not apoptotic to cancer cells, and it did not rescue cells from C75. These data implied that fatty acid oxidation is not involved in the mechanism of cytotoxicity of C75. Furthermore, C273, an oxidized form of C75, which does not inhibit FAS, is nontoxic to human cancer cells.

The mechanism(s) by which FAS inhibitors decrease AKT activity is not clear. One possible explanation is that FAS inhibition may cause an imbalance in membrane phospholipid levels, which may result in decreased AKT membrane localization and activation. This is supported by several lines of evidence. Firstly, lipid rafts are membrane microdomains, which serve as platforms for cell signaling (Sargiacomo *et al*., 1993), and recent studies have revealed a connection between lipid rafts, AKT, and FAS. When rafts are disrupted, AKT phosphorylation is inhibited and cell survival is reduced (Hill *et al*., 2002; Zhuang *et al*., 2002). Secondly, constitutively active AKT serine 473 kinase activity has been found in plasma membrane rafts, implicating a role for lipid rafts in AKT signaling (Hill *et al*., 2002). Finally, it has been shown that FAS drives the synthesis of phospholipids partitioning into detergent-resistant membrane microdomain-raft aggregates (Swinnen *et al*., 2003). Moreover, RNA interference-mediated silencing of FAS inhibits growth and induces apoptosis of LNCaP prostate cancer cells (De Schrijver *et al*., 2003). Since FAS plays a critical role in membrane raft phospholipid synthesis, a decrease in phospholipid levels would likely impair AKT activation. Our *in vitro* and *in vivo* data indicate that FAS inhibition indeed results in decreased AKT activity. However, other possibilities, including inhibition of PI3K or activation of PTEN or protein phosphatase-2A (Resjo *et al*., 2002) by lipid intermediates that accumulate following FAS inhibition, may also contribute to the decreased levels of phospho-AKT. Our *in vivo* studies of the effect of C75 on SKOV3 tumor growth in a murine xenograft model are consistent with results obtained with breast cancer and mesothelioma xenograft models (Pizer *et al*., 2000; Gabrielson *et al*., 2001). In addition to an overall significant inhibition of SKOV3 tumor growth, Western blot analysis of tumors showed decreased AKT activity in most C75-treated mice, concordant with reduced FAS protein levels. Thus, FAS inhibition may have significant promise as a therapeutic approach in human ovarian cancer. In summary, data presented here demonstrate a significant correlation between the expression of FAS and active AKT in ovarian cancer and indicate that inhibition of PI3K/AKT signaling increases sensitivity to FAS inhibitor-induced apoptosis in ovarian carcinoma cells with constitutively active AKT. Our findings are consistent with a working model in which AKT activation regulates FAS expression, at least in part, whereas FAS activity modulates AKT activation. Furthermore, these data suggest that AKT activity and FAS expression are useful biomarkers in ovarian cancer and may serve as important targets for therapeutic invention in this disease.

Materials and methods

Cell culture

Five ovarian cancer cell lines were used: SKOV3, C200, a cisplatin-resistant ovarian cancer cell line derived from A2780 (Godwin *et al*., 1992), OVCAR4, OVCAR5, and OVCAR10. SKOV3 cells were cultured in McCoy's 5A medium supplemented with 10% FBS, 2 mM L-glutamine, 50 U/ml penicillin, and 50 μg/ml streptomycin. C200, OVCAR4, OVCAR5, and OVCAR10 were cultured in RPMI 1640 medium supplemented with 10% FBS, 2 mM L-glutamine, 50 U/ml penicillin, and 50 μg/ml streptomycin. HEK293 cells were cultured in DMEM supplemented with 10% FBS, 2 mM L-glutamine, 50 U/ml penicillin, and 50 μg/ml streptomycin. All cultures were maintained at 37°C in a humidified incubator containing 5% CO_2. For certain experiments, cells were starved in serum-free medium for 20 h prior to treatment. C75 was purchased from Alexis Biochemicals (San Diego, CA, USA); LY294002 and cerulenin were purchased from Calbiochem (San Diego, CA, USA).

Generation of PTEN-inducible cell line IT-3015

A Tet-On gene expression system (BD Biosciences Clontech, Palo Alto, CA, USA) was used to establish the IT-3015 cell line. First, the *PTEN*-null Ishikawa cells were transfected with the pTet-on regulation vector. Stable transfectants were screened by culturing with 500 μg/ml G418. The cloned G418-resistant cells (IT-30) were then infected with pREV-TRE2hyg-*PTEN*. To this end, the PT67 packaging cell line was transfected with the pRev-TRE retrovirus vector in which the murine mammary tumor virus promoter drives a hygromycin resistance gene and the Tet-sensitive promoter (Tet response element upstream of the minimal CMV IE promoter) regulates the inserted *PTEN*. Stable transfectants were screened with 250 μg/ml hygromycin B. The cloned G418-resistant and hygromycin B-resistant cells were screened for expression of PTEN. After screening, cells were cultured in Dulbecco's modified Eagle's medium with 10% FBS containing 100 μg/ml G418 and 100 μg/ml hygromycin B.

siRNA transfection

AKT1 siRNA SMART™ pool and a nonspecific control pool were purchased from DHARMACON Research Inc. (Lafayette, CO, USA). At 1 day before transfection, HEK293 cells were seeded in six-well plates and incubated in DMEM supplemented with 10% FBS without antibiotics. Cells at 90% confluency were transfected with *AKT1* siRNA or nonspecific siRNA according to the manufacturer's instructions. Briefly, 1 ml of Opti-MEM I reduced serum medium containing 200 nmol *AKT1* siRNA SMART pool and 20 μl Lipofectamine 2000 (Invitrogen, Carlsbad, CA, USA) was added to each well. After incubating the cells for 15 h, the lipid and siRNA complex was removed, fresh growth medium was added, and the cells were collected at 60 h post-transfection. Whole cell lysates were prepared and Western blot analysis was carried out as described below.

Preparation of whole cell homogenates

After treatment, cells were washed once in PBS and then scraped into whole cell lysis buffer (25 mM Hepes, pH 7.7, 75 mM NaCl, 2.5 mM $MgCl_2 \cdot 6H_2O$, 0.2 mM EDTA, 0.1% Triton X-100, 0.5 mM DTT, 20 mM β-glycerophosphate) containing 1 × complete protease inhibitors (Roche Molecular Biochemicals, Indianapolis, IN, USA), 1 mM PMSF, and phosphatase inhibitors Na_3VO_4 (1 mM) and NaF (50 mM). Cell lysates were sonicated and centrifuged at 10 000 *g* for 20 min at 4°C. Supernatants were used as whole cell extracts for Western blot analysis. Xenograft tumors were snap-frozen in liquid nitrogen and ground into powder, using a mortar and pestle, under frozen conditions. Whole cell lysis buffer was added to the powder, and the homogenates were sonicated and centrifuged at 10 000 *g* for 20 min at 4°C. Supernatants were used as whole cell extracts for Western blot analysis. The concentration of protein was determined by Bio-Rad protein assay reagent using BSA as a standard.

Western blot analysis

Western blot analysis was carried out as described elsewhere (Wang and Smart, 1999). Briefly, whole cell extract proteins (50–100 μg) were separated electrophoretically on 4–20% Novex Tris-glycine polyacrylamide gels (Invitrogen). Proteins were transferred to Immobilon™-P membrane (Millipore Corporation, Bedford, MA, USA), blocked in 5% nonfat dry milk, 1% BSA, and 0.1% Tween 20. Membranes were probed with polyclonal antibody against phospho-AKT (serine 473) (Cell Signaling Technology, Beverly, MA, USA), polyclonal antibodies against total AKT and actin (Santa-Cruz Biotechnology, Santa Cruz, CA, USA), or a monoclonal FAS antibody (BD Transduction Laboratories, San Diego, CA, USA), polyclonal AKT1-specific antibody (Upstate, Lake Placid, NY, USA), polyclonal AKT2-specific antibody (Cell Signaling Technology). Immunoreactive bands were visualized by Western Lightning™ Chemiluminescence Reagent Plus (Perkin Elmer Life Science, Boston, MA, USA) and exposed to X-ray film. All experiments on Western blot analysis were performed three times.

Immunohistochemical analysis

An ovarian cancer tissue microarray was prepared by the Biosample and Tissue Procurement Core Facility at Fox Chase Cancer Center. Individual sections (4 μm thick) were deparaffinized and hydrated in water, followed by antigen retrieval in 10 mM citrate buffer, pH 6.0. Preparations were incubated in 3% H_2O_2 for 20 min, washed with H_2O or PBS, and blocked with 10% serum for 30 min. Polyclonal FAS antibody (Biotrend Chemical, Destin, FL, USA) was used at 5 μg/ml to detect the expression of FAS, and phospho-AKT (Ser473) antibody (Cell Signaling Technology) was used at a dilution of 1 : 50 to detect active forms of all three AKT isoforms. Primary antibodies were detected with biotinylated secondary antibody (BioGenex, San Ramon, CA, USA). The specificity of phospho-AKT (Ser473) antibody was demonstrated by pre-absorbing the antibody with a phospho-AKT (Ser473) blocking peptide (Cell Signaling Technology). Tissue sections were stained with DAB chromagen and counterstained with hematoxylin. Surrounding non-neoplastic stroma served as an internal negative control for each slide. The slides were scored semiquantitatively. A score of 0 indicated no staining, 0.5 was generally negative with some focal staining, 1 was indicative of weak focal staining, 2 indicated clearly positive staining, and a score of 3 was intensely positive. We define scores of 2 or 3 as indicating elevated phospho-AKT staining. Tumors with weak or no staining were considered as negative for phospho-AKT and FAS. Both Fisher's exact test and Jonckheere–Terpstra test were used to analyse the correlation of phospho-AKT and FAS in these tumors.

Detection of apoptosis by ELISA

Cells were treated with cerulenin or C75 with or without LY294002 for 48 h. Cells were lysed using lysis buffer provided in the Cell Death Detection ELISA kit (Roche Molecular

Biochemicals). Apoptosis was determined by measuring DNA fragmentation following the manufacturer's instructions.

In vivo *xenograft model*

SCID mice were bred in-house at Fox Chase Cancer Center. The body weight of each mouse was monitored weekly. SKOV3 cells were injected into mice i.p. at 5×10^6 in 200 μl PBS. After 1 week, mice were divided randomly into two treatment groups: control ($n = 6$) and C75-treated ($n = 6$) mice. Control mice received 5% DMSO in 200 μl of PBS i.p. weekly for 4 weeks. C75 at 20 mg/kg body weight was administered i.p. weekly for 4 weeks. At 3 days after the last treatment, mice were killed and the individual tumors were weighed and then snap-frozen in liquid nitrogen for storage. All animal experiments complied with institutional animal care guidelines.

Abbreviations

FAS, fatty acid synthase; PI3K, phosphatidylinositol 3-OH kinase; SCID, severe combined immunodeficient.

Acknowledgements

We thank Dr AJP Klein-Szanto for immunohistochemical analysis and H Wang for statistical analysis. This work was supported by National Cancer Institute Grants CA83638 (SPORE in Ovarian Cancer), CA77429, and CA06927, and by an appropriation from the Commonwealth of Pennsylvania. The following Fox Chase Cancer Center shared facilities were used in the course of this work: Cell Culture Facility, Biosample and Tissue Procurement Core, and Laboratory Animal Facility. HQ Wang is supported by a Board of Directors Postdoctoral Fellowship at Fox Chase Cancer Center and by an NIH Institutional Training Grant CA-09035-28. FASgen did not contribute reagents or support for these studies. However, we acknowledge that under a licensing agreement between FASgen and the Johns Hopkins University, FPK is entitled to a share of royalty received by the University on products that may be developed from FAS technology. FPK owns FASgen stock, which is subject to certain restrictions under University policy. The Johns Hopkins University, in accordance with its conflict of interest policies, is managing the terms of this arrangement.

References

Alo PL, Visca P, Framarino ML, Botti C, Monaco S, Sebastiani V, Serpieri DE and Di Tondo U. (2000). *Oncol. Rep.*, 7, 1383–1388.

Alo PL, Visca P, Marci A, Mangoni A, Botti C and Di Tondo U. (1996). *Cancer*, 77, 474–482.

Aunoble B, Sanches R, Didier E and Bignon YJ. (2000). *Int. J. Oncol.*, 16, 567–576.

Brognard J, Clark AS, Ni Y and Dennis PA. (2001). *Cancer Res.*, 61, 3986–3997.

Camassei FD, Cozza R, Acquaviva A, Jenkner A, Rava L, Gareri R, Donfrancesco A, Bosman C, Vadala P, Hadjistilianou T and Boldrini R. (2003a). *Invest. Ophthalmol. Vis. Sci.*, 44, 2399–2403.

Camassei FD, Jenkner A, Rava L, Bosman C, Francalanci P, Donfrancesco A, Alo PL and Boldrini R. (2003b). *Med. Pediatr. Oncol.*, 40, 302–308.

Cheng JQ, Godwin AK, Bellacosa A, Taguchi T, Franke TF, Hamilton TC, Tsichlis PN and Testa JR. (1992). *Proc. Natl. Acad. Sci. USA*, 89, 9267–9271.

Clark AS, West K, Streicher S and Dennis PA. (2002). *Mol. Cancer Ther.*, 1, 707–717.

D'Agnolo G, Rosenfeld IS, Awaya J, Omura S and Vagelos PR. (1973). *Biochim. Biophys. Acta*, 326, 155–156.

Datta SR, Brunet A and Greenberg ME. (1999). *Genes Dev.*, 13, 2905–2927.

De Schrijver E, Brusselmans K, Heyns W, Verhoeven G and Swinnen JV. (2003). *Cancer Res.*, 63, 3799–3804.

Epstein JI, Carmichael M and Partin AW. (1995). *Urology*, 45, 81–86.

Gabrielson EW, Pinn ML, Testa JR and Kuhajda FP. (2001). *Clin. Cancer Res.*, 7, 153–177.

Gansler TS, Hardman III W, Hunt DA, Schaffel S and Hennigar RA. (1997). *Hum. Pathol.*, 28, 686–692.

Godwin AK, Meister A, O'Dwyer PJ, Huang CS, Hamilton TC and Anderson ME. (1992). *Proc. Natl. Acad. Sci. USA*, 89, 3070–3074.

Hill MM, Feng J and Hemmings BA. (2002). *Curr. Biol.*, 12, 1251–1255.

Hu L, Hofmann J, Lu Y, Mills GB and Jaffe RB. (2002). *Cancer Res.*, 62, 1087–1092.

Jackowski S, Wang J and Baburina I. (2000). *Biochim. Biophys. Acta*, 1483, 301–315.

Jin W, Wu L, Liang K, Liu B, Lu Y and Fan Z. (2003). *Br. J. Cancer*, 89, 185–191.

Knuefermann C, Lu Y, Liu B, Jin W, Liang K, Wu L, Schmidt M, Mills GB, Mendelsohn J and Fan Z. (2003). *Oncogene*, 22, 3205–3212.

Kuhajda FP, Pizer ES, Li JN, Mani NS, Frehywot GL and Townsend CA. (2000). *Proc. Natl. Acad. Sci. USA*, 97, 3450–3454.

Kusakabe T, Nashimoto A, Honma K and Suzuki T. (2002). *Histopathology*, 40, 71–79.

Ng SSW, Tsao MS, Chow S and Hedley DW. (2000). *Cancer Res.*, 60, 5451–5455.

Page C, Lin HJ, Jin Y, Castle VP, Nunez G, Huang M and Lin J. (2000). *Anticancer Res.*, 20, 407–416.

Philp AJ, Campbell IG, Leet C, Vincan E, Rockman SP, Whitehead RH, Thomas RJ and Phillips WA. (2001). *Cancer Res.*, 61, 7426–7429.

Piyathilake CJ, Frost AR, Manne U, Bell WC, Weiss H, Heimburger DC and Grizzle WE. (2000). *Hum. Pathol.*, 31, 1068–1073.

Pizer ES, Chrest FJ, DiGiuseppe JA and Han WF. (1998). *Cancer Res.*, 58, 4611–4615.

Pizer ES, Jackisch C, Wood FD, Pasternack GR, Davidson NE and Kuhajda FP. (1996a). *Cancer Res.*, 56, 2745–2747.

Pizer ES, Pflug BR, Bova GS, Han WF, Udan MS and Nelson JB. (2001). *Prostate*, 47, 102–110.

Pizer ES, Thupari J, Han WF, Pinn ML, Chrest FJ, Frehywot GL, Townsend CA and Kuhajda FP. (2000). *Cancer Res.*, 60, 213–218.

Pizer ES, Wood FD, Heine HS, Romantsev FE, Pasternack GR and Kuhajda FP. (1996b). *Cancer Res.*, 56, 1189–1193.

Resjo S, Goransson O, Harndahl L, Zolnierowicz S, Manganiello V and Degerman E. (2002). *Cell Signal.*, 14, 231–238.

Sargiacomo M, Sudol M, Tang Z and Lisanti MP. (1993). *J. Cell Biol.*, 122, 789–807.

Schmidt M, Hovelmann S and Beckers TL. (2002). *Br. J. Cancer*, 87, 924–932.

Shayesteh L, Lu Y, Kuo WL, Baldocchi R, Godfrey T, Collins C, Pinkel D, Powell B, Mills GB and Gray JW. (1999). *Nat. Genet.*, 21, 99–102.

Sun M, Wang G, Paciga JE, Feldman RI, Yuan ZQ, Ma XL, Shelley SA, Jove R, Tsichlis PN, Nicosia SV and Cheng JQ. (2001). *Am. J. Pathol.*, **159**, 431–437.

Swinnen JV, Van Veldhoven PP, Timmermans L, De Schrijver E, Brusselmans K, Vanderhoydonc F, Van de Sande T, Heemers H, Heyns W and Verhoeven G. (2003). *Biochem. Biophys. Res. Commun.*, **302**, 898–903.

Testa JR and Bellacosa A. (2001). *Proc. Natl. Acad. Sci. USA*, **98**, 10983–10985.

Thupari JN, Landree LE, Ronnett GV and Kuhajda FP. (2002). *Proc. Natl. Acad. Sci. USA*, **99**, 9498–9502.

Van de Sande T, De Schrijver E, Heyns W, Verhoeven G and Swinnen JV. (2002). *Cancer Res.*, **62**, 642–646.

Wang D and Sul HS. (1998). *J. Biol. Chem.*, **273**, 25420–25426.

Wang HQ and Smart RC. (1999). *J. Cell Sci.*, **112** (Part 20), 3497–3506.

Yang YA, Han WF, Morin PJ, Chrest FJ and Pizer ES. (2002). *Exp. Cell Res.*, **279**, 80–90.

Yuan ZQ, Sun M, Feldman RI, Wang G, Ma X, Jiang C, Coppola D, Nicosia SV and Cheng JQ. (2000). *Oncogene*, **19**, 2324–2330.

Zhou W, Simpson PJ, McFadden JM, Townsend CA, Medghalchi SM, Vadlamudi A, Pinn ML, Ronnett GV and Kuhajda FP. (2003). *Cancer Res.*, **63**, 7330–7337.

Zhuang L, Lin J, Lu ML, Solomon KR and Freeman MR. (2002). *Cancer Res.*, **62**, 2227–2231.